

Washington University in St. Louis

Washington University Open Scholarship

Arts & Sciences Electronic Theses and
Dissertations

Arts & Sciences

Spring 5-15-2015

Guanine Nucleotide Synthesis and The Enteric Nervous System

Jonathan Ian Lake

Washington University in St. Louis

Follow this and additional works at: https://openscholarship.wustl.edu/art_sci_etds



Part of the [Biology Commons](#)

Recommended Citation

Lake, Jonathan Ian, "Guanine Nucleotide Synthesis and The Enteric Nervous System" (2015). *Arts & Sciences Electronic Theses and Dissertations*. 433.

https://openscholarship.wustl.edu/art_sci_etds/433

This Dissertation is brought to you for free and open access by the Arts & Sciences at Washington University Open Scholarship. It has been accepted for inclusion in Arts & Sciences Electronic Theses and Dissertations by an authorized administrator of Washington University Open Scholarship. For more information, please contact digital@wumail.wustl.edu.

WASHINGTON UNIVERSITY IN ST. LOUIS

Division of Biology & Biomedical Sciences
Molecular Cell Biology

Dissertation Examination Committee:

Robert Heuckeroth, Chair

David Ornitz, Co-chair

Thomas Baranski

Aaron DiAntonio

Gregory Longmore

Jason Mills

Guanine Nucleotide Synthesis and The Enteric Nervous System
by
Jonathan Ian Lake

A dissertation presented to the
Graduate School of Arts and Sciences
of Washington University in
partial fulfillment of the
requirements for the degree
of Doctor of Philosophy

May 2015
St. Louis, Missouri

Table of Contents

List of Figures	vi
List of Tables.....	viii
Acknowledgements	ix
Abstract	xiii
Chapter 1: Introduction	1
Chapter 2: Enteric Nervous System Development: Migration, Differentiation, and Disease.....	3
2.1 Summary	3
2.2 Introduction	4
2.3 The time course of ENS development.....	5
2.4 Human genetics of Hirschsprung Disease and associated syndromes	6
2.5 Critical molecular mediators of ENS development:	9
2.6 The RET/GFR α 1/GDNF Pathway:	9
2.7 EDNRB, ET-3 and ECE1:.....	10
2.8 Transcription factors important for ENCDC colonization of the bowel:.....	11
2.9 Morphogens in ENS development	12
2.10 Intracellular signaling molecules in the developing ENS	16
2.11 Progress in answering persistent questions in ENS developmental biology.....	20
2.11.1 Why do ENS precursors migrate through the bowel?.....	20
2.11.2 What is the function of EDNRB in ENS development?	28
2.11.3 What controls neuronal versus glial differentiation of ENS precursors and what controls neuronal subtype specification?.....	32
2.11.4 What controls neurite outgrowth and axon pathfinding in the ENS?	37
2.11.5 What is the normal role of cell death in the developing and mature ENS?	38
2.11.6 Applying our understanding of ENS development to human disease.....	39
2.11.7 Why is HSCR partially penetrant and why does the extent of aganglionosis vary between individuals?.....	40
2.11.8 Why is HSCR more common in males than in females?	42

2.11.9 Why does Down syndrome predispose to HSCR?	43
2.12 Stem cells in the ENS: therapeutic possibilities and natural roles	44
2.13 Prevention of HSCR and other intestinal motility disorders	46
2.14 Conclusion	49
2.15 References	60
Chapter 3: Hirschsprung-like disease is exacerbated by reduced de novo GMP	
synthesis	80
3.1 Summary	81
3.2 Introduction	81
3.3 Results	83
3.3.1 Medications that inhibit ENS development	83
3.3.2 MPA impaired mammalian ENS development	84
3.3.3 MPA impaired development of cultured ENCDCs	87
3.3.4 MPA selectively reduced ENCDC DNA synthesis in vivo	87
3.3.5 MPA reduced ENCDC migration by reducing proliferation	91
3.3.6 MMF increased penetrance and extent of aganglionosis	95
3.4 Discussion	100
3.5 Materials and Methods	106
3.5.1 Zebrafish	106
3.5.2 Mice	106
3.5.3 MPA and MMF treatment	107
3.5.4 Primary ENCDC culture	107
3.5.5 X-inactivation mosaic analysis	108
3.5.6 Immunohistochemistry	108
3.5.7 Quantitative Reverse Transcriptase PCR (qRT-PCR)	110
3.5.8 Microscopy and Quantification	110
3.5.9 Statistical Analysis	111
3.5.10 Study Approval	112
3.6 Supplemental Data	113
3.7 References	125

Chapter 4: Neural crest requires <i>Impdh2</i> for development of the enteric nervous system, Great vessels, and craniofacial skeleton.....	130
4.1 Summary	130
4.2 Introduction	131
4.3 Results	133
4.3.1 <i>Impdh2</i> deletion in the neural crest results in craniofacial and cardiac defects.	133
4.3.2 Neural crest-specific deletion of <i>Impdh2</i> results in bowel aganglionosis.	135
4.3.3 <i>Impdh2</i> deleted ENCDCs colonize the bowel abnormally.....	137
4.3.4 Wnt1-Cre incompletely recombines the <i>Rosa26^{EYFP}</i> reporter in the ENS of <i>Impdh2</i> conditional knockouts	139
4.4 Discussion	141
4.4.1 A neural-crest autonomous requirement for <i>Impdh2</i>	141
4.4.2 Incomplete recombination in conditional deletion of <i>Impdh2</i>	142
4.5 Conclusions	144
4.6 Materials and Methods	145
4.6.1 <i>Impdh2</i> Gene Targeting.....	145
4.6.2 Animals and Genotyping.....	147
4.6.3 Bone and Cartilage Staining.....	148
4.6.4 Whole-mount Immunofluorescent Staining	149
4.6.5 Microscopy and Measurement	150
4.6.6 Statistical Analysis	151
4.5 Supplemental Data	152
4.6 References	155
Chapter 5: <i>IMPDH2</i> variation in a Hirschsprung Disease Cohort	159
5.1 Summary	159
5.2 Introduction	159
5.3 Results	164
5.3.1 Pooled Resequencing	164
5.3.2 Variation in <i>IMPDH1</i> and <i>IMPDH2</i>	164
5.3.3 Activity of the P123R IMPDH2 variant is reduced relative to wild-type.....	166
5.3.4 Heterozygous loss of <i>Impdh2</i> does not enhance <i>Ret</i> or <i>Sox10</i> mutations.	166

5.4 Discussion	170
5.4.1 Expected Characteristics of a 3p21 HSCR Modifier Allele.....	170
5.4.2 Prevalence of the IMPDH2:p.P123R Nonsynonymous Substitution.....	173
5.4.3 Functional Consequences of the IMPDH2:p.P123R Variant.....	173
5.4.4 The Haplosufficiency of <i>Impdh2</i> in Mouse HSCR Models	174
5.5 Conclusion.....	176
5.6 Materials and Methods	177
5.6.1 Isolation of Human Genomic DNA	177
5.6.2 Quantification and Whole-Genome Amplification of Human Genomic DNA.....	177
5.6.3 Pooled Variant Detection in <i>IMPDH2</i> and <i>IMPDH1</i>	178
5.6.4 PCR-Restriction Fragment Length Polymorphism Genotyping Assay.....	180
5.6.5 Plasmids	181
5.6.6 Production of Recombinant Human IMPDH2 in <i>E. coli</i>	182
5.6.7 IMPDH Activity Assay	183
5.6.8 Curve Fitting	183
5.6.9 Animals and Whole-Mount Immunofluorescence	184
5.9 References	185
Chapter 6: Conclusions and Future Research Directions.....	189
6.1 Environmental factors affecting ENS development.....	189
6.2 Requirement of <i>Impdh2</i> for ENS Development.....	191
6.3 Hirschsprung Disease Genetics: <i>IMPDH2</i> and 3p21	193
6.4 References	195
Curriculum vitae.....	197

List of Figures

Figure 2.1: Initial Colonization of the Mouse Gastrointestinal Tract by Enteric Neural Crest-Derived Cells	7
Figure 2.2: Primary and Secondary Migration of Mouse ENCDCs	8
Figure 2.3: Molecules and Pathways Implicated in ENS Development	17
Figure 3.1: MPA inhibited ENS development in developing zebrafish and mouse.	86
Figure 3.2: MPA reduced ENCDC migration, DNA synthesis, and lamellipodia in explant cultures	88
Figure 3.3: MMF treatment reduces ENCDC migration and DNA synthesis in vivo	90
Figure 3.4: Mosaic analysis reveals that effects of GTP depletion on migration and lamellipodia are non-cell autonomous	93
Figure 3.5: MMF treatment interacts with Ret and Sox10 mutations to increase penetrance and severity of HSCR-like pathology	99
Supplemental Figure 3.1: Model.....	113
Supplemental Figure 3.2: IMPDH expression in the developing mouse bowel	115
Supplemental Figure 3.3: MPA and MMF have similar effects on ENCDCs, TuJ1 reactivity, and bowel length	116
Supplemental Figure 3.4: MPA induces apoptosis of ENCDCs in culture.....	117
Supplemental Figure 3.5: MPA does not alter neurite growth.....	117
Supplemental Figure 3.6: MMF does not significantly alter ENCDC differentiation	118
Supplemental Figure 3.7: MMF does not induce ENCDC apoptosis in vivo	119
Supplemental Figure 3.8: Live imaging of isolated and crowded ENCDC motility	120
Supplemental Figure 3.9: MMF reduces bowel length at near-term.....	121
Figure 4.1: <i>Impdh2</i> deletion by Wnt1-Cre results in craniofacial and cardiac defects at term ...	134
Figure 4.2: <i>Impdh2</i> deletion by Wnt1-Cre causes highly penetrant aganglionosis of variable length at term.....	136
Figure 4.3: <i>Impdh2</i> conditional knockout fetuses have cranial neural crest and ENCDC abnormalities at E13.5	138

Figure 4.4: Residual enteric neurons and ENCDCs in <i>Impdh2</i> conditional knockouts display incomplete recombination.	140
Supplemental Figure 4.1: Production and structure of the <i>Impdh2^{loxP}</i> and <i>Impdh2^{Del}</i> alleles.....	152
Supplemental Figure 4.2: BrdU incorporation in ENCDCs of <i>Impdh2</i> conditional knockout fetuses.	153
Supplemental Figure 4.3: Incomplete <i>Rosa26^{EYFP}</i> recombination by Wnt1-Cre in the absence of selective pressure.....	154
Figure 5.1: Intervals in the 3p21 region linked to HSCR.....	161
Figure 5.2: Sequencing coverage of <i>IMPDH1</i> and <i>IMPDH2</i>	165
Figure 5.3: IMPDH activity of IMPDH2 variants is reduced	169
Figure 5.4: No effect of heterozygous loss of <i>Impdh2</i> on the ENS of <i>Ret</i> and <i>Sox10</i> mutants...	171
Figure 5.5: Estimating proportion of 3p21 risk carriers within HSCR patients.....	172
Figure 5.6: Multispecies IMPDH2 alignment in context of P123R mutation.....	175

List of Tables

Table 2.1 Genes affecting ENS development	50
Table 3.1: Compounds that inhibited ENS development in zebrafish	85
Supplemental Table 3.2: Incidence of neural tube and heart defects in the offspring of MMF treated dams	122
Supplemental Table 3.3: Genotyping oligonucleotides	123
Supplemental Table 3.4: Primary antibodies	124
Table 5.1: Variation detected in <i>IMPDH2</i> and <i>IMPDH1</i> in a HSCR cohort	167
Table 5.2: Kinetic parameters of recombinant <i>IMPDH2</i> variants	168
Table 5.3: Primers and amplification conditions for pooled sequencing	179

Acknowledgments

I would not be here if my mentor, Dr. Robert Heuckeroth, had not hit me in the head with a candy bar on a parabolic trajectory while giving a medical school lecture on gastrointestinal motility. That's the joke version of the story, though the anecdote is true. In reality, I joined his laboratory because he is obviously passionate about investigating interesting scientific problems and committed to rigorous basic research but has always stayed mindful of the bedside. I am greatly indebted to him for his scientific leadership, the collegiate and encouraging lab environment that he fostered, our long and continuing discussions of "crazy ideas", and his willingness to go where the science leads.

My thesis committee members, Drs. David Ornitz, Gregory Longmore, Jason Mills, Aaron DiAntonio, and Thomas Baranski provided valuable scientific guidance, insight, and advice. Their input helped focus nebulous screen results into the plan of action that led here.

The members of the Heuckeroth laboratory have been instrumental to this project in particular and my graduate school experience in general. Drs. Ming Fu and Hongtao Wang taught me everything I know about our experimental systems, were generous with their time and expertise, and are generally responsible for any of my experiments ever working. Elizabeth Wright-Jin, Marina Avetisyan, and Ellen Schill dared to join me in the lab as graduate students and my time here has been greatly enriched for their help, friendship, good humor, support, creativity, and cakes. Former lab members Dr. Meredith Hitch, Aishwarya Kundu Roy, Shahriyar Majidi, Dani Brenner, Kelsey Rebehn, Cassie Graham, and Jung-ha Park also helped make my time in the lab better and gave me

opportunities to teach and learn. Olga Tusheva and Brittany Graham worked long hours sorting fish embryos into 96-well plates with me and were absolutely instrumental to the zebrafish screen's logistical and scientific success.

The success of the zebrafish project also depended critically on the help of our collaborators Drs. Stephen Johnson and Matthew Goldsmith, as well as everyone in their laboratories who helped us acquire embryos and the skills to handle them. Drs. Todd Druley, Robi Mitra, and Francesco Vallania contributed critical methods, analytical software, and support for my human sequencing project while Dr. Allen Mitchell and Dawn Jacobs allowed us access to human DNA samples from the Pregnancy Health Interview Study. Much of this work also depends on mutant mice provided by collaborators and other investigators. The *Sox10^{LacZ}* allele was originally obtained from Dr. Michael Wegner, and Dr. Michelle Southard-Smith advised us on strain backgrounds and sent us congenic *Sox10^{LacZ}* animals. Dr. Sanjay Jain provided *Ret⁹* mice and advice on *Ret* genetics. The *Impdh2^{loxP}* allele was created by Albert Zimmermann and the mice carrying it were provided ahead of publication by Dr. Beverly Mitchell, who also provided the *Hprt⁻* mice that serendipitously became a pivotal part of the mycophenolate study. Other investigators also contributed essential reagents: Dr. Vanda Lennon provided ANNA-1 serum and Dr. Craig Smith provided anti-SoxE antibody. Core facilities at Washington University School of Medicine were also important to the success of this project. The compound library used in the zebrafish screen was obtained through the Chemical Genetics Screening Core and the Digestive Diseases Research Core Center provided access to imaging equipment. The Mouse Genetics Core and its staff,

especially Mia Wallace, Angela Bartels, and Michelle Schaeg, were absolutely critical for the feasibility and success of all of my experiments that required mouse breeding.

The faculty, support staff, and students who worked in the Department of Pediatrics during my time in the lab were always helpful, available, and generous with their time and knowledge. I would especially like to thank Drs. Christina Gurnett, David Haslam, Patrick Jay, Audrey Odom, Bradley Segura, Michael Shoykhet, Philip Tarr, and David Wilson for valuable discussions and help over the course of my time in the laboratory.

I am lucky to have found close friends outside the lab who make me glad to have come to St. Louis, particularly Eddy Hawkins, Radhika Jagannathan, Ramon Jin, Huay-Zong Law, Mike Lee, Esther and Ansel Hsiao, Ariel Lyons-Warren, Kazuo Omi, Steve Persaud, and Feng Su. Greg Bean and Sam Hundert have been long-suffering and tolerant roommates and are friends for life. My friends from home, especially Chemi “Chops” Jacob, Rafael Kupferman, Yonaton Zarbiv, and the entire Zarbiv family always let me know that I was missed and not forgotten even as years went by.

The support, encouragement, understanding, and help I have gotten from my family has been essential throughout my time in the lab, but especially so when I am on any kind of deadline. My father, Dr. Philip Lake, is the reason I set out to do science so many years ago, and my mother Dr. Gail Feingold always reminds me to do a thorough physical exam. My brother Michael Lake is the hardest working person I know, an inspiration, and always has my back. My family has always supported my efforts even when the distance seemed great and the situations were difficult.

I also must make a special point to thank everyone who supported and tolerated my sudden, frequent, and sometimes prolonged absences in 2010 and 2011. Because of Bob's unflagging support, the help of everyone in the lab, and the patience and encouragement of Brian Sullivan and Dr. Wayne Yokoyama, I knew that I could concentrate on the people who needed me. During that difficult time, my father, brother and my uncle Dr. Aaron Feingold kept me sane and held the line with me. Because of a stranger's generosity, my mother's exceptional bravery, the understanding and support of my family, and a truly exceptional amount of luck, I was able to come back to St. Louis and work with renewed purpose.

Funding for this project was provided by the Children's Discovery Institute of Washington University and St. Louis Children's Hospital (CH-II-1008-123, CH-II-2010-390), NIH RO1 DK087715, NIH RO1 DK057038, and Burroughs Wellcome Fund Clinical Scientist Award in Translational Research (1008525). During part of my time in the laboratory, I was supported by the Washington University School of Medicine MSTP Training Grant (GM07200).

Jonathan Lake

Washington University in St. Louis

May 2015

ABSTRACT OF THE DISSERTATION

Guanine Nucleotide Synthesis and The Enteric Nervous System

by

Jonathan Ian Lake

Doctor of Philosophy in Biology & Biomedical Sciences

(Molecular Cell Biology)

Washington University in St. Louis, 2015

Professor Robert Heuckeroth, Chair

Professor David Ornitz, Co-Chair

There are currently no prevention strategies for Hirschsprung disease (HSCR), a potentially lethal birth defect caused by the failure of the enteric nervous system (ENS) to develop completely, resulting in an aganglionic segment of intestine. HSCR can result from one or a combination of partially-penetrant mutations in genes affecting the enteric neural crest-derived cells (ENCDCs) that colonize the intestine to form the ENS. While the genetics of HSCR and ENS development has been extensively studied, little is known about environmental risk factors for HSCR. To investigate maternal medication exposure as a possible HSCR risk factor, we conducted a chemical screen in zebrafish embryos for drugs that inhibit ENS development. Among several identified inhibitors of ENS development, we selected the antimetabolite immunosuppressant medication mycophenolic acid (MPA) and its prodrug mycophenolate mofetil (MMF) for further study. Here we demonstrate that maternal MPA or MMF exposure impairs ENS development in mice through MPA-mediated inhibition of inosine-5'-monophosphate dehydrogenase (IMPDH), which catalyzes the rate-limiting step of *de novo* guanosine monophosphate (GMP) synthesis. This inhibition results in reduced ENCDC proliferation that then impairs colonization of the intestine. We also show that MMF exposure is sufficient to cause permanent ENS defects and greatly enhances the penetrance and severity of aganglionosis in the *Sox10* and *Ret* mouse models of HSCR. Prompted by this interaction

between IMPDH inhibition and ENS development and by the proximity of an essential IMPDH gene, *IMPDH2*, to a mapped HSCR susceptibility region, we sequenced *IMPDH2* in a cohort of HSCR patients. We detected a single individual heterozygous for a nonsynonymous variant, P123R, and show that it produces an enzyme with slightly reduced activity. Furthermore, we deleted *Impdh2* in neural crest derivatives in mice, resulting in major developmental defects including drastically reduced ENCDC colonization of the intestine. However, heterozygosity for a null allele of *Impdh2* did not affect the penetrance of either *Sox10* or *Ret* mutations. These studies reinforce the importance of ENCDC proliferation to ENS development, demonstrate a dramatic gene-drug interaction, and provide the first evidence that maternal medications may increase HSCR risk.

Chapter 1: Introduction

Hirschsprung disease (HSCR), or congenital megacolon, is a birth defect affecting 1 in 5000 infants (1) in which a portion of the enteric nervous system (ENS) fails to form. HSCR is lethal if not surgically treated and is an oligogenic disease with incomplete penetrance and variable severity. The incomplete penetrance of HSCR mutations is generally attributed to either interactions between multiple mutations or to random developmental noise. While the human genetics of HSCR and developmental pathways of ENS development have been very heavily studied, the contribution of environmental factors to this birth defect's penetrance may be overlooked. Investigating the effect of environmental factors on ENS development could lead to prevention or mitigation strategies for HSCR. To date, little attention has been paid to the possible role of nongenetic factors on HSCR, though animal data and some limited human data suggests that the fetal microenvironment exerts an influence. Since medications represent a group of compounds that have known biological relevance, often have well-understood mechanisms, and are actively used by people, they are an ideal tool with which to screen for environmental exposures that influence phenotype.

The studies described here attempt to address this gap. In Chapter 2, I review the genetics and cell biology of ENS development and the pathological processes that occur in HSCR (2.3–2.10). I also discuss areas of ENS development and HSCR pathology where mechanisms remain unexplained or data appears contradictory (2.11). I then review the evidence from animal models and human studies that supports a role for gene-environment interactions in ENS development and HSCR (2.13).

In Chapter 3, I describe a chemical screen in developing zebrafish that I conducted together with other lab members and our detection of mycophenolic acid (MPA) as an inhibitor of ENS development. I then describe my subsequent investigation into the mechanism of MPA's effects on ENS development and demonstrate gene-drug interactions in mouse models of HSCR.

While the chemical screen was intended to detect compounds that affect ENS development, it also prompted us to examine the genes in target pathways, the most prominent being the genes encoding inosine 5' monophosphate dehydrogenase (IMPDH), the target of MPA. In Chapter 4, I examine the developmental role of one of the genes that encodes this enzyme, *Impdh2*, in the mouse ENS using conditional deletion within the neural crest. There, I demonstrate that *Impdh2* expression in the neural crest is essential for development of the craniofacial skeleton and for colonization of the bowel by ENS progenitors.

In Chapter 5, I investigate the possible relationship between genetic variation in the human *IMPDH2* gene and HSCR, since this gene is located in a chromosomal region associated with HSCR susceptibility. Sequencing of a cohort of HSCR patients revealed one rare IMPDH2 variant that reduces its enzymatic activity, but mouse experiments did not support an *Impdh2* interaction with HSCR model mutations.

Together, these studies demonstrate the requirement for a basic metabolic process, de novo guanine nucleotide synthesis, in ENS precursors, reinforce the critical role of proliferation in this developmental process, and demonstrate proof-of-principle gene-environment interactions in ENS development.

Chapter 2: Enteric Nervous System Development:

Migration, Differentiation, and Disease.

This chapter has been published as a review article by Jonathan I. Lake and Robert O. Heuckeroth in *American Journal of Physiology - Gastrointestinal and Liver Physiology* 2013, Volume 305, Issue 1, pp. G1-G24

2.1 Summary

The enteric nervous system (ENS) provides the intrinsic innervation of the bowel and is the most neurochemically diverse branch of the peripheral nervous system, consisting of two layers of ganglia and fibers encircling the entire gastrointestinal tract. The ENS is vital for life and is capable of autonomous regulation of motility and secretion. Developmental studies in model organisms and genetic studies of the most common congenital disease of the ENS, Hirschsprung Disease (HSCR) have provided a detailed understanding of ENS development. The ENS originates in the neural crest, mostly from the vagal levels of the neuraxis, which invades, proliferates, and migrates within the intestinal wall until the entire bowel is colonized with enteric neural crest-derived cells (ENCDCs.) After initial migration, the ENS develops further by responding to guidance factors and morphogens that pattern the bowel concentrically, differentiating into glia and neuronal subtypes, and wiring together to form a functional nervous system. Molecules controlling this process are required for ENS development in humans, including GDNF and its receptor RET, endothelin-3 and its receptor EDNRB, and transcription factors such as SOX10 and PHOX2B. Important areas of active investigation include

mechanisms that guide ENCDC migration, the role and signals downstream of EDNRB, and control of differentiation, neurochemical coding, and axonal targeting. Recent work also focuses on disease treatment by exploring the natural role of ENS stem cells and investigating potential therapeutic uses. Disease prevention may also be possible by modifying the fetal microenvironment to reduce the penetrance of HSCR-causing mutations.

2.2 Introduction

The gastrointestinal tract requires finely tuned control over muscular activity and fluid secretion to efficiently break down macroscopic food particles, efficiently extract nutrients, and maintain a healthy luminal microbiome. An important arbiter of these processes is the enteric nervous system (ENS), a network of neurons and glia within the wall of the bowel that controls most aspects of intestinal function. In humans, the ENS contains about 500 million neurons of more than 15 functional classes comprising a wide range of neurotransmitters, projection patterns, and electrical properties (71). When the ENS is missing (aganglionosis) or defective, children develop constipation, vomiting, abdominal pain, growth failure, and may die. Because ENS development and function are complex, the regulatory molecules that control ENS morphogenesis are also diverse. Disruption of one or more of these signals contributes to a spectrum of diseases. The ENS is derived from the neural crest (NC), a highly migratory and proliferative cell population originating at the junction of the neural plate and the adjacent ectoderm. NC cells invade the bowel and migrate through the mesenchyme in a process that is lengthy in both distance traveled and time required. Failure of enteric neural crest-derived cells (ENCDCs) to colonize the distal bowel causes Hirschsprung disease (HSCR), a common (1 in 5000 live births) and life-threatening developmental disorder. Because enteric neurons are

required to actively relax intestinal smooth muscle, aganglionic bowel is tonically contracted causing functional obstruction. HSCR is a non-Mendelian genetic disease with partial penetrance and variable expressivity. Several excellent reviews of HSCR genetics (2, 111) and ENS developmental biology (12, 40, 79, 81, 89, 90, 120, 140), have been published recently, but these fields are advancing rapidly. Here, we will review recent studies in the field in the context of existing models of ENS development and genetics and highlight areas that require additional investigation.

2.3 The time course of ENS development

ENS precursors originate in the vagal and sacral segments of the neural tube. The vagal NC is the major source of ENS precursors (217), while the sacral NC makes a small contribution to the distal bowel (28, 52) and anterior trunk NC makes a small contribution to the foregut ENS (57). Because vagal NC are most extensively studied and form the vast majority of the ENS, we will focus our discussion on vagal NC while highlighting a few important differences in sacral ENCDC biology. At embryonic day 9.5 (E9.5) in mouse (108) and prior to week 4 in human embryos (63), pre-enteric neural crest-derived cells (pre-ENCDCs) invade the foregut and begin their long rostrocaudal journey down the bowel. By E14 in mice and week 7 in humans (66), this linear migration is complete (Figure 2.1). In mice and humans, ENCDC also undergo inward radial migration after initially colonizing the bowel (103), forming the two layers of ganglia that comprise the myenteric and submucosal plexi (Figure 2.2). Unless otherwise indicated we will refer to mouse gestational ages. As the enteric neural crest-derived cells (ENCDCs) migrate, they proliferate extensively, and then differentiate into neurons and glia and condense into

ganglia to form a network throughout the bowel. Recent data also suggest that ENS stem cells are present in both fetal and adult mammals raising interest in the possibility of autologous stem cell therapy for treatment of Hirschsprung disease and other intestinal motility disorders (14, 138, 139). Formation of the ENS therefore requires extensive cell migration, controlled cell proliferation, regulated differentiation, directed neurite growth and the establishment of a network of interconnected neurons. Given these complex cellular events, each of which must be guided by specific molecular signals, it is not surprising that the genetics of ENS disease is complicated.

2.4 Human genetics of Hirschsprung Disease and associated syndromes

Most cases of HSCR are sporadic and occur as an isolated anomaly, but approximately 20% are familial and 30% have either cytogenetic abnormalities or additional developmental defects that constitute a recognizable clinical syndrome. Currently, at least ten distinct genetic syndromes are strongly associated with HSCR, and many other disorders affecting genes without a clear role in ENS development occasionally include HSCR. These are beautifully discussed in recent reviews (2, 111). There is also a strong male predominance (4:1 male/female ratio) in children with HSCR restricted to the rectum and sigmoid colon (i.e., short segment disease) and a weaker male predominance in children with long segment disease. Sibling recurrence rates for HSCR vary from 1% to 33% depending on the gender of the proband, the length of aganglionosis, and the gender of the new child. This is consistent with the hypothesis that affected females and those with longer aganglionic regions are likely to carry greater genetic liability than males with short segment HSCR. These complex genetic patterns are to be expected given the developmental pathways needed to form the ENS and the many molecules

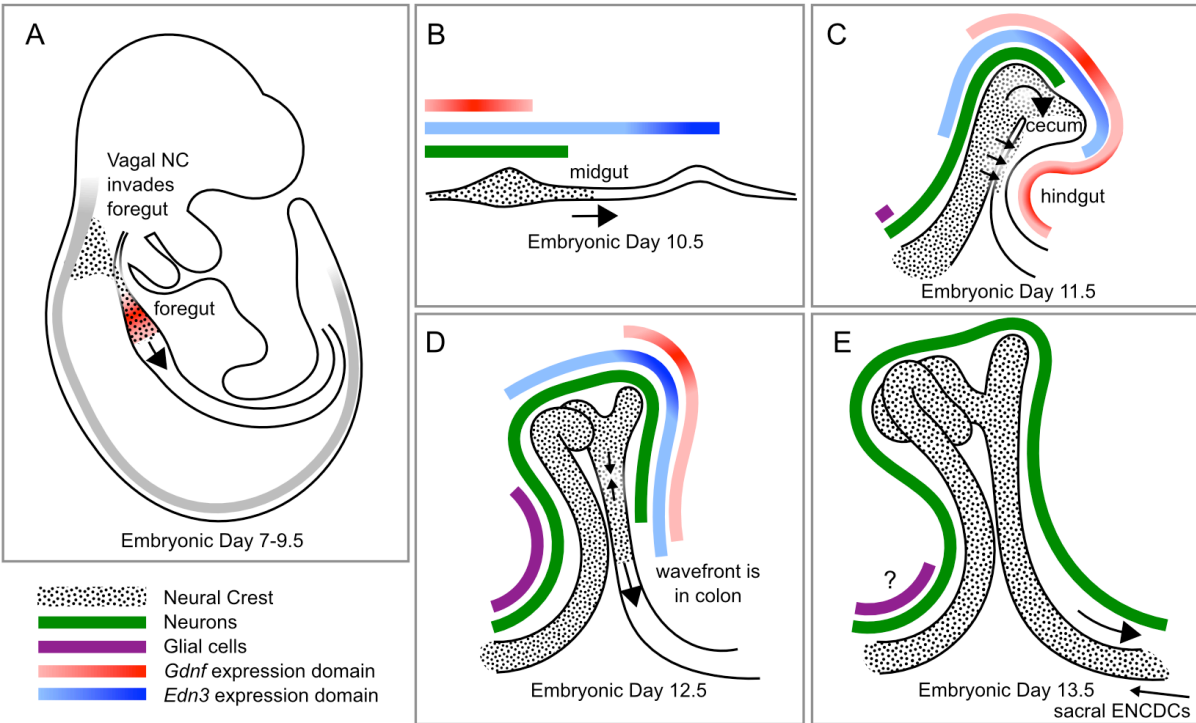


Figure 2.1: Initial Colonization of the Mouse Gastrointestinal Tract by Enteric Neural Crest-Derived Cells

During neural tube closure, neural crest cells (black) delaminate from the vagal region of the dorsal neural tube and migrate (arrows denote direction) in the ventral stream to the region adjacent to the foregut, which expresses glial cell line-derived neurotrophic factor (GDNF) (A). After these pre-ENCDCs invade the foregut, they migrate rostrocaudally, proliferate, and differentiate first into neurons (green) and later into glia (purple: earliest glial marker BFABP) (B, C, D, E). As this process proceeds, the bowel lengthens and changes shape, first from a straight line (B) to a single bend with midgut and hindgut closely apposed (C) followed by growth of the cecal appendage and further lengthening of the entire bowel (D, E). From E11-E12, ENCDCs invade the colon by crossing the mesentery and transiting the cecum (C). The cecal and trans-mesenteric populations then fuse to form the ENS in the rostral colon (D) and the trans-mesenteric population populates the terminal colon as the smaller sacral ENCDC population enters the bowel and migrates caudorostrally (E). Regions of peak *Gdnf* (red) and endothelin-3 (*Edn3*) (blue) production are shown (A,B,C,D, E). The peaks of *Gdnf* expression partially but imperfectly mirror the extent of ENCDC migration, while peak *Edn3* expression is centered at the cecum. A smaller domain of *Gdnf* expression in the antimesenteric side of the terminal colon may attract ENCDCs across the mesentery (C). Human ENS development proceeds through a similar process.

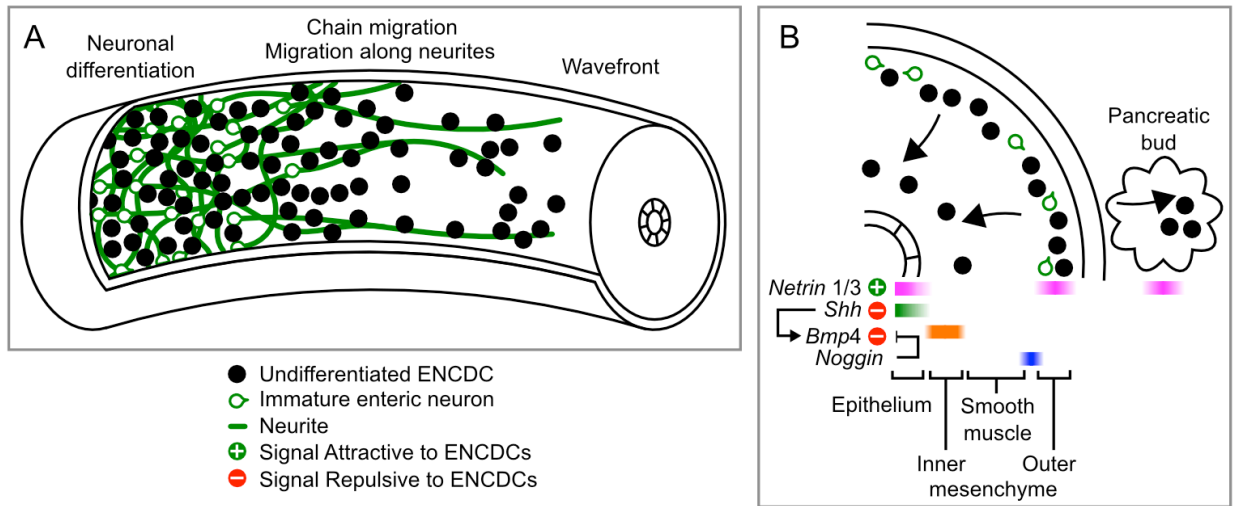


Figure 2.2: Primary and Secondary Migration of Mouse ENCDCs

While the wavefront of ENCDCs in the bowel moves steadily rostrocaudally, individual ENCDCs have complex and unpredictable behaviors. At and immediately behind the wavefront (**A, middle and right**), ENCDCs migrate in chains and are often closely associated with the caudally-projecting neurites of immature neurons, which extend up to the wavefront. ENCDC connections are transient, and cells often swap neighbors within a chain or detach to switch chains or divide. The onset of neuronal lineage differentiation occurs very close to the wavefront (**A, left**) and these cells retain some of their motility as they begin to extend neurites. In colonized regions in mice (**B, cross sectional illustration**) a secondary centripetal migration of ENCDCs is triggered by trophic factors and the morphogens that control the patterning of the bowel wall. Netrin 1 and Netrin 3 are attractive to ENCDCs and are expressed in the epithelium, outer mesenchyme, and pancreatic buds, triggering the secondary migration of ENCDCs toward these structures. This broad attractive signal is probably refined by repulsive signals from sonic hedgehog (SHH) in the epithelium and later bone morphogenetic protein 4 (BMP4) expression in the inner mesenchyme, which SHH induces. A layer of BMP antagonist *Noggin* expressing cells is located just inside the primary ENCDC migration layer, which may protect that region from the influence of BMP4. The precise timing of these signals in relation to each other and the secondary migration process has not yet been established. A similar secondary migration occurs in humans, but this process appears to proceed differently in birds.

that guide this development. Many mouse models with varying degrees of bowel aganglionosis, hypoganglionosis, and other defects have been isolated or engineered (Table 2.1), many of which are caused by disruption of orthologs of human HSCR genes.

2.5 Critical molecular mediators of ENS development:

The process of ENS development is controlled by cell surface receptors and their ligands, transcription factors that regulate their expression, morphogens, and proteins that transmit signals from the cell surface the cytoskeleton and the nucleus. Very brief summaries of these proteins are provided before discussing their role in cell biology and development.

2.6 The RET/GFR α 1/GDNF Pathway:

RET is a transmembrane tyrosine kinase receptor that is expressed in ENCCs as they migrate through the bowel. It is the signaling receptor for four ligands (glial cell line-derived neurotrophic factor (GDNF), neurturin, artemin and persephin) that activate RET by binding to the glycosylphosphatidylinositol linked GDNF family of Receptors (GFR α 1, GFR α 2, GFR α 3 and GFR α 4 respectively). RET signaling supports ENS precursor survival, proliferation, migration, differentiation, and neurite growth (80, 92, 95, 146, 192, 219). Heterozygous inactivating mutations in *RET* occur in about 15% of children with sporadic HSCR, and 50% of children with familial HSCR (2, 111). A common intronic enhancer polymorphism (RET+3 or rs2435357) is an important risk factor for HSCR that impairs *RET* expression (58). This polymorphism underlies many cases of HSCR because of its high prevalence in the population. In both mice and humans, total RET deficiency causes complete intestinal aganglionosis,

highlighting the central role of RET signaling in ENS development (175, 177). RET's coreceptor GFR α 1 and ligand GDNF are the critical RET activators during fetal development, and loss of *Gdnf* and *Gfral* causes nearly identical phenotypes to *Ret* in mutant mice. Indeed, these genes may be involved in rare cases of HSCR. Constitutively active mutations in *RET* cause the hereditary cancer syndromes multiple endocrine neoplasia type 2 (MEN2A and MEN2B) and familial medullary thyroid carcinoma (FMTC). MEN2A is genetically heterogeneous and paradoxically associated with HSCR despite mutations that constitutively activate *RET*. In contrast, MEN2B is almost always caused by the same M918T mutation and causes ganglioneuromas to form within the ENS, impairing bowel function.

2.7 EDNRB, ET-3 and ECE1:

Another signaling pathway, centered on endothelin receptor B (EDNRB) and its ligand endothelin-3 (ET-3) is required for ENS development in the colon. EDNRB is a G-protein coupled receptor expressed in neural crest derivatives including the developing ENS. Hypomorphic or null-mutations in *EDNRB*, *EDN3* (encoding the prepropeptide for ET-3), or the ligand-processing protease *ECE* can cause Hirschsprung disease, usually in the context of Waardenburg syndrome type 4 (WS4), a disorder that includes pigmentation defects, sensorineural deafness, dysmorphic facial features and aganglionic megacolon in humans. Spontaneous mutation of EDNRB has also occurred in domesticated mice, rats, and horses, producing a similar phenotype.

2.8 Transcription factors important for ENCDC colonization of the bowel:

Several transcription factors play critical roles in early ENS development. In part they are important because they influence the expression of *RET* (*SOX10*, *PAX3*, *PHOX2B*) (118, 119, 124, 154) or *EDNRB* (*SOX10*) (228), but this is clearly not their only role. While these transcription factors are critical for cells in multiple organ systems, we will concentrate on their roles in ENS development.

SOX10 is an SRY-related HMG-box transcription factor expressed in the neural tube prior to NC delamination, in migratory ENCDCs, and in mature enteric glia. In humans, heterozygous mutations in *SOX10* cause WS4 with a highly penetrant HSCR component (1, 10, 63). Experiments with homozygous *Sox10*-null mice revealed apoptotic cell death of neural crest cells prior to their entry to the foregut (109). Haploinsufficiency for *Sox10* appears to decrease the number of ENCDCs that initially colonize the bowel, eventually resulting in colonic aganglionosis. In addition to these requirements for survival, appropriate population size, and ENS gene transactivation, *SOX10* has a critical role in maintaining ENCDCs in an undifferentiated state. Overexpression and loss-of-function experiments in primary cell culture (19, 112) and in chick embryos (137) indicate that *SOX10* prevents precursors from differentiating into neurons.

PHOX2B is a homeodomain transcription factor expressed in the neural crest-derived autonomic nervous system, including the developing ENS and adult enteric neurons. *PHOX2B* is required for *Ret* expression in mouse pre-ENCDCs (154), and heterozygous *PHOX2B* polyalanine-expansion mutations cause congenital central hypoventilation syndrome (CCHS, central sleep apnea) in people, a syndrome that may include Hirschsprung disease (Haddad syndrome) (2, 11).

Other transcription factors implicated in ENS development include PAX3 and ZFHX1B. In humans, heterozygous *PAX3* mutations cause Waardenburg syndrome without HSCR (158), but PAX3 is required for development of the ENS in mouse (118). PAX3 also activates *Ret* transcription in concert with SOX10. *ZFHX1B* (*ZEB2/SIP1*) mutations cause HSCR in the context of Mowat-Wilson syndrome, which also includes microcephaly, mental retardation, and dysmorphic facial features (31, 204). In mice, ablation of *Zfhx1b* within the neural crest prevents ENCDC migration beyond the proximal duodenum (163). NKX2-1 and HOXB5 also physically associate with *RET*'s promoter and increase its expression (124, 227). Their necessity *in vivo* remains uncertain in the mouse, though mutations in both genes have been detected in the DNA of some HSCR patients (75, 131).

Several other transcription factors have been linked to the ENS in model systems, but have unexpected mutant phenotypes or an unknown relevance to human disease. ASCL1 (MASH1) and HAND2 (dHAND) are transcription factors required for the development of subsets of autonomic neurons. In *Ascl1*^{-/-} mice, ENCDCs colonize the bowel, but develop into a sparse and abnormal ganglionic network (15) and do not form serotonergic neurons (15) or esophageal neurons (85). Loss of *Hand2* (93) results in a complex phenotype involving a failure of multiple aspects of ENS development. Both *Ascl1* and *Hand2* will be discussed in the context of neuronal subtype specification.

2.9 Morphogens in ENS development

Organization of the ENS requires the establishment of two ganglion cell networks in precise locations within the bowel wall (Figure 2.2B). Neurons and glia cluster together into ganglia, and then neurons extend neurites that initially fasciculate before innervating targets.

Molecules controlling ENS morphogenesis are relatively poorly understood, but several classic morphogens are now known to have important roles in ENS development. Some specific trophic factors are also critical for subsets of enteric neurons, but their absence does not cause intestinal aganglionosis or malformed ganglia.

The hedgehog pathway is involved both indirectly and directly in the developing ENS. Hedgehog proteins have important roles as morphogens. For example, localized sonic hedgehog (SHH) expression is critical for defining anterior-posterior patterning of digits in the limb (10) and dorsoventral patterning in the spinal cord (50). Similarly in the bowel, localized expression of hedgehog proteins in epithelium is essential for concentric patterning of the bowel wall (165). The hedgehog ligands SHH and Indian hedgehog (IHH) are expressed by the gut epithelium during bowel development (13, 165, Figure 2.2B). However, loss of SHH or IHH have very different effects in mice, despite signaling through the same receptor and transduction machinery. Targeted mutation of *Shh* results in excessive numbers of enteric neurons and improper colonization of villi by enteric neuron cell bodies, whereas loss of *Ihh* causes dilated segments of bowel and aganglionosis in parts of the GI tract (165). Oddly, ectopic expression of the hedgehog pathway's transcriptional effector GLI in developing mice produced an effect similar to loss of *Ihh* (216). These disparate phenotypes in mice with hedgehog signaling pathway mutations are incompletely understood. It is possible that *Ihh* and *Shh* mutant phenotypes differ because of important temporal or spatial expression requirements for these proteins. Some of these phenotypes are consistent with known hedgehog effects on ENCCs since SHH promotes proliferation, inhibits neuronal differentiation, and prevents premature centripetal invasion of ENCCs into the future submucosa (64, 187).

A second role for hedgehog in the developing ENS is indirect. Hedgehog signaling induces bowel mesenchyme to secrete bone morphogenetic protein 4 (BMP4), another important modulator of ENS patterning. During initial ENCDC migration, BMP4 expression is induced in a ring of mesenchyme adjacent to the epithelium. Noggin, a BMP antagonist, is secreted by cells surrounding the BMP4 producing mesenchyme (82) and presumably reduces the effect of BMP4 on migratory ENCDCs (67). Interestingly, BMP effects on ENCDC migration differ between mouse and chick. In organotypic and explant cultures of embryonic mouse bowel, inhibiting BMP4 signaling with noggin enhances ENCDC migration (67), while chick embryos that overexpress noggin in the mesenchyme inhibit ENCDC migration (82). However, BMP4 clearly enhances neuronal aggregation in both organisms (38, 64, 82), and is probably important for the clustering of ENCDCs into definitive ganglia. BMP4 also induces the fasciculation of neurites in cell and organotypic culture systems. BMP effects on aggregation and fasciculation appear to be mediated through the addition of the polysaccharide polysialic acid (PSA) to neural cell adhesion molecule (NCAM) expressed by ENCDCs and enteric neurons (62, 67).

Netrins, diffusible ligands involved in central nervous system (CNS) and peripheral nervous system (PNS) patterning, are also involved in the radial migration of the ENS that occurs after initial colonization of the bowel. In mice, Netrins 1 and 3 are produced by the outer bowel mesenchyme in the presumptive myenteric region and by the intestinal mucosa and pancreatic buds (103), which are also invaded by ENCDC during this secondary migration (Figure 2.2B). Deleted in colon cancer (DCC), a netrin receptor, is expressed in migrating ENCDCs and is required for netrins to attract ENCDCs, since *Dcc*^{-/-} mice do not develop a submucosal plexus. Enteric neurons also produce netrins after they differentiate (167), attracting extrinsic fibers from the vagus nerve. Interestingly, laminin, an extracellular matrix molecule

that accumulates in the epithelial basal lamina and around enteric ganglia, converts the attractive effect of netrins on vagal axons to repulsion (166). It is unclear if this repulsion of fibers also applies to migrating ENCDCs, but if it does then such an effect could contribute to the cohesion of ganglia and the exclusion of ENCDCs from the epithelium.

Semaphorins are diffusible ligands involved primarily in axon growth cone repulsion. In the developing colon and cecum, *Sema3A* is expressed by the inner mesenchyme, while the coreceptor for *Sema3A*, neuropilin-1, is expressed in all ENCDCs (4). Despite its wide expression, *Sema3A* appears to specifically affect sacral ENCDCs and the extrinsic axons that they migrate upon. Normally, sacral ENCDCs are sequestered until embryonic day 13.5 within the pelvic ganglia that flank the end of the colon. They begin migrating up the colon, closely associated with extrinsic nerve fibers, just before the arrival of the vagal ENCDC wavefront (110, 209). In *Sema3A*^{-/-} embryos, sacral ENCDCs migrate into the colon early, demonstrating that *Sema3A* serves as a repulsive cue (4).

Retinoic acid (RA) is a diffusible morphogen produced locally in tissues by the retinaldehyde dehydrogenase (RALDH) enzymes. Mice lacking *Raldh2* die prior to ENS development, but viability can be prolonged by exogenous RA supplementation. These partially rescued embryos lack ENCDCs entirely (148), indicating a clear role for RA in ENS development. *In vitro*, Retinoic acid has dramatic effects on both ENCDCs and differentiating enteric neurons. For example, RA is required for the efficient migration of ENCDCs, and acts by reducing levels of phosphatase and tensin homolog (PTEN) protein, a critical negative regulator of ENCDC migration and proliferation that we will discuss below. RA also induces shorter neurites in enteric neurons, a response opposite to that of most other neurons (174). Because RA

is essential for normal ENS development, mouse embryos with impaired RA production due to deficiency in its dietary source, Vitamin A, also have defects in ENS development (65).

2.10 Intracellular signaling molecules in the developing ENS

The trophic factors and morphogens that control ENS development depend on complex intracellular signaling pathways for their action (Figure 2.3). This implicates a large number of additional proteins whose function in the ENS has not been directly tested, and whose expression patterns are not always restricted to the neural crest. For example, SHH, IHH, and GLI activity implicates important functions for the Patched (PTCH1 or PTCH2) receptor and for Smoothed (SMO). Similarly, BMP4 activity implies important roles for SMADs, and RA activity implies that at least some of the retinoid receptors and metabolizing enzymes (RAR α , RAR β , RAR γ , RXR α , RXR β , RXR γ , RALDH1, RALDH2, RALDH3, ADH, RDH, CYP26A, CYP26B, CYP26C, STRA6) will have essential functions that still need to be evaluated. This situation is not confined to morphogen pathways and also applies to signals downstream of critical ENS development genes. To illustrate the complexity of these signaling pathways, we will briefly review the intracellular consequences of RET signaling, some of which have been directly demonstrated in ENCDCs and others inferred from non-ENCDC RET-expressing tissues and studies in cell culture.

The *RET* gene produces two protein isoforms, RET9 and RET51, which differ in their intracellular domains and have some distinct signaling properties in different cell types. After stimulation by a GDNF-family ligand complexed with the appropriate GFR coreceptor, RET dimerizes and becomes autophosphorylated. Phosphorylated RET activates many intracellular signaling pathways including phosphatidylinositol 3-kinase (PI 3-kinase) (146, 182),

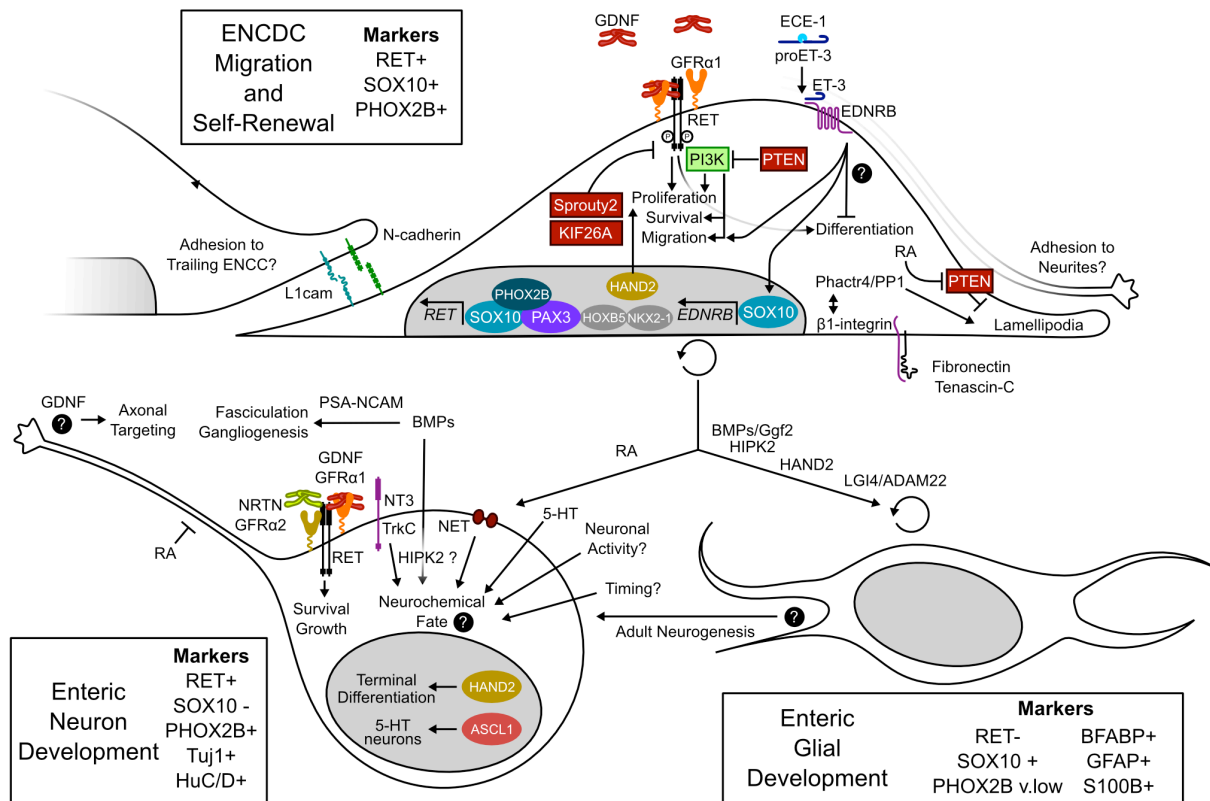


Figure 2.3: Molecules and Pathways Implicated in ENS Development

The roles of molecules and pathways discussed in this review are shown in the contexts of ENCDC migration (**top**), neuronal differentiation (**bottom left**), and glial differentiation (**bottom right**). Markers used to distinguish these developmental stages are listed outside the cells. Intracellular signaling molecules with important activating or inhibitory roles in RET signaling within ENCDCs are boxed (**red: inactivating, green: activating**). Transcription factors with known (color) or likely (gray) roles in ENS development are shown in nuclei. Important mechanisms that remain unresolved are highlighted with black question marks including the mechanism and targets of endothelin-3 (ET-3)/endothelin-receptor type B (EDNRB) signaling in ENCDCs, the conditions that specify each subtype of neuron, the factors other than GDNF that control axonal targeting and circuit formation, and the role of neurogenesis in adults. RA, retinoic acid; PSA-NCAM, polysialic acid-neural cell adhesion molecule; ECE1, endothelin-converting enzyme 1; PP1, protein phosphatase 1; PTEN, phosphatase and tensin homolog; ENCDC, enteric neural crest-derived cell.

extracellular-regulated mitogen-activated protein kinase (MAPK), c-Jun N-terminal kinase (JNK), p38 MAPK, phospholipase C γ (PLC- γ), and the small GTPase Rac (70). These pathways are activated by adapter complexes that bind to phosphorylated RET intracellular domains. c-SRC also binds directly to activated RET and contributes to PI 3-kinase activation (59, 60). Important docking tyrosines known to be required for ENS development include tyrosine 981, the docking site for SRC, and tyrosine 1015, which activates phospholipase C-gamma. Tyrosine 1062 of the RET9 isoform is especially critical for ENS development (102, 211), and serves as a docking site for adapter proteins SHC and GRB2, mediating activation of the MAPK and PI3K pathways. Negative regulators of RET are also required for normal ENS development and maturation. Mice lacking *Sprouty2*, a negative regulator of receptor tyrosine kinase signaling, have hyperganglionosis, esophageal dysmotility, and intestinal motility defects due to hypersensitivity of RET to GDNF signaling (189). Another recent study implicates KIF26A, an atypical kinesin, in the negative regulation of RET through the binding and inhibition of GRB2. Mice lacking *Kif26a* develop megacolon and hyperganglionosis, and appear to have defects in neurite growth despite an overactive GDNF/RET signaling system (226). Overactivation of RET also occurs in the context of MEN2A, which is occasionally co-incident with HSCR. This paradoxical situation demonstrates that the same mutation can have activating effects in one system (i.e., oncogenesis) and inactivating effects in another (ENS development). One possible mechanism for this is that some MEN2A mutations, which result in inappropriate intermolecular disulfide bond formation, activate RET via constitutive dimer formation but disrupt RET structure and prevent its efficient expression at the cell surface (188). Protein trafficking to the cell surface may be more efficient in some cells than in others, or perhaps the rapid rate of ENDCD division does not permit the accumulation of poorly trafficked but hyperactive protein.

Of the pathways activated downstream of RET, the PI 3-kinase pathway appears to be most critical for ENCC migration. Studies of ENCC migration in the presence of PI 3-Kinase inhibitors have demonstrated the importance of this pathway for migration towards GDNF (146). PI3-kinase phosphorylates phosphatidylinositol (4,5)-bisphosphate (PIP₂) to generate phosphatidylinositol (3,4,5)-triphosphate (PIP₃), which recruits the kinases PDK1 and AKT to the membrane. In addition to targets downstream of AKT, PIP₃ accumulation increases the local activity of the Rho GTPases RAC1 and CDC42 through their guanine nucleotide exchange factors, contributing to cell motility and neurite extension (83). This process also recruits the partitioning defective (PAR) complex of polarity proteins (PAR3/PAR6/PKC ζ), which influence axon specification and growth. PKC ζ , an atypical protein kinase C, is then activated by PIP₃ and PDK1 and may locally inhibit glycogen synthase kinase beta (GSK3 β), which must be disabled for definition and efficient growth of axons. In differentiating enteric neurons, inhibition of PKC ζ or GSK3 β increased the number of neurons developing multiple axons and decreased neurite growth (202). PKC ζ and GSK3 β inhibition also reduced ENCC invasion of the colon in organ culture assays, suggesting a role for polarity effectors in the migration of undifferentiated ENCCs or a role for neurite growth in the colonization process.

Molecules that inhibit the PI 3-kinase cascade are also involved in ENS development. PTEN is a tumor suppressor protein that reverses the reaction catalyzed by PI3-kinase, preventing activation of downstream effectors. In the ENS, PTEN serves as a “brake” on ENCC migration, proliferation, and growth. One recent study genetically ablated *Pten* within the mouse neural crest, which caused intestinal hyperganglionosis and megacolon. These animals also have overactivation of AKT and other downstream targets of the PI3-Kinase pathway within the ENS (162). Enteric neuron hyperplasia began at embryonic day 16, several days after the

colonization of the colon by ENCDCs. Another recent study complements these post-colonization findings, showing that PTEN levels must be reduced within migratory ENCDCs at the wavefront for efficient migration (65). Furthermore, in cultured cells responding chemotactically to GDNF, PTEN was polarized away from the leading edge of the cell and PTEN overexpression impaired ENCDC migration.

2.11 Progress in answering persistent questions in ENS developmental biology

Despite dramatic advances in our understanding of the molecular and cellular mechanisms of ENS development, many important questions remain only partially addressed.

2.11.1 Why do ENS precursors migrate through the bowel?

It has been difficult to identify a master mechanism that controls the migration of ENCDCs. Clearly, The GDNF-RET-GFR α 1 signaling pathway is critical for the migration of ENCDCs out of explants (146, 219) and for their directional migration through Boyden chamber membranes (65). GDNF is also mitogenic to ENCDCs and, at later stages of development, trophic for differentiating enteric neurons. The expression of RET in the vagal NC begins at or before E9, prior to the invasion of the foregut (57). At the same time, the foregut mesenchyme begins to express *Gdnf* mRNA, so the GDNF protein can attract pre-ENCDCs adjacent to the foregut (146). In addition, *Gdnf* expression along the gut mesenchyme appears to be spatiotemporally patterned. At E9.5, *Gdnf* mRNA is abundant in the stomach. By E10.5, *Gdnf* mRNA extends to the cecum and is most intense in this region. At both these time-points, the ENCDC wavefront is rostral to the *Gdnf* expression peak. However, the cecum sustains the highest level of *Gdnf* mRNA until ENCDCs complete their colonization of the terminal colon (146). This suggests a role for a gradient of GDNF in promoting ENCDC migration, at least up

to the point where ENCDCs pass through the cecum, after which GDNF chemoattraction cannot explain their continued migration since *Gdnf* mRNA levels are lower in more distal bowel. GDNF is clearly chemoattractive to ENCDCs in cell and organotypic culture (65, 146, 219), but the ability of endogenous GDNF to induce directed chemotaxis of ENCDCs within the bowel mesenchyme has been difficult to demonstrate *in vivo*. In addition to attracting pre-ENCDCs into the foregut, another place where long-range GDNF signals might have an important role is during the entry of the very first ENCDCs into the colon at E11 in mouse. A recent study has determined that most of these pioneer cells actually enter the colon by crossing the mesentery between the closely apposed midgut and hindgut (Figure 2.1C). Unlike the majority of ENCDCs, which migrate through the bowel wall, these cells exit the midgut and migrate across the mesentery as isolated cells. This study also showed that a thin band of antimesenteric colon mesenchyme expresses *Gdnf* mRNA at this time point and that the mesenteric crossing process requires GFR α 1, suggesting that a long-range gradient of GDNF attracts these ENCDCs into the colon. By combining organ culture and a mouse line expressing a photoconvertible fluorescent protein in ENCDCs, the authors were able to mark these cells and demonstrate that the ENS in the distal colon is derived almost entirely from ENCDCs that cross the mesentery.

A model that explains many aspects of vagal ENCDC migration within the bowel mesenchyme (170, 193) is based on the observation that neural crest cells only migrate efficiently through the bowel when at high densities and proliferating. According to this model, migration need not be directed toward a particular attractive signal at the end of the bowel. Instead, the only mechanisms required to produce a directionally migrating wavefront of cells are a proliferating cell population, a limited “carrying capacity” of the local microenvironment, and random motility of ENCDCs. Proliferation in one region proceeds until a limiting cell density is

reached, and then stops. The translocation of the wavefront proceeds mostly by the proliferation and random movement of cells at the wavefront (181). Thus, migration of individual cells need not be directional for a moving wavefront to develop (180).

There is ample evidence to support this model. The first experiments demonstrating a neural crest origin for the enteric ganglia showed that removing the vagal neural crest abolished ganglia throughout the digestive tract, and that partial ablation produced partial aganglionosis, always in the distal region of the bowel (217). Indeed, mechanically reducing the numbers of ENCDCs in bowel explants reduces the population's migration speed (218) and reduces their invasion of the colon (53). ENCDC proliferation is also required for wavefront advance (181). In addition, there is strong evidence that ENCDC migration is not intrinsically unidirectional through the bowel, since ENCDCs grafted at the caudal ends of aneural bowel can migrate caudorostrally (181, 220), and vagal neural tube grafted into the sacral level of the neuraxis of chick embryos results in ENCDCs that efficiently migrate caudorostrally through the bowel (27). Finally, it is likely that the bowel microenvironment has a limited carrying capacity for ENCDCs. Even in the absence of any other limiting factors, availability of GDNF limits the proliferation of ENCDCs above a maximal density (80, 208).

The proliferation dependent model cannot explain all aspects of ENCDC colonization. According to simulations based on this model, purely random diffusion would be sufficient to create a migrating wavefront (180), but observations of migrating ENCDCs demonstrate complex and nonrandom patterns of movement (Figure 2.2A). ENCDCs migrate in contact with one another in structures that, near the wavefront, resemble caudally projecting "chains" of cells. Time-lapse imaging of fluorescent ENCDCs in organ culture reveals that the ENCDCs in these chains climb upon each other and have unpredictable trajectories (218). ENCDCs can detach

from chains, sometimes forming new chains, or can advance along an existing chain (54).. However, the overall structure of the chains and the spaces between them are persistent over time despite the dynamic behavior of each ENCDC. These complex behaviors strongly suggest additional signals governing ENCDC guidance that remain to be discovered. Furthermore, early neuronal differentiation begins almost immediately behind the wavefront, and neurites grow along chains of ENCDC. The nascent neuronal cell bodies also migrate along these neurites, which generally project rostrocaudally (86, 220). At the wavefront itself, migration trajectories of ENCDCs are also predominantly caudal (151, 218), suggesting that wavefront ENCDCs migrate toward a local cue. It is possible that the ENCDC population generates a gradient of GDNF by consuming or competing for GDNF. Endocytosis or simply receptor binding of GDNF by ENCDCs may deplete most of the available GDNF behind the wavefront, creating a local gradient that travels with the wavefront.

Another phenomenon that might contribute to the directed migration of wavefront cells is contact inhibition of locomotion. Recent experiments in *Xenopus* neural crest demonstrated that directional migration of neural crest cells is inhibited by contact with other neural crest cells, but not with other cell types (32). Furthermore, the authors found that non-canonical Wnt signaling (planar cell polarity) at cell-cell contacts mediates this repulsion. Disrupting this pathway inhibits directional migration (34). This pathway, in turn, is dependent on the function of primary cilia on neural crest cells and is disturbed in Bardet-Beidel Syndrome (BBS), an HSCR-associated condition caused by ciliary gene dysfunction (168). The caudally-directed migration of individual ENCDCs at the wavefront could be driven by such a mechanism. Some aspects of colonization might be explained by this behavior, such as the failure of vagal ENCDCs to

colonize already colonized bowel, but others such as chain migration seem incompatible with this mechanism.

The proliferation dependent and contact-mediated repulsion models of migration may explain some otherwise perplexing non-cell-autonomous effects of ENS gene mutations. Mouse chimera and grafting experiments have shown that mixing migration-capable neural crest cells with a sufficient number of neural crest cells with genetic lesions in *Ret* (16), *Ednrb* (107), or *Sox10* (106) impairs migration of wild-type ENCDC enough to cause distal aganglionosis in chimeric embryos and grafted bowel tissue. Wild-type ENCDC were also able to rescue the migration of *Ednrb* null mutant ENCDCs in some chimeric embryos. Since RET, EDNRB and SOX10 are primarily expressed within ENCDCs, the observed non-cell-autonomous effects exerted on neighboring normal ENCDCs are surprising. These results are consistent with a proliferation dependent model of migration, which predicts that if some part of the migratory population is defective for proliferation or survival, as is the case in these models, incompetent cells at the leading edge of the wavefront can inhibit the progress of the cells in the more proximal bowel by reducing the size of the proliferating cell population and blocking progress forward. Similarly, the ability of normal ENCDCs to rescue the migration of mutant ENCDCs may be rooted in an increased overall population size or proliferative capacity. However, it may also occur because wild type cells actively invade aganglionic bowel forming a substrate for mutant cells to migrate on via chain migration or migration along neurites.

Several processes occur simultaneously during colonization of the bowel, including some that fit a proliferation model (wavefront movement), some that appear more chemotactic (movement of individual cells at the wavefront), and some related to cell or matrix adhesion (fiber-climbing and chain-migration). Determining experimentally which of these processes are

critical for colonization has been difficult, largely because mechanisms responsible for directed migration, proliferation, and neurite growth share many molecules and pathways, making any experimental separation difficult. Despite this difficulty, roles for several molecules involved in neuronal polarity and cell motility have been demonstrated. As discussed previously, inhibiting the neuronal polarity effectors GSK3 β and PKC ζ impairs ENCDC migration (202). Also, chemical inhibition of the RAC and CDC42 GTPases or the RHO effectors ROCKI/II in the cecum and colon reduced both migration and neurite growth without affecting proliferation (185). In another study, genetic ablation of *Rac1* and *Cdc42* in the early neural crest impaired neural crest cell proliferation and thereby prevented colonization of the distal bowel by ENCDCs, but did not cause migration defects in early NC cells emigrating from the neural tube (69). While both studies implicate Rho-family GTPases in ENS development, they suggest different roles of these molecules in different stages of neural crest development.

Finally, we should not neglect the critical role of the extracellular matrix (ECM) and the ENCDC proteins that interact with the ECM during bowel colonization. The ECM provides both a mechanical substrate and important signals for ENCDC migration and differentiation. During the process of ENCDC migration, the bowel mesenchyme matures from a uniform-appearing population of mesenchymal cells into layers with distinct morphologies and ECM molecule expression patterns (147). Maturation occurs in a bidirectional wave from rostral and caudal ends of the bowel, and occurs more quickly than ENCDC colonization, so the ECM in contact with ENCDCs is constantly changing. Laminin influences axon guidance, as noted previously, and also enhances neuronal differentiation (43) Since newly differentiated neurons migrate more slowly than undifferentiated ENCDCs (86), the high levels of laminin in the colon may contribute to distal bowel aganglionosis.

Important roles have also been assigned to several ECM-interacting molecules. β 1 integrin (*Itgb1*) is important for ENCDC migration, and its loss from ENCDCs results in colonic aganglionosis and structural abnormalities of the ENS (24). Integrins are cell surface receptors for ECM molecules that participate in both adhesion and signaling. β 1 integrins are necessary for optimal ENCDC migration on fibronectin, which is present throughout the bowel and is enriched in the hindgut. β 1 integrin is especially critical for migration on the ECM molecule tenascin-C, which is expressed at high levels in the hindgut and otherwise inhibits ENCDC migration (21). β 1 integrin is also important for transducing signals from the ECM, and dysregulation of these signals impairs ENS development. PHACTR4, a protein recently shown to be required for directed ENCDC migration, interacts with the actin cytoskeleton and protein phosphatase 1 (PP1). PHACTR4, through its interaction with PP1, modulates β 1 integrin signaling and activates the actin-severing protein cofilin, contributing to the formation of directionally stable lamellipodia (225). This manifests as hypoganglionosis in *Phactr4*^{humdy/humdy} mutant mice, which lack interaction between PHACTR4 and PP1. During development, these embryos have less directed ENCDC migration at the wavefront, despite having a normal random migration velocity.

Adhesion between an individual ENCDC and other ENCDCs is also important for migration. The homophilic adhesion molecules N-cadherin, NCAM, and L1CAM are expressed by migrating ENCDCs, and loss of either N-cadherin or L1CAM results in delayed ENCDC migration and potentiates aganglionosis (5, 24, 206), though neither is sufficient to cause aganglionosis by themselves. Finally, as previously discussed in the context of BMP signaling, the posttranslational addition of polysialic acid to NCAM influences ENCDC aggregation and migration efficiency (62, 67).

Migration and proliferation differ significantly between ENCDCs derived from the vagal and sacral neural crest. Sacral crest-derived ENCDCs migrate in isolation rather than in chains (209), always moving along extrinsic neuronal fibers that project into the hindgut. Although sacral ENCDCs arrive in the terminal hindgut at the same time as vagal ENCDCs, they continue to migrate caudorostrally through vagal crest-colonized bowel. In contrast, vagal ENCDCs will not enter previously colonized bowel (97). The proliferative capacity of sacral ENCDCs is also very different from vagal ENCDCs. While sacral ENCDCs normally comprise about 10-20% of the most distal region of the ENS (28, 209), their population only slightly expands if the vagal neural crest is mechanically ablated in chick embryos (26) and the hindgut is otherwise devoid of ENCDCs. Vagal-to-sacral transplantation experiments in the chick (27) have demonstrated at least some of these differences in behavior reflect intrinsic differences between sacral and vagal neural crest rather than different signals along the migration routes. While vagal and sacral ENCDCs express the same ENCDC-specific markers (3, 49), an RNA microarray comparing vagal and sacral chick neural tube explants (49) indicated that sacral-derived crest expressed less RET mRNA than vagal crest, and their behavior was partially transformed to that of vagal crest by RET overexpression. A study in mice where the vagal wavefront was significantly delayed (neural-crest specific *Ednrb* deletion) confirmed the finding that RET expression was reduced in sacral ENCDCs (61). Notably, In the *Ret*^{-/-} and *Gfra1*^{-/-} mouse models of total intestinal aganglionosis (57, 30) and a conditional *Ednrb* ablation model of colonic aganglionosis (61), rare intrinsic neurons can be found within the most distal bowel. These almost certainly represent the remnants of the sacral ENCDC population. Since these neurons are rare and their numbers approach neither the expected sacral-derived densities observed in the chick nor those estimated in mouse organ culture experiments (28, 209), it seems likely that mutations affecting vagal

ENCDCs also affect sacral ENCDCs, which likely accounts for their absence in the terminal colon of HSCR patients. To our knowledge, it is not known whether the aganglionic segment of HSCR-affected terminal colon contains any residual neurons, but they would likely be difficult to detect using routine diagnostic histology and would not form a functional ENS.

2.11.2 What is the function of EDNRB in ENS development?

Although EDNRB/EDN3 signaling is essential for efficient colonization of the colon and clearly influences ENCDC differentiation and migration, many of the cellular and molecular effects of EDNRB/EDN3 signaling on the developing ENS remain confusing. Total loss of EDNRB signaling results in colonic aganglionosis, abnormalities of the ENS in the small bowel (33), and a developmental delay in ENCDC migration (55). This is a much milder phenotype than is associated with a loss of RET signaling. There are two primary processes that EDNRB affects within ENCDCs: it prevents premature neuronal differentiation and it is required for efficient migration within the colon. Here we will summarize the well-established actions of EDNRB and discuss some apparently contradictory observations demonstrating species specific, region specific, and cell-type specific roles for EDNRB in the ENS.

In culture, there is significant evidence that the EDNRB ligand ET-3 maintains ENCDCs in an undifferentiated state (19, 92, 213). ET-3 alone does not appear to cause proliferation, but ET-3 treatment causes overpopulation of the developing ENS in avian gut explants (143) and acts together with GDNF to increase the proliferation of undifferentiated mouse ENCDCs (8). ET-3 administration to cultured enteric progenitors maintains their expression of SOX10 and their undifferentiated state (19), suggesting that EDNRB signaling might be required to prevent premature loss of SOX10 protein. These observations are consistent with a role for ET-3/EDNRB signaling in repressing neuronal differentiation that might otherwise be triggered by

the high GDNF levels in the cecum and rising laminin levels in the colon (55). Since neurons are post-mitotic, enhanced neuronal differentiation will reduce the proliferative drive that supports bowel colonization by ENCDCs. The similarity of the phenotypes that result from *EDNRB* or *SOX10* mutations (colonic aganglionosis) and their genetic interaction when mutated (discussed below) further suggests that *EDNRB* and *SOX10* are components of a common pathway that keeps ENCDCs undifferentiated. In mouse ENCDCs, *Ednrb* expression is directly regulated by *SOX10* binding to promoter elements upstream of *Ednrb* (228), possibly forming a positive feedback loop contingent on ET-3 signaling.

It is unclear whether increased neuronal differentiation occurs *in vivo* when *EDNRB* signaling is defective. The best evidence, from homozygous null *Edn3* mouse embryos, showed an increase in the percentage of wavefront ENCDCs positive for neuron-specific β III tubulin, indicating an increase in early neuronal differentiation (19). However, in a recent study that used a conditional allele of *Ednrb* allowing specific ablation from the neural crest, the wavefront did not display an increased proportion of ENCDCs positive for the neuronal marker Hu (55). In another study of *Ednrb*-null rat embryos, the wavefront also failed to display an increase in peripherin positive cells (116). This same study showed that rat enteric neural crest stem cells (NCSCs), a defined subpopulation of crest-derived cells in the gut, respond to ET-3 in culture by differentiating into myofibroblast-like cells. It is unclear whether differences between cell types, the mutation status of *Edn3* or *Ednrb*, the neuronal markers chosen, or the species studied account for these differing results suggesting the need for additional investigation of the role of *EDNRB* signaling in the ENS.

Despite the fact that ENCDCs lacking *Ednrb* have a migratory delay throughout ENS development, ENCDCs have a specific requirement for *EDNRB* signaling as they migrate

through the colon. In grafting experiments performed in organotypic culture, neural crest cells from normal bowel colonized normal embryonic colon, but did not invade embryonic colon from mice with *Edn3* mutations (101). *Edn3* mRNA appears to be expressed in a spatially and temporally regulated manner that tracks the migration of ENCDCs, and EDNRB signaling is required during a very narrow temporal window roughly corresponding to colonic migration. At E10, *Edn3* mRNA is expressed throughout the midgut, but levels become elevated in the cecum at E10.5 and this domain of expression extends into the hindgut at E11, when ENCDCs are migrating through the cecum (8). This is identical to the temporal interval when EDNRB signaling is required for ENS development (E10.5 to E12.5) as shown using a tetracycline-regulated *Ednrb* knock-in mouse (178). Like the effects on differentiation, some of the effects of ET-3/EDNRB signaling on migration are also contradictory and difficult to interpret. One issue is that ET-3 appears to have divergent effects on ENCDC migration under different conditions. ET-3 impairs GDNF's chemoattractive effects on ENCDCs in explants cultured in collagen gels (8, 116, 143), but appears to encourage migration through the colon in explant cultures (143), and to partially rescue colon colonization when RET signaling is dysfunctional (203). EDNRB antagonists also cause colonic hypoganglionosis or aganglionosis in culture (143, 212), and acute chemical inhibition of EDNRB in colonic ENCDCs produces immediate retraction of cell processes and loss of motility that occurs too quickly to result from effects on differentiation (55). In addition to its expression in ENCDCs, EDNRB is expressed to some degree in the mesenchyme (8) of mouse bowel. This observation, combined with the finding that laminin- α expression by enteric smooth muscle cells is negatively regulated by ET-3 (213) suggested that EDNRB signaling in the mesenchyme might be necessary to create a colonic microenvironment permissive to ENCDC colonization. However, mesenchymal expression of EDNRB is not

conserved in the chick (143, 144). Furthermore, neural-crest specific ablation of *Ednrb* produces the same ENS phenotype as a null allele (56) and colonic aganglionosis in rats lacking *Ednrb* can be rescued with a transgene that expresses functional EDNRB specifically in ENCDCs (78), indicating that neural crest cells are the critical targets of the ET-3 signaling required for ENS development.

The importance of each second messenger pathway activated downstream of EDNRB is also unclear. One disease-causing mutation in *EDNRB* has been linked to a selective loss of $G_{\alpha q}/G_{\alpha 11}$ coupling and intracellular Ca^{2+} signaling (100, 161) while two others have been shown to perturb $G_{\alpha i}$ coupling and prevent the reduction in cyclic-AMP levels that occurs with $G_{\alpha i}$ activation (68). Of these possibilities, there is more evidence for EDNRB signaling through cyclic-AMP in ENCDCs. Indeed, neural crest-restricted deletion of $G_{\alpha q}/G_{\alpha 11}$ did not result in any ENS defects (51). In primary enteric progenitor cell culture, the anti-differentiation actions of ET-3 were mimicked by inhibition of the cAMP-regulated protein kinase A (PKA), and suppressed by increasing cyclic-AMP (8). In the same study, a protein kinase C inhibitor did not appear to inhibit the effects of EDNRB stimulation, which would be likely if some of the actions of EDNRB were mediated through $G_{\alpha q}/G_{\alpha 11}$. Interestingly, cAMP-dependent and cAMP-independent activation of PKA downstream of BMP signaling have important roles controlling differentiation of another neural-crest derived population, noradrenergic sympathetic neurons (129). However, inhibiting PKA activity is probably not uniformly beneficial to the developing ENS. PKA has been shown to phosphorylate RET at a serine residue (70) important for lamellipodia formation in culture. Targeted mutation of this site to prevent phosphorylation results in distal colonic aganglionosis and ENCDC migration defects (6). Moreover, the same study demonstrated that PKA inhibition reduced ENCDC migration in the colon. This

requirement of PKA activity for migration is difficult to reconcile with the evidence for inhibition of cAMP signaling required to maintain ENCDCs in an undifferentiated state. Intermediate levels of PKA activation or fine temporal or spatial control of cAMP or PKA may be required for normal ENS development. Further study of the ET-3/EDNRB signaling pathway in ENCDCs is necessary to better understand these important molecules.

2.11.3 What controls neuronal versus glial differentiation of ENS precursors and what controls neuronal subtype specification?

Although appropriate differentiation into the many neuronal classes and into glia and is absolutely critical for ENS function, the signals that control these cell fate decisions are less well understood than the process of initial ENS colonization by the multipotent ENCDCs.

ENCDC, neuron, or glial cell?

Presumably, an ENCDC must decide whether to self-renew or differentiate into a neuronal or a glial progenitor. While SOX10 has a central role in maintaining ENCDCs (19, 112), it is not sufficient for maintaining an undifferentiated state, since both ENCDCs and adult enteric glia express SOX10. Notch signaling is implicated in gliogenesis in other areas of the PNS, but appears to have a different role in the ENS. Mice with neural crest incapable of receiving Notch signals develop a hypocellular ENS as newborns, accompanied by reduced Sox10 expression in migrating ENCDCs and inappropriately high level of neuronal differentiation in the population of migrating ENCDCs. Thus, in the developing ENS, Notch is required to prevent premature neuronal differentiation and depletion of undifferentiated ENCDCs. One signal recently demonstrated to be important for enteric glial development is the secreted factor LGI4, which is produced by migrating ENCDCs in the bowel and glia themselves. Mutations in *Lgi4* or its receptor *ADAM22* reduce the number of enteric glia and

alter ENS structure (150). BMP signaling may be involved in specifying enteric glia, since it induces glial differentiation of ENCDCs *in vitro* and these developing glia become dependent on glial growth factor 2 (Ggf2, a NRG1 isoform) signaling through ErbB3 for survival (39). RA signaling also increases neuronal differentiation and the proliferation of cells with early neuronal markers, but not at the expense of glia (174).

Neurogenesis in the ENS is asynchronous

Cells expressing early neuronal markers (Tubb3/Tuj1 and HuC/HuD) and bearing long processes appear in the ENS almost immediately after colonization begins (86, 221). A core population remains as undifferentiated ENCDCs and are presumably responsible for propagating the ENCDC wavefront down the bowel. Other cells express pan-neuronal markers and extend neurites but remain in the cell cycle and continue to migrate. Still others exit the cell cycle during specific intervals (a neuron's "birth date"), and differentiate into diverse enteric neuron subtypes. Neuronal birth dating is a technique that exploits labels such as BrdU or tritiated thymidine that are permanently integrated into the DNA of replicating cells. The label is administered at one selected time point and development is allowed to continue. Neuronal precursors that incorporate the label and then become postmitotic retain high levels of the label, while cells that continue to divide dilute the label to undetectable levels. Thus, this technique marks cells preparing for their final division. In the mouse, serotonergic neurons are born earliest (embryonic days 9-15), and birth of cholinergic neurons peaks at E14 and continues until E17. Birth dates for dopaminergic, peptidergic, nitrergic, and GABA-ergic neurons peak at E14 in the myenteric plexus and close to P0 in the submucosal plexus, extending into postnatal life for up to two weeks after birth (41, 156). While the expression of a neurochemical phenotype occurs some time after a given neuron's birth, the tight association between the time of cell cycle exit and neurochemical

phenotypes suggests that the timing of cell cycle exit may control some aspect of neurochemical fate. Alternatively, an upstream mechanism that remains unknown may determine both birth date and ultimate fate.

Signals and genes affecting neuronal subtypes

There are relatively few genetic models that lack subsets of enteric neurons. This is likely due to the difficulty of identifying subtle ENS phenotypes, which may not lead to life threatening bowel dysfunction. A prominent exception is serotonin (5-hydroxytryptamine, 5-HT) producing neurons that are absolutely dependent on the transcription factor ASCL1. Serotonergic and, to a lesser extent, calretinin-expressing neurons also require the norepinephrine transporter (NET, *Slc6a2*) to develop in proper numbers (125). Another transcription factor required for terminal differentiation of enteric neurons is HAND2, a basic helix-loop-helix transcription factor needed for heart and neural crest development. *Hand2* is not required for ENCDC migration down the bowel, but its deletion results in profound defects in overall ENS structure (93), reductions in neuronal density (93, 48), severe bowel distension likely caused by ENS defects (123) and either subtype-selective (93, 123) or a more general failure (48) to differentiate into functional neurons. Overexpression studies demonstrate that HAND2 is sufficient to both support neurogenesis (93) and specify vasoactive intestinal peptide (VIP) expression in cultured chick ENCDCs, while early neural crest-specific deletion of mouse *Hand2* results in a loss of VIP-expressing neurons (93). In a mouse model where *Hand2* is deleted in a specific subset of ENCDCs, (123) precursor proliferation, gliogenesis, and the specification of many (cholinergic, nitrergic, and calretinin-expressing) but not all neuronal subtypes were impaired within the population derived from *Hand2* deleted ENCDCs, Reductions in numbers of specific neuronal subtypes (nitrergic and calretinin-expressing but not substance P-expressing) also result from haploinsufficiency for and

hypomorphic alleles of *Hand2* (47). Since *Hand2* is expressed and experimentally deleted in both undifferentiated ENCDCs and differentiating neurons and glia, the precise stage where loss of *Hand2* alters neuronal subtype specification or gliogenesis is not yet known.

Another signal critical for specific cell populations in the ENS is neurotrophin-3 (NT-3), which signals through the p75 neurotrophin receptor and the TrkC receptor. Mice lacking NT-3 or TrkC had significantly fewer neurons throughout the ENS, with a particular deficit in the submucosal plexus (42). Calcitonin gene-related peptide (CGRP) reactive submucosal neurons are most sensitive to loss of NT-3/TrkC signaling. However, this signaling pathway does not appear to uniquely identify a single type of neuron. BMP2 and BMP4 signaling also influence neuronal subtype and enhance the development of this TrkC⁺ population (38, 41). When the BMP inhibitor Noggin was expressed ectopically in all enteric neurons *in vivo*, the overall neuronal density in the ENS increased markedly, but the number and proportion of TrkC⁺ neurons was reduced. Conversely, a transgene expressing BMP4 increased the proportion of TrkC⁺ neurons in the adult ENS. These studies implicate BMP signaling in both specification of a particular neuronal subtype (TrkC⁺) and limiting the numbers of other neurons (TrkC⁻). In particular, the density and proportion of early-born classes of neuron were increased and of late-born classes were decreased when BMP signaling was inhibited by the Noggin transgene (41). In accordance with the effects of BMPs on glial differentiation in culture, the same Noggin transgene also reduced the density and proportion of glia in the ENS (39).

Early neuronal activity shapes late-differentiating neurons

Since enteric neurons are “born” asynchronously, the activity of early-born neurons has the potential to shape developmental decisions in later-born neuronal populations. Serotonin producing neurons are one of the earliest-born populations in the ENS (156) and the 5-HT

produced by these cells has a significant effect on the development of later-born neuronal populations (126). ENCDCs express many classes of serotonin receptors and 5-HT promotes the neuronal differentiation of ENCDCs in culture. Mice with enteric neurons unable to synthesize 5-HT develop fewer neurons of several late-born classes including dopaminergic, GABA-ergic, and a subset of nitrergic neurons. Serotonergic neurons, in turn, require the norepinephrine transporter for proper development, which suggests that norepinephrine uptake may shape neuronal differentiation. Recent work has also demonstrated that nascent enteric neurons are electrically active very early in the colonization process (87), and that inhibition of this activity reduces the number of early-born nitrergic neurons close to the ENCDC wavefront (88), suggesting that the interdependence of different types of enteric neuron is not limited to the late-born populations. Finally, neuronal activity may be important for ENCDC colonization of the bowel, since Tetanus and Botulinum neurotoxins slow neurite extension and ENCDC migration (201).

Lineage restriction and decision points

There are a few known progenitor states that mark major decision points in the enteric neuron generation program. One important mark of lineage restriction is the transiently catecholaminergic (TC) class of immature enteric neuron. Neurons expressing catecholaminergic markers are common early in the colonization process, but definitive catecholaminergic neurons represent a small fraction of the mature ENS. The early, transiently catecholaminergic (TC) lineage encompasses many terminal fates, but it includes all future serotonergic neurons (7) and excludes certain fates, including late-born CGRP-producing neurons (15). TC status is clearly a marker of an important decision-making step, but the factors controlling this decision remain unknown, though *Ascl1* may contribute since it is required for development of the TC lineage

(15). Also, since TC cells produce norepinephrine and both TC-cells and the TC-derived lineage express the norepinephrine transporter, the TC-lineage may influence its own developmental fate by signaling through norepinephrine.

2.11.4 What controls neurite outgrowth and axon pathfinding in the ENS?

The ENS is controlled by the organized connections between neurons of different types in different regions. In the CNS and other regions of the PNS, target-derived trophic factors ensure that specific neuronal subtypes are matched qualitatively and quantitatively to their targets. This system works well because axon tips and neuronal cell bodies are usually distant from each other and in quite distinct environments. In contrast, ENS neurons often have a similar environment at the axon tip and cell body (e.g. for cells whose soma and neurites remain within the myenteric plexus) making it difficult to imagine how target derived trophic factors might direct the proper wiring of the adult ENS. While distribution of neuronal classes clearly differs between different areas of the ENS, each ganglion is indistinguishable from its immediate oral or aboral neighbor. Few conditions leading to defects in targeting of neuronal projections have been demonstrated in the ENS at least in part because there has until recently been no simple way to track neurites of single enteric neurons. One study has demonstrated that the targeting of projections from myenteric nitrergic neurons is controlled by GDNF during perinatal and postnatal development. When GDNF was ectopically expressed in enteric glia using the glial fibrillary acid protein (GFAP) promoter, NADPH diaphorase positive (a marker of nitric oxide synthase) fibers redistributed densely around enteric glia, suggesting a role for GDNF in axon targeting for this subtype of enteric neuron (208). In contrast, neither cholinergic nor serotonergic neuron fibers redistributed toward enteric glia in these GDNF overexpressing mice. A recent study used ligand regulated Cre recombinase and a fluorescent recombination reporter

to label single enteric neurons in fetal bowel (173). Using this system, they were able to detect very subtle structural ENS defects and demonstrated that enteric neurons require the planar cell polarity signaling components *Celsr3* and *Fzd3* for proper wiring. Further study and innovative methods will be required to better understand the maturation of the nascent ENS into functional circuits.

2.11.5 What is the normal role of cell death in the developing and mature ENS?

Programmed cell death in the form of apoptosis plays a critical role matching neuron numbers to target size and ensuring correct targeting of neurites in the developing vertebrate CNS and other regions of the PNS. In fact, in most regions of the nervous system more than half of the neurons generated undergo apoptosis, often after target innervation (25). In contrast, during normal ENS development, some apoptosis occurs in pre-ENCDCs (i.e., before these cells enter the bowel) and this may be important for limiting ENS density in the proximal bowel (205). However, after ENCDC entry into the bowel, programmed cell death in the form of apoptosis does not appear to play a role in ENS development in wild type mice. In contrast, cell death does occur in the ENS of mice with specific gene defects. In support of this statement, activated caspase-3 (a marker of cells undergoing apoptosis) is extremely rare in the fetal, newborn, and adult ENS (80) of wild type mice. Rare instances of nuclear fragmentation and death have been observed in migrating SOX10+ ENCDCs (45), although these events are so infrequent that they are unlikely to influence the size of the ENCDC population. Moreover, *Bax*^{-/-} and *Bid*^{-/-} mice, which have defective apoptosis in other developing neuronal populations, have an essentially normal ENS (80). Thus, programmed cell death appears to be involved in regulating the number of ENCDC precursors that initially arrive in the bowel, but seems unlikely to control later developmental processes such as neuronal subtype ratios and ENS wiring.

However, it should also be noted that ENCDC apoptosis is a critical consequence of complete *Ret* and *Sox10* deficiency. Furthermore, under certain circumstances, an unusual form of cell death occurs in the ENS. When GFR α 1 is genetically ablated after ENCDC migration is complete, neurons undergo non-apoptotic cell death, and do not display ultrastructural signs of necrosis or autophagy (198). A subsequent study also demonstrated that a similar atypical ENCDC death occurs in the colons of mice with reduced *Ret* expression (*Ret*^{9/-}) (199), a model that very closely resembles *RET* mediated HSCR in humans. Thus, this atypical cell death may prove to be a critical contributor to the most common form of HSCR.

2.11.6 Applying our understanding of ENS development to human disease

These exciting advances in our understanding of the mechanisms of ENS development raise new hope that novel strategies can be developed to reduce the frequency and severity of human intestinal motility disorders. Managing HSCR remains a challenge in the modern era. One to 10% of children with HSCR still die despite advances in surgical treatment and post-operative management (2, 159). Furthermore, long-segment aganglionosis can necessitate the removal of enough small bowel to cause short gut syndrome resulting in long term dependence on parenteral nutrition, which has serious risks of infection and liver damage. Several other less well understood clinical conditions are caused by altered ENS activity. For example, chronic idiopathic intestinal pseudoobstruction (CIIP), a condition where intestinal motility is abnormal but neurons are present, can also be caused by structural and functional ENS defects that may or may not be obvious on routine clinical biopsies. Based on murine models where the ENS is formed, but the bowel does not function properly, pseudoobstruction of neuronal origin is likely to be due to a variety of failures in post-colonization ENS development such as neurotransmitter selection, axonal targeting, or synaptogenesis. For example, *RET* activating mutations that cause

MEN2B and mutations in *FLNA* (77) cause dysmotility, but the motility defects remain incompletely characterized. In contrast to the major defects that may underlie chronic pseudoobstruction, even more subtle changes to the physiology of the ENS may contribute to irritable bowel syndrome and other “functional” motility disorders. In fact, genetic lesions that alter the structure of the ENS can produce or modify bowel inflammation, suggesting that developmental abnormalities of the ENS can contribute to the severity of inflammatory bowel disease (29, 134). Understanding neuronal cell fate decisions and the wiring process that generates the normal ENS will help us better understand how these pathophysiological events impair intestinal function, and may suggest novel clinical interventions for intestinal motility and inflammatory diseases.

2.11.7 Why is HSCR partially penetrant and why does the extent of aganglionosis vary between individuals?

Human birth defects including HSCR result from genetic defects, non-genetic factors or interactions between genes and “fetal environmental” factors. In some cases, single-gene defects are the major risk factor for HD occurrence and have very high penetrance. However, no known HSCR associated gene defect is fully penetrant. A partial explanation for this observation is that genetic interactions critically influence HD penetrance. For example, there is a well-established genetic interaction between *EDNRB* and *RET* mutations in both humans and in mice. Alleles of each gene that produce mild phenotypes or no phenotype in isolation can cause severe disease in compound heterozygous mice and humans (36, 136). In mice, non-penetrant and weakly-penetrant alleles of *Ednrb* (or *Edn3*) can also worsen the severity of the ENS phenotype resulting from *Sox10* mutations (33, 183). In addition to *RET* coding mutations, a common intron one polymorphism that reduces *RET* expression (*RET*+3 or rs2435357) is highly associated with

sporadic HSCR and modifies the penetrance of HSCR in various predisposing syndromes (58, 152, 160). Recent studies have also implicated neuregulin 1 (*NRG1*) as a modifier of *RET*-dependent HSCR risk (76). Additionally, genes at several other chromosomal loci may influence HSCR risk in people with *RET* mutations (17, 72, 74, 190), though identifying the specific genes has been challenging.

Genetic interactions cannot explain all of HSCR's variability, since HSCR-like phenotypes in many inbred animal models are partially penetrant and of variably severity. *Sox10^{Dom}* is an excellent example of this phenomenon (33). "Developmental noise" or random occurrences at the level of individual ENCDC movement might influence migration processivity and speed. This could be translated into a variable extent of aganglionosis as the bowel wall eventually becomes relatively non-permissive to continued invasion (55, 97) after E14 and the migration wavefront is frozen in position, forming the transition zone between ganglionic and aganglionic bowel. The non-permissiveness of older bowel is relative rather than absolute, as illustrated by *Tcofl* (Treacher Collins-Franceschetti syndrome 1) mutant mice, where heterozygous mice do not fully colonize the bowel at E14.5 due to depletion of early neural crest precursors but continue to migrate, fully colonizing the colon by E18.5 (9). *Tcofl* ENCDCs, however, have abnormally low rates of differentiation and may in fact be more capable of migrating through older bowel than wild-type ENCDCs. Another situation where ENCDCs complete their migration despite a significant colonization delay occurs in the rescued *Ret^{0/-}* mouse model. These mice develop colonic aganglionosis after a moderate ENCDC migration delay and ENCDC death in the colon (199), but in mice that also overexpress the pro-survival protein Bcl-XL, the colon is eventually fully colonized even though ENCDC migration is not rescued and is incomplete at E13.5. In these situations, it seems that abnormal "hardier"

ENCDCs are capable of compensating for a developmental delay that would normally contribute to aganglionosis (197).

2.11.8 Why is HSCR more common in males than in females?

Another perplexing issue in the study of HSCR and ENS development is the male bias for penetrant disease. Interestingly, the male bias is much more pronounced in patients with short-segment disease (5.5:1) than in those with longer regions of aganglionosis (1.75:1) (2). Conceptually, this makes sense if we consider male sex as a mild predisposing factor for aganglionosis. Among syndromic HSCR cases, length of aganglionosis mostly correlates with penetrance of a mutation (160), and strongly penetrant mutations are not dependent on a weak modifier like sex. The molecular basis of this sex bias has been difficult to determine, despite several genetic models of colonic aganglionosis that demonstrate a similar predominance of affected males (33, 136, 199). Mutations in one X-linked gene, *LICAM*, are rarely associated with HSCR and a group of syndromes involving multiple nervous system abnormalities and hydrocephalus. Murine studies have demonstrated that null mutations in *Licam* can interact with *Sox10* mutations to increase the penetrance of aganglionosis and result in more severe pathology (206). Since *LICAM* mutations cause syndromic disease, they are unlikely to account for the male predominance in isolated HSCR unless a new and much less severe variant is found to be associated with HSCR. Another possible explanation for the male bias is suggested by the lower levels of colonic *Edn3* and *Ece1* expression in males compared to females during the time that ENCDC colonize distal bowel (203). However, the reasons for this difference remain unclear as neither testosterone nor Müllerian inhibitory factor (MIF) had any measurable effect on either ENCDC migration or gene expression. Adding ET-3 to cultured Ret mutant male mouse bowel, however, increased the extent of colonization *in vitro* suggesting that EDNRB signaling is

limiting in male mice. Clarifying the mechanisms behind these sex differences will require a better understanding of sexual dimorphism at the level of gene-expression with more detailed analysis of cis and trans regulatory elements (e.g. for *Edn3* and *Ece1*) and the epigenetic marks that control gene expression for critical regulators of ENS development.

2.11.9 Why does Down syndrome predispose to HSCR?

Down syndrome (Trisomy 21) is the most common genetic disorder that predisposes to HSCR. Overall occurrence of HSCR in Down syndrome is low (about 1%), and the common *RET* +3 polymorphism is highly associated with HSCR among children with Down syndrome, suggesting that some level of *RET* dysfunction is required for penetrant disease (160). Despite the fact that HSCR occurs in Down syndrome with a low penetrance relative to single-gene syndromes like WS4 and Mowat-Wilson syndrome, Down syndrome contributes to 2-10% of HSCR cases (2) because it is quite common (about 1 in 800 births). Increased chromosomal copy number of genes expressed in the ENS or surrounding tissues could be important for the HSCR-predisposing effect of trisomy 21. However, no genes confirmed to be important to ENS development reside on chromosome 21, though some candidates have been identified (135). One of these is *DSCAM*, an immunoglobulin-superfamily cell adhesion molecule expressed widely in the CNS and the developing ENS (214). A high-resolution copy number study of individuals with partial trisomy 21 and birth defects including HSCR demonstrated a shared 13-megabase region containing *DSCAM* that was duplicated in the 3 study participants with HSCR (113). It will be interesting to see whether *DSCAM* or other genes from this critical region impair ENS development if overexpressed.

2.12 Stem cells in the ENS: therapeutic possibilities and natural roles

During ENS colonization, ENCDCs serve as stem cells for the ENS and engage in both self-renewing replication and terminal differentiation into neurons and glia. Similar cells exist in the adult and newborn bowel in humans and rodents (Reviewed in 90, 98). Understanding these cells is critical for any future attempts to use them in therapy for HSCR, gastroparesis, achalasia, intestinal pseudoobstruction syndrome or possibly CNS disorders. Some stem cell types that have been transplanted into the rodent bowel are not neural crest derivatives, but instead begin as embryonic stem cells (99) or CNS neural stem cells (NSCs), which can improve gastric emptying in a mouse model of gastroparesis (141) when transplanted into the pylorus. However, we will focus our discussion on stem cells derived from the ENS.

Cultures of multipotent and self-renewing enteric neurospheres can be established from embryonic and postnatal mouse bowel (20, 186). Human enteric neurospheres have also been grown from full-thickness bowel explants (1, 138) and endoscopic mucosal biopsy samples (139) of children with HSCR and others of various ages. These human cells can colonize embryonic bowel (127, 139), differentiate into some types of neuron and glia in appropriate positions, and restore some contractile function (127) in grafting studies. Many criteria have been used to enrich cells isolated from bowel for ENS stem cells, including RET expression (145), selection using reporters recapitulating the expression patterns of ENS genes (44, 45, 91), selection for proliferative capacity in culture (20), and coexpression of p75NTR and the HNK-1 carbohydrate epitope (207). Another well-defined population of stem cells present in embryonic and postnatal bowel of rats coexpress alpha-4 integrin and high levels of p75NTR, and is both multipotent and self-renewing (14, 115) in culture. Many challenges lie between our current capability to expand a population of progenitors and the prospect of colonizing neonatal aganglionic bowel. To date,

engraftment and migration of grafted cells through non-embryonic bowel has been quite limited (139, 196), and it is unclear what functional capabilities these cells could have once engrafted, although they do extend neuronal processes. One aspect that has received less attention is the use of ENS-derived stem cells for transplant into the CNS. These ENS-derived stem cells may be an ideal therapeutic source since they are already capable of differentiating into cells expressing neurotransmitters lost in adult nervous system diseases. Furthermore, human ENS stem cells derived from a patient's own mucosal biopsies are proliferative, neurogenic, and non-immunogenic without the need for genetic modification. They may be the most easily accessible neuronal stem cell in the body, and their use in both CNS and ENS transplantation is worth investigating.

Although much effort has been focused on isolation and growth of ENS-derived stem cells in culture, these cells may serve a homeostatic role in postnatal ENS development, possibly in response to injury and aging. Recent work has demonstrated the existence of an extraganglionic cell that responds to 5-HT₄ receptor stimulation by proliferating, becoming immunoreactive for SOX10, Phox2B and HuC/HuD, and very slowly migrating into ganglia (130). Two recent studies used lineage tracing to demonstrate that enteric glia in the adult rat and mouse ENS have significant neurogenic potential in culture, but only form neurons *in vivo* under very restricted circumstances. Adult cells labeled by an inducible recombinase under control of SOX10-genomic sequences (*Sox10-CreERT2*) never became neurons *in vivo*, except after ENS injury by benzalkonium chloride (121). However, a simultaneous study by another group demonstrated that neurogenesis from cells labeled by a GFAP-controlled recombinase (GFAP-Cre) did not occur after the same type of ENS injury. Furthermore, they did not detect any proliferative neurogenesis in adult mice and rats exposed to an array of chemical, physical,

infectious and dietary insults (105). Taken together, these studies suggest that some neurogenesis in the adult ENS can occur via proliferation of an extraganglionic cell after 5-HT₄ receptor stimulation or possibly through non-proliferative differentiation of an as-yet unidentified SOX10-positive, GFAP-negative (or GFAP-Cre transgene non-expressing) cell after injury. Further work will be needed to identify the source cells for both these fascinating processes. Since neuronal progenitors within the postnatal and adult central nervous system express glial markers (114), the population currently considered to be uniformly enteric glia may contain a distinct subpopulation with the capacity to generate neurons.

2.13 Prevention of HSCR and other intestinal motility disorders

While progress is being made toward novel transplantation strategies that might help treat HSCR or other serious motility disorders, HSCR prevention strategies deserve more focused study. Given the myriad of molecules and pathways involved in ENS development, it is very likely that one or more can be affected by some aspect of the prenatal environment. Currently, counseling for parents of a child with sporadic HSCR is limited to providing information about the sibling recurrence risk, which varies depending on the sex of the proband and the length of aganglionosis. *RET* sequencing in HSCR patients is also becoming more common, since 1-2 % of children that present with HSCR actually have *RET* mutations that cause MEN2A. However, knowing the nature of the mutation does not influence the treatment of HSCR.

Since treatment for HSCR remains imperfect, and even diagnosed and treated HSCR causes significant morbidity, identifying environmental factors that could modify disease penetrance or expressivity would be extremely valuable. The vast majority of sporadic HSCR

(80%) occurs because ENCCs fail to colonize the final 5-10% of the bowel. At this critical point, small effects on ENCC migration efficiency, proliferation, or survival can mean the difference between a functional colon and aganglionic bowel causing life-threatening disease. By identifying and eliminating environmental factors that impair ENS development, we may be able to prevent some cases of short-segment disease and reduce the morbidity of more extensive aganglionosis. To date, very few associations between environmental factors and ENS development have been found, but this has not been systematically investigated. Only a few small clinical studies address whether the prenatal environment affects HSCR risk. One study of children with trisomy 21, for example, found that consumption of more than 3 cups of coffee a day and possibly maternal fever were associated with increased HSCR occurrence (195). An earlier study performed before the identification of any HSCR susceptibility genes also proposed an association between HSCR and hyperthermia during gestation (128), though a subsequent study failed to find any correlation (122). More subtle disorders of intestinal motility may also be rooted in environmental disruption of ENS development. In a recent retrospective study (149), tricyclic antidepressant use during the first trimester and selective serotonin reuptake inhibitor (SSRI) use during the second or third trimester of pregnancy was associated with increases in laxative use (a surrogate for constipation) during early childhood. This is especially interesting because tricyclic antidepressants inhibit the function of many receptors and transporters including the norepinephrine transporter, which, as discussed previously, is required for normal TC-lineage differentiation into serotonergic neurons. In turn, SSRIs might interfere with the normal role of 5-HT in later neurogenesis.

Animal models and culture studies now provide strong evidence that specific gene-environment interactions influence ENS development and/or HSCR risk. Treatment of cultured

fetal mouse colon with the Rho-kinase inhibitor Y-27632 for example, inhibited ENCC migration significantly more in *Ret*^{+/-} explants than in controls (185). Furthermore, oxidative stress in the early neural crest, induced by injection of pregnant mice with H₂O₂, reduced the extent of ENCC migration into distal bowel in *Tcofl*^{+/-} embryos while not affecting the extent of ENCC bowel colonization in wild-type littermates (9). A dramatic and clinically relevant gene-environment interaction was also observed in a mouse model of vitamin A deficiency (65). Mice maintain significant stores of vitamin A in their livers in the form of retinol, so *Rbp4*^{-/-} mice, which cannot mobilize these stores and depend on dietary retinol, were used to assess the effects of vitamin A depletion during ENS development. *Rbp4*^{-/-} mice fed a vitamin-A deficient diet during neural crest development had striking ENCC migration delays in the colon compared to *Rbp4*^{-/-} mice fed a diet containing vitamin A. Additionally, *Rbp4*^{-/-} *Ret*^{+/-} mice had a much more severe delays in ENCC colonization of the bowel when deprived of dietary vitamin A, and even manifested a significant developmental delay when fed a vitamin-A sufficient diet. Similarly, in humans carrying HSCR risk alleles, otherwise subclinical vitamin A deficiency could synergize with genetic defects to worsen the severity of HSCR or increase the likelihood that HSCR will occur. Genetic models of HSCR susceptibility that more closely approximate sporadic HSCR and a careful examination of the signals involved in ENS development will be critical for identifying and characterizing other environmental insults that impair ENS development and to test prevention strategies.

Finally, large scale human epidemiologic studies are now appropriate and will be needed to validate and identify non-genetic factors that increase HSCR risk. Given the strength of the experimental data demonstrating that non-genetic factors can alter HSCR risk, the known effect of many medicines on proteins needed for ENS development, and our ability to couple genetic

and epidemiologic data, this is the ideal time to launch a systematic national or international case-control study of non-genetic HSCR risk factors. The implications of this work will have immediate benefit to families since many children with HSCR are now becoming parents, and families who have one affected child are at dramatically higher risk of having a second child with HSCR.

2.14 Conclusion

Much of our understanding of ENS development has been informed by developmental and genetic studies of very severe ENS defects, in a generally successful effort to understand the etiology of Hirschsprung disease and ENDCD colonization of the bowel. However, we have highlighted several areas where aspects of both global ENS development (cell motility, colonization, cell death, gene and environmental interactions) and processes with more restricted effects (neuronal fate decisions, axon pathfinding, postnatal ENS stem cells) remain unexplained. To address these gaps in our understanding, it will be necessary to find new and more precise ways to perturb ENS development in experimental systems and expand the study of subtle and difficult to identify ENS phenotypes. Understanding normal ENS development and its modes of failure will translate into better outcomes for those affected by developmental defects of the ENS, whether these improvements come in the form of more informative genetic counseling, prevention strategies to mitigate the penetrance and expressivity of mutations, or via stem-cell therapy.

Table 2.1

Genes involved in RET and EDNRB signaling			
Gene	Mouse Model	ENS Phenotype in Mouse	Human Disease Association(2)
<i>Ret</i> receptor tyrosine kinase	Monoisoformic alleles that are hypomorphic in the ENS despite not having any mutations:	Homozygous <i>Ret</i> ^{miRet51/miRet51} . Colonic aganglionosis (84)	HSCR, Total intestinal aganglionosis, MEN2A, MEN2B
		Hemizygous <i>Ret</i> ^{9/-} : Colonic aganglionosis (199)	
	Serine phosphorylation site mutation <i>Ret</i> ^{S697A}	Homozygous: Colonic aganglionosis (6)	
	Tyrosine phosphorylation site mutations such as <i>Ret</i> ^{Y1062F} (104) <i>Ret</i> ^{RET9(1062F)} <i>Ret</i> ^{RET9(Y981F)} <i>Ret</i> ^{RET9(Y1015F)} <i>Ret</i> ^{RET51(Y1062F)} <i>Ret</i> ^{RET51(Y1015F)} (102)	Homozygous: Range of phenotypes from occasional hypoganglionosis to total intestinal aganglionosis. Effects of a given mutation depend on which isoform is mutated. Mutations affecting monoisomorphic RET9 have more deleterious effects than mutations affecting RET51.	
	Missense MEN2A mutation <i>Ret</i> ^{C620R}	Homozygous: Total intestinal aganglionosis Heterozygous: Hypoganglionosis (35)	
	Dominant negative allele: <i>Ret</i> ^{RET9-L985P-Y1062F}	Heterozygous: Aganglionosis extending into the small bowel.	
	Null alleles	Homozygous: Total intestinal aganglionosis (175)	
Heterozygous: Subtle reductions in neuron size and fiber density. Bowel contractility is abnormal (80)			

Genes involved in RET and EDNRB signaling (continued)			
Gene	Mouse Model	ENS Phenotype in Mouse	Human Disease Association
<i>Gdnf</i> neurotrophin, RET ligand	Null allele	Homozygous: Total intestinal aganglionosis (172)	Mutations found in some HSCR cases
		Heterozygous: Reduced enteric neuron density (80)	
<i>Gfra1</i> RET coreceptor	Null allele	Homozygous: Total intestinal aganglionosis (30)	
		Heterozygous: Subtle reductions in neuron size and fiber density. Bowel contractility is abnormal (80)	
<i>Nrtn</i> neurotrophin, RET ligand	Null allele	Homozygous: Reduced soma size and fiber density in the myenteric plexus. Abnormal motility (94)	Mutations found in some HSCR cases
<i>Gfra2</i> RET coreceptor	Null allele	Homozygote: Reduced fiber density and abnormal motility (169)	
<i>Ednrb</i> G-protein coupled receptor	Null allele: <i>Ednrb^{s-1}</i>	Homozygote: Colonic aganglionosis with hypoganglionosis of the small intestine (96) Heterozygote: hypoganglionosis of the small intestine (33)	HSCR, WS4
	Hypomorphic allele: <i>Ednrb^s</i>	Homozygote: Rare colonic aganglionosis (136)	
<i>Edn3</i> EDNRB ligand	Null allele: <i>Edn3^{ls}</i>	Homozygote: Colonic aganglionosis (155)	WS4, very rare
<i>Ece1</i> EDN3 processing protease	Null allele:	Homozygote: Colonic aganglionosis (215)	One case of HSCR with multiple birth defects
Genes involved in ENS development and implicated in syndromic HSCR			
<i>BBS1-11</i> intraciliary transport proteins	ENS not yet studied in mouse models. Morpholino knockdown in zebrafish causes ENS precursor migration defects (194)		Bardel-Biedl syndrome (±HSCR)
<i>KIAA1279</i> (<i>Kbp</i>) unclear function	No mouse model exists. Zebrafish <i>kbp^{st23}</i> loss-of-function mutation reduces axon growth in the ENS (132)		Goldberg-Shprintzen syndrome (+HSCR)

Genes involved in ENS development and implicated in syndromic HSCR (continued)			
Gene	Mouse Model	ENS Phenotype in Mouse	Human Disease Association
<i>L1cam</i> L1 family cell adhesion molecule	Null allele	Transient ENCDC migration delay at E11.5 (5)	X-linked congenital hydrocephalus, MASA Syndrome (\pm HSCR)
<i>Pds5A</i> and <i>Pds5B</i> cohesin regulatory factor	Null alleles	Homozygotes: Delayed ENS colonization (223) , partially penetrant colonic aganglionosis (224)	Cornelia de Lange syndrome (One family)
<i>Phox2b</i> homeodomain transcription factor	Null allele	Homozygous: Total intestinal aganglionosis (154)	Congenital central hypoventilation syndrome, Haddad syndrome
<i>Sox10</i> SRY-related HMG-box transcription factor	Dominant Negative <i>Sox10^{Dom}</i>	Heterozygous: Colonic aganglionosis (117)	HSCR, WS4
		Homozygous: Total intestinal aganglionosis (109)	
	Null allele <i>Sox10^{LacZ}</i>	Heterozygous: Colonic aganglionosis (23)	
		Homozygous: Total intestinal aganglionosis (23)	
<i>Zfx1b</i> (SIP1, ZEB2) zinc-finger/homeodomain protein	Null allele	Homozygous: Failure of vagal neural crest delamination. ENCDCs do not enter the bowel. (164)	Mowat-Wilson syndrome (+HSCR)
Genes involved in ENS development or associated with HSCR			
<i>Aldh1a2</i> (Raldh2) retinoic acid synthesis enzyme	Null allele	Homozygous: Neural crest cells never enter the bowel (148)	

Genes involved in ENS development or associated with HSCR (continued)			
Gene	Mouse Model	ENS Phenotype in Mouse	Human Disease Association
<i>Ascl1</i> (MASH1) basic helix-loop-helix transcription factor	Null allele	Serotonergic neurons absent from ENS (15), no neurons develop in the esophagus (85)	
<i>Dcc</i> receptor for netrin-1	Null allele	Homozygous: Failure of ENCDCs to migrate to submucosal plexus and pancreas (103)	
<i>HOXB5</i> homeodomain transcription factor	Dominant negative Tg(enb5), Tg(b3-IIIa-Cre), mosaic expression	Hypoganglionosis and aganglionosis of the ENS, <i>Ret</i> expression and migration reduced in the subset of cells that express dominant negative <i>HOXB5</i> (131)	Variants associated with HSCR (37, 131)
<i>Ihh</i> hedgehog ligand	Null allele	Homozygous: ENS is absent in some regions of the small bowel and colon (165)	
<i>Kif26a</i> negative regulator of RET signaling	Null allele	Homozygous: Myenteric neuronal hyperplasia, pseudoobstruction (226)	
<i>Lgi4</i> , <i>Adam22</i> Secreted factor and receptor involved in glial development and myelination	Null alleles	Homozygous: Reduced numbers of glial cells, impaired glial marker expression, abnormal ENS structure. (150)	
<i>NKX2-1</i> homeodomain transcription factor	ENS not studied in mouse models. Protein is detectable in human but not mouse ENCDCs.		Mutations found in some HSCR cases. (73)
<i>NRG1</i> ERBB3 Ligand	ENS not yet studied in mouse models		HSCR (76)
<i>NRG3</i> ERBB4 Ligand	ENS not yet studied in mouse models		HSCR (191)
<i>Ntrk3</i> (TrkC) receptor for NT-3	Null allele	Reduced numbers of enteric neurons, evidence for a selective reduction in late-born CGRP neurons (42)	Mutations found in some HSCR cases

Genes involved in ENS development or associated with HSCR (continued)			
Gene	Mouse Model	ENS Phenotype in Mouse	Human Disease Association
<i>Ntf3</i> (NT-3) neurotrophin, TrkC/p75NTR ligand	Null allele	Reduced numbers of enteric neurons (42)	Mutations found in some HSCR cases
<i>Pax3</i> paired-box transcription factor	Null allele <i>Pax3^{Sp}</i>	Homozygous: Total intestinal aganglionosis (118)	Heterozygous mutations associated with Waardenburg syndrome without HSCR.
<i>Phactr4</i> regulator of the actin cytoskeleton and cell adhesion	Mouse hypomorphic allele <i>Phactr4^{humdy}</i>	Homozygous: Colonic hypoganglionosis (225)	
<i>PROK1</i> <i>PROKR1</i> <i>PROKR2</i> Prokineticin and receptors	ENS not yet studied in mouse models. Receptors are expressed in cultured human enteric neurosphere-like bodies. (171)		Mutations found in some HSCR cases.
<i>Shh</i> hedgehog ligand	Null allele	Homozygous: Ectopic neurons located in mucosa (165)	
<i>Slc6a2</i> (NET) norepinephrine reuptake transporter	Null allele	Homozygous: Decreased neuronal numbers, selective decreases in numbers of serotonin and calretinin reactive neurons (125)	
<i>Tcof1</i> nucleolar factor	Null allele	Heterozygotes: Delayed colonization of the bowel by ENCDCs. Migration continues between E14 and E18 to colonize the entire bowel (9)	
<i>Tlx2</i> (Hox11L1) homeodomain transcription factor	Null allele	Homozygous: Myenteric neuronal hyperplasia, pseudoobstruction (179)	

Genes involved in ENS development or associated with HSCR (continued)			
Gene	Mouse Model	ENS Phenotype in Mouse	Human Disease Association
<i>Tph2</i> neuronal serotonin biosynthesis enzyme	Null allele	Homozygous: Decreased numbers of myenteric neurons, selective decreases in numbers of dopaminergic and GABAergic neurons (126)	
<i>Spry2</i> regulator of receptor tyrosine kinases	Null allele	Homozygous: Myenteric neuron hyperplasia, pseudoobstruction, achalasia (189)	
Other genes associated with syndromic HSCR			
<i>DHCR7</i> final enzyme in cholesterol biosynthesis	ENS not yet studied in mouse models		Smith-Lemli-Opitz syndrome (±HSCR)
<i>RMRP</i> mitochondrial RNA-processing noncoding RNA	No viable mouse model		Cartilage-hair-hypoplasia (±HSCR)
<i>TCF7L2</i> , (TCF4) transcription factor involved in Wnt signaling.	ENS not yet studied in mouse models		Pitt-Hopkins syndrome, 1 case includes HSCR
Transgenic models where overexpression alters ENS development			
Mouse Model	Description	ENS Phenotype	
Tg(DBH-NT3)	Ectopic neuronal and ENDCDC expression of NT-3	Increased numbers of enteric neurons and neuronal hypertrophy (42)	
Tg(GFAP-GDNF)	Ectopic glial expression of GDNF	Increased numbers of submucosal neurons, increased numbers of nitrergic neurons, aberrant clustering of nitrergic axons around myenteric ganglia (208)	
Tg(HoxA4)	Global overexpression of homeodomain transcription factor	Colonic hypoganglionosis with neuronal hypertrophy. (210)	

Transgenic models where overexpression alters ENS development (continued)		
Mouse Model	Description	ENS Phenotype
Tg(Mt1-GLI)	Ectopic and inducible expression of GLI1, activator of genes downstream of hedgehog pathway	Megacolon with hypoganglionosis, perinatal and adult death. Severity is related to expression level (216)
Tg(NSE-Noggin)	Ectopic neuronal expression of BMP antagonist noggin	Increased numbers of enteric neurons, with a selective decrease in the size of the TrkC expressing population. (38)
Conditional Mutations		
Gene	Mouse Model*	ENS Phenotype
<i>Cdh2</i> (N-Cadherin) homophilic cell adhesion molecule	Tg(Ht-PA-Cre) <i>Cdh2</i> ^{LoxP}	Delayed colonization of the colon. Severe migration defects in <i>Cdh2 Itgb1</i> double-conditional ENCDCs (24)
<i>Dicer1</i> miRNA processing enzyme	Tg(Wnt1-Cre) <i>Dicer1</i> ^{LoxP}	Post-colonization loss of ENS cells (222)
<i>ErbB2</i> EGF-receptor family member without known ligand. Heterodimerizes with ERBB3/4.	Tg(Nestin-Cre) <i>ErbB2</i> ^{LoxP}	Postnatal loss of colonic neurons (46) , thought to be due to loss of <i>ErbB2</i> in the epithelium, not the neural crest.
<i>Ercc1</i> nucleotide excision repair factor	Tg(Tyr-Cre) <i>Ercc1</i> ^{LoxP}	Postnatal death of colonic neurons (176)
<i>Itgb1</i> (Beta-1 Integrin) cell-ECM adhesion molecule	Tg(Ht-PA-Cre) <i>Itgb1</i> ^{LoxP}	Colonic aganglionosis (22)

Conditional Mutations (continued)		
Gene	Mouse Model*	ENS Phenotype
<i>Hand2</i> basic helix-loop-helix transcription factor	Tg(Wnt1-Cre) <i>Hand2</i> ^{LoxP}	Tg(Wnt1-Cre), <i>Hand2</i> ^{LoxP/LoxP} (93) : Disrupted patterning of nascent enteric ganglia and fiber network, reduction in neuronal density. Failure of neurons to colocalize Tuj1 and Hu markers, selective loss of VIP-immunoreactive neurons. Tg(Wnt1-Cre), <i>Hand2</i> ^{LoxP/null} : Loss of markers of terminal neuronal differentiation (Hu, microtubule-associated protein 2) and some neuronal subtypes (nNOS, dopamine β-hydroxylase). Fetal death at E14 (48). More severe phenotype may be the result of heterozygosity for null allele (47).
<i>Pofut1</i> required for notch signaling	Tg(Wnt1-Cre) <i>Pofut1</i> ^{LoxP}	Hypoganglionosis (153)
<i>Pten</i> phosphatase and tumor suppressor	Tg(Tyr-Cre) <i>Pten</i> ^{LoxP}	Hypertrophy and hyperplasia of enteric neurons (162)
<i>Rac1</i> and <i>Cdc42</i> Rho-family GTPases	Tg(Wnt1-Cre) <i>Rac1</i> ^{LoxP} or Tg(Wnt1-Cre) <i>Cdc42</i> ^{LoxP}	Failure of ENCDCs to proliferate and colonize distal bowel (69)
<i>Tfam</i> mitochondrial transcription factor	<i>CNP</i> ^{Cre} , <i>Tfam</i> ^{LoxP} recombination in Schwann cells and ENS precursors	Postnatal death of specific subsets of enteric neurons (200)
<i>Zfhx1b</i> (SIP1, ZEB2) zinc-finger/homeo-domain protein	Tg(Wnt1-Cre) <i>Zfhx1b</i> ^{LoxP}	Aganglionosis of the entire bowel distal to the stomach and rostral duodenum. (163)
Genetic Interactions in Model Systems		
Genes or alleles		ENS Phenotype
<i>Ret</i> ^{+/-}	<i>Ednrb</i> ^{s/s} <i>Ednrb</i> ^{s-l/s}	Highly penetrant aganglionosis in double-mutant animals. (136) In isolation, <i>Ret</i> ^{+/-} is not penetrant, and these <i>Ednrb</i> genotypes have extremely low penetrance.
<i>Ret</i> ^{Y1062F/Y1062F}	<i>Spry2</i> ^{-/-}	Partial rescue of nitrergic neuron density in the stomach. No effect on the remainder of the ENS. (142)
<i>Ednrb</i> ^{sl/sl}	<i>Ret</i> ^{+/miRet51}	Partial rescue: double mutant embryos have a shorter aganglionic segment than <i>Ednrb</i> ^{sl/sl} single mutants (8)

Genetic Interactions in Model Systems (continued)		
Genes or alleles		ENS Phenotype
<i>Sox10^{Dom/+}</i>	<i>Ednrb^{s/+}</i> <i>Ednrb^{s/s}</i> <i>Ednrb^{l^s-l/+}</i> <i>Ednrb^{s-l/s-l}</i>	Double mutant embryos have more penetrant aganglionosis (33) , a more severe ENCC developmental delay, and more pre-ENCC cell death than <i>Sox10^{Dom/+}</i> embryos (183)
<i>Sox10^{Dom/+}</i>	<i>Edn3^{ls/ls}</i> <i>Edn3^{ls/+}</i>	Double mutant embryos have a more severe ENCC developmental delay than <i>Sox10^{Dom/+}</i> embryos (183)
<i>Sox10^{LacZ/+}</i>	<i>Zfhx1b^{-/+}</i>	Double mutant embryos have a more severe ENCC developmental delay and more extensive aganglionosis than <i>Sox10^{LacZ/+}</i> embryos (184) . The <i>Zfhx1b^{-/+}</i> genotype does not cause aganglionosis by itself.
<i>Sox10^{LacZ/+}</i>	<i>Sox8^{LacZ/+}</i> <i>Sox8^{LacZ/LacZ}</i>	Double mutant embryos have a more severe ENCC developmental delay, more extensive aganglionosis, and more pre-ENCC cell death than <i>Sox10^{LacZ/+}</i> embryos (133). <i>Sox8</i> mutations do not affect ENS development in isolation.
<i>Sox10^{LacZ/+}</i>	<i>L1cam^{+/-}</i> <i>L1cam^{-/Y}</i>	Double mutant embryos have a more severe ENCC developmental delay, more extensive aganglionosis, and more pre-ENCC cell death than <i>Sox10^{LacZ/+}</i> embryos (206). <i>L1cam</i> mutations individually produce transient delays in ENS development.
Gene-environment interactions		
Genetic factor	Environmental factor	ENS Phenotype
<i>Ret^{+/-} Rbp4^{-/-}</i>	Vitamin A deficiency during gestation	Aganglionosis of the colon and small bowel. <i>Rbp4^{-/-}</i> mice depleted of vitamin A and <i>Ret^{+/-} Rbp4^{-/-}</i> fed vitamin A also developed aganglionosis, but less severely. (65)
<i>Tcof1^{+/-}</i>	H ₂ O ₂ exposure at E7.5	More severe ENCC migration delay than <i>Tcof1</i> mutation alone. H ₂ O ₂ had no effect on ENCC migration in wild-type mice. (9)

Genes affecting ENS development. Genes involved in HSCR disease or known to be important to ENS development are listed and their mutant phenotypes described. In addition, genetic interactions and gene-environment interactions that have been demonstrated in the mouse are listed. While many of the genes with well-documented roles in the ENS are also HSCR susceptibility genes, most are rare. Conversely, the normal ENS developmental role of several HSCR susceptibility genes in has not been explored. Human gene symbols are listed when mouse models have not been studied. Otherwise, mouse symbols are listed. While the *Hoxb5* dominant negative mouse is a transgenic, it is listed together with the loss-of-function mutations due to the possible association of *HOXB5* with HSCR. The conditional mutations are listed here when they provided additional information about the role of each gene in ENS development.

*Tg(Wnt1-Cre), Tg(Ht-PA-Cre), lines result in recombination in the neural crest, while the Tg(Tyr-Cre) line results in recombination in a subset of the vagal neural crest including the ENS. Human chromosomal regions with as-yet unidentified susceptibility loci and the genetic interactions that have been identified in humans are not included in this table. BMP, bone morphogenetic protein; CGRP, calcitonin gene-related peptide; ECM, extracellular matrix; EDNRB, endothelin receptor type B; ENCDC, enteric neural crest-derived cell; E7.5, E11.5, E14, and E18, embryonic days 7.5, 11.5, 14, and 18; MEN2A and MEN2B, multiple endocrine neoplasia 2A and 2B; nNOS, neuronal nitric oxide synthase.

2.15 References

1. Almond S, Lindley RM, Kenny SE, Connell MG, Edgar DH. Characterisation and transplantation of enteric nervous system progenitor cells. *Gut* 56: 489–496, 2007.
2. Amiel J, Sproat-Emison E, Garcia-Barcelo M, Lantieri F, Burzynski G, Borrego S, Pelet A, Arnold S, Miao X, Griseri P, Brooks AS, Antinolo G, de Pontual L, Clement-Ziza M, Munnich A, Kashuk C, West K, Wong KK-Y, Lyonnet S, Chakravarti A, Tam PK-H, Ceccherini I, Hofstra RMW, Fernandez R. Hirschsprung disease, associated syndromes and genetics: a review. *J. Med. Genet.* 45: 1–14, 2008.
3. Anderson R, Stewart A, Young H. Phenotypes of neural-crest-derived cells in vagal and sacral pathways. *Cell Tissue Res.* 323: 11–25, 2006.
4. Anderson RB, Bergner AJ, Taniguchi M, Fujisawa H, Forrai A, Robb L, Young HM. Effects of different regions of the developing gut on the migration of enteric neural crest-derived cells: a role for *Sema3A*, but not *Sema3F*. *Dev. Biol.* 305: 287–299, 2007.
5. Anderson RB, Turner KN, Nikonenko AG, Hemperly J, Schachner M, Young HM. The cell adhesion molecule *L1* is required for chain migration of neural crest cells in the developing mouse gut. *Gastroenterology* 130: 1221–1232, 2006.
6. Asai N, Fukuda T, Wu Z, Enomoto A, Pachnis V, Takahashi M, Costantini F. Targeted mutation of serine 697 in the *Ret* tyrosine kinase causes migration defect of enteric neural crest cells. *Development* 133: 4507–4516, 2006.
7. Baetge G, Pintar JE, Gershon MD. Transiently catecholaminergic (TC) cells in the bowel of the fetal rat: Precursors of noncatecholaminergic enteric neurons. *Dev. Biol.* 141: 353–380, 1990.
8. Barlow A, de Graaff E, Pachnis V. Enteric nervous system progenitors are coordinately controlled by the G protein-coupled receptor *EDNRB* and the receptor tyrosine kinase *RET*. *Neuron* 40: 905–916, 2003.
9. Barlow AJ, Dixon J, Dixon MJ, Trainor PA. Balancing neural crest cell intrinsic processes with those of the microenvironment in *Tcof1* haploinsufficient mice enables complete enteric nervous system formation. *Hum. Mol. Genet.* 21: 1782–1793, 2012.
10. Bastida MF, Ros MA. How do we get a perfect complement of digits? *Curr. Opin. Genet. Dev.* 18: 374–380, 2008.
11. Benailly HK, Lapierre JM, Laudier B, Amiel J, Attié T, Blois MD, Vekemans M, Romana SP. *PMX2B*, a new candidate gene for Hirschsprung's disease. *Clin. Genet.* 64: 204–209, 2003.

12. Bergeron K-F, Silversides DW, Pilon N. The developmental genetics of Hirschsprung's disease. *Clin. Genet.* 83: 15–22, 2013.
13. Bitgood MJ, McMahon AP. Hedgehog and Bmp Genes Are Coexpressed at Many Diverse Sites of Cell–Cell Interaction in the Mouse Embryo. *Dev. Biol.* 172: 126–138, 1995.
14. Bixby S, Kruger GM, Mosher JT, Joseph NM, Morrison SJ. Cell-intrinsic differences between stem cells from different regions of the peripheral nervous system regulate the generation of neural diversity. *Neuron* 35: 643–656, 2002.
15. Blaugrund E, Pham TD, Tennyson VM, Lo L, Sommer L, Anderson DJ, Gershon MD. Distinct subpopulations of enteric neuronal progenitors defined by time of development, sympathoadrenal lineage markers and Mash-1-dependence. *Development* 122: 309–320, 1996.
16. Bogni S, Trainor P, Natarajan D, Krumlauf R, Pachnis V. Non-cell-autonomous effects of Ret deletion in early enteric neurogenesis. *Development* 135: 3007–3011, 2008.
17. Bolk S, Pelet A, Hofstra RMW, Angrist M, Salomon R, Croaker D, Buys CHCM, Lyonnet S, Chakravarti A. A human model for multigenic inheritance: Phenotypic expression in Hirschsprung disease requires both the RET gene and a new 9q31 locus. *Proc. Natl. Acad. Sci. U. S. A.* 97: 268–273, 2000.
18. Bondurand N, Dastot-Le Moal F, Stanchina L, Collot N, Baral V, Marlin S, Attie-Bitach T, Giurgea I, Skopinski L, Reardon W, Toutain A, Sarda P, Echaieb A, Lackmy-Port-Lis M, Touraine R, Amiel J, Goossens M, Pingault V. Deletions at the SOX10 Gene Locus Cause Waardenburg Syndrome Types 2 and 4. *Am. J. Hum. Genet.* 81: 1169–1185, 2007.
19. Bondurand N, Natarajan D, Barlow A, Thapar N, Pachnis V. Maintenance of mammalian enteric nervous system progenitors by SOX10 and endothelin 3 signalling. *Development* 133: 2075–2086, 2006.
20. Bondurand N, Natarajan D, Thapar N, Atkins C, Pachnis V. Neuron and glia generating progenitors of the mammalian enteric nervous system isolated from foetal and postnatal gut cultures. *Development* 130: 6387–6400, 2003.
21. Breau MA, Dahmani A, Broders-Bondon F, Thiery J-P, Dufour S. β 1 integrins are required for the invasion of the caecum and proximal hindgut by enteric neural crest cells. *Development* 136: 2791–2801, 2009.
22. Breau MA, Pietri T, Eder O, Blanche M, Brakebusch C, Fässler R, Thiery JP, Dufour S. Lack of β 1 integrins in enteric neural crest cells leads to a Hirschsprung-like phenotype. *Development* 133: 1725–1734, 2006.
23. Britsch S, Goerich DE, Riethmacher D, Peirano RI, Rossner M, Nave K-A, Birchmeier C, Wegner M. The transcription factor Sox10 is a key regulator of peripheral glial development. *Genes Dev.* 15: 66–78, 2001.

24. Broders-Bondon F, Paul-Gilloteaux P, Carlier C, Radice GL, Dufour S. N-cadherin and β 1-integrins cooperate during the development of the enteric nervous system. *Dev. Biol.* 364: 178–191, 2012.
25. Burek MJ, Oppenheim RW. Programmed cell death in the developing nervous system. *Brain Pathol.* 6: 427–446, 1996.
26. Burns AJ, Champeval D, Le Douarin NM. Sacral Neural Crest Cells Colonise Aganglionic Hindgut in Vivo but Fail to Compensate for Lack of Enteric Ganglia. *Dev. Biol.* 219: 30–43, 2000.
27. Burns AJ, Delalande J-MM, Douarin NML. In ovo transplantation of enteric nervous system precursors from vagal to sacral neural crest results in extensive hindgut colonisation. *Development* 129: 2785–2796, 2002.
28. Burns AJ, Le Douarin NM. The sacral neural crest contributes neurons and glia to the post-umbilical gut: spatiotemporal analysis of the development of the enteric nervous system. *Development* 125: 4335–4347, 1998.
29. Bush TG, Savidge TC, Freeman TC, Cox HJ, Campbell EA, Mucke L, Johnson MH, Sofroniew MV. Fulminant jejuno-ileitis following ablation of enteric glia in adult transgenic mice. *Cell* 93: 189–201, 1998.
30. Cacalano G, Fariñas I, Wang L-C, Hagler K, Forgie A, Moore M, Armanini M, Phillips H, Ryan AM, Reichardt LF, Hynes M, Davies A, Rosenthal A. GFR α 1 is an essential receptor component for GDNF in the developing nervous system and kidney. *Neuron* 21: 53–62, 1998.
31. Cacheux V, Dastot-Le Moal F, Kaariainen H, Bondurand N, Rintala R, Boissier B, Wilson M, Mowat D, Goossens M. Loss-of-function mutations in SIP1 Smad interacting protein 1 result in a syndromic Hirschsprung disease. *Hum. Mol. Genet.* 10: 1503–1510, 2001.
32. De Calisto J, Araya C, Marchant L, Riaz CF, Mayor R. Essential role of non-canonical Wnt signalling in neural crest migration. *Development* 132: 2587–2597, 2005.
33. Cantrell VA, Owens SE, Chandler RL, Airey DC, Bradley KM, Smith JR, Southard-Smith EM. Interactions between Sox10 and EdnrB modulate penetrance and severity of aganglionosis in the Sox10^{Dom} mouse model of Hirschsprung disease. *Hum. Mol. Genet.* 13: 2289–2301, 2004.
34. Carmona-Fontaine C, Matthews HK, Kuriyama S, Moreno M, Dunn GA, Parsons M, Stern CD, Mayor R. Contact inhibition of locomotion in vivo controls neural crest directional migration. *Nature* 456: 957–961, 2008.
35. Carniti C, Belluco S, Riccardi E, Cranston AN, Mondellini P, Ponder BAJ, Scanziani E, Pierotti MA, Bongarzone I. The RetC620R Mutation Affects Renal and Enteric Development in a Mouse Model of Hirschsprung's Disease. *Am. J. Pathol.* 168: 1262–1275, 2006.

36. Carrasquillo MM, McCallion AS, Puffenberger EG, Kashuk CS, Nouri N, Chakravarti A. Genome-wide association study and mouse model identify interaction between RET and EDNRB pathways in Hirschsprung disease. *Nat. Genet.* 32: 237–244, 2002.
37. Carter TC, Kay DM, Browne ML, Liu A, Romitti PA, Kuehn D, Conley MR, Caggana M, Druschel CM, Brody LC, Mills JL. Hirschsprung's disease and variants in genes that regulate enteric neural crest cell proliferation, migration and differentiation. *J. Hum. Genet.* 57: 485–493, 2012.
38. Chalazonitis A, D'Autréaux F, Guha U, Pham TD, Faure C, Chen JJ, Roman D, Kan L, Rothman TP, Kessler JA, Gershon MD. Bone morphogenetic protein-2 and -4 limit the number of enteric neurons but promote development of a TrkC-expressing neurotrophin-3-dependent subset. *J. Neurosci.* 24: 4266–4282, 2004.
39. Chalazonitis A, D'Autréaux F, Pham TD, Kessler JA, Gershon MD. Bone morphogenetic proteins regulate enteric gliogenesis by modulating ErbB3 signaling. *Dev. Biol.* 350: 64–79, 2011.
40. Chalazonitis A, Gershon MD, Greene LA. Cell death and the developing enteric nervous system. *Neurochem. Int.* 61: 839–847, 2012.
41. Chalazonitis A, Pham TD, Li Z, Roman D, Guha U, Gomes W, Kan L, Kessler JA, Gershon MD. Bone morphogenetic protein regulation of enteric neuronal phenotypic diversity: Relationship to timing of cell cycle exit. *J. Comp. Neurol.* 509: 474–492, 2008.
42. Chalazonitis A, Pham TD, Rothman TP, DiStefano PS, Bothwell M, Blair-Flynn J, Tessarollo L, Gershon MD. Neurotrophin-3 is required for the survival–differentiation of subsets of developing enteric neurons. *J. Neurosci.* 21: 5620–5636, 2001.
43. Chalazonitis A, Tennyson VM, Kibbey MC, Rothman TP, Gershon MD. The $\alpha 1$ subunit of laminin-1 promotes the development of neurons by interacting with LBP110 expressed by neural crest-derived cells immunoselected from the fetal mouse gut. *J. Neurobiol.* 33: 118–138, 1997.
44. Corpening JC, Cantrell VA, Deal KK, Southard-Smith EM. A Histone2BCerulean BAC transgene identifies differential expression of Phox2b in migrating enteric neural crest derivatives and enteric glia. *Dev. Dyn.* 237: 1119–1132, 2008.
45. Corpening JC, Deal KK, Cantrell VA, Skelton SB, Buehler DP, Southard-Smith EM. Isolation and live imaging of enteric progenitors based on Sox10-Histone2BVenus transgene expression. *genesis* 49: 599–618, 2011.
46. Crone SA, Negro A, Trumpp A, Giovannini M, Lee K-F. Colonic Epithelial Expression of ErbB2 Is Required for Postnatal Maintenance of the Enteric Nervous System. *Neuron* 37: 29–40, 2003.

47. D'Autréaux F, Margolis KG, Roberts J, Stevanovic K, Mawe G, Li Z, Karamooz N, Ahuja A, Morikawa Y, Cserjesi P, Setlick W, Gershon MD. Expression Level of Hand2 Affects Specification of Enteric Neurons and Gastrointestinal Function in Mice. *Gastroenterology* 141: 576–587.e6, 2011.
48. D'Autréaux F, Morikawa Y, Cserjesi P, Gershon MD. Hand2 is necessary for terminal differentiation of enteric neurons from crest-derived precursors but not for their migration into the gut or for formation of glia. *Development* 134: 2237–2249, 2007.
49. Delalande J-M, Barlow AJ, Thomas AJ, Wallace AS, Thapar N, Erickson CA, Burns AJ. The receptor tyrosine kinase RET regulates hindgut colonization by sacral neural crest cells. *Dev. Biol.* 313: 279–292, 2008.
50. Dessaud E, McMahon AP, Briscoe J. Pattern formation in the vertebrate neural tube: a sonic hedgehog morphogen-regulated transcriptional network. *Development* 135: 2489–2503, 2008.
51. Dettlaff-Swiercz DA, Wettschureck N, Moers A, Huber K, Offermanns S. Characteristic defects in neural crest cell-specific $G\alpha_q/G\alpha_{11}$ - and $G\alpha_{12}/G\alpha_{13}$ -deficient mice. *Dev. Biol.* 282: 174–182, 2005.
52. Le Douarin NM, Teillet M-A. The migration of neural crest cells to the wall of the digestive tract in avian embryo. *J. Embryol. Exp. Morphol.* 30: 31–48, 1973.
53. Druckenbrod NR, Epstein ML. The pattern of neural crest advance in the cecum and colon. *Dev. Biol.* 287: 125–133, 2005.
54. Druckenbrod NR, Epstein ML. Behavior of enteric neural crest-derived cells varies with respect to the migratory wavefront. *Dev. Dyn.* 236: 84–92, 2007.
55. Druckenbrod NR, Epstein ML. Age-dependent changes in the gut environment restrict the invasion of the hindgut by enteric neural progenitors. *Development* 136: 3195–3203, 2009.
56. Druckenbrod NR, Powers PA, Bartley CR, Walker JW, Epstein ML. Targeting of endothelin receptor-B to the neural crest. *genesis* 46: 396–400, 2008.
57. Durbec PL, Larsson-Blomberg LB, Schuchardt A, Costantini F, Pachnis V. Common origin and developmental dependence on c-ret of subsets of enteric and sympathetic neuroblasts. *Development* 122: 349–358, 1996.
58. Emison ES, McCallion AS, Kashuk CS, Bush RT, Grice E, Lin S, Portnoy ME, Cutler DJ, Green ED, Chakravarti A. A common sex-dependent mutation in a RET enhancer underlies Hirschsprung disease risk. *Nature* 434: 857–863, 2005.

59. Encinas M, Crowder RJ, Milbrandt J, Johnson EM. Tyrosine 981, a Novel Ret Autophosphorylation Site, Binds c-Src to Mediate Neuronal Survival. *J. Biol. Chem.* 279: 18262–18269, 2004.
60. Encinas M, Tansey MG, Tsui-Pierchala BA, Comella JX, Milbrandt J, Johnson EM. c-Src Is Required for Glial Cell Line-Derived Neurotrophic Factor (GDNF) Family Ligand-Mediated Neuronal Survival via a Phosphatidylinositol-3 Kinase (PI-3K)-Dependent Pathway. *J. Neurosci.* 21: 1464–1472, 2001.
61. Erickson CS, Zaitoun I, Haberman KM, Gosain A, Druckenbrod NR, Epstein ML. Sacral neural crest-derived cells enter the aganglionic colon of *Ednrb*^{-/-} mice along extrinsic nerve fibers. *J. Comp. Neurol.* 520: 620–632, 2012.
62. Faure C, Chalazonitis A, Rhéaume C, Bouchard G, Sampathkumar S -Gopala., Yarema KJ, Gershon MD. Gangliogenesis in the enteric nervous system: Roles of the polysialylation of the neural cell adhesion molecule and its regulation by bone morphogenetic protein-4. *Dev. Dyn.* 236: 44–59, 2007.
63. Fu M, Lui VCH, Sham MH, Cheung ANY, Tam PKH. HOXB5 expression is spatially and temporarily regulated in human embryonic gut during neural crest cell colonization and differentiation of enteric neuroblasts. *Dev. Dyn.* 228: 1–10, 2003.
64. Fu M, Lui VCH, Sham MH, Pachnis V, Tam PKH. Sonic hedgehog regulates the proliferation, differentiation, and migration of enteric neural crest cells in gut. *J. Cell Biol.* 166: 673–684, 2004.
65. Fu M, Sato Y, Lyons-Warren A, Zhang B, Kane MA, Napoli JL, Heuckeroth RO. Vitamin A facilitates enteric nervous system precursor migration by reducing Pten accumulation. *Development* 137: 631–640, 2010.
66. Fu M, Tam PKH, Sham MH, Lui VCH. Embryonic development of the ganglion plexuses and the concentric layer structure of human gut: a topographical study. *Anat. Embryol.* 208: 33–41, 2004.
67. Fu M, Vohra BP., Wind D, Heuckeroth RO. BMP signaling regulates murine enteric nervous system precursor migration, neurite fasciculation, and patterning via altered Ncam1 polysialic acid addition. *Dev. Biol.* 299: 137–150, 2006.
68. Fuchs S, Amiel J, Claudel S, Lyonnet S, Corvol P, Pinet F. Functional characterization of three mutations of the endothelin B receptor gene in patients with Hirschsprung's disease: evidence for selective loss of Gi coupling. *Mol. Med.* 7: 115–124, 2001.
69. Fuchs S, Herzog D, Sumara G, Büchmann-Møller S, Civenni G, Wu X, Chrostek-Grashoff A, Suter U, Ricci R, Relvas JB, Brakebusch C, Sommer L. Stage-Specific Control of Neural Crest Stem Cell Proliferation by the Small Rho GTPases Cdc42 and Rac1. *Cell Stem Cell* 4: 236–247, 2009.

70. Fukuda T, Kiuchi K, Takahashi M. Novel Mechanism of Regulation of Rac Activity and Lamellipodia Formation by RET Tyrosine Kinase. *J. Biol. Chem.* 277: 19114–19121, 2002.
71. Furness JB. *The enteric nervous system*. Malden, MA: Blackwell Publishing, 2006.
72. Gabriel SB, Salomon R, Pelet A, Angrist M, Amiel J, Fornage M, Attié-Bitach T, Olson JM, Hofstra R, Buys C, Steffann J, Munnich A, Lyonnet S, Chakravarti A. Segregation at three loci explains familial and population risk in Hirschsprung disease. *Nat. Genet.* 31: 89–93, 2002.
73. Garcia-Barcelo M, Ganster RW, Lui VCH, Leon TYY, So M-T, Lau AMF, Fu M, Sham M-H, Knight J, Zannini MS, Sham PC, Tam PKH. TTF-1 and RET promoter SNPs: regulation of RET transcription in Hirschsprung's disease. *Hum. Mol. Genet.* 14: 191–204, 2005.
74. Garcia-Barceló M-M, Fong P, Tang CS, Miao X, So M, Yuan Z, Li L, Guo W, Liu L, Wang B, Sun X-B, Huang L-M, Tou J-F, Wong KK-Y, Ngan ES-W, Lui VC, Cherny SS, Sham P, Tam PK. Mapping of a Hirschsprung's disease locus in 3p21. *Eur. J. Hum. Genet* 16: 833–840, 2008.
75. Garcia-Barceló M-M, Lau DK, Ngan ES, Leon TY, Liu T, So M, Miao X, Lui VC, Wong KK, Ganster RW, Cass DT, Croaker GDH, Tam PK. Evaluation of the Thyroid Transcription Factor-1 Gene (TITF1) as a Hirschsprung's Disease Locus. *Ann. Hum. Genet.* 71: 746–754, 2007.
76. Garcia-Barcelo M-M, Tang CS, Ngan ES, Lui VC, Chen Y, So M, Leon TY, Miao X, Shum CK, Liu F, Yeung M, Yuan Z, Guo W, Liu L, Sun X, Huang L, Tou J, Song Y, Chan D, Cheung KMC, Wong KK, Cherny SS, Sham P, Tam PK. Genome-wide association study identifies NRG1 as a susceptibility locus for Hirschsprung's disease. *Proc. Natl. Acad. Sci. U. S. A.* 106: 2694–2699, 2009.
77. Gargiulo A, Auricchio R, Barone MV, Cotugno G, Reardon W, Milla PJ, Ballabio A, Ciccodicola A, Auricchio A. Filamin A is mutated in X-linked chronic idiopathic intestinal pseudo-obstruction with central nervous system involvement. *Am. J. Hum. Genet.* 80: 751–758, 2007.
78. Gariépy CE, Williams SC, Richardson JA, Hammer RE, Yanagisawa M. Transgenic expression of the endothelin-B receptor prevents congenital intestinal aganglionosis in a rat model of Hirschsprung disease. *J. Clin. Invest.* 102: 1092–1101, 1998.
79. Gershon MD. Developmental determinants of the independence and complexity of the enteric nervous system. *Trends Neurosci.* 33: 446–456, 2010.
80. Gianino S, Grider JR, Cresswell J, Enomoto H, Heuckeroth RO. GDNF availability determines enteric neuron number by controlling precursor proliferation. *Development* 130: 2187–2198, 2003.

81. Goldstein A, Hofstra R, Burns A. Building a brain in the gut: development of the enteric nervous system. *Clin. Genet.* (November 20, 2012). doi: 10.1111/cge.12054.
82. Goldstein AM, Brewer KC, Doyle AM, Nagy N, Roberts DJ. BMP signaling is necessary for neural crest cell migration and ganglion formation in the enteric nervous system. *Mech. Dev.* 122: 821–833, 2005.
83. Govek E-E, Newey SE, Aelst LV. The role of the Rho GTPases in neuronal development. *Genes Dev.* 19: 1–49, 2005.
84. De Graaff E, Srinivas S, Kilkenny C, D’Agati V, Mankoo BS, Costantini F, Pachnis V. Differential activities of the RET tyrosine kinase receptor isoforms during mammalian embryogenesis. *Genes Dev.* 15: 2433–2444, 2001.
85. Guillemot F, Lo L-C, Johnson JE, Auerbach A, Anderson DJ, Joyner AL. Mammalian achaete-scute homolog 1 is required for the early development of olfactory and autonomic neurons. *Cell* 75: 463–476, 1993.
86. Hao MM, Anderson RB, Kobayashi K, Whittington PM, Young HM. The migratory behavior of immature enteric neurons. *Dev. Neurobiol.* 69: 22–35, 2009.
87. Hao MM, Boesmans W, Abbeel VV den, Jennings EA, Bornstein JC, Young HM, Berghe PV. Early emergence of neural activity in the developing mouse enteric nervous system. *J. Neurosci.* 31: 15352–15361, 2011.
88. Hao MM, Moore RE, Roberts RR, Nguyen T, Furness JB, Anderson RB, Young HM. The role of neural activity in the migration and differentiation of enteric neuron precursors. *Neurogastroenterol. Motil.* 22: e127–37, 2010.
89. Hao MM, Young HM. Development of enteric neuron diversity. *J. Cell. Mol. Med* 13: 1193–1210, 2009.
90. Heanue TA, Pachnis V. Enteric nervous system development and Hirschsprung’s disease: advances in genetic and stem cell studies. *Nat. Rev. Neurosci.* 8: 466–479, 2007.
91. Heanue TA, Pachnis V. Prospective Identification and Isolation of Enteric Nervous System Progenitors Using Sox2. *Stem Cells* 29: 128–140, 2011.
92. Hearn CJ, Murphy M, Newgreen D. GDNF and ET-3 differentially modulate the numbers of avian enteric neural crest cells and enteric neurons in vitro. *Dev. Biol.* 197: 93–105, 1998.
93. Hendershot TJ, Liu H, Sarkar AA, Giovannucci DR, Clouthier DE, Abe M, Howard MJ. Expression of Hand2 is sufficient for neurogenesis and cell type-specific gene expression in the enteric nervous system. *Dev. Dyn.* 236: 93–105, 2007.

94. Heuckeroth RO, Enomoto H, Grider JR, Golden JP, Hanke JA, Jackman A, Molliver DC, Bardgett ME, Snider WD, Johnson Jr. EM, Milbrandt J. Gene targeting reveals a critical role for Neurturin in the development and maintenance of enteric, sensory, and parasympathetic neurons. *Neuron* 22: 253–263, 1999.
95. Heuckeroth RO, Lampe PA, Johnson EM, Milbrandt J. Neurturin and GDNF promote proliferation and survival of enteric neuron and glial progenitors in vitro. *Dev. Biol.* 200: 116–129, 1998.
96. Hosoda K, Hammer RE, Richardson JA, Baynash AG, Cheung JC, Giaid A, Yanagisawa M. Targeted and natural (piebald-lethal) mutations of endothelin-B receptor gene produce megacolon associated with spotted coat color in mice. *Cell* 79: 1267–1276, 1994.
97. Hotta R, Anderson RB, Kobayashi K, Newgreen DF, Young HM. Effects of tissue age, presence of neurones and endothelin-3 on the ability of enteric neurone precursors to colonize recipient gut: implications for cell-based therapies. *Neurogastroenterol. Motil.* 22: 331–e86, 2010.
98. Hotta R, Natarajan D, Burns AJ, Thapar N. Stem cells for GI motility disorders. *Curr. Opin. Pharmacol.* 11: 617–623, 2011.
99. Hotta R, Pepdjonovic L, Anderson RB, Zhang D, Bergner AJ, Leung J, Pébay A, Young HM, Newgreen DF, Dottori M. Small-molecule induction of neural crest-like cells derived from human neural progenitors. *Stem Cells* 27: 2896–2905, 2009.
100. Imamura F, Arimoto I, Fujiyoshi Y, Doi T. W276 mutation in the endothelin receptor subtype B impairs Gq coupling but not Gi or Go coupling. *Biochemistry* 39: 686–692, 2000.
101. Jacobs-Cohen RJ, Payette RF, Gershon MD, Rothman TP. Inability of neural crest cells to colonize the presumptive aganglionic bowel of ls/ls mutant mice: Requirement for a permissive microenvironment. *J. Comp. Neurol.* 255: 425–438, 1987.
102. Jain S, Knoten A, Hoshi M, Wang H, Vohra B, Heuckeroth RO, Milbrandt J. Organotypic specificity of key RET adaptor-docking sites in the pathogenesis of neurocristopathies and renal malformations in mice. *J. Clin. Invest.* 120: 778–790, 2010.
103. Jiang Y, Liu M, Gershon MD. Netrins and DCC in the guidance of migrating neural crest-derived cells in the developing bowel and pancreas. *Dev. Biol.* 258: 364–384, 2003.
104. Jijiwa M, Fukuda T, Kawai K, Nakamura A, Kurokawa K, Murakumo Y, Ichihara M, Takahashi M. A targeting mutation of tyrosine 1062 in Ret causes a marked decrease of enteric neurons and renal hypoplasia. *Mol. Cell. Biol.* 24: 8026–8036, 2004.
105. Joseph NM, He S, Quintana E, Kim Y-G, Núñez G, Morrison SJ. Enteric glia are multipotent in culture but primarily form glia in the adult rodent gut. *J. Clin. Invest.* 121: 3398–3411, 2011.

106. Kapur RP, Livingston R, Doggett B, Sweetser DA, Siebert JR, Palmiter RD. Abnormal microenvironmental signals underlie intestinal aganglionosis in dominant megacolon mutant mice. *Dev. Biol.* 174: 360–369, 1996.
107. Kapur RP, Sweetser DA, Doggett B, Siebert JR, Palmiter RD. Intercellular signals downstream of endothelin receptor-B mediate colonization of the large intestine by enteric neuroblasts. *Development* 121: 3787–3795, 1995.
108. Kapur RP, Yost C, Palmiter RD. A transgenic model for studying development of the enteric nervous system in normal and aganglionic mice. *Development* 116: 167, 1992.
109. Kapur RP. Early death of neural crest cells is responsible for total enteric aganglionosis in Sox10Dom/Sox10Dom mouse embryos. *Pediatr. Dev. Pathol.* 2: 559–569, 1999.
110. Kapur RP. Colonization of the murine hindgut by sacral crest-derived neural precursors: experimental support for an evolutionarily conserved model. *Dev. Biol.* 227: 146–155, 2000.
111. Kapur RP. Practical pathology and genetics of Hirschsprung’s disease. *Semin. Pediatr. Surg.* 18: 212–223, 2009.
112. Kim J, Lo L, Dormand E, Anderson DJ. SOX10 Maintains Multipotency and Inhibits Neuronal Differentiation of Neural Crest Stem Cells. *Neuron* 38: 17–31, 2003.
113. Korbel JO, Tirosch-Wagner T, Urban AE, Chen X-N, Kasowski M, Dai L, Grubert F, Erdman C, Gao MC, Lange K, Sobel EM, Barlow GM, Aylsworth AS, Carpenter NJ, Clark RD, Cohen MY, Doran E, Falik-Zaccari T, Lewin SO, Lott IT, McGillivray BC, Moeschler JB, Pettenati MJ, Puschel SM, Rao KW, Shaffer LG, Shohat M, Van Riper AJ, Warburton D, Weissman S, Gerstein MB, Snyder M, Korenberg JR. The genetic architecture of Down syndrome phenotypes revealed by high-resolution analysis of human segmental trisomies. *Proc. Natl. Acad. Sci. U. S. A.* 106: 12031–12036, 2009.
114. Kriegstein A, Alvarez-Buylla A. The glial nature of embryonic and adult neural stem cells. *Annu. Rev. Neurosci.* 32: 149–184, 2009.
115. Kruger GM, Mosher JT, Bixby S, Joseph N, Iwashita T, Morrison SJ. Neural crest stem cells persist in the adult gut but undergo changes in self-renewal, neuronal subtype potential, and factor responsiveness. *Neuron* 35: 657–669, 2002.
116. Kruger GM, Mosher JT, Tsai Y-H, Yeager KJ, Iwashita T, Garipey CE, Morrison SJ. Temporally distinct requirements for endothelin receptor b in the generation and migration of gut neural crest stem cells. *Neuron* 40: 917–929, 2003.
117. Lane PW, Liu HM. Association of megacolon with a new dominant spotting gene (Dom) in the mouse. *J. Hered.* 75: 435–439, 1984.

118. Lang D, Chen F, Milewski R, Li J, Lu MM, Epstein JA. Pax3 is required for enteric ganglia formation and functions with Sox10 to modulate expression of c-ret. *J. Clin. Invest.* 106: 963–971, 2000.
119. Lang D, Epstein JA. Sox10 and Pax3 physically interact to mediate activation of a conserved c-RET enhancer. *Hum. Mol. Genet.* 12: 937–945, 2003.
120. Laranjeira C, Pachnis V. Enteric nervous system development: Recent progress and future challenges. *Auton. Neurosci.* 151: 61–69, 2009.
121. Laranjeira C, Sandgren K, Kessar N, Richardson W, Potocnik A, Vanden Berghe P, Pachnis V. Glial cells in the mouse enteric nervous system can undergo neurogenesis in response to injury. *J. Clin. Invest.* 121: 3412–3424, 2011.
122. Larsson LT, Okmian L, Kristoffersson U. No correlation between hyperthermia during pregnancy and Hirschsprung disease in the offspring. *Am. J. Med. Genet.* 32: 260–261, 1989.
123. Lei J, Howard MJ. Targeted deletion of Hand2 in enteric neural precursor cells affects its functions in neurogenesis, neurotransmitter specification and gangliogenesis, causing functional aganglionosis. *Development* 138: 4789–4800, 2011.
124. Leon TYY, Ngan ESW, Hiu-Ching Poon, So M-T, Lui VCH, Tam PKH, Garcia-Barcelo MM. Transcriptional regulation of RET by Nkx2-1, Phox2b, Sox10, and Pax3. *J. Pediatr. Surg.* 44: 1904–1912, 2009.
125. Li Z, Caron MG, Blakely RD, Margolis KG, Gershon MD. Dependence of Serotonergic and Other Nonadrenergic Enteric Neurons on Norepinephrine Transporter Expression. *J. Neurosci.* 30: 16730–16740, 2010.
126. Li Z, Chalazonitis A, Huang Y, Mann JJ, Margolis KG, Yang QM, Kim DO, Côté F, Mallet J, Gershon MD. Essential roles of enteric neuronal serotonin in gastrointestinal motility and the development/survival of enteric dopaminergic neurons. *J. Neurosci.* 31: 8998–9009, 2011.
127. Lindley RM, Hawcutt DB, Connell MG, Almond SN, Vannucchi M, Fausson-Pellegrini MS, Edgar DH, Kenny SE. Human and mouse enteric nervous system neurosphere transplants regulate the function of aganglionic embryonic distal colon. *Gastroenterology* 135: 205–216.e6, 2008.
128. Lipson A. Hirschsprung disease in the offspring of mothers exposed to hyperthermia during pregnancy. *Am. J. Med. Genet.* 29: 117–124, 1988.
129. Liu H, Margiotta JF, Howard MJ. BMP4 supports noradrenergic differentiation by a PKA-dependent mechanism. *Dev. Biol.* 286: 521–536, 2005.

130. Liu M-T, Kuan Y-H, Wang J, Hen R, Gershon MD. 5-HT₄ receptor-mediated neuroprotection and neurogenesis in the enteric nervous system of adult mice. *J. Neurosci.* 29: 9683–9699, 2009.
131. Lui VCH, Cheng WWC, Leon TYY, Lau DKC, Garcia-Bareclo M, Miao XP, Kam MKM, So MT, Chen Y, Wall NA, Sham MH, Tam PKH. Perturbation of Hoxb5 signaling in vagal neural crests down-regulates Ret leading to intestinal hypoganglionosis in mice. *Gastroenterology* 134: 1104–1115, 2008.
132. Lyons DA, Naylor SG, Mercurio S, Dominguez C, Talbot WS. KBP is essential for axonal structure, outgrowth and maintenance in zebrafish, providing insight into the cellular basis of Goldberg-Shprintzen syndrome. *Development* 135: 599–608, 2008.
133. Maka M, Claus Stolt C, Wegner M. Identification of Sox8 as a modifier gene in a mouse model of Hirschsprung disease reveals underlying molecular defect. *Dev. Biol.* 277: 155–169, 2005.
134. Margolis KG, Stevanovic K, Karamooz N, Li ZS, Ahuja A, D’Autréaux F, Saurman V, Chalazonitis A, Gershon MD. Enteric neuronal density contributes to the severity of intestinal inflammation. *Gastroenterology* 141: 588–598.e2, 2011.
135. McCallion A, Emison E, Kashuk C, Bush R, Kenton M, Carrasquillo M, Jones K, Kennedy G, Portnoy M, Green E, others. Genomic variation in multigenic traits: Hirschsprung disease. In: *Cold Spring Harbor symposia on quantitative biology*. 2003, p. 373–382.
136. McCallion AS, Stames E, Conlon RA, Chakravarti A. Phenotype variation in two-locus mouse models of Hirschsprung disease: Tissue-specific interaction between Ret and Ednr β . *Proc. Natl. Acad. Sci. U. S. A.* 100: 1826–1831, 2003.
137. McKeown SJ, Lee VM, Bronner-Fraser M, Newgreen DF, Farlie PG. Sox10 overexpression induces neural crest-like cells from all dorsoventral levels of the neural tube but inhibits differentiation. *Dev. Dyn.* 233: 430–444, 2005.
138. Metzger M, Bareiss PM, Danker T, Wagner S, Hennenlotter J, Guenther E, Obermayr F, Stenzl A, Koenigsrainer A, Skutella T, Just L. Expansion and differentiation of neural progenitors derived from the human adult enteric nervous system. *Gastroenterology* 137: 2063–2073.e4, 2009.
139. Metzger M, Caldwell C, Barlow AJ, Burns AJ, Thapar N. Enteric nervous system stem cells derived from human gut mucosa for the treatment of aganglionic gut disorders. *Gastroenterology* 136: 2214–2225.e3, 2009.
140. Metzger M. Neurogenesis in the enteric nervous system. *Arch. Ital. Biol.* 148: 73–83, 2010.

141. Micci M, Kahrig K, Simmons R, Sarna S, Espejonavarro M, Pasricha P. Neural stem cell transplantation in the stomach rescues gastric function in neuronal nitric oxide synthase-deficient mice. *Gastroenterology* 129: 1817–1824, 2005.
142. Miyamoto R, Jijiwa M, Asai M, Kawai K, Ishida-Takagishi M, Mii S, Asai N, Enomoto A, Murakumo Y, Yoshimura A, Takahashi M. Loss of Sprouty2 partially rescues renal hypoplasia and stomach hypoganglionosis but not intestinal aganglionosis in Ret Y1062F mutant mice. *Dev. Biol.* 349: 160–168, 2011.
143. Nagy N, Goldstein AM. Endothelin-3 regulates neural crest cell proliferation and differentiation in the hindgut enteric nervous system. *Dev. Biol.* 293: 203–217, 2006.
144. Nataf V, Lecoin L, Eichmann A, Le Douarin NM. Endothelin-B receptor is expressed by neural crest cells in the avian embryo. *Proc. Natl. Acad. Sci. U. S. A.* 93: 9645, 1996.
145. Natarajan D, Grigoriou M, Marcos-Gutierrez CV, Atkins C, Pachnis V. Multipotential progenitors of the mammalian enteric nervous system capable of colonising aganglionic bowel in organ culture. *Development* 126: 157–168, 1999.
146. Natarajan D, Marcos-Gutierrez C, Pachnis V, de Graaff E. Requirement of signalling by receptor tyrosine kinase RET for the directed migration of enteric nervous system progenitor cells during mammalian embryogenesis. *Development* 129: 5151–5160, 2002.
147. Newgreen DF, Hartley L. Extracellular matrix and adhesive molecules in the early development of the gut and its innervation in normal and spotting lethal rat embryos. *Acta Anat (Basel)* 154: 243–260, 1995.
148. Niederreither K, Vermot J, Roux IL, Schuhbauer B, Chambon P, Dollé P. The regional pattern of retinoic acid synthesis by RALDH2 is essential for the development of posterior pharyngeal arches and the enteric nervous system. *Development* 130: 2525–2534, 2003.
149. Nijenhuis CM, ter Horst PGJ, van Rein N, Wilffert B, de Jong-van den Berg LTW. Disturbed development of the enteric nervous system after in utero exposure of selective serotonin re-uptake inhibitors and tricyclic antidepressants. Part 2: Testing the hypotheses. *Br. J. Clin. Pharmacol.* 73: 126–134, 2012.
150. Nishino J, Saunders TL, Sagane K, Morrison SJ. Lgi4 promotes the proliferation and differentiation of glial lineage cells throughout the developing peripheral nervous system. *J. Neurosci.* 30: 15228–15240, 2010.
151. Nishiyama C, Uesaka T, Manabe T, Yonekura Y, Nagasawa T, Newgreen DF, Young HM, Enomoto H. Trans-mesenteric neural crest cells are the principal source of the colonic enteric nervous system. *Nat. Neurosci.* 15: 1211–1218, 2012.
152. Nunez-Torres R, Fernandez R, Acosta MJ, del Valle Enguix-Riego M, Marba M, de Agustin JC, Castano L, Antinolo G, Borrego S. Comprehensive analysis of RET common and

rare variants in a series of Spanish Hirschsprung patients confirms a synergistic effect of both kinds of events. *BMC Med. Gen.* 12: 138, 2011.

153. Okamura Y, Saga Y. Notch signaling is required for the maintenance of enteric neural crest progenitors. *Development* 135: 3555–3565, 2008.

154. Pattyn A, Morin X, Cremer H, Goridis C, Brunet J-F. The homeobox gene *Phox2b* is essential for the development of autonomic neural crest derivatives. *Nature* 399: 366–370, 1999.

155. Pavan WJ, Liddell RA, Wright A, Thibaudeau G, Matteson PG, McHugh KM, Siracusa LD. A high-resolution linkage map of the lethal spotting locus: a mouse model for Hirschsprung disease. *Mamm. Genome* 6: 1–7, 1995.

156. Pham TD, Gershon MD, Rothman TP. Time of origin of neurons in the murine enteric nervous system: Sequence in relation to phenotype. *J. Comp. Neurol.* 314: 789–798, 1991.

157. Pingault V, Bondurand N, Kuhlbrodt K, Goerich DE, Prehu M-O, Puliti A, Herbarth B, Hermans-Borgmeyer I, Legius E, Matthijs G, Amiel J, Lyonnet S, Ceccherini I, Romeo G, Smith JC, Read AP, Wegner M, Goossens M. *SOX10* mutations in patients with Waardenburg-Hirschsprung disease. *Nat Genet* 18: 171–173, 1998.

158. Pingault V, Ente D, Dastot-Le Moal F, Goossens M, Marlin S, Bondurand N. Review and update of mutations causing Waardenburg syndrome. *Hum. Mutat.* 31: 391–406, 2010.

159. Pini Prato A, Rossi V, Avanzini S, Mattioli G, Disma N, Jasonni V. Hirschsprung's disease: what about mortality? *Pediatr. Surg. Int.* 27: 473–478, 2011.

160. De Pontual L, Pelet A, Clement-Ziza M, Trochet D, Antonarakis SE, Attie-Bitach T, Beales PL, Blouin J-L, Moal FD-L, Dollfus H, Goossens M, Katsanis N, Touraine R, Feingold J, Munnich A, Lyonnet S, Amiel J. Epistatic interactions with a common hypomorphic *RET* allele in syndromic Hirschsprung disease. *Hum. Mutat.* 28: 790–796, 2007.

161. Puffenberger EG, Hosoda K, Washington SS, Nakao K, deWit D, Yanagisawa M, Chakravarti A. A missense mutation of the endothelin-B receptor gene in multigenic hirschsprung's disease. *Cell* 79: 1257–1266, 1994.

162. Puig I, Champeval D, De Santa Barbara P, Jaubert F, Lyonnet S, Larue L. Deletion of *Pten* in the mouse enteric nervous system induces ganglioneuromatosis and mimics intestinal pseudoobstruction. *J. Clin. Invest.* 119: 3586–3596, 2009.

163. Van de Putte T, Francis A, Nelles L, van Grunsven LA, Huylebroeck D. Neural crest-specific removal of *Zfhx1b* in mouse leads to a wide range of neurocristopathies reminiscent of Mowat-Wilson syndrome. *Hum. Mol. Genet.* 16: 1423–1436, 2007.

164. Van de Putte T, Maruhashi M, Francis A, Nelles L, Kondoh H, Huylebroeck D, Higashi Y. Mice lacking *Zfhx1b*, the gene that codes for SMAD-interacting protein-1, reveal a role for

multiple neural crest cell defects in the etiology of Hirschsprung disease–mental retardation syndrome. *Am. J. Hum. Genet.* 72: 465–470, 2003.

165. Ramalho-Santos M, Melton DA, McMahon AP. Hedgehog signals regulate multiple aspects of gastrointestinal development. *Development* 127: 2763–2772, 2000.

166. Ratcliffe EM, D’Autréaux F, Gershon MD. Laminin terminates the Netrin/DCC mediated attraction of vagal sensory axons. *Dev. Neurobiol.* 68: 960–971, 2008.

167. Ratcliffe EM, Fan L, Mohammed TJ, Anderson M, Chalazonitis A, Gershon MD. Enteric neurons synthesize netrins and are essential for the development of the vagal sensory innervation of the fetal gut. *Dev. Neurobiol.* 71: 362–373, 2011.

168. Ross AJ, May-Simera H, Eichers ER, Kai M, Hill J, Jagger DJ, Leitch CC, Chapple JP, Munro PM, Fisher S, Tan PL, Phillips HM, Leroux MR, Henderson DJ, Murdoch JN, Copp AJ, Eliot M-M, Lupski JR, Kemp DT, Dollfus H, Tada M, Katsanis N, Forge A, Beales PL. Disruption of Bardet-Biedl syndrome ciliary proteins perturbs planar cell polarity in vertebrates. *Nat. Genet.* 37: 1135–1140, 2005.

169. Rossi J, Luukko K, Poteryaev D, Laurikainen A, Sun YF, Laakso T, Eerikäinen S, Tuominen R, Lakso M, Rauvala H, Arumäe U, Pasternack M, Saarma M, Airaksinen MS. Retarded growth and deficits in the enteric and parasympathetic nervous system in mice lacking GFR α 2, a functional neurturin receptor. *Neuron* 22: 243–252, 1999.

170. Rovasio R, Delouree A, Yamada K, Timpl R, Thiery J. Neural crest cell migration: requirements for exogenous fibronectin and high cell density. *J. Cell Biol.* 96: 462–473, 1983.

171. Ruiz-Ferrer M, Torroglosa A, Núñez-Torres R, de Agustín JC, Antiñolo G, Borrego S. Expression of PROKR1 and PROKR2 in human enteric neural precursor cells and identification of sequence variants suggest a role in HSCR. *PLoS ONE* 6: e23475, 2011.

172. Sánchez MP, Silos-Santiago I, Frisé J, He B, Lira SA, Barbacid M. Renal agenesis and the absence of enteric neurons in mice lacking GDNF. *Nature* 382: 70–73, 1996.

173. Sasselli V, Boesmans W, Berghe PV, Tissir F, Goffinet AM, Pachnis V. Planar cell polarity genes control the connectivity of enteric neurons. *J. Clin. Invest.* (March 8, 2013). doi: 10.1172/JCI66759.

174. Sato Y, Heuckeroth RO. Retinoic acid regulates murine enteric nervous system precursor proliferation, enhances neuronal precursor differentiation, and reduces neurite growth in vitro. *Dev. Biol.* 320: 185–198, 2008.

175. Schuchardt A, D’Agati V, Larsson-Blomberg L, Costantini F, Pachnis V. Defects in the kidney and enteric nervous system of mice lacking the tyrosine kinase receptor Ret. *Nature* 367: 380–383, 1994.

176. Selfridge J, Song L, Brownstein DG, Melton DW. Mice with DNA repair gene *Erccl* deficiency in a neural crest lineage are a model for late-onset Hirschsprung disease. *DNA Repair* 9: 653–660, 2010.
177. Shimotake T, Go S, Inoue K, Tomiyama H, Iwai N. A homozygous missense mutation in the tyrosine kinase domain of the RET proto-oncogene in an infant with total intestinal aganglionosis. *Am. J. Physiol. Gastrointest. Liver Physiol.* 96: 1286–1291, 2001.
178. Shin MK, Levorse JM, Ingram RS, Tilghman SM. The temporal requirement for endothelin receptor-B signalling during neural crest development. *Nature* 402: 496–501, 1999.
179. Shirasawa S, Yunker AMR, Roth KA, Brown GA, Horning S, Korsmeyer SJ. *Enx* (*Hox11L1*)-deficient mice develop myenteric neuronal hyperplasia and megacolon. *Nat. Med.* 3: 646–650, 1997.
180. Simpson MJ, Landman KA, Hughes BD. Looking inside an invasion wave of cells using continuum models: proliferation is the key. *J. Theor. Biol.* 243: 343–360, 2006.
181. Simpson MJ, Zhang DC, Mariani M, Landman KA, Newgreen DF. Cell proliferation drives neural crest cell invasion of the intestine. *Dev. Biol.* 302: 553–568, 2007.
182. Srinivasan S, Anitha M, Mwangi S, Heuckeroth RO. Enteric neuroblasts require the phosphatidylinositol 3-kinase/Akt/Forkhead pathway for GDNF-stimulated survival. *Mol. Cell. Neurosci.* 29: 107–119, 2005.
183. Stanchina L, Baral V, Robert F, Pingault V, Lemort N, Pachnis V, Goossens M, Bondurand N. Interactions between *Sox10*, *Edn3* and *Ednrb* during enteric nervous system and melanocyte development. *Dev. Biol.* 295: 232–249, 2006.
184. Stanchina L, Van de Putte T, Goossens M, Huylebroeck D, Bondurand N. Genetic interaction between *Sox10* and *Zfhx1b* during enteric nervous system development. *Dev. Biol.* 341: 416–428, 2010.
185. Stewart AL, Young HM, Popoff M, Anderson RB. Effects of pharmacological inhibition of small GTPases on axon extension and migration of enteric neural crest-derived cells. *Dev. Biol.* 307: 92–104, 2007.
186. Suárez-Rodríguez R, Belkind-Gerson J. Cultured Nestin-Positive Cells from Postnatal Mouse Small Bowel Differentiate Ex Vivo into Neurons, Glia, and Smooth Muscle. *Stem Cells* 22: 1373–1385, 2004.
187. Sukegawa A, Narita T, Kameda T, Saitoh K, Nohno T, Iba H, Yasugi S, Fukuda K. The concentric structure of the developing gut is regulated by Sonic hedgehog derived from endodermal epithelium. *Development* 127: 1971–1980, 2000.

188. Takahashi M, Iwashita T, Santoro M, Lyonnet S, Lenoir GM, Billaud M. Co-segregation of MEN2 and Hirschsprung's disease: The same mutation of RET with both gain and loss-of-function? *Hum. Mutat.* 13: 331–336, 1999.
189. Taketomi T, Yoshiga D, Taniguchi K, Kobayashi T, Nonami A, Kato R, Sasaki M, Sasaki A, Ishibashi H, Moriyama M, Nakamura K, Nishimura J, Yoshimura A. Loss of mammalian Sprouty2 leads to enteric neuronal hyperplasia and esophageal achalasia. *Nat Neurosci* 8: 855–857, 2005.
190. Tang CS, Sribudiani Y, Miao XP, Vries AR, Burzynski G, So MT, Leon YY, Yip BH, Osinga J, Hui KJWS, Verheij JBG, Cherny SS, Tam PKH, Sham PC, Hofstra RMW, Garcia-Barceló MM. Fine mapping of the 9q31 Hirschsprung's disease locus. *Hum. Genet.* 127: 675–683, 2010.
191. Tang CS-M, Cheng G, So M-T, Yip BH-K, Miao X-P, Wong EH-M, Ngan ES-W, Lui VC-H, Song Y-Q, Chan D, Cheung K, Yuan Z-W, Lei L, Chung PH-Y, Liu X-L, Wong KK-Y, Marshall CR, Scherer S, Cherny SS, Sham P-C, Tam PK-H, Garcia-Barceló M-M. Genome-wide copy number analysis uncovers a new HSCR gene: NRG3. *PLoS Genetics* 8: e1002687, 2012.
192. Taraviras S, Marcos-Gutierrez CV, Durbec P, Jani H, Grigoriou M, Sukumaran M, Wang LC, Hynes M, Raisman G, Pachnis V. Signalling by the RET receptor tyrosine kinase and its role in the development of the mammalian enteric nervous system. *Development* 126: 2785–2797, 1999.
193. Thiery JP, Duband JL, Tucker GC. Cell Migration in the Vertebrate Embryo: Role of Cell Adhesion and Tissue Environment in Pattern Formation. *Annu. Rev. Cell. Biol.* 1: 91–113, 1985.
194. Tobin JL, Di Franco M, Eichers E, May-Simera H, Garcia M, Yan J, Quinlan R, Justice MJ, Hennekam RC, Briscoe J, Tada M, Mayor R, Burns AJ, Lupski JR, Hammond P, Beales PL. Inhibition of neural crest migration underlies craniofacial dysmorphology and Hirschsprung's disease in Bardet–Biedl syndrome. *Proc. Natl. Acad. Sci. U. S. A.* 105: 6714–6719, 2008.
195. Torfs CP, Christianson RE. Maternal risk factors and major associated defects in infants with Down syndrome. *Epidemiology* 10: 264–270, 1999.
196. Tsai Y -H, Murakami N, Garipey CE. Postnatal intestinal engraftment of prospectively selected enteric neural crest stem cells in a rat model of Hirschsprung disease. *Neurogastroenterol. Motil.* 23: 362–369, 2011.
197. Uesaka T, Enomoto H. Neural precursor death is central to the pathogenesis of intestinal aganglionosis in ret hypomorphic mice. *J. Neurosci* 30: 5211–5218, 2010.
198. Uesaka T, Jain S, Yonemura S, Uchiyama Y, Milbrandt J, Enomoto H. Conditional ablation of GFR α 1 in postmigratory enteric neurons triggers unconventional neuronal death in the colon and causes a Hirschsprung's disease phenotype. *Development* 134: 2171–2181, 2007.

199. Uesaka T, Nagashimada M, Yonemura S, Enomoto H. Diminished Ret expression compromises neuronal survival in the colon and causes intestinal aganglionosis in mice. *J. Clin. Invest.* 118: 1890–1898, 2008.
200. Viader A, Wright-Jin EC, Vohra BPS, Heuckeroth RO, Milbrandt J. Differential regional and subtype-specific vulnerability of enteric neurons to mitochondrial dysfunction. *PLoS ONE* 6: e27727, 2011.
201. Vohra BP., Tsuji K, Nagashimada M, Uesaka T, Wind D, Fu M, Armon J, Enomoto H, Heuckeroth RO. Differential gene expression and functional analysis implicate novel mechanisms in enteric nervous system precursor migration and neuritogenesis. *Dev. Biol.* 298: 259–271, 2006.
202. Vohra BPS, Fu M, Heuckeroth RO. Protein kinase C ζ and glycogen synthase kinase-3 β control neuronal polarity in developing rodent enteric neurons, whereas SMAD specific E3 ubiquitin protein ligase 1 promotes neurite growth but does not influence polarity. *J. Neurosci.* 27: 9458–9468, 2007.
203. Vohra BPS, Planer W, Armon J, Fu M, Jain S, Heuckeroth RO. Reduced endothelin converting enzyme-1 and endothelin-3 mRNA in the developing bowel of male mice may increase expressivity and penetrance of Hirschsprung disease-like distal intestinal aganglionosis. *Dev. Dyn.* 236: 106–117, 2007.
204. Wakamatsu N, Yamada Y, Yamada K, Ono T, Nomura N, Taniguchi H, Kitoh H, Mutoh N, Yamanaka T, Mushiake K, Kato K, Sonta S, Nagaya M. Mutations in SIP1, encoding Smad interacting protein-1, cause a form of Hirschsprung disease. *Nat. Genet.* 27: 369–370, 2001.
205. Wallace AS, Barlow AJ, Navaratne L, Delalande J-M, Tauszig-Delamasure S, Corset V, Thapar N, Burns AJ. Inhibition of cell death results in hyperganglionosis: implications for enteric nervous system development. *Neurogastroenterol. Motil.* 21: 768–e49, 2009.
206. Wallace AS, Schmidt C, Schachner M, Wegner M, Anderson RB. L1cam acts as a modifier gene during enteric nervous system development. *Neurobiology of Disease* 40: 622–633, 2010.
207. Walters LC, Cantrell VA, Weller KP, Mosher JT, Southard-Smith EM. Genetic background impacts development potential of enteric neural crest-derived progenitors in the Sox10Dom model of Hirschsprung disease. *Hum. Mol. Genet.* .
208. Wang H, Hughes I, Planer W, Parsadonian A, Grider JR, Vohra BP., Keller-Peck C, Heuckeroth RO. The Timing and Location of Glial Cell Line-Derived Neurotrophic Factor Expression Determine Enteric Nervous System Structure and Function. *J. Neurosci.* 30: 1523, 2010.

209. Wang X, Chan AKK, Sham M-H, Burns AJ, Chan WY. Analysis of the sacral neural crest cell contribution to the hindgut enteric nervous system in the mouse embryo. *Gastroenterology* 141: 992–1002.e6, 2011.
210. Wolgemuth DJ, Behringer RR, Mostoller MP, Brinster RL, Palmiter RD. Transgenic mice overexpressing the mouse homoeobox-containing gene Hox-1.4 exhibit abnormal gut development. *Nature* 337: 464–467, 1989.
211. Wong A, Bogni S, Kotka P, de Graaff E, D’Agati V, Costantini F, Pachnis V. Phosphotyrosine 1062 Is Critical for the In Vivo Activity of the Ret9 Receptor Tyrosine Kinase Isoform. *Mol. Cell Biol.* 25: 9661–9673, 2005.
212. Woodward MN, Kenny SE, Vaillant C, Lloyd DA, Edgar DH. Time-dependent effects of endothelin-3 on enteric nervous system development in an organ culture model of hirschsprung’s disease. *J. Pediatr. Surg.* 35: 25–29, 2000.
213. Wu JJ, Chen JX, Rothman TP, Gershon MD. Inhibition of in vitro enteric neuronal development by endothelin-3: mediation by endothelin B receptors. *Development* 126: 1161–1173, 1999.
214. Yamakawa K, Huot Y, Haendelt M, Hubert R, Chen X, Lyons G, Korenberg J. DSCAM: a novel member of the immunoglobulin superfamily maps in a Down syndrome region and is involved in the development of the nervous system. *Hum. Mol. Genet.* 7: 227–237, 1998.
215. Yanagisawa H, Yanagisawa M, Kapur RP, Richardson JA, Williams SC, Clouthier DE, de Wit D, Emoto N, Hammer RE. Dual genetic pathways of endothelin-mediated intercellular signaling revealed by targeted disruption of endothelin converting enzyme-1 gene. *Development* 125: 825–836, 1998.
216. Yang JT, Liu CZ, Villavicencio EH, Yoon JW, Walterhouse D, Iannaccone PM. Expression of human GLI in mice results in failure to thrive, early death, and patchy Hirschsprung-like gastrointestinal dilatation. *Mol. Med.* 3: 826–835, 1997.
217. Yntema CL, Hammond WS. The origin of intrinsic ganglia of trunk viscera from vagal neural crest in the chick embryo. *J. Comp. Neurol.* 101: 515–541, 1954.
218. Young HM, Bergner AJ, Anderson RB, Enomoto H, Milbrandt J, Newgreen DF, Whittington PM. Dynamics of neural crest-derived cell migration in the embryonic mouse gut. *Dev. Biol.* 270: 455–473, 2004.
219. Young HM, Hearn CJ, Farlie PG, Canty AJ, Thomas PQ, Newgreen DF. GDNF is a chemoattractant for enteric neural cells. *Dev. Biol.* 229: 503–516, 2001.
220. Young HM, Jones BR, McKeown SJ. The projections of early enteric neurons are influenced by the direction of neural crest cell migration. *J. Neurosci.* 22: 6005–6018, 2002.

221. Young HM, Turner KN, Bergner AJ. The location and phenotype of proliferating neural-crest-derived cells in the developing mouse gut. *Cell Tissue Res.* 320: 1–9, 2005.
222. Zehir A, Hua LL, Maska EL, Morikawa Y, Cserjesi P. Dicer is required for survival of differentiating neural crest cells. *Dev. Biol.* 340: 459–467, 2010.
223. Zhang B, Chang J, Fu M, Huang J, Kashyap R, Salavaggione E, Jain S, Shashikant K, Deardorff MA, Uzielli MLG, Dorsett D, Beebe DC, Jay PY, Heuckeroth RO, Krantz I, Milbrandt J. Dosage effects of cohesin regulatory factor Pds5 on mammalian development: implications for cohesinopathies. *PLoS ONE* 4: e5232, 2009.
224. Zhang B, Jain S, Song H, Fu M, Heuckeroth RO, Erlich JM, Jay PY, Milbrandt J. Mice lacking sister chromatid cohesion protein PDS5B exhibit developmental abnormalities reminiscent of Cornelia de Lange syndrome. *Development* 134: 3191–3201, 2007.
225. Zhang Y, Kim T-H, Niswander L. Phactr4 regulates directional migration of enteric neural crest through PP1, integrin signaling, and cofilin activity. *Genes Dev.* 26: 69–81, 2012.
226. Zhou R, Niwa S, Homma N, Takei Y, Hirokawa N. KIF26A is an unconventional kinesin and regulates GDNF-RET signaling in enteric neuronal development. *Cell* 139: 802–813, 2009.
227. Zhu J, Garcia-Barcelo M-M, Tam PKH, Lui VCH. HOXB5 cooperates with NKX2-1 in the transcription of human RET. *PLoS ONE* 6: e20815, 2011.
228. Zhu L, Lee H-O, Jordan CS, Cantrell VA, Southard-Smith EM, Shin MK. Spatiotemporal regulation of endothelin receptor-B by SOX10 in neural crest-derived enteric neuron precursors. *Nat. Genet.* 36: 732–737, 2004.

Chapter 3: Hirschsprung-like disease is exacerbated by reduced de novo GMP synthesis

This chapter describes the rationale and results of our broad attempt to detect environmental factors that impair enteric nervous system (ENS) development using a chemical screen in zebrafish. This screen led to the detection of several inhibitors of ENS development including mycophenolic acid. The systemic effects of MPA and its prodrug mycophenolate mofetil (MMF) on ENS development were then confirmed in the mouse, and we demonstrated using in vivo and primary culture systems that MPA impairs ENS development primarily through its antiproliferative effects on enteric neural crest-derived cells (ENCDCs). Finally, we demonstrate a profound gene-environment interaction between mouse mutation models of Hirschsprung disease and MMF exposure, the first demonstration that Hirschsprung disease phenotypes can be enhanced by an environmental exposure.

Since these experiments indicate that MPA/MMF exerts its antiproliferative effects on ENCDCs through its inhibition of inosine 5'-monophosphate dehydrogenase (IMPDH) and de novo guanine nucleotide synthesis, these experiments also form the rationale for our subsequent investigations into the *Impdh2* gene in the developing mouse ENS and the possible association between the *IMPDH2* gene and human Hirschsprung disease.

The contents of this chapter have been published: Lake JI, Tusheva OA, Graham BL, Heuckeroth RO. Hirschsprung-like disease is exacerbated by reduced de novo GMP synthesis. *The Journal of Clinical Investigation* 2013;123(11):4875–4887.

3.1 Summary

Hirschsprung disease is a partially penetrant oligogenic birth defect that occurs if enteric nervous system (ENS) precursors fail to colonize distal bowel during early pregnancy. We hypothesized that non-genetic factors might contribute to this disease. Here we show that mycophenolate, an inhibitor of *de novo* guanine nucleotide biosynthesis, and eight other drugs identified using a zebrafish screen impair ENS development. Murine studies *in vivo* confirm that mycophenolate selectively impairs ENS precursor proliferation, delays precursor migration, induces bowel aganglionosis, and increases the penetrance and severity of Hirschsprung-like pathology in *Sox10* and *Ret* mutant mice. Mycophenolate also reduces ENS precursor migration, lamellipodia formation, proliferation, and survival *in vitro*. Using X-inactivation mosaicism for the purine salvage gene *Hprt*, we show that reduced ENS precursor proliferation most likely causes mycophenolate-induced migration defects and aganglionosis. Mycophenolate is the first medicine identified that causes major ENS malformations and Hirschsprung-like pathology. These studies demonstrate a critical role for *de novo* guanine nucleotide biosynthesis in enteric nervous system development and suggest that some cases of Hirschsprung disease may be preventable.

3.2 Introduction

Hirschsprung disease (HSCR) is a common (1 in 5000) birth defect where the enteric nervous system is missing from distal bowel (aganglionosis). Because the ENS controls intestinal motility, HSCR causes severe constipation, abdominal distension, bilious vomiting, growth

failure and life-threatening infection (1). Survival requires surgical excision of aganglionic bowel. After surgery, however, enterocolitis (i.e., bowel inflammation) occurs commonly (35%), and ~5% of affected children still die from HSCR. Infrequently, long-segment HSCR necessitates intravenous nutrition with accompanying life-threatening infections. Most children with HSCR (80%) have only a short segment of aganglionosis, suggesting that slightly enhanced bowel colonization by ENS precursors could prevent disease. New strategies are needed to enhance bowel colonization by ENS precursors and to reduce HSCR occurrence.

While HSCR undoubtedly requires genetic defects (2), almost all predisposing mutations have partial penetrance and variable expressivity. For example, inactivating *RET* mutations occur in 15-20% of sporadic and 50% of familial HSCR, but only about half of children with inactivating *RET* mutations have HSCR (2). Genetic interactions also influence HSCR risk (3–6), however, much variability in occurrence and severity of HSCR and other human birth defects remains unexplained. We hypothesized that non-genetic factors might affect HSCR occurrence. If so, then some cases of HSCR might be preventable by changes in prenatal care.

HSCR is caused by failure of distal bowel colonization by enteric neural-crest derived cells (ENCDCs) during week four to seven of human gestation (7–9). Normally, ENCDCs proliferate vigorously and migrate rostrocaudally to colonize the entire intestine. A similar process occurs in mice from embryonic day 9.5 (E9.5) to E13.5 and in zebrafish from 36-96 hours post fertilization (hpf). Many genes (7, 10) in addition to *RET* are needed for ENS development including *SOX10*, *PHOX2B*, *EDNRB*, *EDN3*, *GDNF*, intracellular signaling molecules (11, 12), cytoskeletal components (13, 14), and adhesion proteins (15–17). 30% of children with HSCR have additional birth defects and at least 30 genetic syndromes are HSCR-associated (2). The diverse molecular mechanisms supporting ENS development suggest that many non-genetic

factors could influence ENCDC bowel colonization and HSCR occurrence by modifying the activity or abundance of needed molecules. Furthermore, chemical perturbation of the developing ENS may identify new pathways involved in ENCDC migration, self renewal, proliferation, or survival.

To identify medicines that might increase HSCR risk, gain new insight into HSCR genetics, and identify new modulators of ENS developmental biology, we conducted a zebrafish chemical screen. Here we show that mycophenolic acid (MPA), a commonly used immunosuppressant, caused ENS developmental defects in fish and impaired ENCDC colonization of the bowel in mice *via* inhibition of inosine monophosphate dehydrogenase (IMPDH), the rate limiting enzyme in *de novo* GMP synthesis. Guanine nucleotides are essential for DNA replication, transcription, and for > 200 GTP-dependent proteins. Our analyses suggest that reduced ENCDC proliferation after GTP depletion is the primary cause of MPA induced bowel aganglionosis (Supplemental Figure 3.1) and show that IMPDH inhibition can greatly increase the penetrance and severity of genetic defects affecting the ENS. These studies reinforce the central role of ENCDC proliferation in bowel colonization and raise the intriguing possibility that drugs, nutritional deficiencies, or gene polymorphisms that reduce cell proliferation during early pregnancy may increase HSCR occurrence.

3.3 Results

3.3.1 Medications that inhibit ENS development

Zebrafish were treated with 1508 individual drugs from the Johns Hopkins Clinical Compound Library (18) (Supplemental Table 3.1, available at <http://www.jci.org/articles/view/69781/sd/1>) for the entire duration of ENCDC colonization of

the bowel (34 to 96 hours post fertilization (hpf)). Using Elav13/4 (HuC/HuD) immunohistochemistry to visualize neurons (19), we identified 9 compounds that consistently impaired ENS development, are systemically administered, and were not overtly toxic at doses impacting the ENS (Table 3.1). Dose-response studies permitted determination of TD₅₀ for ENS defects for these drugs. We analyzed mycophenolic acid (MPA) in more detail because MPA dramatically impaired fish ENS development (Figure 3.1A-C), is commonly used in humans, has a well-understood molecular mechanism, and has a TD₅₀ within human therapeutic levels (20).

3.3.2 MPA impaired mammalian ENS development

MPA inhibits IMPDH, a protein detected in all E10.5-E12.5 bowel cells (Supplemental Figure 3.2), that is slightly more abundant in ENCDCs than in neighboring mesenchyme. To determine if MPA impairs mouse ENS development, we injected pregnant dams with MPA daily from E10.5 through E12.5 and analyzed fetal bowel at E13.5. Since we expected that MPA metabolism and effects might vary depending on genetic background, we used both the outbred CF1 strain due to its high fertility and large litters and the C57Bl/6 (B6) standard laboratory strain. CF1 fetuses tolerated 100 mg/kg/day (36% of adult human therapeutic dose allometrically scaled to mice (21)), but no B6 fetuses survived >25 mg/kg/day. In both strains, MPA caused dose-dependent reductions in the extent of ENCDC colonization of the bowel (Figure 3.1D-E) as indicated by the extent of TuJ1-positive neurites in the colon. While we have previously demonstrated that the caudal extent of TuJ1 reactivity indicates the position of the ENCDC wavefront (12), these structures might not be tightly associated after MPA treatment. To directly assess the position of the wavefront, we mated B6 females to *Wnt1-Cre Rosa26^{EYFP/EYFP}* males, marking all neural crest-derived cells with enhanced yellow fluorescent protein (EYFP). We examined the position of the most distal staining in the bowel using EYFP, TuJ1 and SOX10

Table 3.1: Compounds that inhibited ENS development in zebrafish

Compound	TD₅₀ in zebrafish ENS	C_{max} in mammals	Indication	Primary mechanism	Target molecule
Artesunate	500 nM	1-3 µM	Antimalarial	Unknown	Unknown
Benzbromarone	600 nM	6-8 µM	Uricosuric	Inhibits uric acid reabsorption	URAT1
Cinchophen ^A	<100 nM	unknown	Analgesic/anti-inflammatory (veterinary)	Possibly cyclooxygenase inhibition	Unknown
Closantel	1.8 µM	82 µM	Anthelmintic (veterinary)	Possibly mitochondrial uncoupling	Unknown
Diclazuril	1 µM	5 µM	Antifungal (veterinary)	Unknown	Unknown
Flubendazole	2 µM	20 nM	Anthelmintic (veterinary)	Inhibits microtubule assembly	beta-tubulin (invertebrate)
Lovastatin (Mevinolin)	0.4 µM	0.1 µM	Antihyperlipidemic	Inhibits cholesterol biosynthesis	HMG-CoA Reductase
Mycophenolic Acid	1 µM	1-10 µM	Immunosuppressant	Inhibits de novo GMP synthesis	IMPDH
Oxibendazole	200 nM	30 nM	Anthelmintic (veterinary)	Inhibits microtubule assembly	beta-tubulin (invertebrate)

A – Dose response not performed.

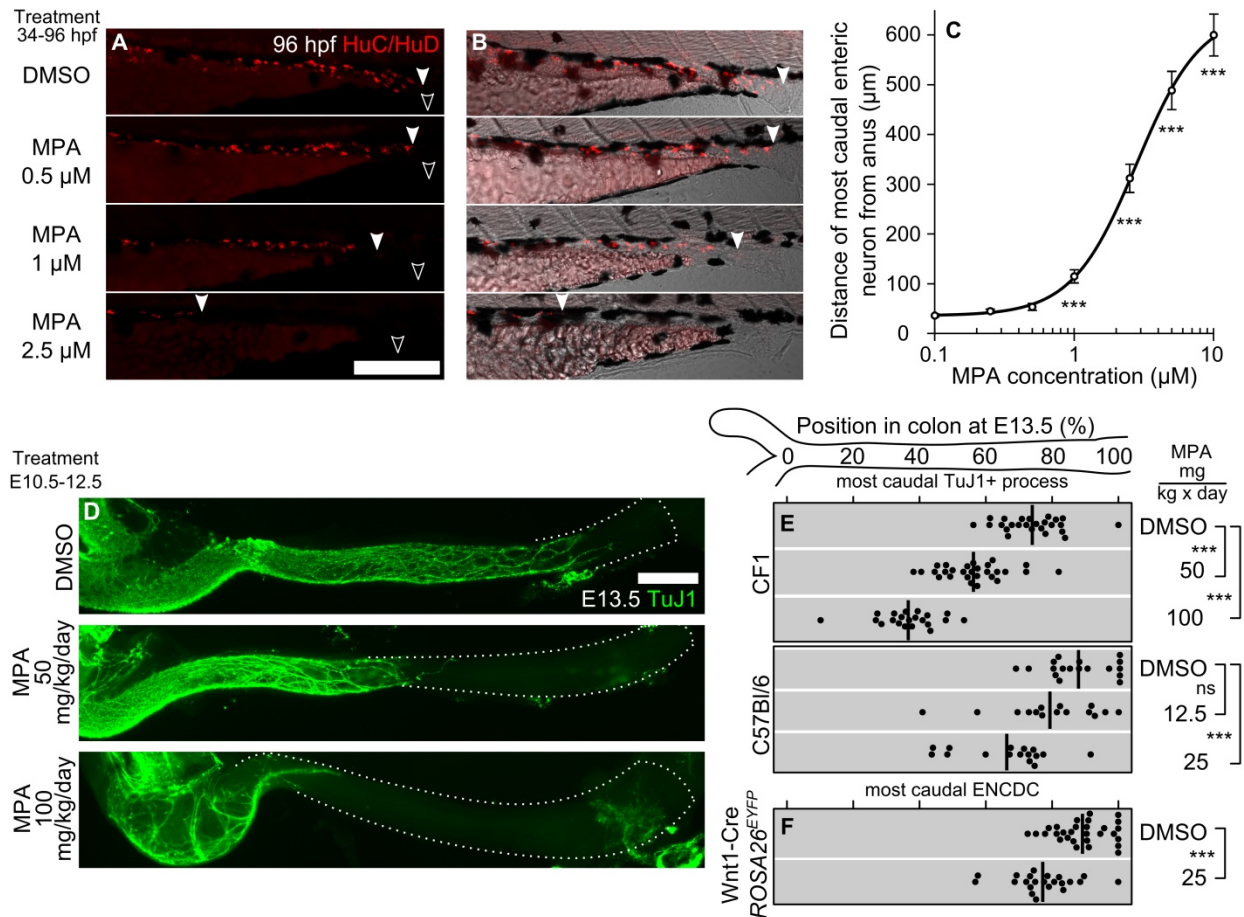


Figure 3.1

MPA inhibited ENS development in developing zebrafish and mouse. Developing wild-type zebrafish were exposed to DMSO or MPA from 34 hpf to 96 hpf and larvae (N>200) were immunostained for (A) neuronal marker HuC/D (elavl3/4) (filled arrowheads = most caudal enteric neuron, empty arrowheads = vent, scale bar = 250 μm), (B) merged with transmitted light. (C) Average uncolonized distal intestine is plotted vs. MPA dose and compared to control (Kolmogorov-Smirnov test). MPA exposure by maternal intraperitoneal injection from E10.5-E12.5 impairs enteric neuron colonization of the mouse hindgut at E13.5 (D) as visualized by the neuronal marker TuJ1 (left side = ileocecal junction, dotted line = colon outline, scale bar = 1 mm). The position within each E13.5 colon of the most caudal (E) neuronal process (marked by TuJ1) or (F) ENCDC cell body (ascertained by the lineage-marker EYFP or by SOX10 staining in EYFP-negative littermates) in each E13.5 fetus is plotted for each MPA dose and mouse strain (thick lines = mean, statistical tests are ANOVAs and t-test). *** = $P < 0.001$, ** = $P < 0.01$, * = $P < 0.05$, ns = not significant.

immunoreactivity. Both SOX10 and TuJ1 reliably reflected the extent of bowel colonization seen with EYFP after control or MPA treatment (Supplemental Figure 3.3) confirming that MPA impaired ENCDC colonization (Figure 3.1F). While MPA treatment reduced fetal size and colon length (Supplemental Figure 3.3), it also increased the absolute length of uncolonized colon, suggesting a greater effect of MPA on ENS development than on colon growth.

3.3.3 MPA impaired development of cultured ENCDCs

MPA could reduce migration *in vivo* by direct effects on ENCDCs or indirect effects on other fetal cells. To study ENCDCs moving on an acellular, migration-permissive surface, we cultured E12.5 midgut slices on fibronectin (12). MPA drastically reduced RET-positive cell migration (Figure 3.2A-B,E) out of bowel explants and reduced the percentage of migrating ENCDCs with lamellipodia (Figure 3.2F,G-I). MPA also significantly reduced DNA synthesis (Figure 3.2A-B,D) and induced ENCDC apoptosis (Supplemental Figure 3.4). MPA did not, however, alter neurite growth in post-mitotic enteric neurons (BrdU-negative, TuJ1-positive) grown in low density dissociated cell culture (22) (Supplemental Figure 3.5). To confirm that MPA effects were due to reduced guanine nucleotide levels, we treated cells with guanosine to restore GTP through the purine salvage pathway. Guanosine efficiently rescued MPA's effects on ENCDC migration (3. 2C, E), DNA synthesis (Figure 3.2D), and lamellipodia (Figure 3.2F, J), indicating that MPA effects are due to IMPDH inhibition.

3.3.4 MPA selectively reduced ENCDC DNA synthesis *in vivo*

To deliver MPA more consistently than drug injections permit, the prodrug mycophenolate mofetil (MMF) was given in drinking water at a dose (1 mg/mL) that improves survival in a mouse lupus model (23). B6 females mated to Wnt1-Cre *Rosa26*^{EYFP/EYFP} males were MMF treated from E10.5-E13.5 and injected with BrdU one hour prior to analysis. MMF decreased

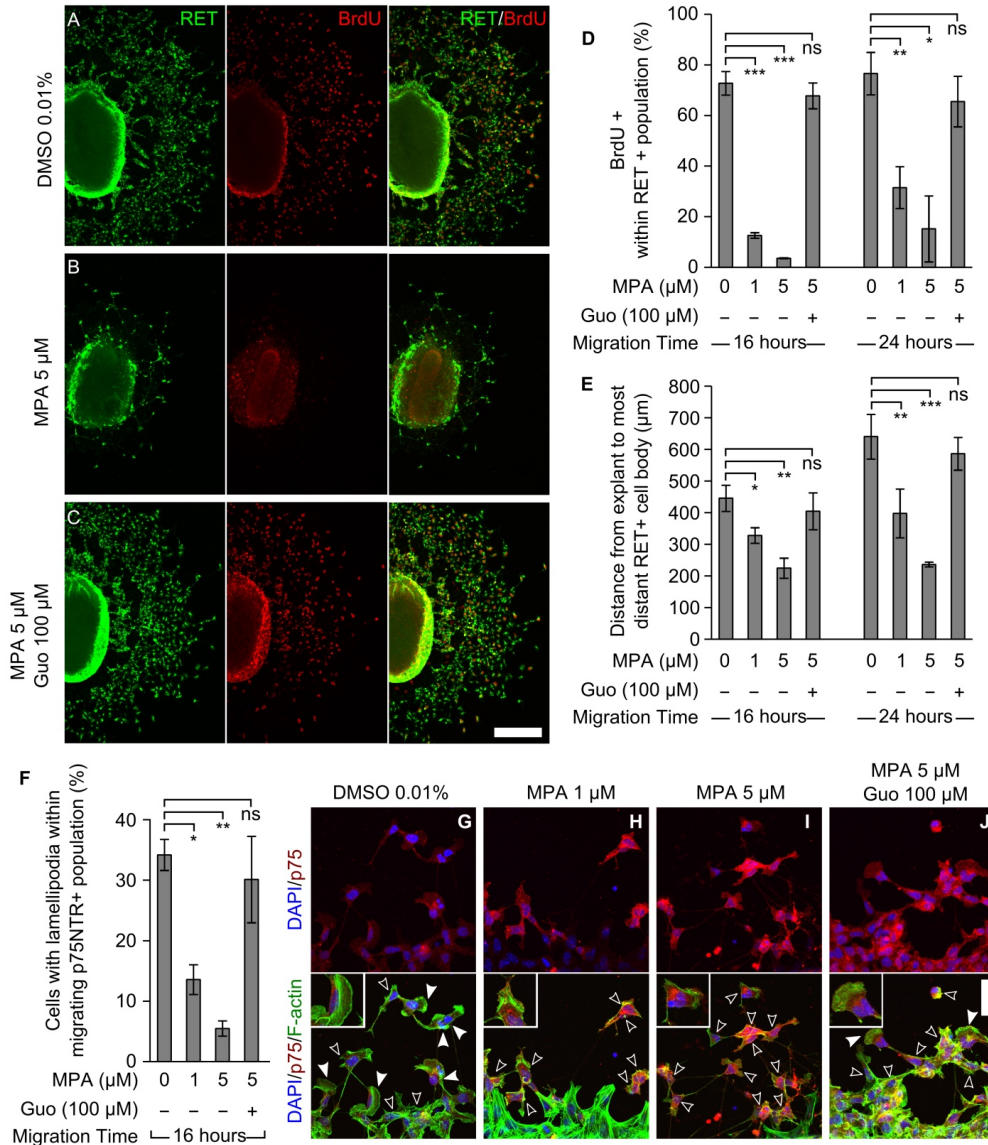


Figure 3.2

MPA reduced ENCDC migration, DNA synthesis, and lamellipodia in explant cultures. (A-C) Low-magnification confocal micrographs of 24-hour E12.5 midgut explant cultures immunostained for RET and BrdU (explant is on left side of each panel, scale bar = 250 μm). Guanosine (Guo) (C) completely reverses the proliferation and migration reduction caused by MPA (B). (D) Quantification of BrdU labeling index and (E) distance migrated by the RET-expressing population after 16 and 24 hours in culture (repeated-measures ANOVA). (F) MPA reduced the percentage of cells with lamellipodia within the neural crest-derived cell population (stained with anti-p75NTR) most distant from the explant, an effect also reversed by guanosine (ANOVA). (G-J) Optical sections of p75NTR and phalloidin stained ENCDCs demonstrate the changes in cell shape associated with MPA treatment (filled arrowhead shows ENCDC with lamellipodium; empty arrowhead shows ENCDC without lamellipodia, scale bar = 50 microns). Insets show detail of ENCDC at the leading edge. *** = $P < 0.001$, ** = $P < 0.01$, * = $P < 0.05$, ns = not significant.

distal colon colonization by ENCDCs (Figure 3.3A-D), recapitulating the effect of injected MPA. SOX10 and RET immunohistochemistry showed that neuronal differentiation in littermate fetuses was unaffected by MMF (Supplemental Figure 3.6A-C). Since MPA might affect transcription of mesenchyme-derived signals required for colonization of the bowel, we measured *Gdnf*, *Edn3*, and *Ece1* mRNA levels in E13.5 bowel using qRT-PCR, but found no differences (Supplemental Figure 3.6D). In contrast to our in vitro data, cleaved-caspase 3 positive cells were rare in both ENCDC and surrounding mesenchyme after MMF treatment (Supplemental Figure 3.7), but were readily detected in limb bud interdigital web. These results agree with recent studies that showed low but detectable rates of nuclear fragmentation (24) and cleaved-caspase 3 (25) reactivity in wild-type ENCDCs. While ENCDCs also can die through unconventional, caspase-independent processes in circumstances such as partial loss of RET expression (26), ENCDCs in culture readily undergo canonical apoptosis in response to MPA, so we limited our examination of cell death to cleaved-caspase 3. Consistent with MPA effects on ENCDCs in culture, MMF reduced proliferation of colon ENCDCs. In contrast to its effects on ENCDCs, MMF actually increased the fraction of surrounding mesenchymal cells incorporating BrdU in (Figure 3.3E-G). Since this was unexpected given the reduction in bowel size resulting from either MPA or MMF treatment (Supplemental Figure 3.3), we counted mitotic figures within these populations. The mitotic index (Figure 3.3H) was reduced within ENCDCs in concordance with the reduction in BrdU incorporation. In contrast to BrdU results, however, the mitotic index in the mesenchyme was not increased, indicating that MMF treated mesenchymal cells entered S-phase but did not divide at elevated rates. MMF therefore selectively reduced ENCDC proliferation and distal bowel colonization in vivo without increasing caspase-mediated apoptosis or altering neuronal differentiation.

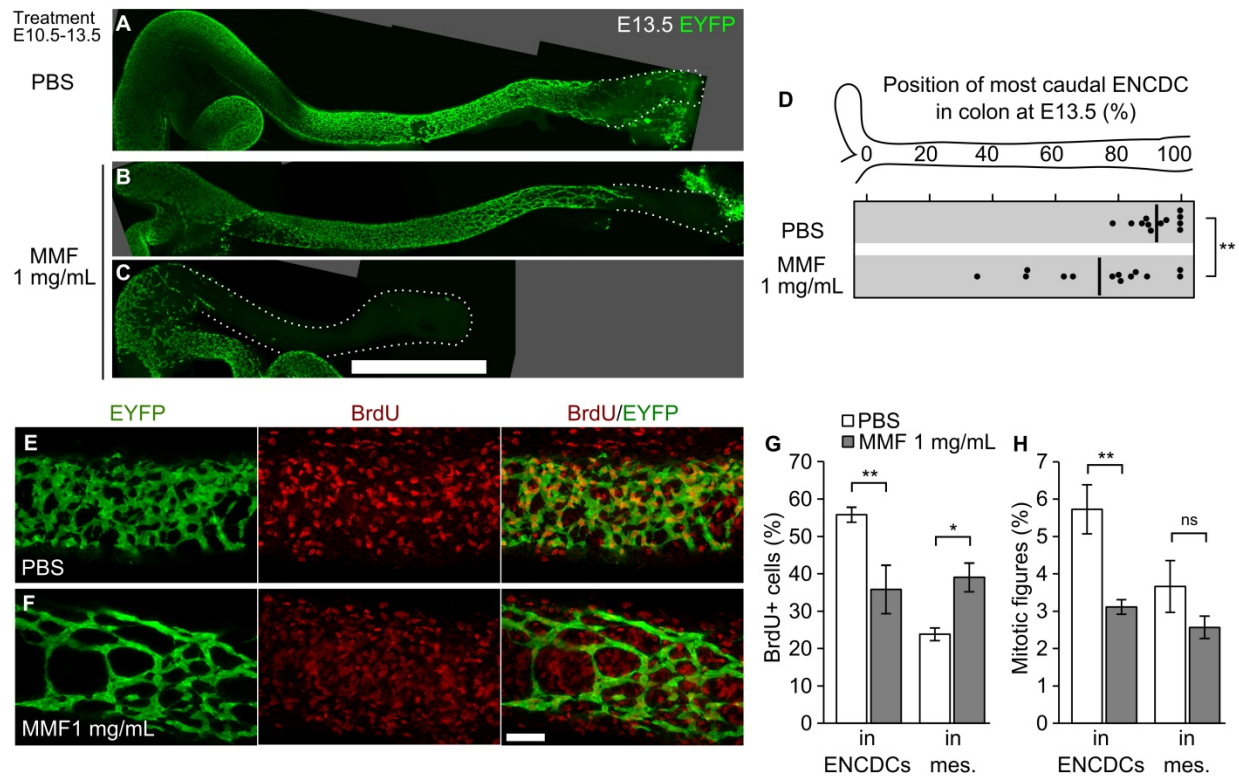


Figure 3.3

MMF treatment reduces ENCDC migration and DNA synthesis in vivo. (A-D) Oral treatment of pregnant B6 dams with MMF from E10.5-E13.5 reduces the colonization of the hindgut at E13.5. Stitched maximum-intensity projections of untreated (A), mildly affected (B) and severely affected (C) fetal colons with EYFP-marked ENCDCs demonstrate MMF's inhibitory effect on ENCDC wavefront migration in vivo (dotted lines = outline of bowel, scale bar = 1 mm). (D) The position within each E13.5 colon of the most caudal ENCDC cell body (ascertained by EYFP or by SOX10 staining in EYFP-negative littermates) is plotted for each treatment. (Thick line = mean, statistic is Student's t-test). (E-F) 8 μ m-thick maximum-intensity projections of EYFP and BrdU labeled E13.5 colons (scale bar = 50 μ m) and (G) counting of BrdU positive cells within these volumes demonstrate a reduced proportion of BrdU positive ENCDCs and an increased proportion of BrdU-positive mesenchymal cells after MMF treatment (ANOVA). (H) Counting of mitotic figures shows that the proportion of ENCDCs undergoing mitosis was reduced, while the mitotic index of the mesenchyme was not significantly changed (ANOVA on log-transformed values). mes = non-ENCDC mesenchyme. * = $P < 0.05$, ** = $P < 0.01$, *** = $P < 0.001$, ns = not significant.

3.3.5 MPA reduced ENCDC migration by reducing proliferation

Guanine nucleotide depletion must underlie MPA effects because guanosine rescues these effects in vitro. GTP is essential for DNA, RNA, and protein synthesis as well as for GTPases and many other proteins. To distinguish between primary effects of guanine nucleotide depletion on cell motility versus effects on ENCDC proliferation that secondarily reduce distal bowel colonization, we determined which effects of GTP depletion are cell autonomous. This is important since either reduced ENCDC proliferation or reduced cell intrinsic motility could prevent ENCDC migration into distal bowel (27). We used mice with a null mutation in the purine salvage gene *Hprt* (28), which is required for guanosine to rescue GTP depletion (29). Since *Hprt* is X-linked, one copy of the *Hprt* locus is randomly inactivated in each cell of a female. Thus, in all the cells of *Hprt*⁻ males or half of the cells of *Hprt*^{+/-} females, HPRT protein is absent and guanosine supplementation will not rescue GTP depletion. Leveraging this system to determine which GTP depletion effects are cell autonomous requires a cellular marker indicating which X chromosome is active. To achieve this, male mice carrying an X-linked EGFP transgene (30) were mated to *Hprt*^{+/-} females, and E12.5 midgut explants were cultured with 5 μM MPA and 100 μM guanosine, conditions that completely rescue MPA effects in wild-type explants. Four possible genotypes resulted from this mating (enumerated in Figure 3.4A). One of these genotypes (female X-EGFP⁺; *Hprt*^{+/-}) produces an embryo containing a mixture of cells with normal HPRT activity (EGFP-positive) and EGFP-negative cells with no HPRT activity. Therefore, each explant from fetuses of this genotype contains a mixture of guanosine-rescuable ENCDCs (EGFP-positive) and EGFP-negative cells that cannot convert guanosine to GMP, GTP, or dGTP. The other three genotypes serve as controls. As expected, MPA and guanosine treated male (*Hprt*^{-/Y}) explants had much less migration (Figure 3.4F), less BrdU

incorporation (Figure 3.4D), and fewer lamellipodia (Figure 3.4H) than wild-type explants, confirming that HPRT is required for guanosine rescue. In female wild-type explants, ENCDCs incorporated BrdU equally within EGFP-positive and negative populations as expected. In contrast, EGFP-negative cells in female heterozygote mosaic ($X\text{-EGFP}^+$; $Hprt^{+/-}$) cultures incorporated very little BrdU compared to neighboring EGFP-positive cells (Figure 3.4E), confirming that DNA synthesis is cell-autonomous with respect to GTP depletion and that guanine nucleotides are inefficiently transferred from rescued wild-type to mutant cells.

Unexpectedly, the overall migration from $Hprt^{+/-}$ explants was equivalent to wild-type (Figure 3.4F). Moreover, despite absent BrdU incorporation, within $Hprt^{+/-}$ cultures HPRT-deficient ENCDCs (EGFP-negative) migrated indistinguishably from neighboring HPRT-expressing EGFP-positive cells (Figure 3.4G). Furthermore, consistent with competence to migrate, the proportion of EGFP-negative ENCDCs with lamellipodia in $Hprt^{+/-}$ cultures was not reduced (Figure 3.4I). Thus, while DNA synthesis, cell migration, and lamellipodia are all affected by GTP depletion and require HPRT for guanosine rescue, only effects on DNA synthesis are cell-autonomous with respect to GTP pools. ENCDC with adequate GTP fully rescue the ability of adjacent GTP-depleted ENCDC to migrate in culture. Consistent with these results, time-lapse imaging of isolated ENCDCs confirmed that MPA does not reduce cell motility. However, in explant cultures where dense clusters of ENCDCs migrate outward, time-lapse imaging confirmed slower migration of MPA treated ENCDCs (Supplemental Figure 3.8). Because ENCDC proliferation also drives migration in vivo (27), these data suggest that the primary defect that causes HSCR-like delays in ENCDC migration after MPA/MMF treatment is reduced cell proliferation that secondarily reduces ENCDC colonization of distal bowel.

Figure 3.4

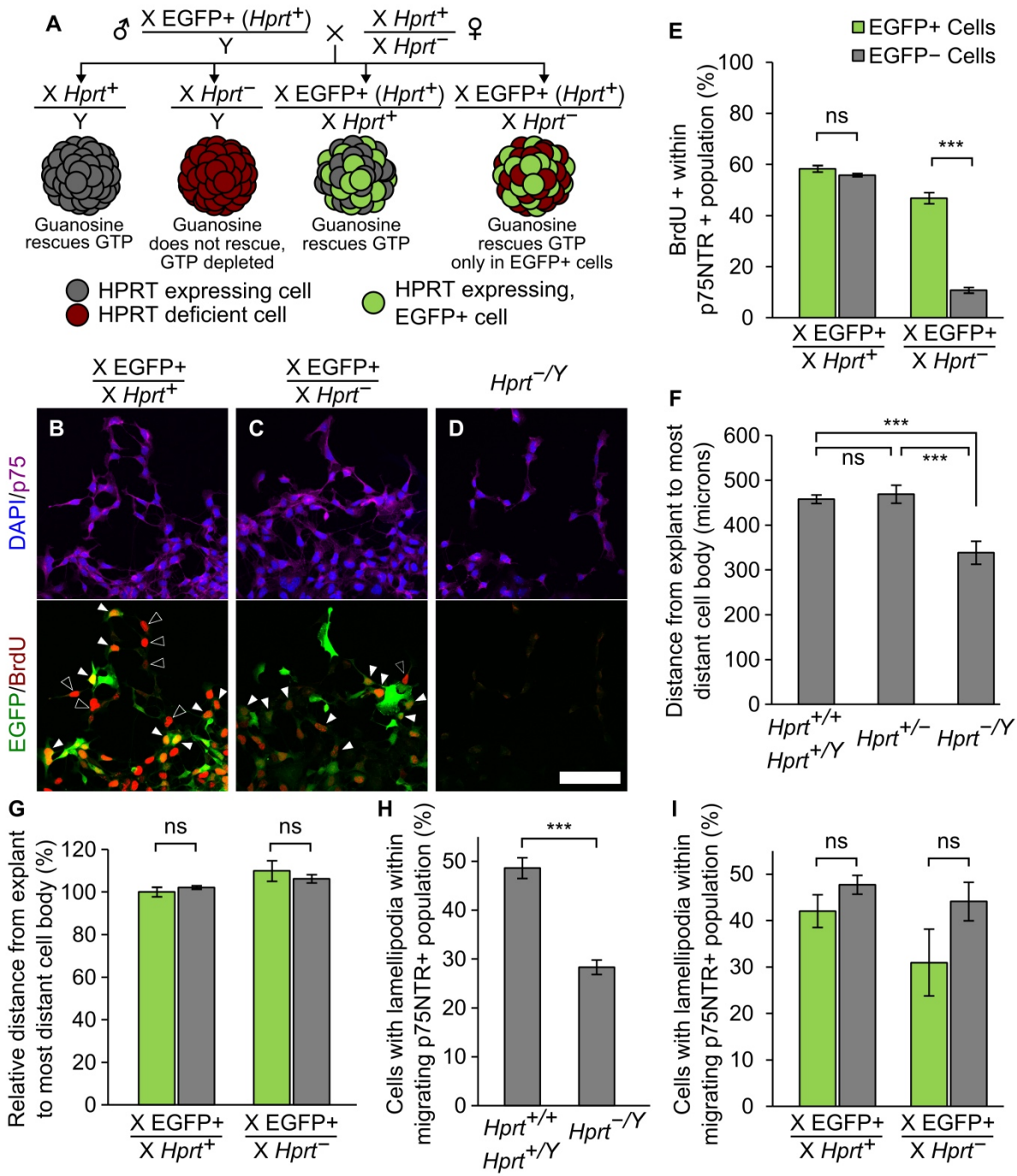


Figure 3.4

Mosaic analysis reveals that effects of GTP depletion on migration and lamellipodia are non-cell autonomous. (A) Schematic of the mating scheme, genotypes, HPRT and EGFP expression patterns, and the GTP depletion status of each population when cultured in the presence of both MPA and guanosine. These conditions create mixed cultures of GTP-depleted and EGFP-marked, guanosine-rescued ENCDCs in X-EGFP⁺, *Hprt*^{+/-} explants, allowing migration of individual GTP-depleted ENCDCs to be examined in the context of a field of rescued ENCDCs. (B-D) BrdU labeling reveals that guanosine rescues DNA synthesis in all ENCDCs in X-EGFP⁺, *Hprt*^{+/+} explants (B) but only rescues DNA synthesis within the HPRT-expressing ENCDCs marked by EGFP in X-EGFP⁺, *Hprt*^{+/-} explants (C). As expected, guanosine fails to rescue DNA synthesis in *Hprt*^{-/-} ENCDCs (D). Filled arrowheads = BrdU, EGFP double positive ENCDCs, empty arrowheads = BrdU positive/GFP negative ENCDCs, scale bar = 50 μm. (E) Quantification of BrdU labeling in mosaic explants (paired t-test). (F) ENCDC migration out of explants was impaired in *Hprt*^{-/-} explants, as expected, but *Hprt*^{+/+} and *Hprt*^{+/-} explants produced similar ENCDC migration distances (ANOVA). (G) Quantification of migration within the depleted (EGFP-negative) and rescued (EGFP-positive) populations of female *Hprt*^{+/-} cells demonstrated that GTP-depleted cells did not migrate any less efficiently than rescued cells (Wilcoxon signed-rank test) when surrounded by rescued cells. (H) Similarly, while lamellipodia were reduced in *Hprt*^{-/-} explants (t-test), they were not reduced (I) within the GTP-depleted ENCDC population in *Hprt*^{+/-} explant cultures (paired t-test). *** = $P < 0.001$, ns = not significant.

3.3.6 MMF increased penetrance and extent of aganglionosis

MPA is teratogenic (31) in humans and some MPA-associated malformations are plausibly due to defective neural crest-derived cell development (32). However, aganglionosis has not been described in MPA-exposed children or animals. We hypothesized that MPA's effects on perinatal ENS structure might be more dramatic when combined with predisposing but incompletely penetrant mutations, and that HSCR might only be induced by MPA when such mutations are present. We therefore exposed the developing ENS of *Sox10^{LacZ/+}* mice to MPA. *Sox10^{LacZ/+}* mice have partially penetrant aganglionosis and hypoganglionosis (33), modeling high-penetrance HSCR in Waardenburg syndrome type IV. Explant cultures of *Sox10^{LacZ/+}* E12.5 bowel had equivalent ENCDC migration and BrdU labeling to wild-type under control conditions. Importantly, MPA had similar effects on WT and *Sox10^{LacZ/+}* ENCDC (Figure 3.5A-B). Thus, in this short-term culture, MPA was not more toxic to mutant than to wild-type ENCDCs.

Next, we examined the interaction between MMF and *Sox10* in vivo. Since *Sox10* is haploinsufficient in the developing ENS, we crossed *Sox10^{LacZ/+}* males with B6 females (34) and treated with MMF throughout prenatal ENS development (E7.5-E18.5). We attempted postnatal evaluation, but some MMF-treated pups had exencephaly and died immediately after birth. To avoid missing more severely affected animals, we harvested E18.5 fetuses. Occasionally, control dams delivered at E18.5, but ENS structure was similar to fetuses that had not delivered. Whole-mount immunohistochemistry for neuronal processes (TuJ1) and somata (HuC/D) demonstrated that *Sox10* mutations and MMF individually caused partially-penetrant colonic hypoganglionosis

and aganglionosis (Figure 3.5C). The combination of *Sox10* mutation and MMF resulted in extensive bowel aganglionosis.

We next tested MPA on *Ret*^{+/-} ENCDCs in culture, since *RET* is mutated in most human HSCR (2) cases. *Ret*^{+/-} mice, however, are never aganglionic or hypoganglionic (35). In contrast to *Sox10*^{LacZ/+}, *Ret*^{+/-} ENCDCs did not migrate as efficiently as WT in culture, although BrdU labeling was unaffected by *Ret* genotype (Figure 3.5D-E). MPA and *Ret* heterozygosity had additive effects on distance migrated, consistent with known roles for RET in ENCDC migration (11, 36) and MPA's primary effect on proliferation.

Since heterozygous null *Ret* mutations do not delay ENCDC colonization of fetal bowel (35) and only slightly alter adult ENS structure (37), we used a hypomorphic allele, *Ret*^o, that causes partially penetrant aganglionosis (38) to test MMF effects in vivo. *Ret*^{+^o/+} males were bred to *Ret*^{+/-} females on a B6 background and pregnant dams were treated with MMF from E7.5 to E18.5. We expected *Ret*^{o/-} fetuses to have partially penetrant aganglionosis even without MMF (26), but found no aganglionosis and only one mouse with obvious hypoganglionosis (Figure 3.5F, H). Other genotypes did not have detectable ENS abnormalities in control fetuses. In contrast, two of six MMF-treated *Ret*^{+/+} fetuses had hypoganglionic or aganglionic colons (Figure 3.5F, I). Furthermore, MMF-treated *Ret*^{o/+} and *Ret*^{+/-} fetuses had longer regions of aganglionic colon than wild-type, demonstrating a synergistic effect. (Figure 3.5F, J, K). Strikingly, all eight MMF treated *Ret*^{o/-} fetuses had aganglionosis, often extending into small bowel (Figure 3.5F, L). These findings are remarkable since the *Ret*^{o/-} genotype closely mimics heterozygous *RET* mutations that underlie more than 25% of human HSCR. Unlike human HSCR, however, sex did not affect the penetrance or the extent of ENS abnormalities in MMF treated *Ret* mutant mice.

Thus MMF treatment from E7.5 onward caused Hirschsprung-like aganglionosis that was significantly worse in genetically susceptible mice. We also tested the hypothesis that a more limited period of MMF exposure might cause permanent distal bowel aganglionosis. ENCDCs normally first enter the bowel at E9.5 (39) and reach the end of the colon by E13.5, but the colon becomes less permissive (40, 41) to ENCDC migration at E14.5. To determine if MMF treatment during the critical period of ENCDC migration caused permanent or transient distal bowel aganglionosis, we switched dams carrying *Sox10* and *Ret* litters from PBS to MMF for the interval from E9.5-E14.5 and then allowed them to recover on PBS from E14.5 to E18.5. For *Sox10* and *Ret* matings (Figure 3.5C and 3.5F), the colons of all wild-type fetuses and intermediate *Ret* genotype fetuses were completely colonized at E18.5, though one *Sox10*^{+/+} fetus had a hypoganglionic terminal colon. In contrast, aganglionosis was highly though not universally penetrant in *Ret*^{9/-} fetuses treated with MMF from E9.5-E14.5 and was confined to the colon (Figure 3.5F). Furthermore, although the penetrance of aganglionosis in *Sox10*^{LacZ/+} fetuses treated with MMF from E9.5-E18.5 was very similar to those treated with MMF from E7.5-E18.5, the aganglionic segments were shorter on average if mice did not receive MMF before E9.5 and after E14.5. Collectively, these data suggest that significant ENCDC migration delays may be reversible, but the most susceptible genotypes lack the capacity to recover from transient MMF exposure.

It is important to note that the preceding data described colonization of the bowel by ENCDC derived from the vagal region of the neural crest. Interestingly, in mice with aganglionic bowel, the terminal third of the colon often had single neurons or isolated clumps of neurons (<150 neurons per colon) associated with extrinsic nerve bundles and separated from vagal

Figure 3.5

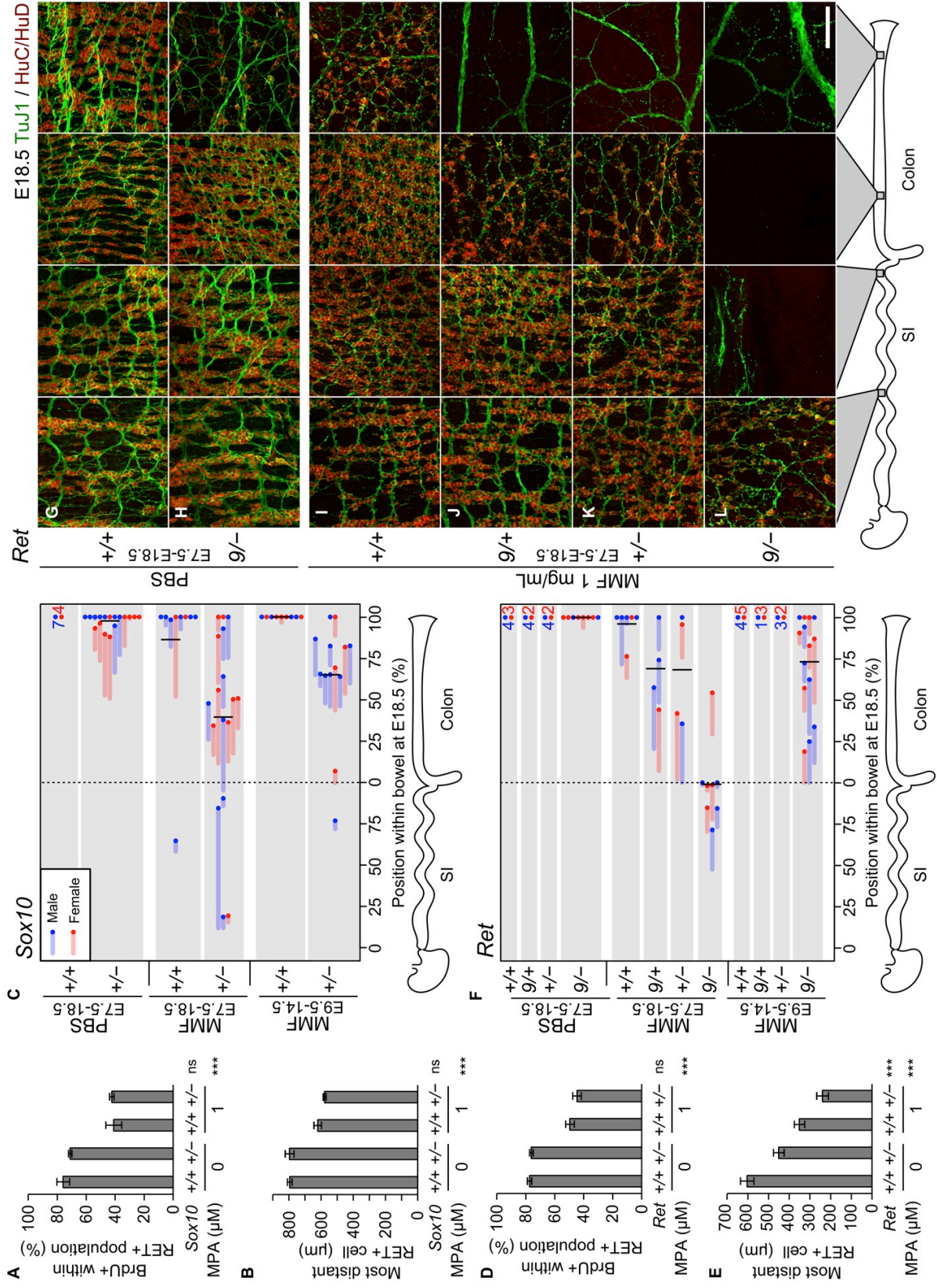


Figure 3.5

MMF treatment interacts with *Ret* and *Sox10* mutations to increase penetrance and severity of HSCR-like pathology. MPA treatment in 24-hour explant cultures reveals that (A, D) neither *Ret* nor *Sox10* heterozygosity impacts BrdU incorporation. (B, E) In contrast, *Ret* but not *Sox10* heterozygosity reduces ENCDC migration distance and MPA treatment has an additive effect on ENCDC migration distance (two-way ANOVA, interaction terms were not statistically significant). (C, F) Pregnant dams were provided MMF or control PBS in drinking water and the ENS was examined at E18.5 with neuronal fiber (TuJ1) and soma (HuC/HuD) markers. The position of the most caudal soma within the intestine is plotted as a dot, and the region of hypoganglionosis is plotted as a line. Mean positions of aganglionosis are indicated with black lines. Groups without abnormal fetuses are summarized as one dot and number. Treatment with MMF from E7.5-E18.5 resulted in hypoganglionosis and aganglionosis with genotype-dependant penetrance and severity. Treatment with MMF from E9.5 to E14.5 to test whether MMF-induced developmental delays are reversible demonstrates genotype-dependent reversal. (G-L) Representative maximum-intensity projections are shown of myenteric plexus in the mid-small bowel, terminal ileum, proximal colon, and terminal colon from PBS-exposed wild-type and *Ret*^{9/-} fetuses and all MMF-treated *Ret* genotypes (scale bar = 100 μm). The PBS-exposed *Ret*^{9/-} colon shown (H) displays distal hypoganglionosis. TuJ1 staining demonstrates thick nerve bundles in the aganglionic terminal colons of J-L and disorganized fibers in hypoganglionic regions. *** = $P < 0.001$, ns = not significant.

ENCDC by long segments of bowel that were completely devoid of enteric neurons. These rare neurons are likely to arise from ENCDCs derived from the sacral region of the neural crest.

In addition to ENS defects, MMF treated mice were small, had reduced bowel length (Supplemental Figure 3.9), exencephaly and congenital heart defects. MMF-induced exencephaly was unaffected by genotype but was only present in litters treated with MMF from E7.5-E18.5 (Supplemental Table 3.2). Most heart defects occurred in *Sox10* or *Ret* mutant fetuses in the E7.5-E18.5 treatment group. Although the number of fetuses was small, the infrequent heart defects in MMF treated control mice raises the possibility that *Sox10* or *Ret* may have unappreciated roles in cardiac crest development that are only demonstrable with additional genetic or environmental insults. We also observed 6 MMF-exposed fetuses with orofacial clefting and three with iris colobomas. These defects are similar to those reported in MMF exposed human infants (31).

3.4 Discussion

Hirschsprung disease and other problems with ENS development are known to occur in individuals with many well established genetic defects (2) suggesting that these disorders are not preventable. The gene defects and chromosomal anomalies that predispose to HSCR, however, are all partially penetrant and cause variable degrees of aganglionosis. In part this variation in phenotype in individuals who share the same underlying primary genetic defect is thought to occur because of interactions between genes needed for normal development. Our current data provide the first direct evidence that specific medicines impact enteric nervous system development to cause distal bowel aganglionosis in mice and fish that mimics human Hirschsprung disease. In addition, the data show dramatic gene-environment interactions.

Importantly, these studies suggest the possibility that any factor that reduces ENCDC proliferation might increase the risk of distal bowel aganglionosis and that some cases of Hirschsprung disease might be prevented by careful optimization of non-genetic risk factors during early pregnancy.

Most compounds found to inhibit distal bowel colonization by ENCDCs in fish lack obvious links to previously recognized ENS developmental pathways. Furthermore, because we tested only one drug concentration, many additional medications are probably detrimental to the developing ENS. Two medications in addition to MPA deserve comment. Mevinolin is a commonly used inhibitor of the rate limiting step in *de novo* cholesterol biosynthesis (HMG-CoA reductase), which is interesting because *DHCR7* mutations disrupt the final step in cholesterol biosynthesis, causing HSCR as a component of Smith–Lemli–Opitz syndrome (42). Artesunate is a common malaria treatment that may increase reactive oxygen species (ROS), and in *Tcofl* mutant mice, additional oxidative stress delays ENCDC migration (43). These findings highlight the many complex pathways needed for ENCDC colonization of fetal bowel and the potential for diverse medicine classes to increase HSCR occurrence. This is especially important since families with one child with HSCR have a 50- to 1600-fold increased risk of having another child with the same life-threatening disease (2).

We investigated the immunosuppressant mycophenolic acid in more detail because MPA profoundly inhibited zebrafish ENS development at concentrations in the low human therapeutic range and because MPA is the only drug identified associated with specific patterns of human birth defects (31). Despite inhibiting the ubiquitous process of GMP biosynthesis, some MPA associated defects (cardiac defects, craniofacial defects, coloboma) suggest that IMPDH inhibition disproportionately affects neural crest-derived cells (32). Interestingly, *Drosophila*

IMPDH mutations (*raspberry*) cause mis-targeting of photoreceptor axons (44), and MPA impairs cranial nerve development in rat embryos (45) demonstrating that defects in other neural cell types can be caused by abnormal purine metabolism. We are not aware of human ENS malformations reported after MPA or MMF exposure, but HSCR occurrence after exposure likely requires predisposing gene mutations. Here we show that MPA caused dose-dependent distal ENS malformations in fish and mice, that MPA impairs ENCDC migration by depleting guanine nucleotides and reducing proliferation, and that mutations that model HSCR-predisposition dramatically increased MMF's teratogenic effects on distal bowel colonization by ENCDCs.

The unique way that the ENS develops that may explain why ENCDCs are particularly sensitive to MPA/MMF. One possibility is that the relatively high rate of ENCDC proliferation compared to neighboring mesenchymal cells requires ENCDC to synthesize guanine nucleotides more rapidly via IMPDH and the *de novo* synthesis pathway. The elevated levels of IMPDH in ENCDC compared to adjacent cells are consistent with this hypothesis, as are the different effects of MMF in different cell types. As expected, MPA/MMF dramatically reduced BrdU incorporation and mitotic figures in ENCDC. Remarkably, MPA/MMF effects in neighboring mesenchyme were more complex. In contrast to ENCDC, a higher proportion of mesenchymal cells incorporate BrdU after MPA/MMF treatment, but without a concomitant increase in mitoses. This might occur if MMF-treated mesenchymal cells have enough guanine nucleotide to enter S-phase, but have a prolonged period of DNA synthesis because of limited dGTP availability. Alternatively, guanine nucleotide depletion could cause DNA damage, and the elevated levels of BrdU incorporation reflect DNA repair. In any case, the effect on mammalian development of blocking a ubiquitous enzyme like IMPDH depends not only on how the drug

affects the biology of individual cells, but also on how important that perturbation is for particular aspects of development. For example, proliferation is essential for ENCDC to efficiently colonize the distal bowel (27). Reduced proliferation of other cell types might lead to smaller organs, but might not cause a structural defect because proliferation is not essential to build that structure during the interval of drug exposure.

For our studies it was important to determine if distal bowel aganglionosis in MPA/MMF treated mice occurred because of reduced ENCDC proliferation (27) or if depletion of guanine nucleotides directly affected proteins needed for cell migration. In mesangial (46) and endothelial (47) cells, for example, MPA-mediated GTP depletion led to reduced levels of active (GTP-bound) Rho-family GTPases including RAC1, a key regulator of the actin cytoskeleton. Our experiments, however, strongly suggested that MPA/MMF in the doses tested did not directly impair cell migration. Specifically, we found that random motility of EYFP-labeled ENCDCs was unchanged by MPA (Supplemental Figure 3.8) when cells were cultured at a density that reduced cell-cell contact. Furthermore, using X-inactivation mosaicism we deleted HPRT and depleted GTP in single ENCDCs that were surrounded by “normal” guanosine rescued ENCDCs. In these cultures, the non-rescued ENCDCs remain BrdU negative, excluding cell-to-cell transfer of any significant amount of guanine nucleotide, but the GTP depleted cells appear to migrate essentially normally. Thus, with two different approaches we demonstrate that GTP-depleted ENCDC can move at normal speeds, but fail to migrate effectively unless they are surrounded by adjacent normally proliferating ENCDC. This result is conceptually related to the findings that *Sox10* and *Ednrb* mutations have non-cell autonomous effects on ENCDC migration in aggregation chimeras (48, 49) and that proliferation inhibitors (27) or mechanical reduction of ENCDC density (35) can reduce ENCDC colonization of cultured bowel. The

molecular mechanisms that allow ENCDCs to sense and react to local ENCDC density or that control the unpredictable trajectories of individual ENCDCs remain unknown, though in other neural-crest cells both diffusible (50) and contact-mediated signals are involved (51).

We therefore propose that reduced ENCDC proliferation parsimoniously explains all other observed effects of MPA on the developing ENS. These results suggest the possibility that any condition that reduces ENCDC proliferation could increase the risk of Hirschsprung disease. In addition to the risk of bowel aganglionosis in wild-type mice after MPA/MMF treatment, our data show dramatic gene-environment interactions between MMF and either *Sox10* or *Ret* mutations at term. MMF caused distal bowel aganglionosis both when administered for the entire period of prenatal neural crest development (E7.5-E18.5) or during the period of ENCDC migration (E9.5-E14.5). Interestingly, ENCDCs were able to recover from a transient MMF-induced developmental delay in wild-type mice and in mice with “mild” *Ret* genotypes, but not in *Sox10*^{LacZ/+} or *Ret*^{9/-} fetuses. Furthermore, MPA/MMF appeared to inhibit bowel colonization by both vagal and sacral neural crest. The sacral neural crest normally migrates proximally through terminal colon and forms 10-20% of the distal colonic ENS (52). Although we observed isolated neurons in each aganglionic colon, sacral ENCDC derivatives, if present, are greatly diminished in number by MMF and/or the genetic lesions evaluated (i.e., less than 2% of anticipated sacral-derived neurons in this region). If the same phenomena occur in humans, then many potentially detrimental drug exposures will only cause Hirschsprung disease in children with underlying predisposing mutations.

A few interesting differences were noted between in vivo versus explant culture results for *Ret* and *Sox10* mutant animals. In vivo, *Ret*^{+/+} and *Ret*^{+/-} ENCDC migrate at the same rate through the colon (35), but we noted reduced migration of *Ret*^{+/-} ENCDC from cultured gut

explants compared to WT cells. This may occur because the supraphysiologic level of GDNF used in culture saturates all RET receptors, whereas in vivo GDNF is limiting even in *Ret*^{+/-} mice (37). In contrast, *Sox10* mutant and WT ENCDC migrated an equal distance from gut explants in vitro, while the same *Sox10* mutation impaired distal bowel colonization in vivo. This illustrates the importance of coupling in vitro and in vivo studies since some defects will not be detected in the culture system currently in use. Differences that might be required to detect *Sox10*-mediated defects include the much longer time that ENCDCs migrate in vivo, the diverse set of factors affecting stem cell renewal, differentiation, and migration, and the three dimensional environment in vivo that requires degradation of the extracellular matrix (53) and may engage alternate integrin or adherence protein signaling.

Collectively, this work provides the first strong evidence that medicines may impact ENS development and that potent gene-environment interactions dramatically alter the risk of Hirschsprung-like disease. Combined with our previous demonstration that vitamin A deficiency increases HSCR-like defects in concert with *Ret* mutations (12), this work adds credibility to the hypothesis that unappreciated maternal non-genetic factors influence HSCR risk. Oral MMF may also be a valuable experimental tool to probe for genetic factors that predispose to ENS abnormalities but that are not severe enough to cause disease in the absence of additional defects.

Finally, these studies demonstrate a profound linkage between basic processes in cell metabolism and specific mammalian ENS developmental defects. This work supports the idea that any stressor that reduces the efficiency of ENCDC proliferation might increase HSCR occurrence and severity in children with predisposing mutations, even without altering “classical” ENS developmental pathways. *De novo* purine biosynthesis, for example, is a multistep process where enzymes require nicotinamide, folate, and vitamin B12. Focused

investigation of clinically-relevant antimetabolic stressors such as folate and B12 deficiency, anti-folate medicines (trimethoprim, methotrexate), and other antimetabolites (e.g. azathioprine, 6-mercaptopurine) may identify immediate candidate interventions for reducing the incidence and severity of HSCR in genetically predisposed children. In parallel with work in model systems, these studies suggest that human case-control epidemiologic investigation is appropriate and may uncover avoidable maternal exposures or health conditions that could reduce the risk of dangerous neural crest-dependent birth defects like HSCR.

3.5 Materials and Methods

3.5.1 Zebrafish

Wild type (AB) in vitro fertilized embryos were treated ($N \geq 6$ embryos per drug) with 10 μM drug and 1% DMSO in E3 Screening Media (54) from 34-96 hpf. 1% DMSO did not induce any defects but may increase sensitivity as 2% DMSO alone inhibited ENCC migration. Distance from most caudal neuron (Elavl3/4-positive) to bowel terminus was measured ($N > 9000$ larvae) using a micrometer-calibrated eyepiece grid. Compounds were retested if mean uncolonized distance was >125 microns, results were consistent between experiments, and the compound might cross the placenta in mammals. Drugs causing death at 10 μM were retested at lower concentrations. Larvae with >100 microns of uncolonized bowel were considered as affected for the TD_{50} calculations.

3.5.2 Mice

Vaginal plug day was considered E0.5. Mice were from Charles River (CF1), or the Jackson Laboratory: C57Bl/6J (referred to as B6), C3HeBFe/J (C3Fe), 129X1Sv/J (129X1), Tg(Wnt1-cre)11Rth (55) referred to as Tg(Wnt1-Cre), *Gt(ROSA)26Sor^{tm1(EYFP)Cos}* (56) referred to

as *Rosa26^{EYFP}*, and Tg(CAG-EGFP)D4Nagy/J (30) referred to as X-EGFP⁺. Other mouse strains and genetic backgrounds used were *Ret^{tm1Jmi}*: a null allele referred to as *Ret^{TGM}* (57) on a B6 background, *Sox10^{tm1Weg}*: a null allele referred to as *Sox10^{LacZ}* (33) on a C3Fe background, and *Ret^{tm2(RET)Jmi}*: a hypomorphic allele referred to as *Ret⁹* (38) and backcrossed to 129X1 for 2-5 generations. Wnt1-Cre *Rosa26^{EYFP/EYFP}* and *Hprt^{b-m3}* (28) (referred to as *Hprt⁻*) were on a mixed background. PCR genotyping (58) for *Sox10^{LacZ}* and Wnt1-Cre used published primers (58). Other primers are listed in Supplemental Table 3.3.

3.5.3 MPA and MMF treatment

Dams were injected daily with MPA (Sigma #M3536) in DMSO or DMSO alone (1.24 μ L/gram body weight, 31.25-250 mM MPA, intraperitoneal), or given prodrug MMF (Accord Healthcare, NDC #16729-094) at 1 mg/mL in 0.25X PBS adjusted to pH 3.6 as drinking water (23). MMF and PBS groups drank equal amounts. Cardiovascular anatomy at E18.5 was visualized under a dissection stereomicroscope by left ventricle injection with India ink (Windsor Newton) diluted 1/10 in water).

3.5.4 Primary ENCDC culture

300–500 micron slices of E12.5 small bowel were cultured on fibronectin-coated (250 μ g/mL, Life Technologies) Lab-Tek Permanox chamber slides (Thermo Fisher) in DMEM (high glucose), 200 mM L-glutamine, 100 IU/mL penicillin, 100 g/mL streptomycin, 1X B-27 supplement (Life Technologies), and MPA in DMSO (0.01% final concentration). Four hours after plating, GDNF (59) at 50 ng/mL was added to trigger migration. Cultures were maintained for an additional 16 or 24 hours (37°C/5% CO₂). BrdU (10 μ M) was added five hours before fixation when appropriate. All culture experiments not involving mutant mice used CF1 fetuses. *Sox10*, *Ret*, and *Hprt* fetuses were cultured individually and genotyped.

For measuring neurite lengths, E12.5 bowel was enzymatically dissociated into a single-cell suspension (22) and cells were cultured in Neurobasal media supplemented with 1X B-27, 200 mM L-glutamine, 100 IU/mL penicillin, and 100 g/mL streptomycin. Cultures were plated at a density 1250 cells per cm² on glass chamber slides (Lab-Tek) coated with poly-D-lysine (100 µg/mL, Sigma) and laminin (BD Biosciences) and cultured for 48 hours before fixation. BrdU (10 µM), DMSO or MPA (5 µM final), and GDNF (50 ng/mL) were added at plating. For time-lapse EYFP microscopy, E12.5 *Wnt1-Cre Rosa26^{EYFP/+}* midguts were cultured as dissociated cells or slices as described above and plated on fibronectin-coated glass chamber slides (Thermo Fisher). Both cells and slices were cultured in phenol red-free DMEM supplemented with B-27, L-glutamine, and antibiotics as described above. All other culture conditions were identical to those of explant cultures.

3.5.5 X-inactivation mosaic analysis

X-EGFP⁺ male mice were bred to *Hprt*^{+/-} females. E12.5 midgut explants resulting from these matings were cultured for 16 hours in the presence of both MPA (5 µM) and guanosine (100 µM) to rescue all wild-type cells while GTP-depleting all cells that do not express HPRT. Since both *Hprt* and the EGFP transgene are subject to mosaic X-inactivation, in *Hprt*^{+/-} explants EGFP marks wild-type (rescued) cells but not mutant (depleted) cells. EGFP expression from the transgene was weak and visualization required immunohistochemistry.

3.5.6 Immunohistochemistry

Zebrafish were fixed and then stained in whole-mount as previously described (19) with anti-HuC/HuD monoclonal 16A11 (250 ng/mL, Life Technologies) and Alexa Fluor 594 anti-mouse secondary (1:250, Life Technologies) before mounting in 50% glycerol/PBS.

E18.5 mouse bowel flushed with PBS was fixed (4% paraformaldehyde/PBS for 30 minutes at 25°C), washed (PBS), and permeabilized/blocked (1 hour at 25°C) in TBST (Tris-buffered saline with 0.1% Triton-X 100), 1% cold water fish skin gelatin (Sigma), 100 mM glycine, and 5% normal serum matching secondary species (Jackson ImmunoResearch). Primary antibodies (Supplemental Table 3.4) were incubated overnight in blocking solution at 4°C. Fluorophore-conjugated secondary (Alexa 488 and 594 donkey anti-rabbit, Alexa 488 and 594 donkey anti-goat, Alexa 647 goat anti-rabbit, or Alexa 647 donkey anti-goat, Life Technologies) incubation was for 1 hour at 25°C. When desired, DAPI (100 ng/mL) and/or Alexa 594 or Alexa 488-conjugated phalloidin (4 units/mL, Life Technologies) were added during secondary incubation.

An acid treatment (4N HCl, 5 minutes, 25°C) step was required for BrdU and RET staining and was performed after blocking (for TuJ1 co-staining) or after antibody staining and a post-fixation step (4% paraformaldehyde/PBS for 10 minutes) for co-staining of other antigens. Samples were washed twice with TBS and blocked again between acid treatment and primary antibody incubation.

E18.5 mouse bowel anti-HuC/HuD staining required an alternate procedure. Fixed samples were treated with 3% H₂O₂/PBS (20 minutes at room temperature) before blocking in PBST (phosphate-buffered saline pH 7.4, 1% Triton-X 100), 10% normal donkey serum, 1% cold water fish skin gelatin, and 100 mM glycine. Endogenous biotin was blocked (Streptavidin/biotin blocking kit, Vector Labs) before an overnight 4°C incubation with biotin-XX conjugated anti-HuC/HuD (400 ng/uL, Life Technologies #A21272) in blocking solution. After 6 PBST washes, tissue was incubated with Alexa-594 streptavidin (1:2000, Life technologies) in PBST (15 minutes at 37°C).

3.5.7 Quantitative Reverse Transcriptase PCR (qRT-PCR)

Intestines (from stomach to colon) were harvested from E13.5 fetuses treated with PBS or MMF (E10.5-E13.5) and individually homogenized in 800 μ L of Trizol (Life Technology) by passage through a 26-gauge needle. RNA was isolated according to manufacturer's instructions with 200 μ g of RNA-grade glycogen (Thermo Scientific) added as a carrier. 1 μ g of each RNA sample was treated with RQ1 DNase (Promega) in a total volume of 10 μ L to degrade genomic DNA according to manufacturer's instructions. 1 μ L of this treated RNA solution was reverse-transcribed with 200 units of SuperScript II Reverse Transcriptase (Life Technologies) according to manufacturer's instructions using 250 ng of random hexamers in a total volume of 21.1 μ L. qPCR reactions were performed on the equivalent of 1.6 ng of input RNA using Power SYBR Green PCR Master Mix (Applied Biosystems) and 20 μ M of each oligonucleotide in a 25 μ L reaction on a Stratagene Mx3005P thermocycler using the following cycling parameters: 10 minutes at 95°C followed by 40 cycles of 30 seconds at 95°C, 1 minute at 55°C, and 1 minute at 72°C. Oligonucleotide sequences for *Gdnf*, *Ece1* (60), and *Gapdh* (61) were described previously, and sequences for *Edn3* were 5' TCACCAGTTATTCCGGGAGAG 3' and 5' TAAGGCCGGTGGGCTTTATC 3'. No-template controls and no-RT enzyme controls were performed for each primer-pair. Three replicate reactions were run for each sample-amplicon combination and average PCR efficiencies for each amplicon were calculated using LinRegPCR software (62) which were then used to calculate efficiency-corrected fold changes (63) using *Gapdh* as a reference gene.

3.5.8 Microscopy and Quantification

Micrographs were acquired with Olympus BX60 or IX71 microscopes, Axiocam CCD camera, and Axiovision software or with an Olympus FV1000 confocal microscope and

Fluoview software. ImageJ was used for image processing limited to cropping, stitching multiple fields (64), rotating, and uniform contrast adjustments. Confocal micrographs are presented as single optical sections or maximum intensity projections.

Uncolonized zebrafish bowel was measured using micrometer-calibrated gridded eyepieces. Mouse bowel colonization was measured with ImageJ. E18.5 bowel was considered hypoganglionic when gaps between myenteric ganglia became perceptibly larger and ganglia contained fewer neurons. For explant cultures, we measured the distance between gut edges and cell bodies of the most distant ENCDC in 8 sectors per explant. In X-inactivation mosaic experiments, overall, EGFP-positive, and EGFP-negative migration were measured. Time-lapse images were acquired every 3 minutes on an AxioObserver.Z1 microscope (Zeiss) equipped with motorized stage, incubator, and CO₂ controller. Cells were tracked with MTrackJ software (65).

All experiments were performed in at least triplicate with separate embryos or separate pools of embryos in culture. For drug treated pregnant mice, at least three litters were collected per treatment. Mean \pm SEM are plotted unless otherwise indicated. Analyses were performed by observers blind to genotype and treatment status.

3.5.9 Statistical Analysis

We used SigmaPlot 11 (Systat Software) or R (R Foundation) for analysis. For fetal bowel colonization, Student's t-test or one-way ANOVA was used. For wild-type explants, repeated measures ANOVA was used unless noted. For mutant explants, two-way ANOVA was used to test influence of genotype, treatment, and interactions. Paired t-tests or Wilcoxon signed-rank tests (when data were non-normally distributed) were used for mosaic analyses. Other parameters were compared with one-way ANOVA, t-test, rank-sum test, or Kolmogorov-Smirnov test as indicated. For all analyses, $P < 0.05$ was considered significant and two-tailed

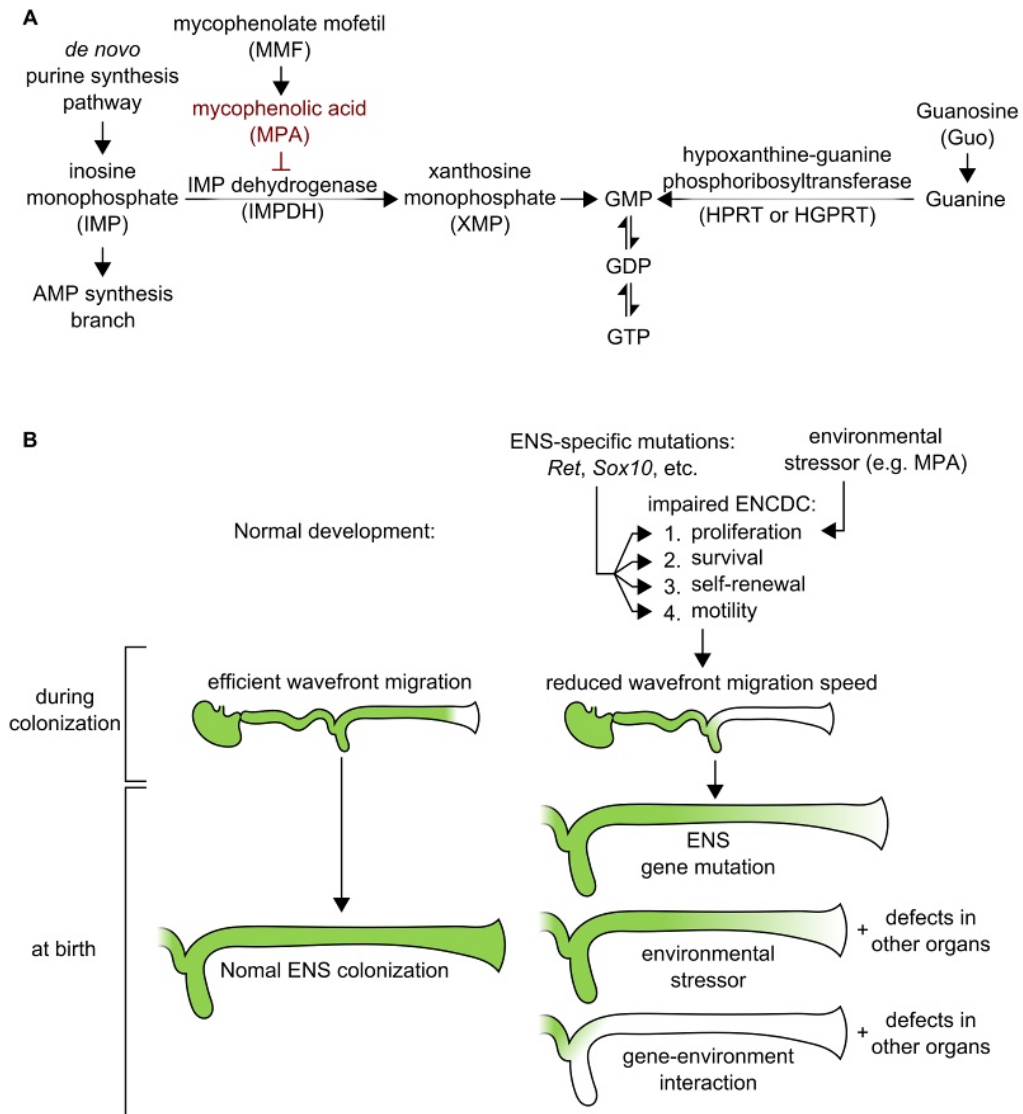
tests were performed. *P* values were adjusted for multiple comparisons by the Holm-Bonferroni procedure based on numbers of planned comparisons. When colonization was normalized to bowel length, absolute length of aganglionic (or abnormal) segments were also tested and always agreed with the normalized results.

3.5.10 Study Approval

Animal experiments were approved by the Washington University Animal Studies Committee.

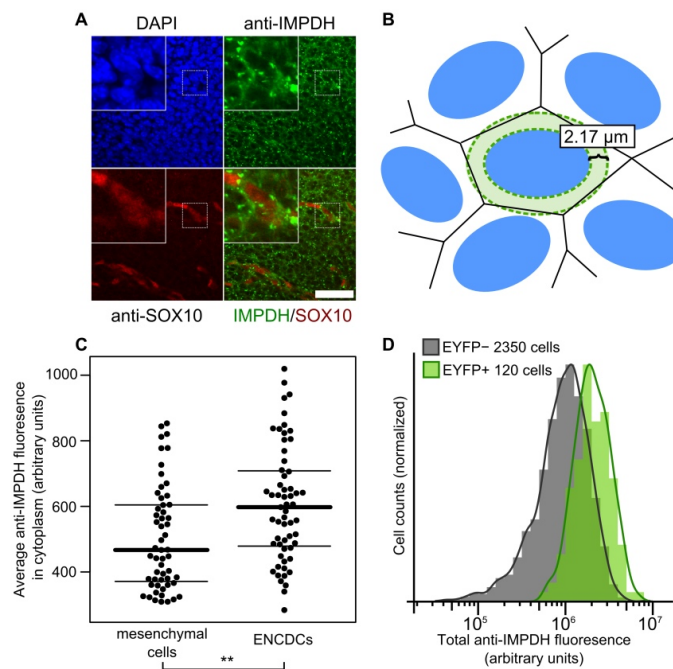
3.6 Supplemental Data

Supplemental Figure 3.1



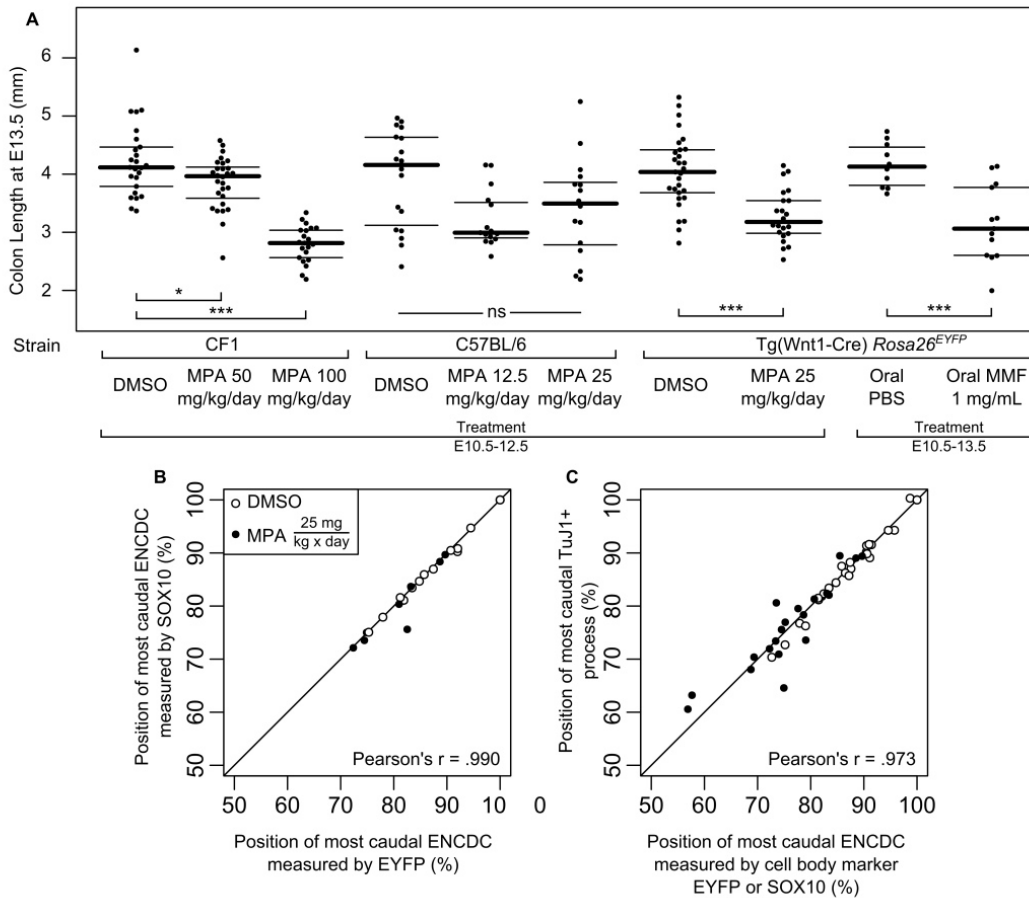
Supplemental Figure 3.1

The *de novo* and salvage purine synthesis pathways are shown converging on GMP synthesis (**A**). Enzymes and intermediates not involved in MPA action and/or guanosine salvage are omitted for simplicity. A model (**B**) for the individual and synergistic effects of MPA (or other similar antiproliferative insults) and HSCR-predisposing mutations on the developing ENS. Normally, the ENCDCs that migrate into the developing bowel complete their colonization of the terminal colon with relatively little time remaining before the bowel microenvironment becomes more resistant to colonization. Either defects in classical ENS development genes or prolonged exposure to antimetabolites (e.g. MPA) can result in partially penetrant aganglionosis because of this developmental window. ENCDCs may be individually more sensitive to MPA than other bowel cells and or simply cannot migrate effectively if proliferation of all cells slows. MPA interacts with genes both affecting proliferation (*Ret*) and other aspects of ENS development (*Sox10*) suggesting that multiplicative effects on disease penetrance and severity can result from two hits in converging but largely separate signaling pathways. Transient environmental insults that are removed as the ENCDC migration window closes can result in phenotypes ranging from complete recovery to lethal aganglionosis dependent on genotype.



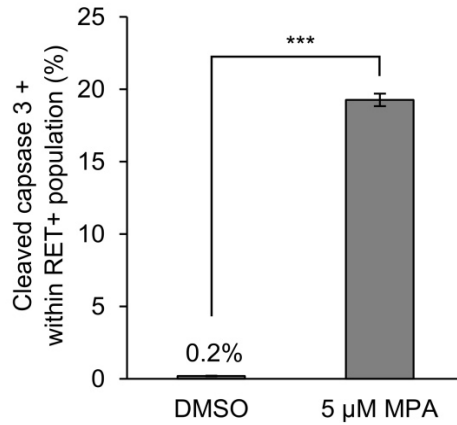
Supplemental Figure 3.2

IMPDH is ubiquitously expressed in the bowel at the time that ENCDCs colonize the colon. Since we anticipated that IMPDH levels might vary by position within the bowel and ENS, we first used whole mount IMPDH immunohistochemistry to visualize and quantify the expression in situ. **(A)** IMPDH reactivity was diffusely cytoplasmic with rod and ring aggregates. Since ENCDCs appeared to have more intense cytoplasmic immunoreactivity for IMPDH, we measured the average fluorescence signal intensity in 2.17 micron thick rings **(B)** (represented by the shaded green region) around mesenchymal and ENCDC (SOX10-positive) nuclei (blue ovals). This strategy was designed to minimize overlap with the cytoplasm of neighboring cells (black lines). **(C)** Intensity values. Each dot is mean fluorescence intensity from a single cell. Measurements are from optical sections of three separate E11.5 colons from the CF1 strain. Thick line = median; thin lines = 25th and 75th percentile. Values have extensive overlap, but ENCDCs have a statistically significant increase in average IMPDH fluorescence intensity. ** = $P < 0.01$, rank-sum test. Since whole bowel staining did not reveal any obvious differences in anti-IMPDH reactivity between regions of the bowel, we quantified **(D)** total cellular anti-IMPDH reactivity in cells dissociated from six E12.5 Tg(Wnt1-Cre); *Rosa26*^{EYFP} bowels that were cultured for 3 hours on fibronectin-coated glass at a density of 3.1×10^4 cells/cm² before fixation and staining. Total-cellular anti-IMPDH fluorescence for each cell was quantified with ImageJ and is shown for EYFP-negative and EYFP-positive populations as histograms.



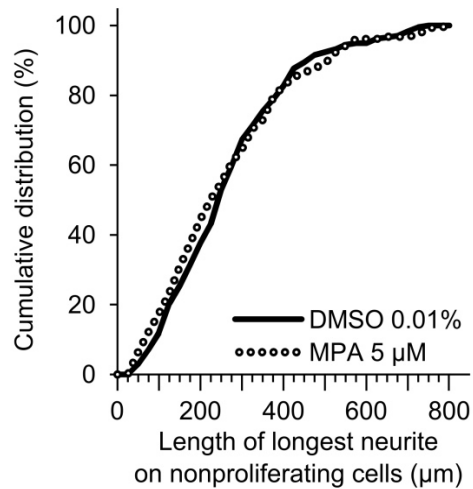
Supplemental Figure 3.3

MPA/MMF treatment from E10.5-E13.5 reduced colon lengths at E13.5. (A) Higher doses of MPA significantly reduced the length of CF1-strain colons at E13.5 ($P < .001$, Kruskal-Wallis test) while lower doses of MPA and oral MMF significantly reduced the length of Wnt1-Cre *Rosa26^{EYFP}*-strain colons (t-tests). Lower doses of MPA did not significantly affect bowel length in C57Bl/6 fetuses, though variability was high (Kruskal-Wallis test). Thick line = median; thin lines = 25th and 75th percentile. *** = $P < 0.001$, * = $P < .05$. (B,C) Plots of ENS colonization extent assessed with double-stained E13.5 Wnt1-Cre *Rosa26^{EYFP}*-strain colons. (B) Cellular markers such as neural-crest lineage marker EYFP or SOX10 have near-perfect concordance for ENS colonization extent measurements. The most caudal TuJ1+ process also reliably indicates colonization extent, albeit with some random error. MPA treatment does not appear to have any systematic effect on the extension of neuronal processes up to ENCDCs at the wavefront.



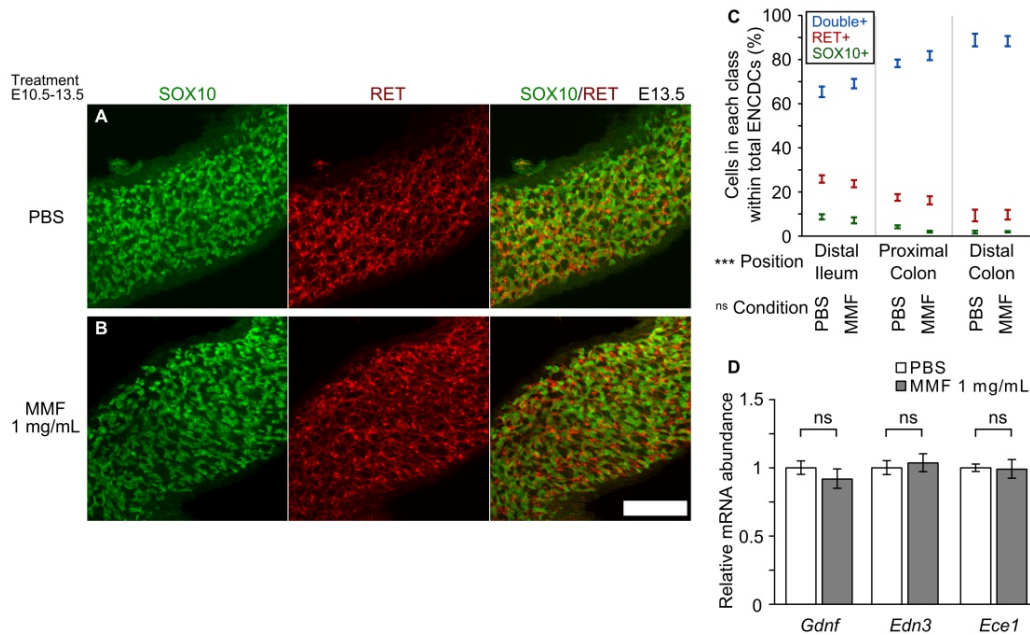
Supplemental Figure 3.4

Cleaved caspase 3 staining of 24-hour explant cultures reveals that MPA induces apoptosis in cultured ENCDCs. *** = $P < 0.001$, t-test.



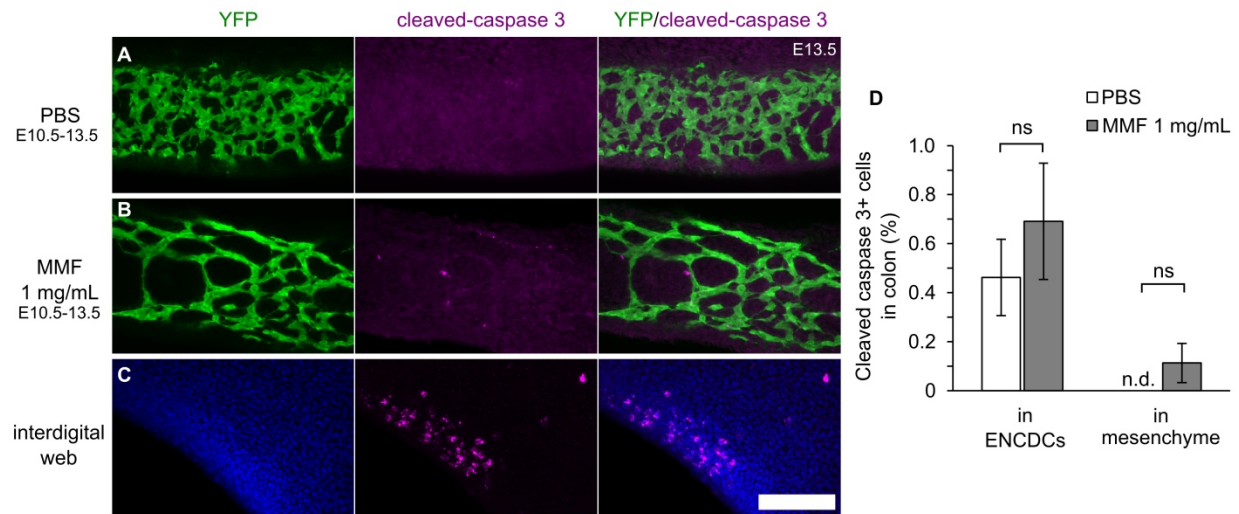
Supplemental Figure 3.5

MPA did not alter neurite growth in post-mitotic neurons. Data show the length of the longest neurite on each TuJ1+ cell that did not incorporate BrdU over the course of 48 hours in culture with GDNF, (n>150 cells/group).



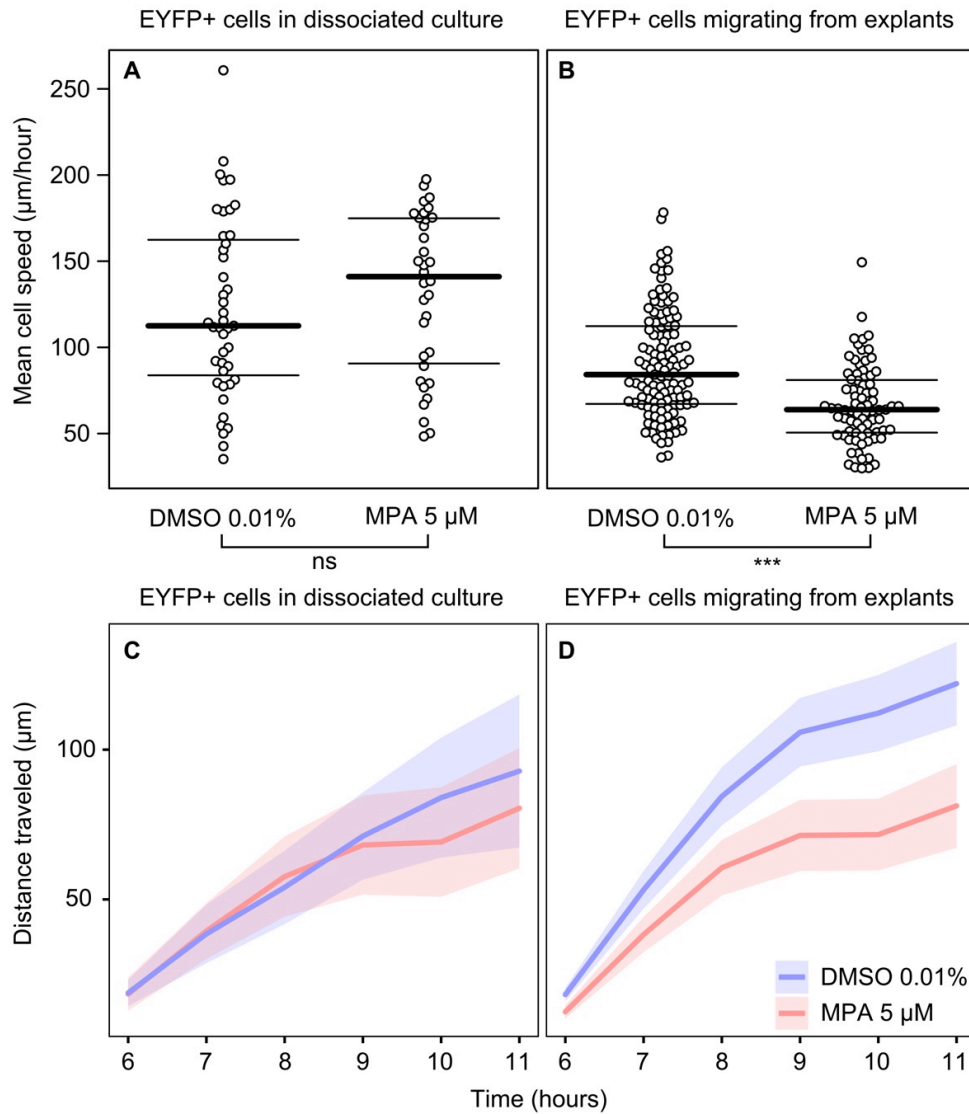
Supplemental Figure 3.6

MMF treatment at doses that significantly reduced ENCDC proliferation and bowel colonization in vivo did not cause premature differentiation at E13.5. 8 μm -thick maximum-intensity projections of SOX10 (pseudocolored green) and RET (pseudocolored red) distal small intestine (**A,B**, scale bar = 100 μm) and quantification of each cell population within total ENCDCs (**C**) demonstrate the expected reduction in the percentage of SOX10, RET double positive progenitor cells within the ENCDC population as we move from distal (e.g. more recently colonized) to proximal. Concomitantly, the RET+, SOX10- and SOX10+, RET- single positive populations increase in proportion as the double-positive proportion falls. Since enteric neurons already exist at this time and are known to lose SOX10 and retain RET expression, the RET single-positive population is very likely a neuronal lineage. Increased differentiation would manifest as a reduction in the proportion of double-positive cells. MMF treatment did not significantly change the percentage of SOX10+, RET+ progenitor cells within the ENCDC population (two-way ANOVA, interaction term was not significant). (**D**) qRT-PCR analysis of mRNAs encoding mesenchyme derived factors important for ENS colonization. RNA was isolated from E13.5 bowels after treatment from E10.5-E13.5 with PBS (5 embryos) or MMF (4 embryos). *Gapdh* is used as an internal reference gene for relative quantitation (t-tests). *** = $P < 0.001$, ns = not significant.



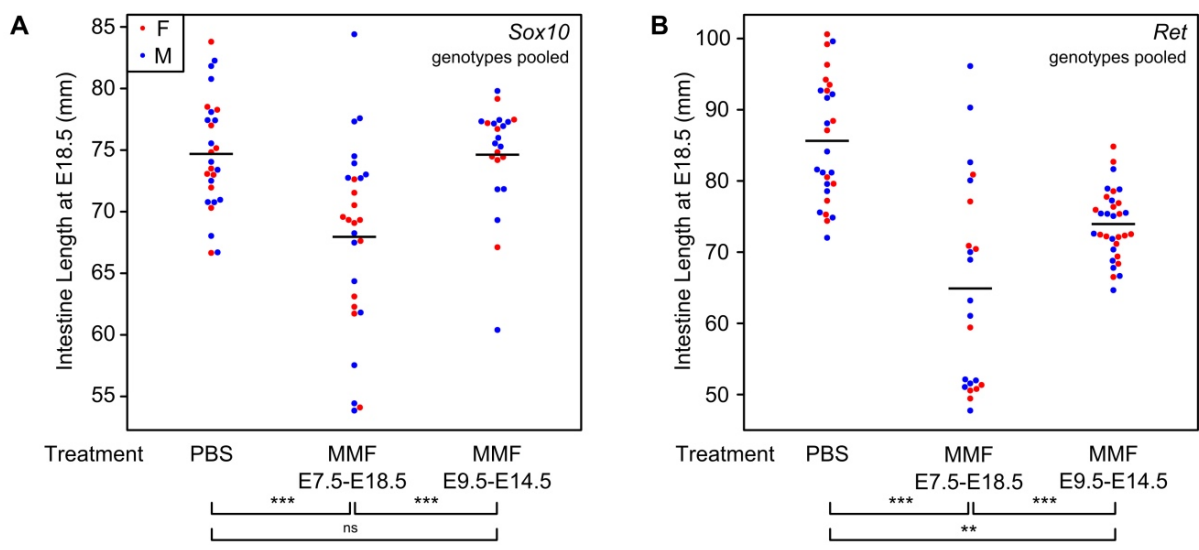
Supplemental Figure 3.7

MMF treatment at doses that significantly reduced ENCDC proliferation and bowel colonization in vivo did not cause detectable canonical caspase-mediated ENCDC apoptosis. Cleaved-caspase 3 reactivity was readily detected in the interdigital web of E13.5 mice (C) but was infrequently detected in ENCDCs or non-neural crest mesenchymal cells with or without MMF treatment (A-B,D) ns = not significant, t-test). Bowels shown in (A-B) are the same as in Figure 3E-F.



Supplemental Figure 3.8

Time lapse imaging of isolated ENCDC and bowel explant cultures reveals that (A, C) MPA does not alter the speeds or migration distance of individual ENCDCs when they are cultured at low density (Kolmogorov-Smirnov test), but does reduce (B, D) the speed and migration of ENCDCs migrating from bowel explants (t-test on log-transformed speeds). Isolated ENCDCs were prepared from the same region of *Wnt1-Cre Rosa26^{EYFP}* bowel as were the explants (small intestine) and were plated at low density (3125 cells/cm²) to minimize cell-cell collisions. Migrating EYFP+ cells were randomly selected for tracking at 8 hours after GDNF addition and tracked for the duration of culture that they remained in the field of view, alive, and non-dividing. Measurements from the middle third (approximately hours 6-11) of 16-hour time-courses were chosen for analysis because most chosen cells stayed in field for this interval. ns = not significant, *** = $P < .05$. Thick lines in A-B = median. Thin lines in A-B = 25th and 75th percentile. Thick lines and shaded region in C-D = Mean and 95% confidence interval.



Supplemental Figure 3.9

MMF treatment during gestation reduces intestine length at E18.5 in (A) *Sox10* and (B) *Ret* interaction experiments. Data are shown with all genotypes pooled since *Ret* or *Sox10* genotype did not affect intestine length. Black lines = mean, *** = $P < 0.001$, ns = not significant, statistical test: Welch ANOVA.

Supplemental Table 3.2: Incidence of neural tube and heart defects in the offspring of MMF treated dams

Paternal Strain / Genotype	Maternal Strain / Genotype	Treatment	Fetus Genotype	N Fetuses	Exencephaly	Heart / Great Vessel Defects
C3HFe/J <i>Sox10^{+/-LacZ}</i>	C57Bl/6	0.25X PBS E7.5-E18.5	<i>Sox10^{+/+}</i>	11	0 (0%)	0 (0%)
			<i>Sox10^{+/-LacZ}</i>	16	0 (0%)	0 (0%)
		MMF 1 mg/mL E7.5-E18.5	<i>Sox10^{+/+}</i>	10	4 (40%)	1 (10%)
			<i>Sox10^{+/-LacZ}</i>	17	6 (35%)	4 (23%)
		MMF 1 mg/mL E9.5-E14.5	<i>Sox10^{+/+}</i>	9	0 (0%)	0 (0%)
			<i>Sox10^{+/-LacZ}</i>	13	0 (0%)	1 (8%) ^A
B6;129X1 <i>Ret^{9/+}</i>	C57Bl/6 <i>Ret^{TGM/+}</i>	0.25X PBS E7.5-E18.5	<i>Ret^{+/+}</i>	7	0 (0%)	0 (0%)
			<i>Ret^{9/+}</i>	6	0 (0%)	0 (0%)
			<i>Ret^{+/-}</i>	6	0 (0%)	0 (0%)
			<i>Ret^{9/-}</i>	8	0 (0%)	0 (0%)
		MMF 1 mg/mL E7.5-E18.5	<i>Ret^{+/+}</i>	5	3 (60%)	0 (0%)
			<i>Ret^{9/+}</i>	4	2 (50%)	0 (0%)
			<i>Ret^{+/-}</i>	4	2 (50%)	0 (0%)
			<i>Ret^{9/-}</i>	8	5 (63%)	3 (38%)
		MMF 1 mg/mL E9.5-E14.5	<i>Ret^{+/+}</i>	9	0 (0%)	0 (0%)
			<i>Ret^{9/+}</i>	4	0 (0%)	0 (0%)
			<i>Ret^{+/-}</i>	5	0 (0%)	0 (0%)
			<i>Ret^{9/-}</i>	14	0 (0%)	0 (0%)

A – Affected fetus was much smaller than littermates

Supplemental Table 3.3: Genotyping oligonucleotides

Gene	Allele	Direction	Sequence	Amplicon Size (bp)
<i>Ret</i>	common	Forward	5'CAG CGC AGG TCT CTC ATC AGT ACC GC AAC C3'	multiple ^A
<i>Ret</i>	wild-type 1	Reverse	5'ACG TCG CTT TCG CCA TCG CCC GTG CGC GCG3'	230
<i>Ret</i>	<i>Ret</i> ^{TGM}	Reverse	5'CCC TGA GCA TGA TCT TCC ATC ACG TCG AAC3'	290
<i>Ret</i>	wild-type 2	Reverse	5'GCG CAG CAG CTA GCC GCA GCG ACC CGG TTC3'	450
<i>Ret</i>	<i>Ret</i> ⁹	Reverse	5'CCC AGT AAG CAT CCC TCG AGA AGT AGA GGC3'	320
<i>Hprt</i>	wild-type	Forward	5'TCT GGT TTT ATA TGG GTA CTG GGG GAT CT3'	218
<i>Hprt</i>	<i>Hprt</i> ^{b-m3}	Forward	5'AGC ATT CCT GCC CCA ACA ATG ATT C3'	288
<i>Hprt</i>	common	Reverse	5'CAT GCA GGC ACT CAC ACA TAC AAG TAA AAA3'	multiple ^B
<i>Sry</i>	N/A	Forward	5'TTG TCT AGA GAG CAT GGA GGG CCA TGT CAA3'	273
<i>Sry</i>	N/A	Reverse	5'CCA CTC CTC TGT GAC ACT TTA GCC CTC CGA3'	
<i>EGFP</i> / <i>EYFP</i>	N/A	Forward	5'GCA CGA CTT CTT CAA GTC CGC CAT GCC3'	265
<i>EGFP</i> / <i>EYFP</i>	N/A	Reverse	5'GCG GAT CTT GAA GTT CAC CTT GAT GCC3'	

A – To detect *Ret*⁺ and *Ret*^{TGM}, a PCR reaction was performed with three primers (common, wild-type 1, and *TGM*). To distinguish *Ret*⁺ and *Ret*⁹, an analogous reaction was used (common, wild-type 2, and *Ret*⁹).

B – To detect *Hprt* genotype, two separate PCR reactions were performed for wild-type (wild-type and common) and *b-m3* (*b-m3* and common).

Supplemental Table 3.4: Primary antibodies

Antibody	Manufacturer / Investigator	Dilution used
rabbit anti-TuJ1	Covance (PRB-435P)	1:10000
goat anti-RET	Neuromics (GT15002)	1:200
rabbit anti-p75NTR	Promega (G323A)	1:200
chicken anti-GFP	Aves Labs (GFP-1020)	1:1000
goat anti-SOX10	Santa Cruz Biotechnology	1:200
rabbit anti-SoxE	Craig Smith, MRCI, Australia	1:4000
rabbit anti-IMPDH	Proteintech (12948-1-AP)	1:100 on bowel; 1:200 on cells
rabbit anti-cleaved Caspase 3	Cell Signaling (#9661)	1:250
Alexa 594-conjugated mouse anti-BrdU	Life Technologies (PRB-1)	1:50
biotin-XX conjugated anti-HuC/HuD	Life Technologies (A21272)	400 ng/mL

3.7 References

1. Heuckeroth RO. Hirschsprung Disease. In: Faure C, Di Lorenzo C, Thapar N eds. *Pediatric Neurogastroenterology*. New York: Humana Press; 2013:271–283
2. Amiel J et al. Hirschsprung disease, associated syndromes and genetics: a review. *J Med Genet*. 2008;45(1):1–14.
3. Carrasquillo MM et al. Genome-wide association study and mouse model identify interaction between RET and EDNRB pathways in Hirschsprung disease. *Nat Genet*. 2002;32(2):237–244.
4. Gabriel SB et al. Segregation at three loci explains familial and population risk in Hirschsprung disease. *Nat Genet*. 2002;31(1):89–93.
5. Emison ES et al. A common sex-dependent mutation in a RET enhancer underlies Hirschsprung disease risk. *Nature*. 2005;434(7035):857–863.
6. De Pontual L et al. Epistatic interactions with a common hypomorphic RET allele in syndromic Hirschsprung disease. *Hum Mutat*. 2007;28(8):790–796.
7. Heanue TA, Pachnis V. Enteric nervous system development and Hirschsprung's disease: advances in genetic and stem cell studies. *Nat Rev Neurosci*. 2007;8(6):466–479.
8. Fu M, Tam PKH, Sham MH, Lui VCH. Embryonic development of the ganglion plexuses and the concentric layer structure of human gut: a topographical study. *Anat Embryol*. 2004;208(1):33–41.
9. Wallace AS, Burns AJ. Development of the enteric nervous system, smooth muscle and interstitial cells of Cajal in the human gastrointestinal tract. *Cell Tissue Res*. 2005;319(3):367–382.
10. Lake JI, Heuckeroth RO. Enteric nervous system development: migration, differentiation, and disease. *Am J Physiol Gastrointest Liver Physiol*. 2013;305(1):G1–G24.
11. Vohra BPS, Fu M, Heuckeroth RO. Protein kinase C ζ and glycogen synthase kinase-3 β control neuronal polarity in developing rodent enteric neurons, whereas SMAD specific E3 ubiquitin protein ligase 1 promotes neurite growth but does not influence polarity. *J Neurosci*. 2007;27(35):9458–9468.
12. Fu M et al. Vitamin A facilitates enteric nervous system precursor migration by reducing Pten accumulation. *Development*. 2010;137(4):631–640.
13. Stewart AL, Young HM, Popoff M, Anderson RB. Effects of pharmacological inhibition of small GTPases on axon extension and migration of enteric neural crest-derived cells. *Dev Biol*. 2007;307(1):92–104.

14. Zhang Y, Kim T-H, Niswander L. Phactr4 regulates directional migration of enteric neural crest through PP1, integrin signaling, and cofilin activity. *Genes Dev.* 2012;26(1):69–81.
15. Anderson RB et al. The cell adhesion molecule L1 is required for chain migration of neural crest cells in the developing mouse gut. *Gastroenterology.* 2006;130(4):1221–1232.
16. Breau MA, Dahmani A, Broders-Bondon F, Thiery J-P, Dufour S. β 1 integrins are required for the invasion of the caecum and proximal hindgut by enteric neural crest cells. *Development.* 2009;136(16):2791–2801.
17. Broders-Bondon F, Paul-Gilloteaux P, Carlier C, Radice GL, Dufour S. N-cadherin and β 1-integrins cooperate during the development of the enteric nervous system. *Dev Biol.* 2012;364(2):178–191.
18. Chong CR, Chen X, Shi L, Liu JO, Sullivan DJ. A clinical drug library screen identifies astemizole as an antimalarial agent. *Nat Chem Biol.* 2006;2(8):415–416.
19. Kuhlman J, Eisen JS. Genetic screen for mutations affecting development and function of the enteric nervous system. *Dev Dyn.* 2007;236(1):118–127.
19. CellCept [package insert]. Genentech Inc., South San Francisco, CA; June 2012 http://www.gene.com/download/pdf/cellcept_prescribing.pdf. Accessed March 7, 2013
21. Reagan-Shaw S, Nihal M, Ahmad N. Dose translation from animal to human studies revisited. *FASEB J.* 2008;22(3):659–661.
22. Sato Y, Heuckeroth RO. Retinoic acid regulates murine enteric nervous system precursor proliferation, enhances neuronal precursor differentiation, and reduces neurite growth in vitro. *Dev Biol.* 2008;320(1):185–198.
23. Jonsson CA, Svensson L, Carlsten H. Beneficial effect of the inosine monophosphate dehydrogenase inhibitor mycophenolate mofetil on survival and severity of glomerulonephritis in systemic lupus erythematosus (SLE)-prone MRL*lpr/lpr* mice. *Clin Exp Immunol.* 1999;116(3):534–541.
24. Corpening JC et al. Isolation and live imaging of enteric progenitors based on Sox10-Histone2BVenus transgene expression. *genesis.* 2011;49(7):599–618.
25. Wallace AS, Schmidt C, Schachner M, Wegner M, Anderson RB. L1cam acts as a modifier gene during enteric nervous system development. *Neurobiology of Disease.* 2010;40(3):622–633.
26. Uesaka T, Nagashimada M, Yonemura S, Enomoto H. Diminished Ret expression compromises neuronal survival in the colon and causes intestinal aganglionosis in mice. *J Clin Invest.* 2008;118(5):1890–1898.
27. Simpson MJ, Zhang DC, Mariani M, Landman KA, Newgreen DF. Cell proliferation drives neural crest cell invasion of the intestine. *Dev Biol.* 2007;302(2):553–568.

28. Hooper M, Hardy K, Handyside A, Hunter S, Monk M. HPRT-deficient (Lesch-Nyhan) mouse embryos derived from germline colonization by cultured cells. *Nature*. 1987;326(6110):292–295.
29. Allison AC, Eugui EM. Mycophenolate mofetil and its mechanisms of action. *Immunopharmacology*. 2000;47(2-3):85–118.
30. Hadjantonakis AK, Cox LL, Tam PP, Nagy A. An X-linked GFP transgene reveals unexpected paternal X-chromosome activity in trophoblastic giant cells of the mouse placenta. *Genesis*. 2001;29(3):133–140.
31. Anderka MT, Lin AE, Abuelo DN, Mitchell AA, Rasmussen SA. Reviewing the evidence for mycophenolate mofetil as a new teratogen: Case report and review of the literature. *Am J Med Genet*. 2009;149A(6):1241–1248.
32. Lin AE et al. An additional patient with mycophenolate mofetil embryopathy: Cardiac and facial analyses. *Am J Med Genet*.
33. Britsch S et al. The transcription factor Sox10 is a key regulator of peripheral glial development. *Genes Dev*. 2001;15(1):66–78.
34. Paratore C, Eichenberger C, Suter U, Sommer L. Sox10 haploinsufficiency affects maintenance of progenitor cells in a mouse model of Hirschsprung disease. *Hum Mol Genet*. 2002;11(24):3075–3085.
35. Young HM et al. Dynamics of neural crest-derived cell migration in the embryonic mouse gut. *Dev Biol*. 2004;270(2):455–473.
36. Natarajan D, Marcos-Gutierrez C, Pachnis V, de Graaff E. Requirement of signalling by receptor tyrosine kinase RET for the directed migration of enteric nervous system progenitor cells during mammalian embryogenesis. *Development*. 2002;129(22):5151–5160.
37. Gianino S, Grider JR, Cresswell J, Enomoto H, Heuckeroth RO. GDNF availability determines enteric neuron number by controlling precursor proliferation. *Development*. 2003;130(10):2187–2198.
38. Jain S et al. Mice expressing a dominant-negative Ret mutation phenocopy human Hirschsprung disease and delineate a direct role of Ret in spermatogenesis. *Development*. 2004;131(21):5503–5513.
39. Kapur RP, Yost C, Palmiter RD. A transgenic model for studying development of the enteric nervous system in normal and aganglionic mice. *Development*. 1992;116(1):167.
40. Druckenbrod NR, Epstein ML. Age-dependent changes in the gut environment restrict the invasion of the hindgut by enteric neural progenitors. *Development*. 2009;136(18):3195–3203.
41. Hotta R, Anderson RB, Kobayashi K, Newgreen DF, Young HM. Effects of tissue age, presence of neurones and endothelin-3 on the ability of enteric neurone precursors to colonize

recipient gut: implications for cell-based therapies. *Neurogastroenterol Motil.* 2010;22(3):331–e86.

42. Curry CJ et al. Smith-Lemli-Opitz syndrome-type II: multiple congenital anomalies with male pseudohermaphroditism and frequent early lethality. *Am J Med Genet.* 1987;26(1):45–57.

43. Barlow AJ, Dixon J, Dixon MJ, Trainor PA. Balancing neural crest cell intrinsic processes with those of the microenvironment in Tcofl haploinsufficient mice enables complete enteric nervous system formation. *Hum Mol Genet.* 2012;21(8):1782–1793.

44. Long H, Cameron S, Yu L, Rao Y. De Novo GMP Synthesis Is Required for Axon Guidance in *Drosophila*. *Genetics.* 2006;172(3):1633–1642.

45. Schmidt F, Eckardt K, Shakibaei M, Glander P, Stahlmann R. Effects of mycophenolic acid alone and in combination with its metabolite mycophenolic acid glucuronide on rat embryos in vitro. *Arch Toxicol.* 2013;87(2):361–370.

46. Mondin M et al. Alterations in cytoskeletal protein expression by mycophenolic acid in human mesangial cells requires Rac inactivation. *Biochem Pharmacol.* 2007;73(9):1491–1498.

47. Krotz F et al. Mycophenolate Acid Inhibits Endothelial NAD(P)H Oxidase Activity and Superoxide Formation by a Rac1-Dependent Mechanism. *Hypertension.* 2007;49(1):201–208.

48. Kapur RP et al. Abnormal microenvironmental signals underlie intestinal aganglionosis in dominant megacolon mutant mice. *Dev Biol.* 1996;174(2):360–369.

49. Kapur RP, Sweetser DA, Doggett B, Siebert JR, Palmiter RD. Intercellular signals downstream of endothelin receptor-B mediate colonization of the large intestine by enteric neuroblasts. *Development.* 1995;121(11):3787–3795.

50. Carmona-Fontaine C et al. Complement Fragment C3a Controls Mutual Cell Attraction during Collective Cell Migration. *Developmental Cell.* 2011;21(6):1026–1037.

51. Carmona-Fontaine C et al. Contact inhibition of locomotion in vivo controls neural crest directional migration. *Nature.* 2008;456(7224):957–961.

52. Wang X, Chan AKK, Sham M-H, Burns AJ, Chan WY. Analysis of the sacral neural crest cell contribution to the hindgut enteric nervous system in the mouse embryo. *Gastroenterology.* 2011;141(3):992–1002.e6.

53. Anderson RB. Matrix metalloproteinase-2 is involved in the migration and network formation of enteric neural crest-derived cells. *Int J Dev Biol.* 2010;54(1):63–69.

54. Murphey RD, Zon LI. Small molecule screening in the zebrafish. *Methods.* 2006;39(3):255–261.

55. Danielian PS, Muccino D, Rowitch DH, Michael SK, McMahon AP. Modification of gene activity in mouse embryos in utero by a tamoxifen-inducible form of Cre recombinase. *Curr Biol*. 1998;8(24):1323–1326.
56. Srinivas S et al. Cre reporter strains produced by targeted insertion of EYFP and ECFP into the ROSA26 locus. *BMC Dev Biol*. 2001;1:4–4.
57. Enomoto H et al. RET signaling is essential for migration, axonal growth and axon guidance of developing sympathetic neurons. *Development*. 2001;128(20):3963–3974.
58. Stratman JL, Barnes WM, Simon TC. Universal PCR genotyping assay that achieves single copy sensitivity with any primer pair. *Transgenic Res*. 2003;12(4):521–522.
59. Creedon DJ et al. Neurturin shares receptors and signal transduction pathways with glial cell line-derived neurotrophic factor in sympathetic neurons. *Proc Natl Acad Sci USA*. 1997;94(13):7018–7023.
60. Vohra BPS et al. Reduced endothelin converting enzyme-1 and endothelin-3 mRNA in the developing bowel of male mice may increase expressivity and penetrance of Hirschsprung disease-like distal intestinal aganglionosis. *Dev Dyn*. 2007;236(1):106–117.
61. Wang H, Zhang Y, Heuckeroth RO. PAI-1 deficiency reduces liver fibrosis after bile duct ligation in mice through activation of tPA. *FEBS Letters*. 2007;581(16):3098–3104.
62. Ramakers C, Ruijter JM, Deprez RHL, Moorman AF. Assumption-free analysis of quantitative real-time polymerase chain reaction (PCR) data. *Neuroscience Letters*. 2003;339(1):62–66.
63. Pfaffl MW. A new mathematical model for relative quantification in real-time RT-PCR. *Nucleic Acids Res*. 2001;29(9):e45.
64. Preibisch S, Saalfeld S, Tomancak P. Globally optimal stitching of tiled 3D microscopic image acquisitions. *Bioinformatics*. 2009;25(11):1463–1465.
65. Meijering E, Dzyubachyk O, Smal I. Methods for Cell and Particle Tracking. In: P. Michael conn ed. *Methods in Enzymology*. Academic Press; 2012:183–200

Chapter 4: Neural crest requires *Impdh2* for development of the enteric nervous system, great vessels, and craniofacial skeleton

4.1 Summary

Mutations that impair the proliferation of enteric neural crest-derived cells (ENCDC) cause Hirschsprung disease, a potentially lethal birth defect where the enteric nervous system (ENS) is absent from distal bowel. Inosine 5' monophosphate dehydrogenase (IMPDH) activity is essential for *de novo* GMP synthesis, and chemical inhibition of IMPDH induces Hirschsprung disease-like pathology in mouse models by reducing ENCDC proliferation. Two IMPDH isoforms are ubiquitously expressed in the embryo, but only IMPDH2 is required for life. To further understand the role of IMPDH2 in ENS and neural crest development, we characterized a conditional *Impdh2* mutant mouse. Deletion of *Impdh2* in the early neural crest using the Wnt1-Cre transgene produced defects in multiple neural crest derivatives including highly penetrant intestinal aganglionosis, agenesis of the craniofacial skeleton, and cardiac outflow tract and great vessel malformations. Analysis using a *Rosa26* reporter mouse suggested that some or all of the remaining ENS in *Impdh2* conditional-knockout animals was derived from cells that escaped Wnt1-Cre mediated DNA recombination. These data suggest that IMPDH2 mediated guanine nucleotide synthesis is essential for normal development of the ENS and other neural crest derivatives.

4.2 Introduction

The enteric nervous system (ENS) is a network of ganglia distributed throughout the digestive tract that autonomously controls motility, secretion, and blood flow (1). The ENS develops from migratory neural crest-derived cells that invade, migrate through, and colonize the nascent bowel while dividing rapidly, eventually reorganizing into discrete ganglia, and differentiating into glia or one of more than fifteen functional classes of neuron (2–4). A complete and functional ENS is required for life. Incomplete colonization of the bowel by ENS precursors results in Hirschsprung disease (HSCR), a life-threatening oligogenic birth defect where a segment of distal bowel is devoid of enteric neurons (aganglionosis). Bowel colonization critically requires that ENCCs proliferate efficiently (5, 6). For this reason, many of the mutations that cause HSCR impair ENS precursor proliferation or self-renewal (2, 7). Inhibition of ENCC proliferation with the antimetabolite immunosuppressant mycophenolic acid (MPA) also causes aganglionosis in mice (6) and enhances the penetrance and phenotypic severity of mutations that model HSCR. MPA blocks the rate-limiting step of *de novo* guanine nucleotide synthesis by inhibiting inosine 5' monophosphate dehydrogenase (IMPDH), a ubiquitous metabolic enzyme whose expression is relatively enriched in ENCC (6). Prenatal MPA exposure in humans is also associated with a specific pattern of birth defects (8), some of which are plausibly due to disruptions in neural crest development (9).

Relatively little is known about the developmental roles of IMPDH, which is present in two isoforms encoded by separate genes in vertebrates. IMPDH2 is widely expressed and is enriched in activated lymphocytes, tumor cells, fetal tissues, and other

proliferative cells (10–12). Homozygous *Impdh2* deletion in mice results in early lethality prior to embryo implantation, while heterozygous deletion results in a subtle reduction in the IMPDH activity of splenic lymphocytes (13). IMPDH1 is also ubiquitously expressed, but does not appear to be regulated by proliferative demand, and has a specialized but poorly-understood role in the retina (12, 14–17), where missense mutations in *IMPDH1* cause a form of autosomal dominant retinitis pigmentosa in humans. In mice, *Impdh1* is dispensable for life and its deletion results in a relatively mild retinal phenotype (16, 18).

Our previous experiments with the non-selective IMPDH inhibitor mycophenolic acid did not target IMPDH inhibition to neural crest derivatives, nor did they indicate whether IMPDH1 and IMPDH2 have redundant roles or whether one isoform is uniquely required for neural crest development. Since *Impdh1* homozygous mutant mice are viable and fertile and thus must form a complete and functional ENS, we hypothesized that *Impdh2* is required within the neural-crest lineage for ENCDCs to proliferate efficiently and colonize the bowel. To further explore the role for this basic metabolic pathway in development, we deleted *Impdh2* in the early neural crest of mice using a Cre/loxP system and Wnt1-Cre mice.

Here we demonstrate that *Impdh2* expression is required in the neural crest for development of the craniofacial skeleton, cardiac outflow tract, and enteric nervous system. In the ENS, loss of *Impdh2* results in extensive bowel aganglionosis. Furthermore, ENCDC that do colonize the bowel in *Impdh2* conditional mutant mice are delayed and demonstrate incomplete Cre/loxP recombination, indicating a strong selective pressure against *Impdh2* deletion. Collectively these data support the need for de-novo guanine nucleotide synthesis and cell proliferation during neural crest

development and are consistent with the hypothesis that IMPDH1 does not adequately supply metabolic guanine nucleotide needs for these neural crest-derived cell populations.

4.3 Results

4.3.1 *Impdh2* deletion in the neural crest results in craniofacial and cardiac defects.

Guanine nucleotides can be produced either *de novo* via IMPDH1/IMPDH2 or by the purine salvage pathway. To determine whether *Impdh2* was required within the neural crest lineage for ENS development or whether *Impdh1* and/or purine salvage from adjacent tissue could provide adequate GMP once embryonic lethality was bypassed, we used the well-characterized Wnt1-Cre transgene (19) to delete a conditional *Impdh2*^{loxP} allele (Supplemental Figure 4.1) in the early neural crest. As expected, both *Impdh2*^{loxP/loxP} and *Impdh2*^{loxP/Del} mice lacking Wnt1-Cre survived to adulthood and were fertile. While Wnt1-Cre *Impdh2*^{loxP/+} mice appeared normal, Wnt1-Cre *Impdh2*^{loxP/loxP} mice did not survive after birth, though they did develop to term. At E18.5, Wnt1-Cre *Impdh2*^{loxP/loxP} fetuses had profound malformations of the anterior head (Figure 4.1A,E) including a near-total absence of the jaw and a protruding brain that was not covered by bone. Eyes were sometimes open, and ear pinnae were rudimentary. Bone and cartilage staining revealed that most skeletal structures anterior to the parietal (dorsal) or basisphenoid (ventral) bones were reduced or ablated, and the remaining structures consisted of irregular spicules of bone and cartilage (Figure 4.1B-D,F-H). Notably, these structures are normally neural crest-derived. Several posterior elements of the skull that are neural crest-derived are also reduced or missing in Wnt1-Cre *Impdh2*^{loxP/loxP} fetuses,

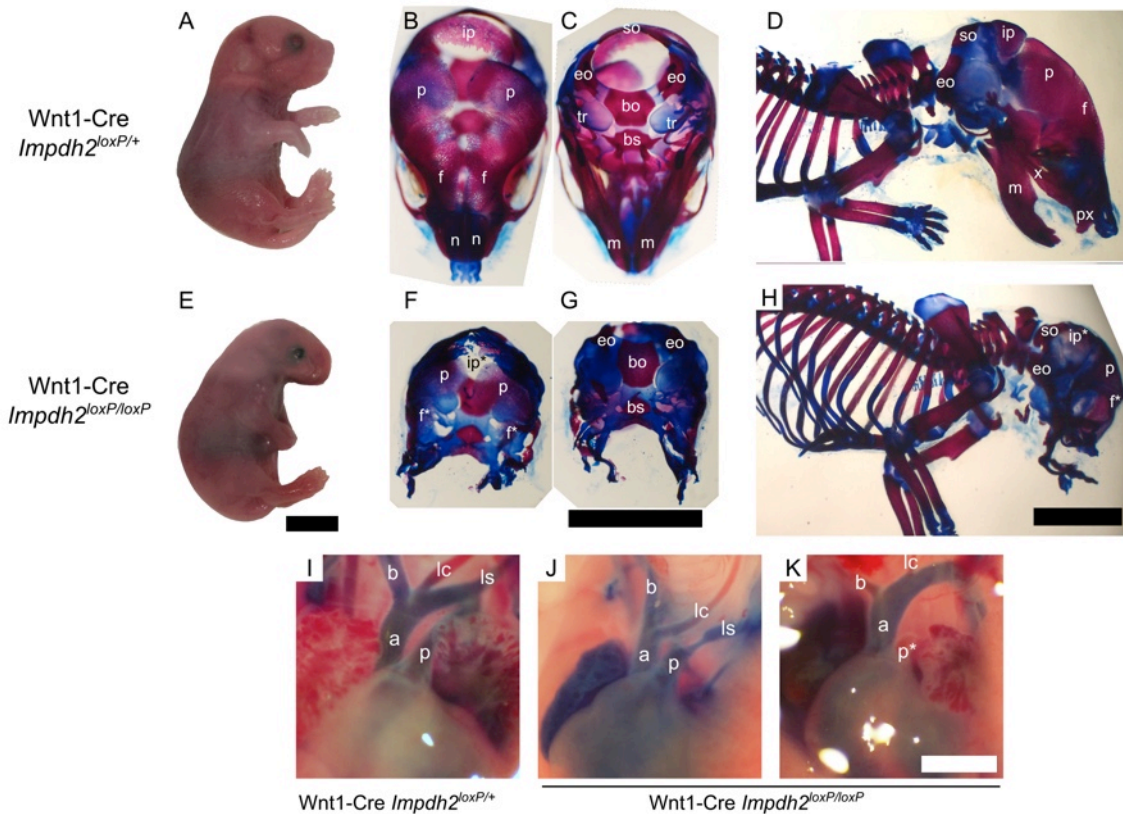


Figure 4.1: *Impdh2* deletion by *Wnt1-Cre* results in craniofacial and cardiac defects at term.

At embryonic day 18.5 (E18.5), (A, E) *Wnt1-Cre Impdh2^{loxP/loxP}* fetuses lack a jaw, external ear, or any mineralized bone in the anterior head. (B, F) superior, (C, G) inferior, and (D, H) lateral views of bone and cartilage stained skulls show that *Wnt1-Cre Impdh2^{loxP/loxP}* fetuses have missing or severely reduced neural-crest derived skeletal structures of the head, including most structures anterior to the parietal and basisphenoid bones as well as the neural crest derived interparietal bone and tympanic rings. bo = basiooccipital bone, bs = basisphenoid bone, eo = exooccipital bone, f = frontal bone, m = mandible, n = nasal bone, p = parietal bone, px = premaxilla, ip = interparietal bone, so = supraoccipital bone, tr = tympanic ring, x = maxilla, * = remnant or abnormal structure. scale bars in panels A-H = 5 mm. Injection of ink into the ventricles of control *Wnt1-Cre Impdh2^{loxP/+}* hearts (I) reveals normal anatomy of the great arteries. *Wnt1-Cre Impdh2^{loxP/loxP}* hearts (J and K) show representative malformations of the great vessels and outflow tract: J shows an interrupted aortic arch, where the left subclavian (ls) arises from the pulmonary artery instead of the aorta. In K, the pulmonary artery fails to label with ink despite ink injection into the right ventricle, indicating pulmonic stenosis or atresia. a = aorta, p = pulmonary artery, b = brachiocephalic trunk, lc = left common carotid artery, ls = left subclavian artery, p* = atretic pulmonary artery. Scale bar = 2 mm.

such as the interparietal bone and tympanic rings (20, 21). Since our previous experiments with IMPDH inhibition also revealed heart defects in exposed fetuses, we examined hearts at E18.5 using dye injection into the left ventricle and observed outflow tract and great vessel defects in 4 of 8 Wnt1-Cre *Impdh2*^{loxP/loxP} fetuses (Figure 4.1I-K).

4.3.2 Neural crest-specific deletion of *Impdh2* results in bowel aganglionosis.

Examination of enteric neurons in E18.5 fetal bowel using ANNA-1 (anti-HuC/HuD) staining revealed normal colonization in *Impdh2*^{loxP/+} fetuses while deletion of *Impdh2* in the neural crest of *Impdh2*^{loxP/loxP} fetuses resulted in severe defects of the ENS including highly-penetrant aganglionosis of variable length (Figure 4.2A-C) ranging from very short colonic aganglionosis to total intestinal aganglionosis. In bowels that had normally-innervated regions, those regions were always oral to hypoganglionic and aganglionic regions, strongly suggesting that *Impdh2* deletion causes a vagal ENCC colonization defect. Some isolated enteric neurons were found in the walls of otherwise aganglionic colons and are possibly of sacral neural crest origin. We were concerned that the variable phenotype seen in the conditional knockout was due to the presence of two “floxed” alleles of *Impdh*, resulting in either incomplete recombination or a failure to reduce IMPDH2 protein levels quickly enough to produce a complete phenotype in the ENS. To address this concern, we converted one copy of *Impdh2*^{loxP} to the deleted allele *Impdh2*^{Del} in the germline and examined the phenotype of Wnt1-Cre *Impdh2*^{loxP/Del} fetuses. This configuration requires only a single recombination event to delete *Impdh2*. This strategy greatly increased the severity of the ENS phenotype. (Figure 4.2A,D).

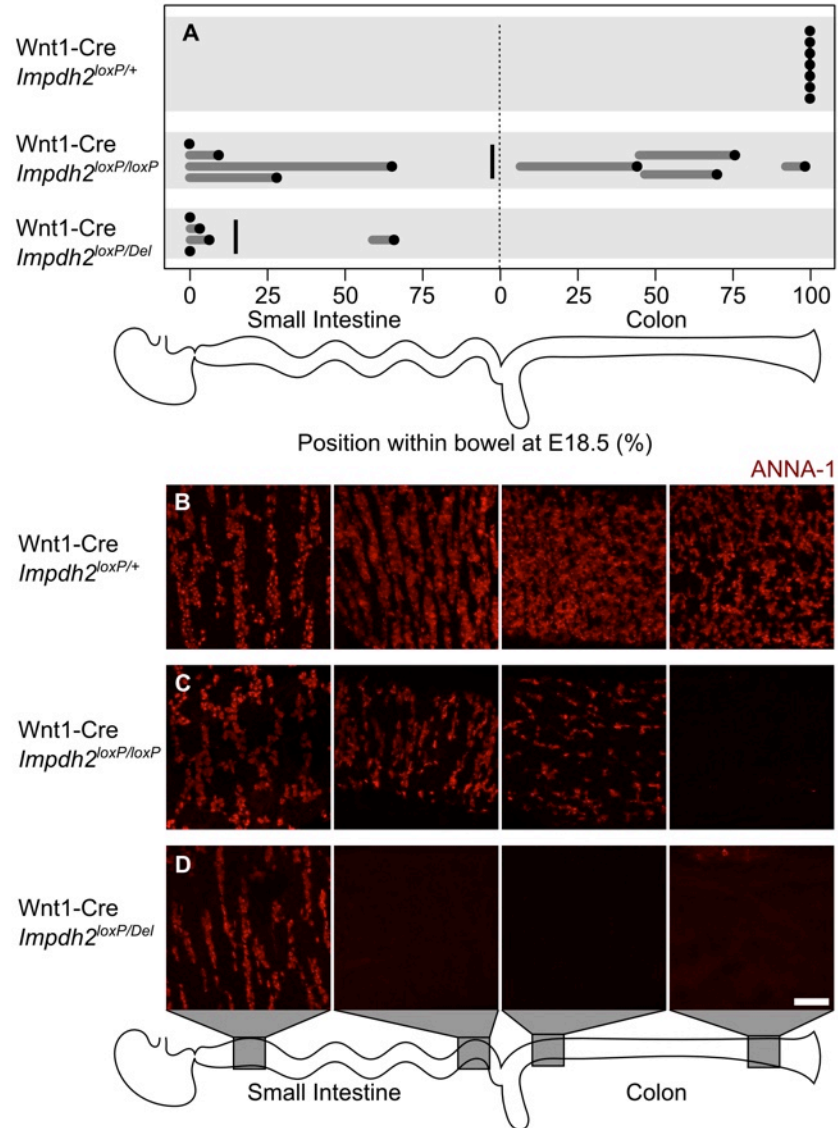


Figure 4.2: *Impdh2* deletion by Wnt1-Cre causes highly penetrant aganglionosis of variable length at term.

(A) At E18.5, all Wnt1-Cre *Impdh2*^{loxP/+} bowels are fully colonized by neurons, while Wnt1-Cre *Impdh2*^{loxP/loxP} and Wnt1-Cre *Impdh2*^{loxP/Del} intestines demonstrate distal aganglionosis reminiscent of Hirschsprung disease. Proximal to aganglionic bowel there is a hypoganglionic transition zone and eventually, in many cases, regions of relatively normal bowel. Dots = position of the most caudal enteric neuron in each intestine, grey lines = hypoganglionic regions. vertical lines = mean positions of the most caudal ENCDC. (B) ANNA-1 (anti-HuC/HuD) staining of enteric neuron somata reveals that Wnt1-Cre *Impdh2*^{loxP/+} bowels contain a dense network of enteric neurons throughout the bowel while (C-D) conditional knockout genotypes contain aganglionic (distal colon), hypoganglionic (C, proximal colon) and relatively normal regions of the ENS (proximal small intestine). ANNA-1 photomicrographs are maximum intensity projections of 20 micron-thick volumes. Scale bar = 100 μ m.

4.3.3 *Impdh2* deleted ENCDCs colonize the bowel abnormally

Because of the distal aganglionosis apparent at E18.5, we examined the effects of *Impdh2* deletion as the ENCDC migration process nears completion at E13.5 using a mouse strain that expresses EYFP after Cre-induced DNA recombination, *Rosa26^{EYFP}*. The craniofacial defects that result from *Impdh2* deletion were readily apparent at E13.5. While lineage-marked EYFP⁺ cranial neural crest cells did migrate to the expected regions of the anterior head in Wnt1-Cre *Impdh2^{loxP/loxP}* and Wnt1-Cre *Rosa26^{EYFP}* *Impdh2^{loxP/Del}* fetuses, the resulting structures were abnormal in Wnt1-Cre *Rosa26^{EYFP}* *Impdh2^{loxP/loxP}* embryos and the pharyngeal arches were almost entirely absent in the *Impdh2^{loxP/Del}* genotype (Figure 4.3A,C,E). In the ENS, Wnt1-Cre *Impdh2^{loxP/+}* colons were uniformly colonized at E13.5 as indicated by EYFP fluorescence or SOX10 staining. In contrast, both Wnt1-Cre *Impdh2^{loxP/loxP}* and Wnt1-Cre *Impdh2^{loxP/Del}* genotypes showed severe colonization defects at E13.5 (Figure 4.3B,D,F-G) and colonization in the Wnt1-Cre *Impdh2^{loxP/Del}* genotype was slightly but significantly reduced relative to Wnt1-Cre *Impdh2^{loxP/loxP}* (Figure 4.3G). The structure of the proximal colonized regions of the ENS was also abnormal in both conditional knockout genotypes. In *Impdh2^{loxP/+}* fetuses, the ENCDCs immediately behind the wavefront were organized into chains of cells (Figure 4.3B), quickly transitioning into a high-density network more proximally. In contrast, Wnt1-Cre *Impdh2^{loxP/loxP}* and Wnt1-Cre *Impdh2^{loxP/Del}* bowel contained long stretches of low-density ENCDC strands and even isolated ENCDCs (Figure 4.3D,F). Notably, the proximal colonized areas of E18.5 bowel appeared essentially normal (Figure 4.2), indicating that these sparse strands of ENCDCs did expand between E13.5 and E18.5 to populate the colonized regions of the proximal bowel. In an effort to determine the fate of

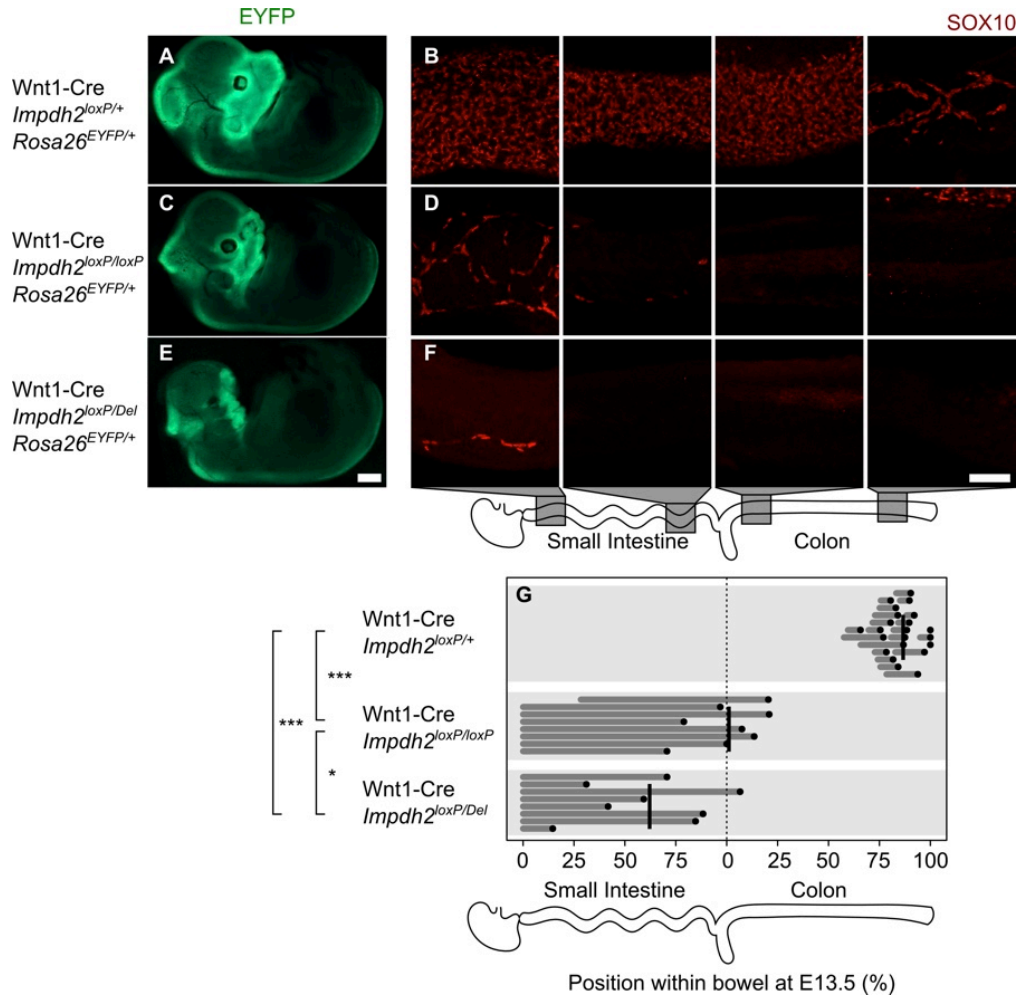


Figure 4.3: *Impdh2* conditional knockout fetuses have cranial neural crest and ENCDC abnormalities at E13.5

(A, C, E) EYFP-positive neural crest derivatives have migrated to the anterior head in all genotypes, but in (C) *Wnt1-Cre Rosa26^{EYFP} Impdh2^{loxP/loxP}* fetuses, EYFP-positive tissue is reduced in size and has not fused at the midline. In (E) *Wnt1-Cre Rosa26^{EYFP} Impdh2^{loxP/Del}* fetuses, EYFP-positive tissue is still present anterolaterally but does not form recognizable branchial arch structures. Scale bar = 1 mm. In (B) control bowel, SOX10-positive enteric neural crest-derived cells (ENCDCs) have colonized almost the entire bowel and have accumulated to a high density in colonized regions (small intestine and proximal colon). In (D) *Wnt1-Cre Impdh2^{loxP/loxP}* and (F) *Impdh2^{loxP/Del}* intestine, colonized regions are both significantly shorter and contain fewer cells, indicating a profound inability for ENCDCs to efficiently populate the intestine. Scale bar = 100 μ m. Measurements (G) of colonization extent as well as colonized regions of bowel containing an unusually low ENCDC density reveal that *Wnt1-Cre Impdh2^{loxP/Del}* intestine has a significantly worse colonization defect than *Wnt1-Cre Impdh2^{loxP/loxP}*. Dots = position of the most caudal ENCDC in each intestine as indicated by EYFP expression in *Rosa26^{EYFP}* bowels or SOX10 staining in *Rosa26⁺* bowels. Grey lines = regions of low ENCDC density. Vertical lines = mean positions of the most caudal ENCDC. * = $P < .05$, *** = $P < .001$ by Welch's t-test on the most-caudal ENCDC positions.

Impdh2-deficient ENCDCs, we measured DNA synthesis and apoptosis at E13.5 using BrdU labeling and cleaved-caspase 3 staining. We did not detect significant numbers of cleaved-caspase 3 reactive ENCDCs of any genotype and found that BrdU incorporation in the EYFP-positive cells of E13.5 *Impdh2*^{loxP/Del} bowel was not significantly reduced relative to EYFP-positive cells at the migration wavefront in *Impdh2*^{loxP/+} fetuses (Supplemental Figure 4.2).

4.3.4 Wnt1-Cre incompletely recombines the *Rosa26*^{EYFP} reporter in the ENS of *Impdh2* conditional knockouts

E18.5 fetuses that also carried the *Rosa26*^{EYFP} reporter displayed an unexpected phenotype. In Wnt1-Cre *Impdh2*^{loxP/+} bowel, all neurons were EYFP-positive (Figure 4.4A), as expected given the Wnt1-Cre fate map (20). However, in every *Impdh2*^{loxP/loxP} *Rosa26*^{EYFP} fetus (N=4 EYFP-positive samples), mixtures of varying numbers of EYFP-positive and EYFP-negative neurons were clearly visible (Figure 4.4B-C). The degree of incomplete recombination varied both between animals and between regions of a single bowel, reflecting the clonal mixing that occurs during ENS development (22–24). When we examined heterozygous Wnt1-Cre *Impdh2*^{loxP/+} *Rosa26*^{EYFP} bowels at E18.5, (N=4 EYFP-positive samples), we were unable to find any EYFP-negative neurons. Similarly, when we examined Wnt1-Cre *Impdh2*^{loxP/+} and Wnt1-Cre *Impdh2*^{loxP/Del} bowels carrying the *Rosa26*^{EYFP} reporter at E13.5 and stained for SOX10, we observed many EYFP-negative ENCDCs in the *Impdh2*^{loxP/Del} genotype (2 of 4 embryos, Figure 4.4D-E). After searching the colonized regions of Wnt1-Cre *Impdh2*^{loxP/+} bowels marked by EYFP (N=6), we found only a few scattered EYFP-negative SOX10-positive ENCDCs in a

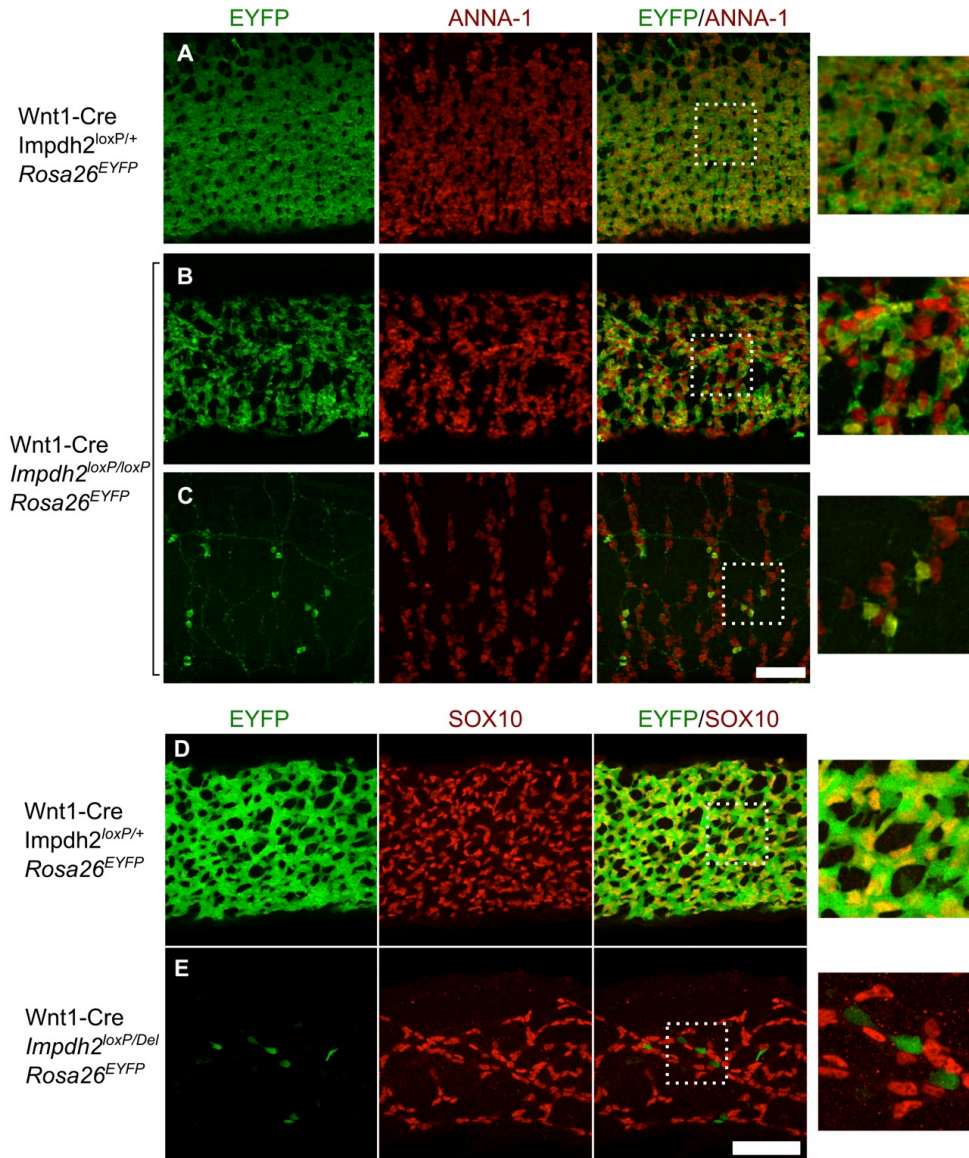


Figure 4.4: Residual enteric neurons and ENCDCs in *Impdh2* conditional knockouts display incomplete recombination.

In (A) *Wnt1-Cre Impdh2^{loxP/+} Rosa26^{EYFP}* control fetuses, all ANNA-1-positive (anti-HuC/HuD, red) enteric neurons are EYFP-positive (green) at E18.5, demonstrating that under normal circumstances *Wnt1-Cre* efficiently recombines the ancestors of essentially all ENCDCs. In (B-C) *Wnt1-Cre Rosa26^{EYFP} Impdh2^{loxP/loxP}* colon (B) and small intestine (C), many enteric neurons are not EYFP-positive, and the degree of incomplete labeling varies. (D-E) A similar phenomenon is already visible in the small intestine at E13.5. ENCDCs (SOX10-positive, red) are always EYFP-positive (green) in (D) control *Wnt1-Cre Rosa26^{EYFP} Impdh2^{loxP/+}* bowel, but in *Wnt1-Cre Rosa26^{EYFP} Impdh2^{loxP/Del}* bowel, many SOX10-positive ENCDCs are EYFP-negative (E). Dashed boxes = magnified insets. All scale bars = 100 μm . All photomicrographs are maximum intensity projections of 20 micron-thick volumes.

single embryo (Supplemental Figure 4.3), indicating that while Wnt1-Cre mediated recombination in the ENS is highly efficient, it is not universal.

4.4 Discussion

4.4.1 A neural-crest autonomous requirement for *Impdh2*

Deletion of *Impdh2* in the early neural crest results in craniofacial defects including near-total ablation of skull structures derived from the neural crest (20, 25). This includes the skeleton anterior to the basisphenoid and parietal bones as well as the tympanic rings and the interparietal bone in the posterior skull (Figure 4.1). In addition, conditional knockout fetuses demonstrated cardiac outflow tract and great vessel defects. These phenotypes bear a striking resemblance to the pan-neural crest defects that result from experimental ablation of the Wnt1-Cre fate map using Cre recombinase-triggered expression of diphtheria toxin fragment-A (26) or HSV-Tk followed by ganciclovir treatment (27), which suggests that neural crest derivatives lacking *Impdh2* fail to expand, survive, or differentiate properly. Taken together with the catastrophic results of *Impdh2* deletion in the ENS, these results reinforce our previous findings that global IMPDH inhibition results in cardiac and ENS defects (6). Our previous work could not separate the effects of IMPDH inhibition on ENCDCs and non-neural crest tissues such as the bowel mesenchyme, which manifested as global growth restriction and reduced intestinal length in exposed fetuses. These experiments clearly show that *Impdh2* is required in ENCDCs and that the resulting ENS defects occur in the context of an entirely normal bowel microenvironment. Moreover, guanine salvage from this normal neighboring

tissue and any residual GMP synthesis by IMPDH1 clearly cannot compensate for the loss of IMPDH2.

4.4.2 Incomplete recombination in conditional deletion of *Impdh2*

The aganglionosis observed in *Impdh2* conditional knockout bowel demonstrates the necessity of IMPDH2 for ENS development, while the incomplete recombination seen in the ENS (Figure 4.4) of these fetuses provides indirect evidence that loss of *Impdh2* selects against neural crest cells populating the bowel. The Wnt1-Cre transgene has been used extensively to delete genes in and mark the cells of the ENS (28–31), and we are unaware of any previous instances where incomplete recombination has been demonstrated in Wnt1-Cre mice, although it has been suggested that it may account for some otherwise contradictory results (32, 33). Indeed, we observed only rare instances of incomplete recombination of the EYFP reporter in E13.5 *Impdh2*^{loxP/+} *Rosa26*^{EYFP} fetuses (Supplemental Figure 4.3), suggesting that Cre-induced recombination is nearly complete in the ENS of Wnt1-Cre mice. The *Impdh2*^{loxP/loxP} conditional knockout, on the other hand, shows clear evidence of incomplete recombination of the *Rosa26* reporter. Since each Cre-catalyzed recombination event is independent, when reporter recombination is obviously incomplete we can no longer assert with confidence that every EYFP-positive cell has recombined the gene of interest. Because the Wnt1-Cre transgene is very efficient in conditional heterozygotes, we suspect that cells escaping recombination had a strong selective advantage early in neural crest development, leading to their overrepresentation in the ENS of conditional knockout fetuses. We also suspected that incomplete deletion of *Impdh2* could account for the variability in ENS phenotype. Since the *Impdh2* allele used in this study lacks an internal recombination reporter and all

available anti-IMPDH antibodies suitable for immunohistochemistry lack specificity for IMPDH2, we attempted to circumvent this problem by using the *Impdh2*^{loxP/Del} *Rosa26*^{EYFP} genotype, reasoning that reducing the number of required recombination events from 3 to 2 might make both deletion and lineage marking more uniform. However, examination of the ENCDC population indicates that this was not entirely successful, since many SOX10-positive cells in *Impdh2*^{loxP/Del} *Rosa26*^{EYFP} bowels still escaped recombination at the *Rosa26* locus. Using the *Impdh2*^{loxP/Del} genotype likely increased deletion efficiency and reduced the number of proliferation competent cells entering the bowel since the migration phenotype in *Impdh2*^{loxP/Del} embryos at E13.5 was significantly worse than in mice with the *Impdh*^{LoxP/LoxP} genotype and ENCDC migration depends largely on population size and proliferation (5, 34). The relatively normal BrdU labeling index in Wnt1-Cre *Impdh2*^{loxP/Del} ENCDCs is also easily accounted for if the ENCDCs that do colonize the bowel in *Impdh* conditional mutant mice have preferentially not undergone recombination at the *Impdh2* locus despite sporadically recombining the *Rosa26*^{EYFP} reporter.

The defect in ENCDC colonization of *Impdh2* conditional knockout fetuses is severe at E13.5, with long stretches of very sparsely populated bowel (Figure 4.3). Continued expansion of this remnant ENCDC population must occur to produce the relatively normal-appearing ENS present in the colonized regions of bowel at E18.5 (Figure 4.2), which also supports the idea that this sparsely colonized network is made up of fugitive ENCDCs whose ancestors escaped recombination and then adaptively expand to fill the underpopulated bowel (35). To our knowledge, it is not known how long Cre expression from the Wnt1-Cre transgene lasts in the migratory neural crest. Expression of

a similar Tg(Wnt1-LacZ) transgene in the developing ENS was lost after E11.5 (36), suggesting that the rare ENCDC that had not yet recombined at that time would permanently escape Cre-mediated DNA recombination. As other studies have shown, reducing the number of ENCDCs that enter the bowel is sufficient to cause aganglionosis even if the remaining ENCDCs are healthy (34), which accounts for the failure of these remaining cells to colonize the more distal portions of the bowel. It is also possible that non-recombined cells support the migration of *Impdh2*-deleted cells through the bowel, since non-cell autonomous rescue of ENCDC migration occurs in aggregation chimeras (37, 38) and in tissue culture (6). In the absence of a method to directly detect *Impdh2* recombination on a cell-by-cell basis, we cannot determine if all ENCDC that colonize the bowel in mutant mice retain IMPDH2 expression.

4.5 Conclusions

Taken together with our prior study demonstrating that chemical inhibition of IMPDH results in aganglionosis by reducing ENCDC proliferation (6), these experiments identify IMPDH2 as uniquely required for the development of the ENS. This is especially interesting since human genetic studies have independently identified a risk locus at 3p21 in Hirschsprung disease (39), and the *IMPDH2* gene is located at 3p21. In that analysis, the 3p21 risk allele appeared to enhance the effect of *RET* mutations, the primary causative mutation in most cases of Hirschsprung disease (7). A subsequent study has mapped this risk locus to an interval 0.6 megabases from *IMPDH2* (40). Other modifier mutations are well-appreciated contributors to Hirschsprung disease (41–43), and future

studies will investigate whether known (44) or novel genetic variation in human *IMPDH2* is associated with Hirschsprung disease.

Because IMPDH inhibition impairs ENS development and the *Impdh2* gene is indispensable for embryonic survival, we examined whether *Impdh2* is required in the neural crest lineage for its proper development. Wnt1-Cre-mediated deletion of *Impdh2* resulted in severe craniofacial, heart, and extensive aganglionosis of the ENS. During initial ENS development, ENCDC colonization in conditional knockout fetuses was impaired and the remaining colonized regions were abnormally hypocellular. Furthermore, both the developing and definitive ENS showed evidence of incomplete recombination that was specific to the conditional knockout genotype, demonstrating that *Impdh2* deletion is strongly selected against in the neural crest cells that eventually become the ENS. These results confirm a critical role for de novo guanine nucleotide synthesis and IMPDH2 in the neural crest lineage, and indicate that IMPDH1 and the salvage pathway cannot compensate for IMPDH2 loss even when other tissues in the developing embryo are normal.

4.6 Materials and Methods

4.6.1 *Impdh2* Gene Targeting

The pOSfirt-loxP vector (Provided by Randy Thresher, Lineberger Comprehensive Cancer Center Animal Models Core) containing a FRT-flanked positive selection marker (MC1-Neo) and a negative selection marker (PGK-TK) was used to assemble the *Impdh2* targeting construct from a 129/SV derived mouse genomic *Impdh2* clone (Agilent Lambda FIX II). A XbaI/XbaI fragment containing *Impdh2* exons 10-14 and 3' flanking

region (4.6 kb ‘long arm’) was filled-in using T4 DNA polymerase (Promega) and cloned into the PmeI site of pOSfirt-loxP using T4 DNA ligase (NEB) 3’ to the FRT-flanked MC1-Neo cassette. A second 3.5 kb fragment was synthesized by PCR using one primer located in intron 1 (5’ AAG GGT ACC CAT ATG TGA AGC AGG GGC AGG GGT TTA GAG G 3’) and a second loxP sequence-containing primer located in intron 9 (5’ CCG GGT ACC ATA ACT TCG TAT AAT GTA TGC TAT ACG AAG TTA TAG AGA TGC CAA GTC AGG CCT TGC C 3’). KpnI restriction sites at both ends of the amplified product were utilized to clone the fragment into the KpnI site of pOSfirt-loxP between the FRT-flanked MC1-Neo cassette and the 4.6 kb “long arm”. The entire PCR insert was sequenced and confirmed to be void of mutations. To complete the targeting construct, a 3.3 kb XbaI/NdeI fragment containing the 5’ end of *Impdh2* (5’ flanking sequence through exon 1, ‘short arm’) was filled-in and ligated into the PmlI site of pOSfirt-loxP containing the other two fragments, between the PGK-TK gene and the FRT-flanked MC1-Neo cassette. Sequencing of the completed targeting vector revealed that the most 5’ portion of this fragment was phage vector DNA located between *Impdh2* genomic sequences and the PGK-TK cassette, and that the homologous ‘short arm’ was 1.3 kb long.

Transfection and selection of E14TG2a (129/Ola) ES cells and generation of chimeras was performed by the Animal Models Core of the UNC-Lineberger Comprehensive Cancer Center. A single correctly targeted ES cell clone was identified using PCR screening and sequencing, and the resulting agouti male chimeras were bred to C57Bl/6 females to accomplish germline transmission. The MC1-Neo cassette was excised by mating to Flp-recombinase expressing mice to produce the *Impdh2*^{loxP} allele.

4.6.2 Animals and Genotyping

Animal experiments were approved by the Washington University Animal Studies. Animal procedures were conducted in accordance with animal research protocols approved by the University of North Carolina – Chapel Hill’s Institutional Animal Care and Use Committee. All mice were maintained on mixed genetic backgrounds with functional HPRT-mediated purine salvage. Since E14TG2a ES cells carry the *Hprt*^{b-m3} null mutation, PCR was used to confirm that the *Impdh2*^{loxP} strain did not carry *Hprt*^{b-m3} (6) prior to experimental matings. Cre-mediated recombination of the *Impdh2*^{loxP} allele results in a frameshift after codon 32 and a premature stop after codon 48, preventing expression of the catalytic domain. To produce a conventional knock-out allele, *Impdh2*^{loxP/+} mice were bred to Tg(ACTB-cre)2Mrt/J “Actin-Cre” mice (45) resulting in pups carrying germline deletions of *Impdh2*, referred to as *Impdh2*^{Del}. Actin-Cre was then removed through further breeding prior to experimental matings. *Impdh2*^{loxP} mice were bred to *Gt(ROSA)26Sor*^{tm1(EYFP)Cos} (46) mice (referred to as *Rosa26*^{EYFP}) which permanently marks all Cre-expressing cells and their descendants with EYFP expression. *Impdh2*^{loxP} and *Impdh2*^{Del} mice were bred to Tg(Wnt1-cre)11Rth (19) mice, (referred to as Wnt1-Cre), which drives loxP recombination in the entire neural crest and the dorsal tissues of the neural tube of the midbrain and hindbrain (20). These strains were intercrossed as indicated using timed matings to produce Wnt1-Cre *Impdh2*^{loxP/+} conditional heterozygotes (control animals) and the two conditional knockout genotypes Wnt1-Cre *Impdh2*^{loxP/loxP} and Wnt1-Cre *Impdh2*^{loxP/Del} with and without the *Rosa26*^{EYFP} reporter.

The vaginal plug day was counted as embryonic day 0.5. For collection of fetal samples, dams were euthanized with CO₂ according to institutionally-approved procedures. Embryonic day 18.5 (E18.5) fetuses were euthanized by decapitation except for fetuses to be processed for bone and cartilage staining, which were anesthetized prior to immersion fixation. Tail DNA was prepared using the HotSHOT method (47) and genotyped using a previously described PCR genotyping protocol (48). Genotyping reactions for Cre recombinase-containing transgenes and Rosa26^{EYFP} used previously described primers (6, 48). The *Impdh2*⁺ and *Impdh2*^{loxP} alleles were genotyped using primer pair *Impdh2*-F: 5'GAC TAC CTG ATT AGC GGA GGC ACC TCT TAC3' and *Impdh*-5FRTlox-R: 5'CAC GCT AAC ATA TTC CAC ATA TCC AGA GAA3', producing a 320 bp band from the wild-type allele and a 450 bp band from the conditional allele. The *Impdh2*^{Del} allele was genotyped with primer pair *Impdh2*-F and *Impdh*-3lox-R: 5'CTG AAA GAC ACC TAT ACC AAG TCC ATA GCC3' resulting in a 650 bp band indicating the presence of the deleted allele. All analyzed mice were hemizygous for the Wnt1-Cre transgene and heterozygous for Rosa26^{EYFP} if it was present.

4.6.3 Bone and Cartilage Staining

Simultaneous staining with alizarin red S and alcian blue was performed essentially as described in (49). E18.5 mouse fetuses were fixed in 95% ethanol for two hours, after which skin and organs were removed and fixation was continued for one week. Samples were moved to acetone for two days and then stained for 3 days at 37 °C in 0.015% alcian blue (Sigma #A5268), 0.005% alizarin red S (Sigma #5533), 5% glacial acetic acid, and 70% ethanol. Samples were washed with water and rocked in a 1% KOH

solution at room temperature until skeletons became visible after 48 hours. Samples were then passed through a graded series of 20–80% glycerol/1% KOH baths over the course of several weeks until tissues cleared. Skeletal preparations were stored and photographed in 100% glycerol.

4.6.4 Whole-mount Immunofluorescent Staining

Enteric neurons were labeled in E18.5 fetal mouse bowel using human ANNA–1 antiserum (A gift of Vanda Lennon, Mayo Clinic), which stains the somas of all enteric neurons (50) with the same pattern as the anti HuC/HuD monoclonal antibody used in previous studies (6). Fetal bowel was harvested, flushed with PBS, fixed with 4% paraformaldehyde in phosphate-buffered saline (PBS) for 30 minutes at room temperature, and then incubated in blocking solution for 1 hour at 37 °C: 5% normal goat serum (Jackson ImmunoResearch #005–000–121), 1% cold water fish-skin gelatin (Sigma #G7765), 100 mM Glycine in Tris-buffered saline pH 7.5 with 1% Triton-X 100 (TBST). Samples were then incubated overnight at 4 °C in ANNA–1 antiserum diluted 1:2000 in ANNA–1 diluent (5% normal goat serum, 1% bovine serum albumin, and 0.2% sodium azide in PBS.) Samples were washed 3 times with PBS and incubated with Alexa–594 conjugated goat anti-human secondary antibody (1:400, Life Technologies #A–11014) at 37 °C for 1 hour in PBS. After 3 washes with PBS, samples with the *Rosa26^{EYFP}* reporter were incubated overnight at 4 °C with chicken anti-GFP (1:1000, Aves Labs #GFP–1020) in blocking solution, washed 3 times with TBST, incubated for 1 hour at 37 °C with Alexa–488 conjugated goat-anti-chicken (1:400, Life Technologies #A–11039), and washed 3 times with PBS.

Embryonic day 13.5 (E13.5) fetuses were pulse-labeled by maternal intraperitoneal bromodeoxyuridine (BrdU) injections (100 µg/gram body weight) with a one-hour chase. Fetal bowel was harvested, processed, and stained for EYFP (Aves Labs GFP-1020), cleaved-caspase 3 (Cell Signaling #9661) or for SOX10 (rabbit anti-SoxE, Craig Smith, MRCI Australia) exactly as described (6), except that rat anti-BrdU (1:400, BU1/75, Abcam #ab6326) and Alexa-594 conjugated donkey anti-rat (1:400, Life Technologies A-21209) was used to visualize BrdU incorporation instead of a fluorophore-conjugated primary antibody. All samples were mounted on slides and visualized in 50% glycerol/PBS.

4.6.5 Microscopy and Measurement

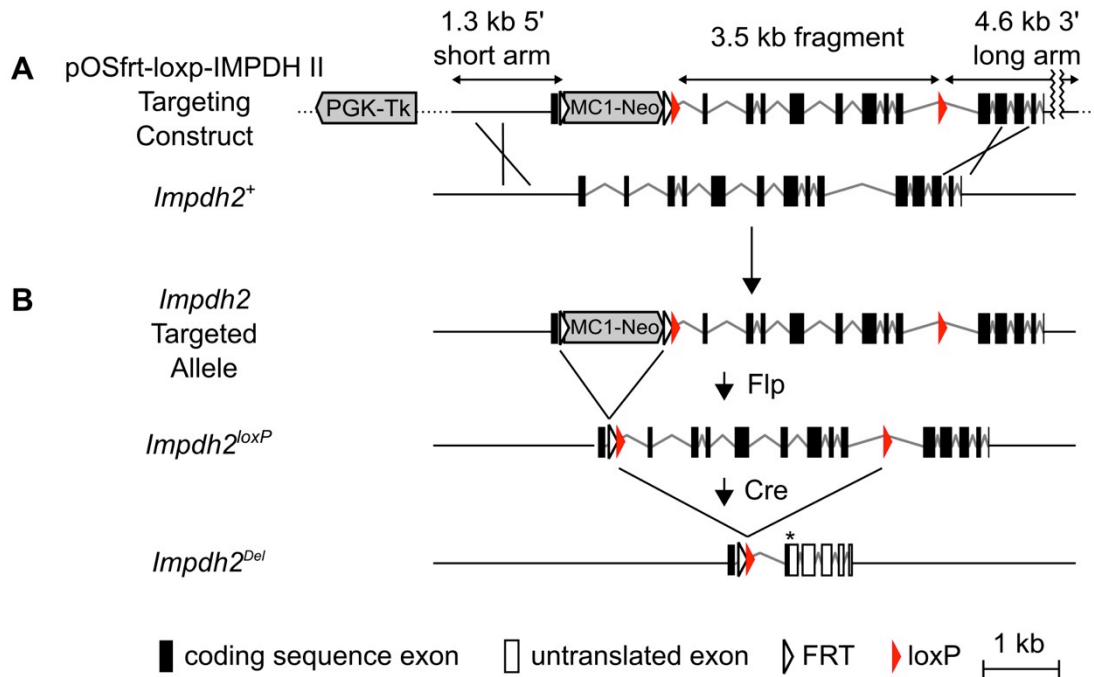
Photographs of whole fetuses, skeletal preparations, and hearts were acquired on an Olympus SZ-40 stereomicroscope. EYFP fluorescent micrographs of whole fetuses were acquired on a Nikon SMZ1500 stereomicroscope using a GFP-B epifluorescence filter. Measurements of colonization, aganglionosis and hypoganglionosis were conducted on an IX71 epifluorescence microscope guided by ANNA-1 staining at E18.5 or by SOX10 and EYFP staining at E13.5. Images of fluorescent whole-mount bowel were acquired as wide-field fluorescent micrographs on a Zeiss Axio Observer.Z1 or as multiple optical sections using either a Zeiss Apotome.2 structured illumination device or an Olympus FV1000 point-scanning confocal microscope. BrdU positivity within EYFP-positive cells was manually counted from confocal volumes. All optically sectioned samples are presented as maximum intensity projections through 20 micron-thick volumes unless otherwise indicated. Image processing was performed in ImageJ software (51) and was limited to stitching of multiple fields (52), rotation, cropping, uniform

brightness and contrast adjustments, and maximum intensity projection of volumes, with the exception of EYFP fluorescent micrographs of whole E13.5 fetuses, which were subjected to local contrast enhancement using contrast limited adaptive histogram equalization (CLAHE) (53) to improve the contrast of EYFP-containing tissue.

4.6.6 Statistical Analysis

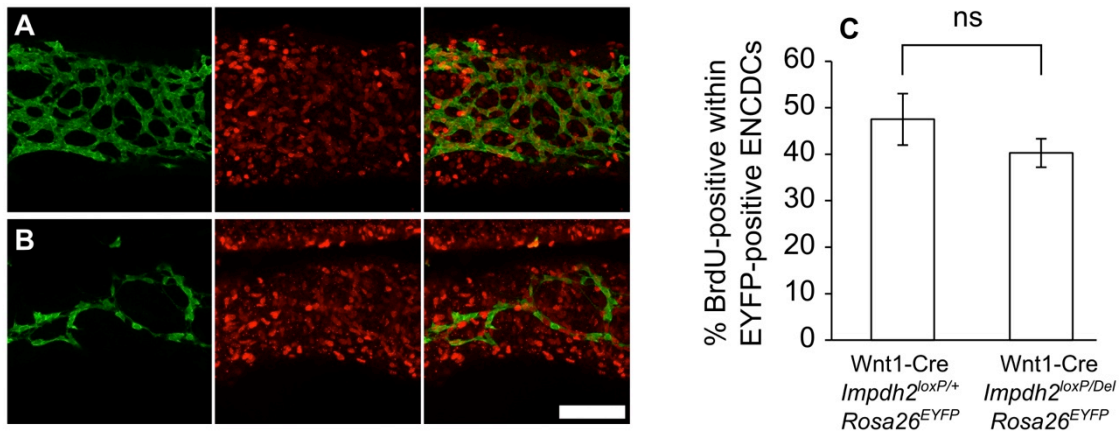
Statistical tests were performed using the R software package (54). Student's *t* test was used to compare E13.5 bowel colonization and rates of BrdU incorporation within ENCDCs. Multiple comparison adjustments were performed with the Holm-Boniferroni method based on the number of planned comparisons.

4.5 Supplemental Data



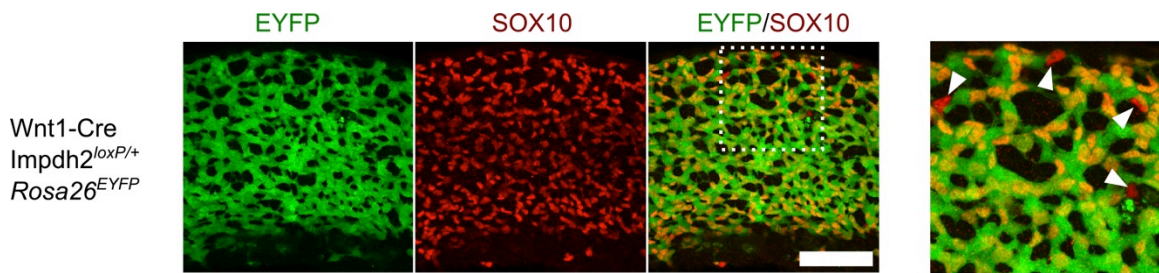
Supplemental Figure 4.1: Production and structure of the *Impdh2*^{loxP} and *Impdh2*^{Del} alleles.

(A) The *Impdh2* targeting construct, shown above the corresponding wild-type *Impdh2* locus, contains loxP sequences (red triangles) in intron 1 and intron 9 while FRT sequences (hollow triangles) flank a MC1-Neo cassette immediately preceding the first loxP site. Flp-mediated recombination excises the MC1-Neo cassette (B) from the targeted allele to produce the conditional *Impdh2*^{loxP} allele. Cre-mediated recombination produces the *Impdh2*^{Del} allele, which results in a frameshift (asterisk) and premature termination codon in the exon 3' to the recombination. After Cre-mediated DNA recombination, the IMPDH catalytic domain will be not be produced.



Supplemental Figure 4.2: BrdU incorporation in ENCDCs of *Impdh2* conditional knockout fetuses.

(A) Immediately behind the migration wavefront in Wnt1-Cre *Rosa26*^{EYFP} *Impdh2*^{loxP/+} bowel, many EYFP-positive ENCDCs (green) incorporate bromodeoxyuridine (BrdU, red and merge). (B) At this time point, very few ENCDCs are present in the small intestine of Wnt1-Cre *Rosa26*^{EYFP} *Impdh2*^{loxP/Del} fetuses. Scale bar = 100 μ m. Pictures are maximum intensity projections of 12 μ m-thick volumes. (C) Quantification of BrdU incorporating nuclei within the EYFP-marked ENCDC population does not demonstrate a significant difference in BrdU incorporation between *Impdh2*^{loxP/+} (N = 5) and *Impdh2*^{loxP/Del} (N = 4) genotypes. Note that different regions of the bowel are being compared, since each contains the migration wavefront in its respective genotype. ns = not significant by pooled-variance t-test. Error bars are s.e.m.



Supplemental Figure 4.3: Incomplete *Rosa26*^{EYFP} recombination by Wnt1-Cre in the absence of selective pressure.

In Wnt1-Cre *Impdh2*^{loxP/+} *Rosa26*^{EYFP} fetuses, Cre/loxP recombination of the EYFP reporter allele is not entirely complete. Individual SOX10-positive, EYFP-negative cells (inset, arrowheads) can be seen, likely representing a clone of ENCDCs derived from a rare neural crest cell that escaped recombination.

4.6 References

1. Furness JB. *The enteric nervous system*. Malden, MA: Blackwell Publishing; 2006.
2. Lake JI, Heuckeroth RO. Enteric nervous system development: migration, differentiation, and disease. *Am. J. Physiol. - Gastrointest. Liver Physiol.* 2013;305(1):G1–G24.
3. Obermayr F, Hotta R, Enomoto H, Young HM. Development and developmental disorders of the enteric nervous system. *Nat. Rev. Gastroenterol. Hepatol.* 2013;10(1):43–57.
4. Goldstein A, Hofstra R, Burns A. Building a brain in the gut: development of the enteric nervous system. *Clin. Genet.* 2013;83(4):307–316.
5. Simpson MJ, Zhang DC, Mariani M, Landman KA, Newgreen DF. Cell proliferation drives neural crest cell invasion of the intestine. *Dev. Biol.* 2007;302(2):553–568.
6. Lake JI, Tusheva OA, Graham BL, Heuckeroth RO. Hirschsprung-like disease is exacerbated by reduced de novo GMP synthesis. *J. Clin. Invest.* 2013;123(11):4875–4887.
7. Amiel J et al. Hirschsprung disease, associated syndromes and genetics: a review. *J. Med. Genet.* 2008;45(1):1–14.
8. Anderka MT, Lin AE, Abuelo DN, Mitchell AA, Rasmussen SA. Reviewing the evidence for mycophenolate mofetil as a new teratogen: Case report and review of the literature. *Am. J. Med. Genet. A.* 2009;149A(6):1241–1248.
9. Lin AE et al. An additional patient with mycophenolate mofetil embryopathy: Cardiac and facial analyses. *Am. J. Med. Genet. A.* [published online ahead of print: March 15, 2011]; doi:10.1002/ajmg.a.33934
10. Zimmermann AG, Sychala J, Mitchell BS. Characterization of the human inosine-5'-monophosphate dehydrogenase type II gene. *J. Biol. Chem.* 1995;270(12):6808–6814.
11. Senda M, Natsumeda Y. Tissue-differential expression of two distinct genes for human IMP dehydrogenase (E.C.1.1.1.205). *Life Sci.* 1994;54(24):1917–1926.
12. Nagai M, Natsumeda Y, Weber G. Proliferation-linked Regulation of Type II IMP Dehydrogenase Gene in Human Normal Lymphocytes and HL-60 Leukemic Cells. *Cancer Res.* 1992;52(2):258–261.
13. Gu JJ et al. Inhibition of T lymphocyte activation in mice heterozygous for loss of the IMPDH II gene. *J. Clin. Invest.* 2000;106(4):599–606.

14. Gunter JH et al. Characterisation of inosine monophosphate dehydrogenase expression during retinal development: Differences between variants and isoforms. *Int. J. Biochem. Cell Biol.* 2008;40(9):1716–1728.
15. Bowne SJ et al. Why Do Mutations in the Ubiquitously Expressed Housekeeping Gene IMPDH1 Cause Retina-Specific Photoreceptor Degeneration?. *Invest. Ophthalmol. Vis. Sci.* 2006;47(9):3754–3765.
16. Aherne A et al. On the molecular pathology of neurodegeneration in IMPDH1-based retinitis pigmentosa. *Hum. Mol. Genet.* 2004;13(6):641–650.
17. Zimmermann A, Gu JJ, Spychala J, Mitchell BS. Inosine monophosphate dehydrogenase expression: Transcriptional regulation of the type I and type II genes. *Adv. Enzyme Regul.* 1996;36:75–84.
18. Gu JJ et al. Targeted Disruption of the Inosine 5'-Monophosphate Dehydrogenase Type I Gene in Mice. *Mol. Cell. Biol.* 2003;23(18):6702–6712.
19. Danielian PS, Muccino D, Rowitch DH, Michael SK, McMahon AP. Modification of gene activity in mouse embryos in utero by a tamoxifen-inducible form of Cre recombinase. *Curr. Biol.* 1998;8(24):1323–1326.
20. Jiang X, Iseki S, Maxson RE, Sucov HM, Morriss-Kay GM. Tissue Origins and Interactions in the Mammalian Skull Vault. *Dev. Biol.* 2002;241(1):106–116.
21. Huang T, Liu Y, Huang M, Zhao X, Cheng L. Wnt1-cre-mediated Conditional Loss of Dicer Results in Malformation of the Midbrain and Cerebellum and Failure of Neural Crest and Dopaminergic Differentiation in Mice. *J. Mol. Cell Biol.* 2010;2(3):152–163.
22. Binder BJ et al. Spatial Analysis of Multi-species Exclusion Processes: Application to Neural Crest Cell Migration in the Embryonic Gut. *Bull. Math. Biol.* 2012;74(2):474–490.
23. Young H m., Newgreen D. Enteric neural crest-derived cells: Origin, identification, migration, and differentiation. *Anat. Rec.* 2001;262(1):1–15.
24. Rothman TP, Le Douarin NM, Fontaine-Pérus JC, Gershon MD. Colonization of the bowel by neural crest-derived cells re-migrating from foregut backtransplanted to vagal or sacral regions of host embryos. *Dev. Dyn. Off. Publ. Am. Assoc. Anat.* 1993;196(3):217–233.
25. Chai Y et al. Fate of the mammalian cranial neural crest during tooth and mandibular morphogenesis. *Development* 2000;127(8):1671–1679.
26. Olaopa M et al. Pax3 is essential for normal cardiac neural crest morphogenesis but is not required during migration nor outflow tract septation. *Dev. Biol.* 2011;356(2):308–322.

27. Porras D, Brown CB. Temporal–spatial ablation of neural crest in the mouse results in cardiovascular defects. *Dev. Dyn.* 2008;237(1):153–162.
28. Zehir A, Hua LL, Maska EL, Morikawa Y, Cserjesi P. Dicer is required for survival of differentiating neural crest cells. *Dev. Biol.* 2010;340(2):459–467.
29. Fuchs S et al. Stage-Specific Control of Neural Crest Stem Cell Proliferation by the Small Rho GTPases Cdc42 and Rac1. *Cell Stem Cell* 2009;4(3):236–247.
30. Okamura Y, Saga Y. Notch signaling is required for the maintenance of enteric neural crest progenitors. *Development* 2008;135(21):3555–3565.
31. Van de Putte T, Francis A, Nelles L, van Grunsven LA, Huylebroeck D. Neural crest-specific removal of *Zfhx1b* in mouse leads to a wide range of neurocristopathies reminiscent of Mowat-Wilson syndrome. *Hum. Mol. Genet.* 2007;16(12):1423–1436.
32. Hendershot TJ et al. Expression of *Hand2* is sufficient for neurogenesis and cell type-specific gene expression in the enteric nervous system. *Dev. Dyn.* 2007;236(1):93–105.
33. D’Autréaux F, Morikawa Y, Cserjesi P, Gershon MD. *Hand2* is necessary for terminal differentiation of enteric neurons from crest-derived precursors but not for their migration into the gut or for formation of glia. *Development* 2007;134(12):2237–2249.
34. Barlow AJ, Wallace AS, Thapar N, Burns AJ. Critical numbers of neural crest cells are required in the pathways from the neural tube to the foregut to ensure complete enteric nervous system formation. *Development* 2008;135(9):1681–1691.
35. Natarajan D, Grigoriou M, Marcos-Gutierrez CV, Atkins C, Pachnis V. Multipotential progenitors of the mammalian enteric nervous system capable of colonising aganglionic bowel in organ culture. *Development* 1999;126(1):157–168.
36. Kapur RP. Colonization of the murine hindgut by sacral crest-derived neural precursors: experimental support for an evolutionarily conserved model. *Dev. Biol.* 2000;227(1):146–155.
37. Kapur RP et al. Abnormal microenvironmental signals underlie intestinal aganglionosis in dominant megacolon mutant mice. *Dev. Biol.* 1996;174(2):360–369.
38. Kapur RP, Sweetser DA, Doggett B, Siebert JR, Palmiter RD. Intercellular signals downstream of endothelin receptor-B mediate colonization of the large intestine by enteric neuroblasts. *Development* 1995;121(11):3787–3795.
39. Gabriel SB et al. Segregation at three loci explains familial and population risk in Hirschsprung disease. *Nat. Genet.* 2002;31(1):89–93.
40. Garcia-Barceló M-M et al. Mapping of a Hirschsprung’s disease locus in 3p21. *Eur. J. Hum. Genet.* 2008;16(7):833–840.

41. Carrasquillo MM et al. Genome-wide association study and mouse model identify interaction between RET and EDNRB pathways in Hirschsprung disease. *Nat. Genet.* 2002;32(2):237–244.
42. De Pontual L et al. Epistatic interactions with a common hypomorphic RET allele in syndromic Hirschsprung disease. *Hum. Mutat.* 2007;28(8):790–796.
43. Garcia-Barcelo M-M et al. Genome-wide association study identifies NRG1 as a susceptibility locus for Hirschsprung's disease. *Proc. Natl. Acad. Sci.* 2009;106(8):2694–2699.
44. Wang J et al. A Novel Variant L263F in Human Inosine 5'-Monophosphate Dehydrogenase 2 Is Associated with Diminished Enzyme Activity. *Pharmacogenet. Genomics* 2007;17(4):283–290.
45. Lewandoski M, Meyers EN, Martin GR. Analysis of Fgf8 Gene Function in Vertebrate Development. *Cold Spring Harb. Symp. Quant. Biol.* 1997;62:159–168.
46. Srinivas S et al. Cre reporter strains produced by targeted insertion of EYFP and ECFP into the ROSA26 locus. *BMC Dev. Biol.* 2001;1:4–4.
47. Truett GE et al. Preparation of PCR-quality mouse genomic DNA with hot sodium hydroxide and tris (HotSHOT). *BioTechniques* 2000;29(1):52, 54.
48. Stratman JL, Barnes WM, Simon TC. Universal PCR genotyping assay that achieves single copy sensitivity with any primer pair. *Transgenic Res.* 2003;12(4):521–522.
49. McLeod MJ. Differential staining of cartilage and bone in whole mouse fetuses by alcian blue and alizarin red S. *Teratology* 1980;22(3):299–301.
50. Lennon VA. The case for a descriptive generic nomenclature: clarification of immunostaining criteria for PCA-1, ANNA-1, and ANNA-2 autoantibodies. *Neurology* 1994;44(12):2412–2415.
51. Schneider CA, Rasband WS, Eliceiri KW. NIH Image to ImageJ: 25 years of image analysis. *Nat. Methods* 2012;9(7):671–675.
52. Preibisch S, Saalfeld S, Tomancak P. Globally optimal stitching of tiled 3D microscopic image acquisitions. *Bioinformatics* 2009;25(11):1463–1465.
53. Schindelin J et al. Fiji: an open-source platform for biological-image analysis. *Nat. Methods* 2012;9(7):676–682.
54. R. Core Team. *R: A Language and Environment for Statistical Computing [Internet]*. Vienna, Austria: 2012:

Chapter 5: *IMPDH2* variation in a Hirschsprung

Disease Cohort

5.1 Summary

In the mouse, IMPDH activity and the *Impdh2* gene are required for normal development of the enteric nervous system. In humans, the *IMPDH2* gene is located at 3p21, a region linked to Hirschsprung disease susceptibility and genetic interactions with *RET*. These observations suggested the possibility that mutations in *IMPDH2* predispose to Hirschsprung disease. We therefore sequenced the *IMPDH1* and *IMPDH2* genes in a cohort of Hirschsprung disease patients and detected one rare nonsynonymous variant that moderately reduced the enzymatic activity of recombinant IMPDH2. Common variants that may affect IMPDH activity were detected at normal frequencies. In parallel, we investigated whether heterozygous loss of *Impdh2* could affect the penetrance of mutations that model Hirschsprung disease in mice, and determined that *Impdh2* interacted with neither the *Sox10* nor the *Ret* mutant alleles tested. Together these results suggest that *IMPDH2* is unlikely to be the Hirschsprung disease susceptibility locus previously mapped to 3p21.

5.2 Introduction

Several factors prompted us to search for one or more mutations in *IMPDH2*, the gene encoding one of the two IMPDH isoforms (1), as possible risk factors for Hirschsprung disease (HSCR). We have shown that IMPDH proteins are enriched in ENCDCs, that IMPDH inhibition

impairs ENS development in vertebrates, and that IMPDH inhibition interacts with *Ret* in a mouse model of HSCR. These findings suggest that mutations that reduce IMPDH activity or expression could interact with established HSCR-predisposing mutations in a manner analogous to the effects of mycophenolic acid (MPA). Furthermore, we have demonstrated that *Impdh2* is required in neural crest-derivatives for the formation of the ENS, while the survival and relatively normal phenotype of *Impdh1*-knockout mice (2) indicates that *Impdh1* is dispensable for ENS development. Most intriguingly, *IMPDH2* is located in a chromosomal region that has been linked to HSCR (3). Specifically, a region in 3p21 was identified along with *RET* and another unidentified locus at 19q12 in a genome-wide linkage study of families with short-segment HSCR. The model that best fit the data indicated that the 3p21 and 19q12 risk alleles modify the effect of a *RET* mutations. More recent work has replicated this association between HSCR and 3p21 in a different population (4), but the causative gene has not yet been identified. This region is rich in genes, and these mapping studies have detected association with two different intervals in this region. *IMPDH2* is located between the regions identified in these two studies (Figure 5.1). To date, no other approaches have been used to identify the gene responsible, refine the interval, or rule out candidates in humans or using model systems.

Genetic variation in both *IMPDH2* and *IMPDH1* has been studied in several contexts. *IMPDH1* (OMIM 146690, RP10, LCA11) mutations cause blindness in autosomal dominant retinitis pigmentosa (adRP) (5, 6) and Leber congenital amaurosis (7), two genetically heterogeneous disorders affecting the retina. These mutations do not affect enzymatic activity, though they may cause aggregation (8, 9) or decrease IMPDH1's ability to bind nucleotides (7, 10) which has as-yet unknown functional significance, but may be involved in transcription (11) or translation (12). Though the mechanism by which these mutations cause disease is not

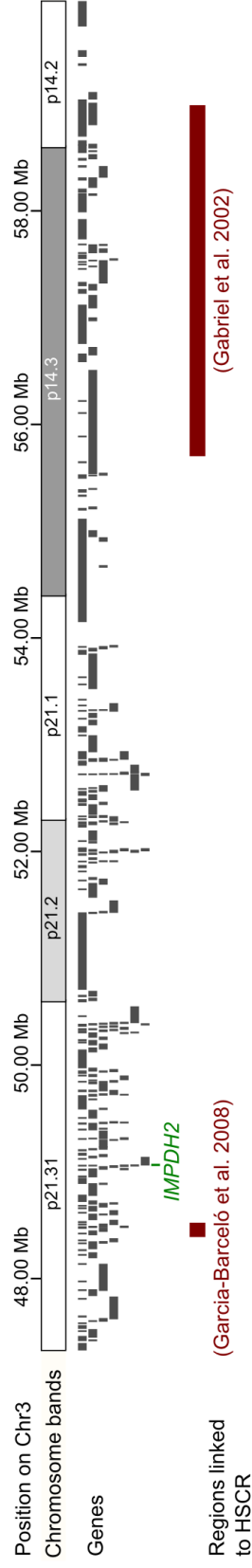


Figure 5.1: Intervals in the 3p21 region linked to HSCR

Using linkage analysis in two different populations, Hirschsprung disease has been linked to two intervals (red blocks) in the 3p21 region. The lack of overlap indicates that the regions that crossed the significance cutoffs in each study were not overlapping, and does not necessarily demonstrate separate loci. *IMPDH2* (green) is located between these two association blocks, while *IMPDH1* is located at 7q31.2, a region not associated with HSCR.

completely understood, failure to synthesize GMP can be excluded as a possible reason, since *Impdh1* knockout mice only develop a late-onset and mild retinopathy that is very different from adRP (8). In contrast, introducing RP10-mutant IMPDH1 to normal mouse retina using viral vectors is toxic to photoreceptors, while overexpression of normal human IMPDH1 causes no pathology (13). This demonstrates that RP10 *IMPDH1* mutations that cause retinitis pigmentosa are dominant and probably not due to a simple loss of GMP synthesis.

Variation in *IMPDH2* and *IMPDH1* have also been investigated in human patients for polymorphisms related to clinical outcomes and therapeutic drug monitoring in mycophenolate mofetil (MMF) / mycophenolate sodium (MPS) immuno-suppression. Two intronic *IMPDH1* SNPs (rs2278293 and rs2278294) were associated with biopsy-proven acute rejection in kidney transplants (14). rs2278294 was also associated with the risk of acute graft-versus-host disease in allogeneic hematopoietic stem-cell transplant recipients (15). Only rs2278294 was associated with rejection of kidney grafts and leukopenia in a subsequent study (16), while conversely only rs2278293 was associated with subclinical acute rejection in a third study of kidney transplant patients (17). Two other groups have failed to find any association with renal transplantation outcomes at either SNP (18, 19). In *IMPDH2*, the minor allele at one common SNP (rs11706052) has been associated with biopsy-proven acute rejection in kidney transplant (20), higher *IMPDH2* activity after transplantation (21), MPA resistance in activated lymphocytes (22), and reduced incidence of lymphopenia (23). However, two other studies have failed to confirm this SNP's association with rejection (14, 16) while a third found only a weak association (18). A rare variant (24) is located in the *IMPDH2* promoter (*IMPDH2*:c.-96T>G) within a putative cyclic-AMP response element. This variant reduced the expression of reporter constructs relative to the wild-type promoter, but this variant is rare and has not been detected subsequently (25).

Still another rare variant, rs72639214, is intronic and associated with lower *IMPDH2* mRNA levels (26). Electrophoretic mobility shift assays showed that the minor allele abolishes binding to nuclear extract, suggesting that this variant impairs binding of a transcription factor. The alleles that may provide reduced rejection or graft-vs-host disease risk are hypothesized to act by reducing the abundance of *IMPDH1/IMPDH2* at the transcriptional or posttranscriptional level and allowing more complete immunosuppression for a given level of MPA, while simultaneously predisposing to side-effects like leukopenia. Rare nonsynonymous variants with functional consequences have also been detected in *IMPDH1* and *IMPDH2*. In *IMPDH1*, excluding mutations linked to retinal disease, one nonsynonymous mutation (rs72624960, *IMPDH1*:p.S275L) has been detected that reduces enzyme activity largely through increased protein degradation and lower steady-state protein levels (26). In *IMPDH2*, the rare variant rs121434586 (*IMPDH2*:p.L263F) demonstrated 10% of the activity of wild-type enzyme (27) and this phenotype also seems to be related to lower protein levels and accelerated degradation (26).

Exhaustively sequencing a human gene even in a small group of patients is a major undertaking using traditional methods, but second-generation sequencing coupled to an appropriate data analysis pipeline allows for detection of single nucleotide variants at single-allele frequencies in pools of hundreds of alleles (28), an approach generally referred to as “amplicon-seq”. New analysis strategies have extended this approach to allow for identification of both missense mutations and small insertions and deletions (indels) with high sensitivity and specificity (29). This strategy estimates minor allele frequencies in a pool but does not identify which individuals have a mutation nor the allelic configuration within any single individual, so

individual DNA samples must be genotyped using other methods if interesting variants are detected.

Using this sequencing strategy, we scanned *IMPDH2* and *IMPDH1* in 51 HSCR patient samples for single-nucleotide variants and short indels. We detected one nonsynonymous variant in *IMPDH2*, IMPDH2:p.P123R (rs142797363), and examined its effect on IMPDH activity in recombinant enzyme preparations. We also demonstrate that heterozygous loss of *Impdh2* does not enhance the phenotype of mouse models of HSCR.

5.3 Results

5.3.1 Pooled Resequencing

The pooled sequencing reaction provided good coverage (>30 reads per strand per allele, Figure 5.2B) of all targeted regions of *IMPDH2* and control sequences. Most exons of *IMPDH1* were also adequately covered, with the exception of exons 1, 4, and 12 (Figure 5.2A) likely due to the GC-richness of their immediate flanking sequences (70-80%). The SPLINTER algorithm detected all four positive control polymorphisms that were present at simulated frequencies of 10/102, and detected 12 of the 13 variants present at 1/102 simulated alleles, indicating high but not perfect sensitivity.

5.3.2 Variation in *IMPDH1* and *IMPDH2*

Only one nonsynonymous variant was detected in the pooled DNA from individuals with Hirschsprung disease: IMPDH2:c.368C>G or IMPDH2:p.P123R, which we confirmed by PCR-RFLP assay and conventional sequencing to be present in one individual in the heterozygous configuration. Neither the L263F *IMPDH2* variant nor the *IMPDH1* S275L variant were detected. Minor alleles at the possibly relevant noncoding SNPs rs2278293, rs2278294, and

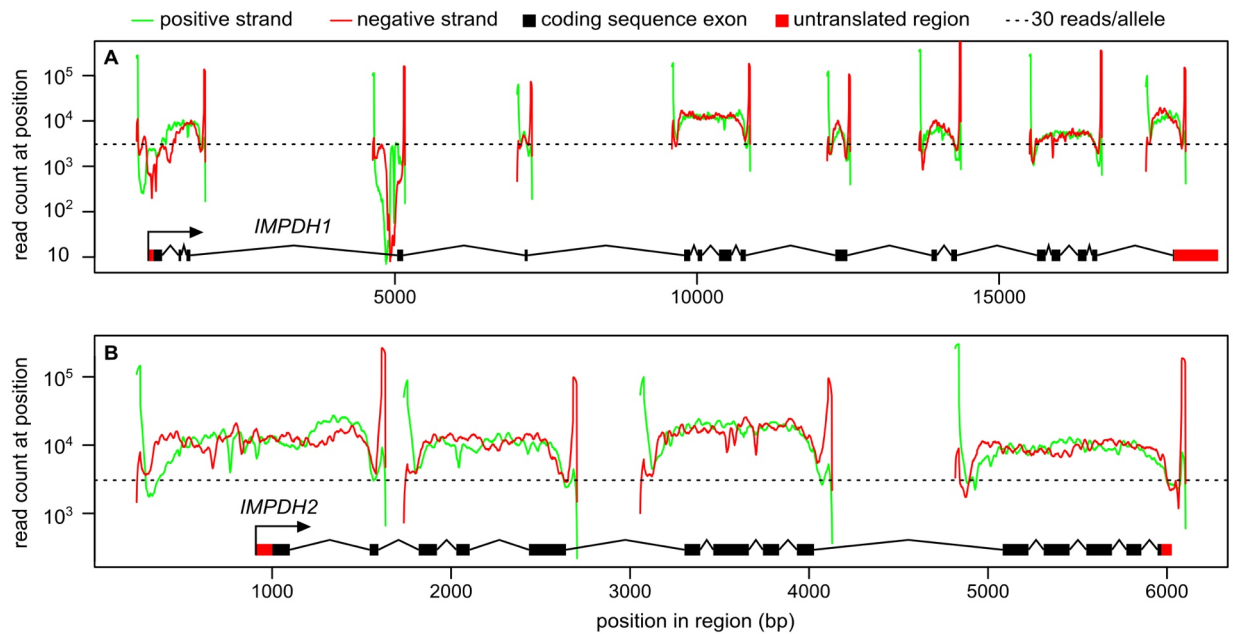


Figure 5.2: Sequencing coverage of *IMPDH1* and *IMPDH2*

Pooled-sequencing coverage plots of all targeted regions in **A)** *IMPDH2* and **B)** *IMPDH1*. For all analyses and this plot, reads were truncated to 22 base pairs before alignment. Coverage of *IMPDH2* noncoding regions is more complete since *IMPDH2* is a much shorter gene. The cutoff for confident variant detection was set at 30 reads/allele in either orientation, though coverage was generally very similar in each direction.

rs11706052 were present at frequencies comparable to previous findings, and the two rarer noncoding *IMPDH2* variants (rs72639214 and c.-96T>G) were not detected (Table 5.1). Other variation was generally intronic and did not appear to be obviously deleterious. Several detected variants were changes in the number of bases in repetitive regions. The *IMPDH2* P123R allele (rs142797363) has been previously detected (38) but nothing is known about its functional consequences.

5.3.3 Activity of the P123R IMPDH2 variant is reduced relative to wild-type.

To determine whether the P123R variant affected enzyme activity, we expressed wild-type, P123R, and known deleterious mutant L263F human IMPDH2 fused to an N-terminal 6xHis tag using an *E. coli* expression system as has been done for IMPDH1 (8) yielding enzymatically active protein. Purified protein yields for wild-type IMPDH2 were consistently higher than those for P123R. L263F produced even less protein, as reported previously in bacterial (27) and mammalian expression systems (26). Activity assays revealed significant differences (Figure 5.3) between wild-type and both variant enzymes. The P123R variant demonstrated a modest but significant reduction in turnover number (K_{cat}) and an increase in K_m for both IMP and NAD^+ substrates (Table 5.2). The L263F variant resulted in larger changes in K_{cat} and both K_m , though the reduction in activity was not as severe as was previously reported (26, 27).

5.3.4 Heterozygous loss of *Impdh2* does not enhance *Ret* or *Sox10* mutations.

Activated splenic lymphocytes from *Impdh2*^{+/-} mice have reduced total IMPDH activity (39), indicating that heterozygous deletion of *Impdh2* effectively simulates a partial loss of activity and can reasonably simulate a loss-of-function mutation. We applied this genetic stressor to the same two mouse models of HSCR that pharmacologic IMPDH inhibition potentiated but

Gene	HGVS Name	Type	SNP id	Minor allele freq.	
				dbSNP	HSCR
IMPDH1	NM_000883.3:c.146+109A>T	Intron	rs2288553	0.121	0.061
IMPDH1	NM_000883.3:c.147-52G>T	Intron	rs2288552	0.077	0.041
IMPDH1	NM_000883.3:c.147-35G>A	Intron	rs2288551	0.077	0.061
IMPDH1	NM_000883.3:c.505-34C>A	Intron	rs72624952	0.010	0.061
IMPDH1	NM_000883.3:c.579+119G>A	Intron	rs2278293*	0.444	0.500
IMPDH1	NM_000883.3:c.580-106G>A	Intron	rs2278294*	0.400	0.408
IMPDH1	NM_000883.3:c.987G>C	Synonymous	rs2288550	0.126	0.133
IMPDH1	NM_000883.3:c.1075-129C>A	Intron	novel	N/A	0.020
IMPDH1	NM_000883.3:c.1405+33C>T	Intron	rs28580600	0.101	0.133
IMPDH1	NM_000883.3:c.1551-114T>G	Intron	rs4731447	0.175	0.061
IMPDH1	NM_000883.3:c.1575G>A	Synonymous	rs2228075	0.279	0.428
IMPDH1	NM_000883.3:c.1694+43G>A	Intron	rs72624969	0.122	0.071
IMPDH1	NM_000883.3:c.1779-407G>C	Intron	rs78763502	0.090	0.133
IMPDH1	NM_000883.3:c.1779-131G>T	Intron	novel	N/A	0.020
IMPDH2	NT_022517.18:g.49007307A>G	5' Flanking (run of As)	adjacent to rs71641216	N/A	0.082
IMPDH2	NT_022517.18:g.49007304delA and g.49007304delAinsAA	5' Flanking (run of As)	rs71641216	no data	0.102
IMPDH2	NM_000884.2:c.368C>G	Pro123Arg	rs142797363	no data	0.041
IMPDH2	NM_000884.2:c.532-177T>C	Intron	novel	N/A	0.010
IMPDH2	NM_000884.2:c.532-169T>C	Intron	novel	N/A	0.031
IMPDH2	NM_000884.2:c.532-168G>A	Intron	novel	N/A	0.010
IMPDH2	NM_000884.2:c.532-161G>A	Intron	novel	N/A	0.020
IMPDH2	NM_000884.2:c.532-160C>T	Intron	novel	N/A	0.020
IMPDH2	NM_000884.2:c.532-159C>T	Intron	novel	N/A	0.020
IMPDH2	NM_000884.2:c.532-156G>A	Intron	novel	N/A	0.020
IMPDH2	NM_000884.2:c.532-139C>T	Intron	novel	N/A	0.031
IMPDH2	NM_000884.2:c.532-138C>T	Intron	novel	N/A	0.031
IMPDH2	NM_000884.2:c.532-137G>A	Intron	novel	N/A	0.071
IMPDH2	NM_000884.2:c.532-120delA	Intron	novel	N/A	0.010
IMPDH2	NM_000884.2:c.532-96G>A	Intron	rs72624911	0.016	0.031
IMPDH2	NM_000884.2:c.819+10T>C	Intron	rs11706052*	0.073	0.092
IMPDH2	NM_000884.2:c.*26Tdel and c.*25_26TinsT	3' UTR (run of Ts)	rs200887858	no data	0.020

Table 5.1: Variation detected in *IMPDH2* and *IMPDH1* in a HSCR cohort

Known variants were queried using NCBI human variation search tool (as of September 2013) (www.ncbi.nlm.nih.gov/projects/SNP/transNP). * = SNPs correlated with human phenotypes.

IMPDH Variant	Kcat (s⁻¹)	Km IMP (μM)	Km NAD⁺ (μM)
Wild-type	0.524 (± 0.015)	36.4 (± 3.44)	95.1602 (± 6.52)
P123R	0.477 (± 0.017) *	47.1 (± 3.92) *	125.8893 (± 10.21) *
L263F	0.431 (± 0.026) **	63.5 (± 10.20) *	187.4732 (± 24.32) **

Table 5.2: Kinetic parameters of recombinant IMPDH2 variants

* = $P < .05$, ** = $P < .01$, two-tailed t-test against wild-type parameter. All values are ± standard error. K_i for substrate inhibition by NAD⁺ was estimated at 279 (± 57.51) μM

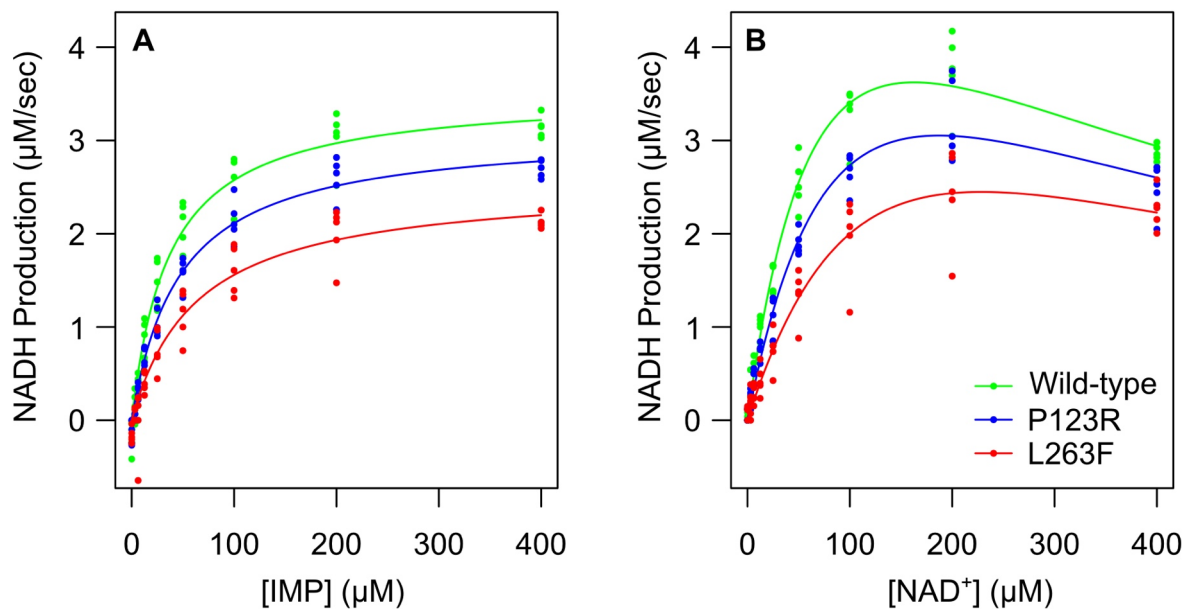


Figure 5.3: IMPDH activity of IMPDH2 variants is reduced

IMPDH activity was measured by monitoring the production of NADH by 15 nM (908 ng/mL) of each IMPDH variant (wild-type = green, P123R = blue, L263F = red) in the presence of the indicated concentrations of (A) IMP and (B) NAD⁺ and 400 µM of the other substrate. The reduction in velocity seen at high concentrations of NAD⁺ (B) is typical of substrate inhibition. Both variants appear to have reduced enzymatic activity.

these crosses resulted in no effect on the penetrance of ENS malformations or the length of bowel affected in either *Sox10* or *Ret* mutant mice (Figure 5.4).

5.4 Discussion

5.4.1 Expected Characteristics of a 3p21 HSCR Modifier Allele

Using the population prevalence of HSCR (1 in 5000), the risk ratio estimate for the modifier allele at 3p21 (4.2), and estimates of the baseline population frequency (3) of the 3p21 modifier allele (4% allele frequency and thus 7.5% heterozygote frequency) we can estimate that about 24% of HSCR patients in the originally studied population were heterozygotes for the 3p21 modifier allele (Figure 5.5). Linkage to 3p21 was identified in short-segment HSCR families and the 3p21 risk allele is a *RET* modifier gene, so we do not expect it to be overrepresented in syndromic cases of HSCR associated with other genes (*EDNRB*, *PHOX2B*, *SOX10*, *KIAA1279*, or *ZFHX1B*). Because of the methods used to identify and enroll patients in the PHIS/BDS study, we lack detailed diagnostic information for each patient. It is a reasonable assumption that isolated (non-syndromic) HSCR requires some form of *RET* mutation, since linkage to the *RET* locus is seen even in the absence of identified functional mutations (3, 40). Since HSCR appears as an isolated trait in 70% of patients and short-segment disease represents 80% of HCSR patients (41), we can estimate the likelihood of a randomly-selected HSCR patient carrying the 3p21 risk allele as about 13.5% and thus sampling a group of as few as 21 HSCR patients is 95% likely to include at least 1 occurrence of the 3p21 mutation. Thus if mutations in *IMPDH2* are the causative lesions at *RET* modifier locus 3p21 we would be able to detect them even in a small cohort of HSCR patients. Because *IMPDH1* contains significant variation in the human population, we included canonical *IMPDH1* exons in the sequencing library.

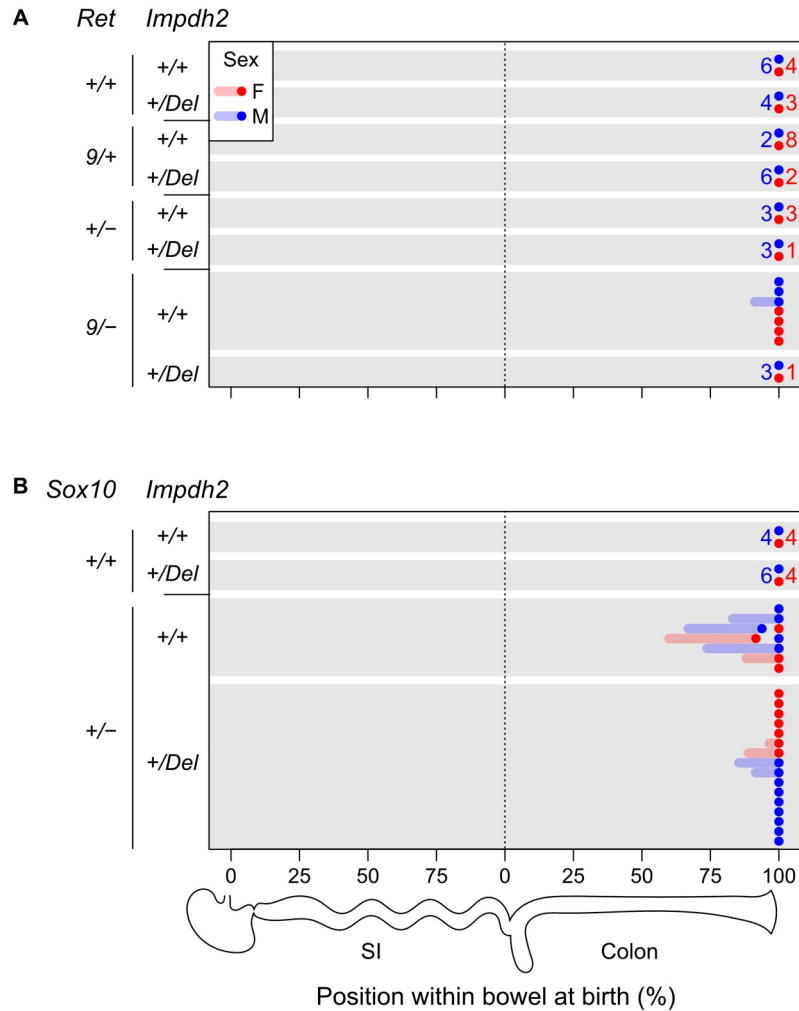


Figure 5.4: No effect of heterozygous loss of *Impdh2* on the ENS of *Ret* and *Sox10* mutants
Impdh2^{+/*Del*} mice were bred to (A) *Ret* and (B) *Sox10* models of Hirschsprung disease and the neonatal (postnatal day zero) bowels were examined for aganglionosis and hypoganglionosis. The most caudal neuronal soma in each animal identified using ANNA-1 (anti-HuC/HuD) immunofluorescence is shown as a point, and the hypoganglionic region is shown with a line projecting to the left. Data are abbreviated with a number indicating sample size when no animal in a group was aganglionic or hypoganglionic. The *Ret*^{9/-} genotype (A, bottom) has low penetrance and severity on its own, and *Impdh2* heterozygosity did not appear to worsen its associated phenotype. The more penetrant *Sox10*^{+/-} phenotype was similarly not enhanced by *Impdh2* heterozygosity (B). Though the penetrance of *Sox10*^{+/-} appeared possibly reduced by *Impdh2*^{*Del*}, this difference was not statistically significant when considering either aganglionosis or hypoganglionosis (Fisher's exact test).

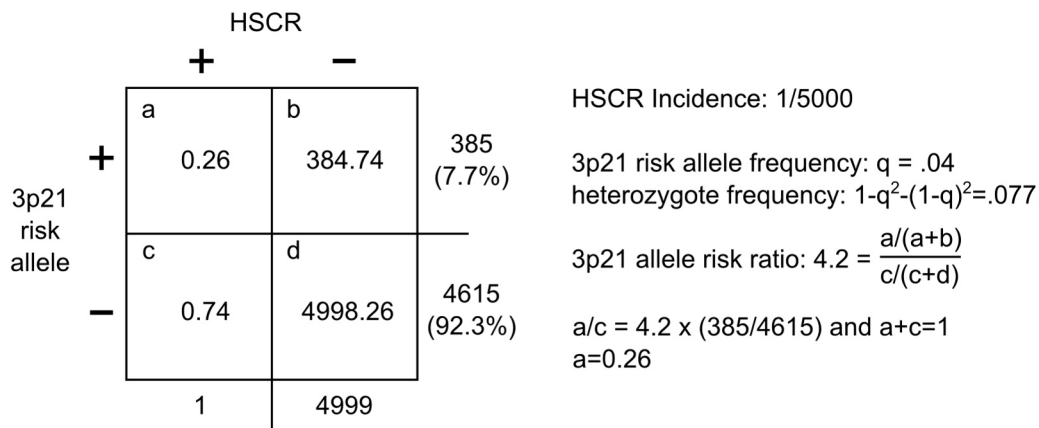


Figure 5.5: Estimating proportion of 3p21 risk carriers within HSCR patients.

Gabriel et al. (3) estimated a risk ratio of 4.2 and population allele frequency of .04 for the 3p21 *RET* modifier allele. To estimate the proportion of allele carriers within the population, we first calculate the frequency of heterozygotes assuming Hardy-Weinberg equilibrium (.077). This allows the calculation of non-carrier non-affected (b) from the disease incidence (1/5000.) a/c, the carrier frequency within an affected cohort, can then be calculated. This assumes that homozygosity is not selected against, but the numbers are very similar if homozygosity is lethal. This estimate does depend on the assumption that the results of one study in HSCR families with multiple cases of disease in each family can be generalized to the population at large.

5.4.2 Prevalence of the IMPDH2:p.P123R Nonsynonymous Substitution

We did detect one nonsynonymous variant that reduces the enzymatic activity of IMPDH2 (IMPDH2:p.P123R), but this variant was present in only in one individual. Allele frequencies calculated by SPLINTER are vulnerable to errors in DNA quantification and pooling, likely accounting for the discrepancy between the number of P123R alleles detected (4/102) by pooled sequencing and those confirmed by individual genotyping (1/102). This variant was also detected by the NHLBI Exome Sequencing Project (ESP), but it was extremely rare. P123R was detected only once in 8600 alleles in a European-American population and was absent from a 4406-allele African-American population. The cohorts included in the ESP contain both normal controls and several cardiac and pulmonary disease cohorts and it was not possible at this time to determine which NHLBI cohort contained the variant. In any case, we expect the 3p21 risk allele previously identified to be present in the general population at a significantly higher frequency than P123R, making IMPDH2 nonsynonymous variants poor candidates for the 3p21 risk factor. Our mutation scan also did not detect major overrepresentation or underrepresentation of any *IMPDH2* or *IMPDH1* variants that have been previously associated with transplantation outcomes and/or IMPDH activity (Table 5.1), nor did we detect the L263F variant.

5.4.3 Functional Consequences of the IMPDH2:p.P123R Variant

Both PolyPhen2 (42) and MutPred (43) phenotype prediction programs suggest that the proline to arginine amino acid substitution might be deleterious, and alignment of IMPDH2 orthologs and IMPDH1 reveals that proline 123 is highly conserved despite many changes in flanking residues (Figure 5.6A). This amino acid, however, is located in the first cystathionine β -synthase (CBS) domain, which is involved in nucleotide binding and is unnecessary for IMPDH's catalytic activity (44). The region containing P123 is generally disordered in crystal

structures of IMPDH1 and IMPDH2 but a structure of *S. pyogenes* IMPDH (PDB: 1ZFJ, 45) does resolve this region and shows that the homologous proline residue (P106) initiates a turn (Figure 5.6B) within the first CBS domain, suggesting that a substitution may have structural consequences. As a control mutation for enzyme kinetics, we used the L263F variant of IMPDH2, assuming that it would produce nearly inactive enzyme. Somewhat surprisingly, IMPDH2 L263F retained a much larger proportion of wild-type catalytic activity in this study than in either a previous study using recombinant IMPDH2 from *E. coli* or affinity-tagged IMPDH2 expressed in mammalian cells (26, 27). Kinetic parameters for both wild-type and L263F enzyme also differed from previously published values, especially the K_m for NAD^+ and IMP. Since previous studies used either C-terminal affinity tags or untagged protein, it is possible that the N-terminal affinity tag alters the stability and kinetic properties of the enzyme.

5.4.4 The Haplosufficiency of *Impdh2* in Mouse HSCR Models

Importantly, the hypothesis that *IMPDH2* might be the HSCR susceptibility locus at 3p21 was formulated based on our previous finding that IMPDH inhibition impairs ENS development and interacts with *Ret* and *Sox10* (Chapter 3). To examine the plausibility that a loss-of-function variant could have an effect similar to global IMPDH inhibition, we tested if *Impdh2* heterozygosity increased bowel aganglionosis in mice with mutations in *Ret* and *Sox10*. While no association between 3p21 and *SOX10* has been documented in HSCR, *Sox10* was included as a potential interactor because IMPDH inhibition strongly enhances *Sox10* phenotypes and because *Sox10*^{LacZ/+} has a much greater penetrance in the ENS than even the highest risk *Ret*^{9/-} genotype. We detected no enhancement of either the *Ret* or *Sox10* ENS phenotype by *Impdh2* heterozygosity. Furthermore the *Ret*^{+/-} *Impdh2*^{+/Del} compound heterozygotes generated as part of the breeding scheme survived to adulthood and were fertile. It seems likely that heterozygosity

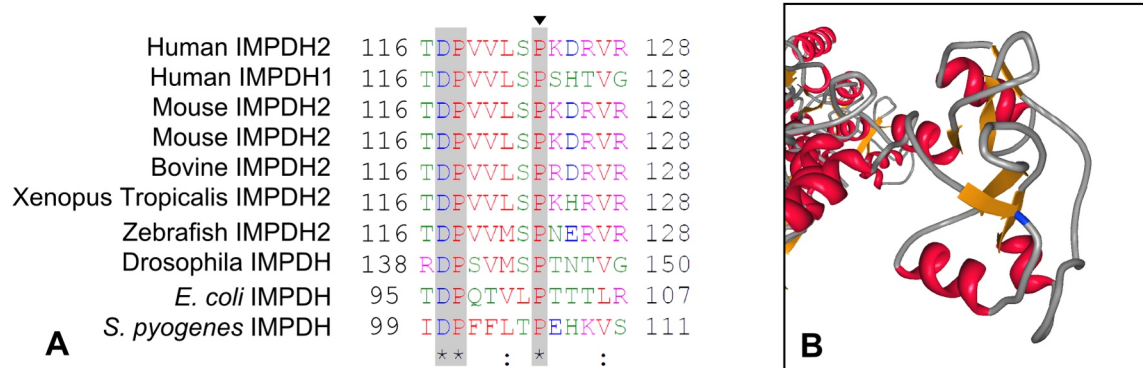


Figure 5.6: Multispecies IMPDH2 alignment in context of P123R mutation

A: Proline 123 is highly conserved across isoforms of human IMPDH and across species, including prokaryotes, despite poor conservation in the rest of this CBS domain at the amino-acid level. **B:** While P123 or its immediate neighbors is generally missing from crystal structures of mammalian IMPDH, the homologous residue (blue section of backbone ribbon) is resolved in a structure of *S. pyogenes* IMPDH, showing that this residue initiates a turn.

for a null allele is a more severe defect than heterozygous P123R or even L263F mutations would create based on our in vitro enzyme kinetics studies, though we cannot discount the possibility that these mutations could have a dominant negative effect through heterotetramerization, cellular toxicity from aggregation, or disruption of one of the noncatalytic roles of IMPDH. Others have speculated that homozygosity for L263F might be incompatible with life (27), but even if P123R or L263F homozygosity were possible, such individuals would be vanishingly rare in the general population given the allele frequencies.

IMPDH2 may have roles in the cell unrelated to its enzymatic activity, which are suggested by its ability to bind single-stranded nucleic acids, which mediates its association with translating polysomes and its role as a transcription factor in *Drosophila* (11, 12, 46). The CBS domain where the P123 residue is located is important for nucleic acid binding activity (46), and our study does not address whether the P123R substitution affects nucleic acid binding. However, any possible disruption to these functions is not directly related to the antiproliferative effects of IMPDH inhibitors that prompted us to examine *IMPDH2* and thus lacks a plausible mechanism to cause ENS-specific disease.

5.5 Conclusion

The 3p21 *RET* modifier locus has thus far eluded identification (3, 4). Mutation scans of *IMPDH2* in a HSCR cohort revealed one rare variant (rs142797363 or IMPDH2:p.P123R) with reduced enzymatic activity. However, other variants that could possibly reduce IMPDH activity were not overrepresented in the sequenced HSCR cohort compared to control populations. Moreover, heterozygous deletion of *Impdh2* did not increase the penetrance or severity of mouse

HSCR models. Based on these findings, it is unlikely that a mutation in *IMPDH2* is the *RET* modifier allele identified through linkage studies.

5.6 Materials and Methods

5.6.1 Isolation of Human Genomic DNA

Cases of Hirschsprung disease were identified by the Pregnancy Health Interview Study (Birth Defects Study), an ongoing case-control surveillance study of birth defects in North America (30). Anonymized human genomic DNA samples were obtained either as isolated DNA in TE buffer or as buccal cells collected and frozen on nylon brushes. DNA was isolated from brushes using the Gentra Puregene Buccal Cell Kit (Qiagen) using a procedure modified to enhance the recovery of low-abundance (<2 µg) samples. Brushes were incubated in cell lysis solution with proteinase K (Qiagen) for 1 hour at 65 °C. After this incubation, lysis buffer containing DNA and debris was recovered from brushes by embedding the brush in a sterile plastic micropipette tip and forcing liquid out with air driven by a syringe. Subsequent isolation steps were performed according to manufacturers instructions, after which the DNA/glycogen pellet was resuspended in 20 µL of DNA hydration solution (Qiagen) and quantified on a Nanodrop spectrophotometer (Thermo Scientific).

5.6.2 Quantification and Whole-Genome Amplification of Human Genomic DNA

Because buccal-derived DNA samples contain variable amounts of microbial DNA, the amount of human DNA in each sample was quantified using a qPCR assay designed against the human-specific Yd6 subfamily of the Alu element retrotransposable element. qPCR reactions consisted of 0.1 µM forward and reverse intra-Yd6 primers (31), 1X SYBR Master Mix (Applied Biosystems), and 1 µL of sample DNA in a total reaction volume of 25 µL. DNA samples were

compared to a standard curve of control human genomic DNA to determine the linear range of the assay and the amount of amplifiable human DNA in each sample. Samples containing too little DNA for pooled sequencing or undetectable amounts of DNA were subjected to whole-genome amplification using the REPLI-g system (Qiagen) according to manufacturer's protocol. 51 HSCR samples were of sufficient quantity to include in the pooled sequencing procedure.

5.6.3 Pooled Variant Detection in *IMPDH2* and *IMPDH1*

PCR amplicons were designed using to include all exons and splice sites of *IMPDH1* (NM_000883.3) and *IMPDH2* (NM_000884.2) except the retina-specific exon 13b of *IMPDH1* (32). All variation coordinates are relative to these cDNA sequences, except for variation in the promoter of *IMPDH2*, which is presented relative to the genomic sequence NT_022517.18. At least 75 bp of all 3' intron sequences and the core promoter of *IMPDH2* (1) were included to capture functional noncoding elements. Primers (Table 5.3) were designed not to overlap any sequence of interest and were selected using Primer3 software (33). DNA samples were pooled to a total weight of 0.4 µg, with 10 ng of the pool used in each subsequent PCR reaction, ensuring that 60 haploid genomes per pooled individual were present in each reaction. To construct a positive control pool simulating unique heterozygous variants in a pool of 51 individuals, plasmids containing defined mutant copies of *TP53* exon 9 were pooled in amounts corresponding to either one allele (13 variants) or ten alleles (4 variants) out of a total of 104 alleles, with the difference made up by wild-type sequence. The negative control DNA used to construct the error model was M13mp18 phage DNA (New England Biolabs). All pooled PCR reactions were performed and products were purified as previously described in (29) and Table 5.3. Purified PCR products were pooled in equimolar amounts, ligated into concatamers, and fragmented by sonication on a Bioruptor XL (Diagenode) as described in (29). A single-end

Amplicon	Primer Sequences	Size (bp)	Annealing Temp (°C)
IMPDH2 Amplicon 1	Fwd: 5'GATGGATGGACCCTGGAGGGAATCT3'	1394	59
	Rev: 5'GCTCACCTTGATGTTTCAGGACCCAA3'		
IMPDH2 Amplicon 2	Fwd: 5'GGGTCCTGGGTGGCTGGATGTAG3'	970	59 ^A
	Rev: 5'CGCGCACCTAGGGGTACGAGACC3'		
IMPDH2 Amplicon 3	Fwd: 5'TGGTGGTCCATAGAACTTCACCCCTG3'	1074	64
	Rev: 5'CCCCTATTGGAGGGCTCTATTGTCCC3'		
IMPDH2 Amplicon 4	Fwd: 5'GGCTGCTAAGACTGCATGTGCCTGA3'	1289	64
	Rev: 5'TGAGGGTGCTGTTTTTGTGTGCATC3'		
IMPDH1 Amplicon 1	Fwd: 5'GTAGGGACACCTCTCCCCCTCATCC3'	1139	61
	Rev: 5'CAAATCCTCTGGACCGGAAGGACAG3'		
IMPDH1 Amplicon 2	Fwd: 5'GCGCGGCTGAGCCCTTTGT3'	392	57
	Rev: 5'CGCGCACCTAGGGGTACGAGACC3'		
IMPDH1 Amplicon 3	Fwd: 5'GGGGGCTGTAGCCTCTGCTCCTCTA3'	248	59
	Rev: 5'GCCCTGAGCAAGAAGTCAGCCTCT3'		
IMPDH1 Amplicon 4	Fwd: 5'GTCATCTTGAGCATATGTCCTGTGTCTG3'	1296	64
	Rev: 5'GCTGTGAAGGAACAACGGGACTGTG3'		
IMPDH1 Amplicon 5	Fwd: 5'GCTGTCACCTAGTGGCTGACTGGGG3'	384	59
	Rev: 5'CTGCTGAACCACTCATCCATCTCCC 3'		
IMPDH1 Amplicon 6	Fwd: 5'TTTCAGGGAAGCAGTCCCCTTTGAG3'	692	65
	Rev: 5'ATACATCTGGGGAACAAAGGCGAGG3'		
IMPDH1 Amplicon 7	Fwd: 5'ATCCAGCCCTGTCCCTTTTCCTGA3'	1200	59
	Rev: 5'TCAGCTTGACCTCAGAACCCTGGC3'		
IMPDH1 Amplicon 8	Fwd: 5'CAGGCCTAAGGCTGCCCCATTTTAG3'	695	64
	Rev: 5'GAGCAGTCCTGACTCTGCAGGGGAT3'		

Table 5.3: Primers and amplification conditions for pooled sequencing

A: Denaturation temperature was raised to 96°C for this GC-rich amplicon

sequencing library was constructed from the fragmented concatamers using genomic DNA library construction reagents (Illumina) according to manufacturer's instructions. The library was sequenced on a Genome Analyzer using one lane of a sequencing flow-cell. 24 bp reads were aligned to reference sequences allowing for two mismatches/indels per read and aligned reads were analyzed unknown variants using SPLINTER software using the positive control sequence and expected variants to set confidence cutoffs (29). Primer binding sites were masked and positions within 5 bp of the 3' end of primer binding sites were excluded because of disproportionately high coverage. Variation in low-coverage (less than 30 reads/allele) regions was also excluded.

5.6.4 PCR-Restriction Fragment Length Polymorphism Genotyping Assay

The P123R (rs142797363) minor allele results in the creation of a MwoI restriction site. PCR primers were designed to produce a 182 bp amplicon for restriction digestion containing the polymorphic site. Presence of the P123R variant is indicated by cleavage of the amplicon into 111 and 71 bp fragments. P123-Forward: 5'GCT TCA GAT CAA GAG CCT GAT GAA AGT AGT3', P123-Reverse: 5'GTC TGT GAT TGG GAT ACC GCA GAA AC3'. A positive control product containing the rs142797363 minor allele was amplified from control genomic DNA in two overlapping amplicons using 1) P123-Forward and mutated reverse primer P123R-OE-R: 5'CGA TCC TTG CGG CTG AGG ACC ACA GGG TCT3' and 2) mutated forward primer P123R-OE-F: 5'GTC CTC AGC CGC AAG GAT CGC GTG CGG GAT3' and P123-Reverse. The two purified amplicons were fused and full length product was synthesized in a PCR reactions using the P123-Forward and P123-Reverse primers. Negative control product was amplified from control genomic DNA using the same primers and was mixed in equimolar amounts with positive control product to simulate heterozygosity. PCR reactions on individual

samples were performed in the following conditions: 5 ng genomic DNA sample, 200 μ M dNTPs, 0.2 μ M each primer, 1.3 M Betaine, 1X KlenTaq LA Buffer pH 9.2, 0.1% (v/v) KlenTaq LA polymerase mix in a total reaction volume of 20 μ L. Cycling conditions were as follows: 94 °C for 3', 40 cycles of [94 °C for 1', 52 °C for 45", and 68 °C for 1'], and 68 °C for 5'. PCR products were digested with MwoI by adding 5 μ L of a solution containing 0.2 units/ μ L MwoI in 1X NEBuffer #4 (New England Biolabs) and incubating at 60 °C for 2 hours. Digested products were separated on a 2% sodium borate-agarose gel. Heterozygous samples were confirmed by automated dye-terminator sequencing of purified PCR products.

5.6.5 Plasmids

Human *IMPDH2* cDNA was amplified from IMAGE clone 3447994 (34) using primers KpnI-EK-IMPDH2-F: 5'CGG GGT ACC GAC GAC GAC GAC AAG ATG GCC GAC TAC CTG ATT AG3' and SacI-IMPDH2-R: 5'CGC GAG CTC TCA GAA AAG CCG CTT CTC ATA3'. Purified PCR products were double-digested with KpnI and SacI restriction enzymes (New England Biolabs) and ligated into pET30a(+) bacterial expression vector (Novagen) digested with KpnI and SacI and treated with Shrimp Alkaline Phosphatase (Promega, producing full-length human IMPDH2 with an N-terminal 6xHis-S-FLAG tag (pET30a-IMPDH2). P123R-IMPDH2 was produced in two amplicons by amplifying the original IMPDH2 clone using 1) KpnI-EK-IMPDH2-F and P123R-OE-R primers and 2) P123R-OE-F and SacI-IMPDH2-R primers. The two purified amplicons were fused using PCR with KpnI-EK-IMPDH2-F and SacI-IMPDH2-R primers, and the resulting product was ligated into pET30a(+) using the same procedure as wild-type IMPDH2 to produce pET30a-P123R-IMPDH2. pET30a-L263F-IMPDH2 was derived from pET30a-IMPDH2 by a linear amplification-based site-directed mutagenesis procedure (35) using L263F-OE-F: 5'GGA CTT GTT CGC CCA GGC TGG TG3' and 5'TGG

GCG AAC AAG TCC AGC CTA TAC TTG TC3' primers. The fidelity of all constructs was confirmed by sequencing.

5.6.6 Production of Recombinant Human IMPDH2 in *E. coli*

The production and purification procedure was modified from (32). pET30a-IMPDH and variant plasmids were transformed into Rosetta (DE3) pLysS *E. coli* (Novagen) and grown in 100 mL LB media with 30 µg/mL kanamycin and 34 µg/mL chloramphenicol. Cultures were grown on a shaker incubator at 37 °C until reaching an OD₆₀₀ of 0.5–0.6. Cultures were cooled to room temperature and were induced with 1 mM IPTG for 14–16 hours while shaking at room temperature. Bacteria were pelleted and resuspended in 6 mL of lysis buffer (50 mM NaH₂PO₄, 300 mM NaCl, 10 mM imidazole, 10% glycerol v/v, pH 8.0) supplemented with Complete Mini protease inhibitor cocktail (Roche), 1 mg/mL lysozyme, 10 µg/mL RNase A, and 5 µg/mL DNase I (Sigma). Suspensions were sonicated with a probe sonicator on ice for a total of 60 seconds in 10 second pulses with 10 second rest periods at a power of 250 W. Lysates were incubated on ice for 15 minutes and then cleared by centrifugation for 30 minutes at 10,000 g at 4 °C. The resulting supernatant was incubated with constant rotation with 1.5 mL of a 50% slurry of Ni-NTA Superflow resin (Qiagen) for 30 minutes at 4 °C. Resin and lysate was decanted into gravity-flow chromatography columns, lysates were allowed to flow through, and the resin was washed twice with 6 mL wash buffer (lysis buffer with an imidazole concentration of 20 mM). Bound protein was eluted with four 0.5 mL volumes of elution buffer (lysis buffer with an imidazole concentration of 250 mM). The fractions containing protein (as indicated by UV absorbance at 280 nm) were pooled and dialyzed twice against 1 L of storage buffer (Tris-Cl 100 mM, KCl 100 mM, 20% glycerol v/v, pH 8.0) overnight at 4 °C. Coomassie stained SDS-PAGE gels revealed a single band at the expected size (60.5 kD). Attempts to enzymatically remove the

6xHis-S-FLAG tag with enterokinase were not successful on-resin or in solution without degrading the protein so tagged protein was used in subsequent assays. Protein concentrations were measured using the Bradford method (Bio-Rad Protein Assay) and protein was stored at $-80\text{ }^{\circ}\text{C}$ until it was assayed.

5.6.7 IMPDH Activity Assay

IMPDH activity for each protein preparation was measured using a procedure modified from (27). Enzymatic activity was measured at $37\text{ }^{\circ}\text{C}$ in 100 mM Tris-Cl, 10 mM KCl, 3 mM EDTA, 2 mM DTT by monitoring production of reduced nicotinamide adenine dinucleotide (NADH) using absorbance at 340 nm (extinction coefficient $6,220\text{ M}^{-1}\text{cm}^{-1}$). 15 nM of enzyme in a 200 μL volume was used for each reaction. Reactions were performed in 96-well plates and NADH production was monitored over a 30 minute period using a Synergy2 temperature-controlled plate reader (Bio-Tek) using an absorbance path length calculated from plate well dimensions. Inosine monophosphate (IMP) or nicotinamide adenine dinucleotide (NAD^+) concentration was varied from 1–400 μM in the presence of 400 μM of the other substrate. The rate of NADH production did not change appreciably in any reaction over the course of 30 minutes, so average rate was assumed to accurately represent initial rate.

5.6.8 Curve Fitting

NADH production rates were fit to standard kinetic models using nonlinear least-squares regression in the R software package (R Foundation for Statistical Computing.) Apparent kinetic parameters for IMP were determined using the model $v = V_{max} \times [\text{IMP}]/(K_m + [\text{IMP}])$. Since the experiment in which NAD^+ concentration was varied revealed significant substrate inhibition at 400 μM , an alternative model including substrate inhibition for NAD^+ was used: $v = V_{max} \times [\text{NAD}]/(K_m + [\text{NAD}^+] + [\text{NAD}^+]^2/K_i)$ (36). K_i for NAD^+ was assumed to be identical between

variants. Differences in each model parameter (V_{max} and K_m) between wild-type and each variant were tested for statistical significance using two-tailed t-tests (37). Reported K_{cat} is calculated from the V_{max} of the IMP experiment.

5.6.9 Animals and Whole-Mount Immunofluorescence

$Impdh2^{Del}$, $Sox10^{LacZ}$ ($Sox10^-$), Ret^{TGM} (Ret^-), and Ret^9 pups were genotyped as previously described in Chapter 3 and 4. $Impdh2^{+/Del} Sox10^{LacZ/+}$ pups were produced by mating heterozygote animals. $Impdh2^{+/Del} Ret^{9/-}$ pups were produced by first breeding $Impdh2^{+/Del}$ and $Ret^{+/-}$ heterozygotes. $Impdh2^{+/Del} Ret^{+/-}$ mice survived normally and were then bred to $Ret^{9/+}$ mice. Postnatal day zero pups were euthanized by decapitation and intestines were collected, fixed, and stained with ANNA-1 antiserum and as previously described in Chapter 4. Bowels were then incubated overnight at 4 °C with rabbit anti-Tuj1 (1:1000, Covance #PRB-435P) in blocking solution: Tris-buffered saline pH 7.5 with 1% Triton-X 100 (TBST), 5% normal donkey serum (Jackson ImmunoResearch), 1% cold water fish skin gelatin (Sigma #G7765), 100 mM Glycine. Samples were washed 3 times with TBST and incubated for 1 hour at 37 °C with Alexa-488 donkey anti-rabbit secondary antibody (1:400, Life Technologies # A-21206) in TBST. Bowels were washed 3 times with TBST before mounting and visualization in 50% glycerol/PBS. Aganglionic and hypoganglionic regions were measured using the same methods described in Chapters 3 and 4.

5.9 References

1. Zimmermann AG, Spychala J, Mitchell BS. Characterization of the human inosine-5'-monophosphate dehydrogenase type II gene. *J Biol Chem*. 1995;270(12):6808–6814.
2. Gu JJ et al. Targeted Disruption of the Inosine 5'-Monophosphate Dehydrogenase Type I Gene in Mice. *Mol Cell Biol*. 2003;23(18):6702–6712.
3. Gabriel SB et al. Segregation at three loci explains familial and population risk in Hirschsprung disease. *Nat Genet*. 2002;31(1):89–93.
4. Garcia-Barceló M-M et al. Mapping of a Hirschsprung's disease locus in 3p21. *Eur J Hum Genet EJHG*. 2008;16(7):833–840.
5. Bowne SJ et al. Mutations in the inosine monophosphate dehydrogenase 1 gene (IMPDH1) cause the RP10 form of autosomal dominant retinitis pigmentosa. *Hum Mol Genet*. 2002;11(5):559–568.
6. Kennan A et al. Identification of an IMPDH1 mutation in autosomal dominant retinitis pigmentosa (RP10) revealed following comparative microarray analysis of transcripts derived from retinas of wild-type and Rho^{-/-} mice. *Hum Mol Genet*. 2002;11(5):547–558.
7. Bowne SJ et al. Spectrum and Frequency of Mutations in IMPDH1 Associated with Autosomal Dominant Retinitis Pigmentosa and Leber Congenital Amaurosis. *Invest Ophthalmol Vis Sci*. 2006;47(1):34–42.
8. Aherne A et al. On the molecular pathology of neurodegeneration in IMPDH1-based retinitis pigmentosa. *Hum Mol Genet*. 2004;13(6):641–650.
9. Wang X, Mion B, Aherne A, Engel PC. Molecular recruitment as a basis for negative dominant inheritance? Propagation of misfolding in oligomers of IMPDH1, the mutated enzyme in the RP10 form of retinitis pigmentosa. *Biochim Biophys Acta BBA - Mol Basis Dis*. 2011;1812(11):1472–1476.
10. Mortimer SE, Hedstrom L. Autosomal dominant retinitis pigmentosa mutations in inosine 5'-monophosphate dehydrogenase type I disrupt nucleic acid binding. *Biochem J*. 2005;390(1):41.
11. Kozhevnikova EN et al. Metabolic Enzyme IMPDH Is Also a Transcription Factor Regulated by Cellular State. *Mol Cell*. 2012;47(1):133–139.
12. Mortimer SE et al. IMP Dehydrogenase Type 1 Associates with Polyribosomes Translating Rhodopsin mRNA. *J Biol Chem*. 2008;283(52):36354–36360.
13. Tam LCS et al. Therapeutic benefit derived from RNAi-mediated ablation of IMPDH1 transcripts in a murine model of autosomal dominant retinitis pigmentosa (RP10). *Hum Mol Genet*. 2008;17(14):2084–2100.

14. Wang J et al. IMPDH1 Gene Polymorphisms and Association With Acute Rejection in Renal Transplant Patients. *Clin Pharmacol Ther.* 2007;83(5):711–717.
15. Cao W et al. Genetic Variations in the Mycophenolate Mofetil Target Enzyme Are Associated with Acute GVHD Risk after Related and Unrelated Hematopoietic Cell Transplantation. *Biol Blood Marrow Transplant.* 2012;18(2):273–279.
16. Gensburger O et al. Polymorphisms in type I and II inosine monophosphate dehydrogenase genes and association with clinical outcome in patients on mycophenolate mofetil: *Pharmacogenet Genomics.* 2010;20(9):537–543.
17. Kagaya H, Miura M, Saito M, Habuchi T, Satoh S. Correlation of IMPDH1 Gene Polymorphisms with Subclinical Acute Rejection and Mycophenolic Acid Exposure Parameters on Day 28 after Renal Transplantation. *Basic Clin Pharmacol Toxicol.* 2010;107(2):631–636.
18. Oetting WS et al. Validation of single nucleotide polymorphisms associated with acute rejection in kidney transplant recipients using a large multi-center cohort. *Transpl Int.* 2011;24(12):1231–1238.
19. Shah S, Harwood SM, Döhler B, Opelz G, Yaqoob MM. Inosine Monophosphate Dehydrogenase Polymorphisms and Renal Allograft Outcome: *Transplant J.* 2012;94(5):486–491.
20. Grinyó J et al. Association of four DNA polymorphisms with acute rejection after kidney transplantation. *Transpl Int.* 2008;21(9):879–891.
21. Sombogaard F et al. Interpatient variability in IMPDH activity in MMF-treated renal transplant patients is correlated with IMPDH type II 3757T>C polymorphism: *Pharmacogenet Genomics.* 2009;19(8):626–634.
22. Winnicki W et al. An inosine 5'-monophosphate dehydrogenase 2 single-nucleotide polymorphism impairs the effect of mycophenolic acid. *Pharmacogenomics J.* 2009;10(1):70–76.
23. Pazik J et al. Lymphocyte Counts in Kidney Allograft Recipients Are Associated With IMPDH2 3757T>C Gene Polymorphism. *Transplant Proc.* 2011;43(8):2943–2945.
24. Garat A et al. IMPDH2 genetic polymorphism: a promoter single-nucleotide polymorphism disrupts a cyclic adenosine monophosphate responsive element. *Genet Test Mol Biomarkers.* 2009;13(6):841–847.
25. Garat A et al. Inter-ethnic variability of three functional polymorphisms affecting the IMPDH2 gene. *Mol Biol Rep.* 2011;38(8):5185–5188.
26. Wu T-Y et al. Pharmacogenetics of the mycophenolic acid targets inosine monophosphate dehydrogenases IMPDH1 and IMPDH2: gene sequence variation and functional genomics. *Br J Pharmacol.* 2010;161(7):1584–1598.

27. Wang J et al. A Novel Variant L263F in Human Inosine 5'-Monophosphate Dehydrogenase 2 Is Associated with Diminished Enzyme Activity. *Pharmacogenet Genomics*. 2007;17(4):283–290.
28. Druley TE et al. Quantification of rare allelic variants from pooled genomic DNA. *Nat Meth*. 2009;6(4):263–265.
29. Vallania FLM et al. High-throughput discovery of rare insertions and deletions in large cohorts. *Genome Res*. 2010;20(12):1711–1718.
30. Mitchell AA, Rosenberg L, Shapiro S, Slone D. Birth defects related to bendectin use in pregnancy: I. oral clefts and cardiac defects. *JAMA*. 1981;245(22):2311–2314.
31. Walker JA et al. Human DNA quantitation using Alu element-based polymerase chain reaction. *Anal Biochem*. 2003;315(1):122–128.
32. Bowne SJ et al. Why Do Mutations in the Ubiquitously Expressed Housekeeping Gene IMPDH1 Cause Retina-Specific Photoreceptor Degeneration? *Invest Ophthalmol Vis Sci*. 2006;47(9):3754–3765.
33. Rozen S, Skaletsky H. Primer3 on the WWW for general users and for biologist programmers. *Methods Mol Biol Clifton NJ*. 2000;132:365–386.
34. Lennon G, Auffray C, Polymeropoulos M, Soares MB. The I.M.A.G.E. Consortium: an integrated molecular analysis of genomes and their expression. *Genomics*. 1996;33(1):151–152.
35. Liu H, Naismith JH. An efficient one-step site-directed deletion, insertion, single and multiple-site plasmid mutagenesis protocol. *BMC Biotechnol*. 2008;8(1):91.
36. Wang W, Hedstrom L. Kinetic mechanism of human inosine 5'-monophosphate dehydrogenase type II: random addition of substrates and ordered release of products. *Biochemistry (Mosc)*. 1997;36(28):8479–8483.
37. Cohen J, Cohen P, West SG, Aiken LS. *Applied Multiple Regression/Correlation Analysis for the Behavioral Sciences*. Routledge; 2003:
27. Exome Variant Server, NHLBI GO Exome Sequencing Project (ESP) [Internet] 2012; <http://evs.gs.washington.edu/EVS/>. Accessed August 2013
39. Gu JJ et al. Inhibition of T lymphocyte activation in mice heterozygous for loss of the IMPDH II gene. *J Clin Invest*. 2000;106(4):599–606.
40. Bolck S et al. A human model for multigenic inheritance: Phenotypic expression in Hirschsprung disease requires both the RET gene and a new 9q31 locus. *Proc Natl Acad Sci U S A*. 2000;97(1):268–273.
41. Amiel J et al. Hirschsprung disease, associated syndromes and genetics: a review. *J Med Genet*. 2008;45(1):1–14.

42. Adzhubei IA et al. A method and server for predicting damaging missense mutations. *Nat Methods*. 2010;7(4):248–249.
43. Li B et al. Automated inference of molecular mechanisms of disease from amino acid substitutions. *Bioinforma Oxf Engl*. 2009;25(21):2744–2750.
44. Hedstrom L. IMP Dehydrogenase: Structure, Mechanism and Inhibition. *Chem Rev*. 2009;109(7):2903–2928.
45. Zhang R et al. Characteristics and crystal structure of bacterial inosine-5'-monophosphate dehydrogenase. *Biochemistry (Mosc)*. 1999;38(15):4691–4700.
46. McLean JE et al. Inosine 5'-monophosphate dehydrogenase binds nucleic acids in vitro and in vivo. *Biochem J*. 2004;379(Pt 2):243–251.

Chapter 6: Conclusions and Future Research

Directions

6.1 Environmental factors affecting ENS development

Through a chemical screen in zebrafish and subsequent studies in primary culture and in vivo in mice, we determined that the antimetabolite immunosuppressant mycophenolic acid (MPA) and its prodrug mycophenolate mofetil (MMF) impair ENS development and interact with *Ret* and *Sox10*, genes that cause Hirschsprung disease (HSCR) in humans and similar ENS defects in mice. To our knowledge, this is also the first chemical screen in which effects on ENS development were assessed. While our laboratory has previously demonstrated that Vitamin A deficiency impairs ENS development and interacts with *Ret* mutations, Vitamin A depletion in mice required both genetic and environmental manipulations of Vitamin A metabolism where the genetic insult was sufficient to interact with *Ret* even when dietary Vitamin A was abundant (1). Mycophenolate exposure is the first solely environmental factor that impacts the development of the ENS in an animal model. Future work will focus on drug exposures that are more likely to occur in pregnancy, since MPA/MMF is already recognized as a hazard (2, 3).

In the chemical screen we identified several other interesting compounds that impaired ENS development, and preliminary work by others in the laboratory indicates that many of them affect murine ENCDCs in culture. Artesunate has become an

important part of combination malaria therapy (4) and pregnant women are likely being exposed to it regularly without apparent harm, though studies have demonstrated teratogenic effects in animals (5). Since this is likely to be a common exposure, it will be important to determine whether it interacts with mild HSCR-predisposing mutations such as *RET* polymorphisms (6), which can be relatively common in the general population. Mevinolin, a widely used cholesterol lowering drug, is contraindicated during pregnancy due to the results of animal studies, case reports of malformations and out of an abundance of caution (7). Separate from the likelihood of exposure and the possibility of adverse events, detecting a drug that affects cholesterol synthesis in our assay highlights the developmental importance of this pathway and suggests that ENS development should be studied in mice lacking *Dhcr7*, a cholesterol synthesis gene implicated in Smith-Lemli-Opitz syndrome, which can include Hirschsprung disease as a component. The chemical library used in this screen is relatively small (9), and does not cover even the modest 2200 compounds approved by the FDA (10). Also, our screen examined only a single, somewhat arbitrarily chosen dose of 10 μ M. Use of a range of doses and expansion of the library to encompass both overlooked pharmaceuticals and bioactive natural products that may be present in the environment or deliberately used will likely yield additional ‘hits’ for further investigation.

Further investigation of a class of drugs, toxins, exposures, and nutritional deficiencies is prompted by the fact that MPA/MMF impairs ENS development through its antiproliferative effects. Many other exposures could plausibly reduce proliferation in ENS precursors, contributing to the failure of ENS development during the critical period in which precursor migration is possible. Our data suggest that such insults might also

increase the likelihood that a *RET* mutation will result in penetrant disease. Interestingly, flubendazole has recently been shown to act as an inhibitor of microtubule polymerization in tumor cells and delays the growth of leukemia xenografts (8), suggesting that it may also act on the developing ENS through an antiproliferative mechanism. More common exposures that might modulate cell proliferation include Vitamin B12 and folic acid deficiencies, as well as commonly used antifolate drugs such as trimethoprim/sulfamethoxazole. These and other exposures are amenable to experimental testing against HSCR animal models analogous to the experiments performed using MMF.

MPA/MMF itself may prove to be a useful experimental tool in the search for candidate genes affecting the ENS. Much as MMF treatment was capable of uncovering the phenotype of low penetrance and nonpenetrant *Ret* genotypes, this simple pharmacological manipulation might induce aganglionosis in the context of mutations such as *Phox2b* and *Zfhx1b* that, like *Ret*, cause no ENS phenotype in the heterozygous state in the mouse but result in HSCR in humans.

6.2 Requirement of *Impdh2* for ENS Development

Prompted by the effects of MPA/MMF on ENS development, we then demonstrated that *Impdh2* is required within the neural crest for the development of the ENS and other neural crest derivatives using a tissue specific knockout mouse model. *Impdh2* deletion ablated most ENS precursors and appeared to provide a selective advantage to neural crest cells that did not efficiently express Cre. Implicitly, this shows that IMPDH1 is insufficient to substitute for IMPDH2 and that salvage cannot substitute

for de novo guanine nucleotide synthesis, even when neighboring non-neural crest tissues are normal.

Given the reduction in the number of ENS precursors, it is somewhat surprising that we were able to detect neither a reduction in proliferation nor apoptosis in EYFP marked ENS precursors at embryonic day 13.5 (E13.5). It is possible that these cells are dying through non-apoptotic processes or have already been eliminated before entering the bowel. Wnt1-Cre probably begins to recombine loxP sites at E8 (11, 12), and our current studies leave a large time interval unexplored. While the developing ENS at embryonic day 12.5 and 11.5 was already hypocellular, examination of the pre-enteric migratory streams of vagal neural crest cells at a time point such as E9.5 (13) will probably be necessary to determine the fate of recombined cells. At this time, given the evidence of incomplete recombination and the defects in multiple neural crest derivatives, we cannot exclude the possibility that *Impdh2* deletion is lethal to all cells, and the cells that are in the bowel at E13.5 appear normal because they escaped Cre-mediated recombination.

In parallel with the studies performed in vivo, we established a mouse embryonic fibroblast (MEF) cell line from an *Impdh2*^{loxP/loxP} *Rosa26*^{EYFP} embryo. Preliminary attempts at Cre-mediated deletion of *Impdh2* in culture do not appear to have resulted in adverse effects on these cells and thus suggest that not all cells require IMPDH2, but more work is needed both to confirm complete recombination and analyze the phenotype of these cells. In vivo, PCR analysis of ENS precursors sorted using the EYFP reporter would definitively determine whether any of the cells that enter the bowel have recombined both copies of *Impdh2*.

Alternatively, deletion of *Impdh2* could be delayed until a later time using 4-hydroxytamoxifen inducible Cre recombinase lines with activity in the developing ENS, such as *Ret*^{CreERT2} (14) or Tg(Sox10:iCreERT2) (15). Normally, at E12.5, enough ENS precursors have entered the bowel to perform organotypic culture experiments incorporating time lapse imaging capable of observing non-apoptotic/non-necrotic cell death (13). Moreover, guanosine supplementation experiments performed on these cells could definitively determine whether or not any of the proposed nonenzymatic functions of IMPDH2 are important for ENS development.

6.3 Hirschsprung Disease Genetics: *IMPDH2* and 3p21

Because human *IMPDH2* is located in a genomic region associated with HSCR, we sequenced *IMPDH1* and *IMPDH2* in a cohort of patient samples. While we found one heterozygous *IMPDH2* variant that moderately reduced the activity of recombinant IMPDH2, we did not observe any differences in the frequency of common variants associated with IMPDH function. Moreover, heterozygosity for loss of mouse *Impdh2* did not influence the penetrance of ENS defects in *Ret* or *Sox10* mutants.

Thus, *IMPDH2* is unlikely to be the *RET* modifier locus at 3p21 and the causative gene remains unidentified. Mapping studies have demarcated large regions containing many genes, making a candidate approach difficult, and the relatively modest effect of the variant combined with the requirement for a *RET* mutation for penetrant disease complicates the human genetics. We could turn once again to the zebrafish for a higher-throughput system with which to test the large number of candidate genes. This system has been successfully used to demonstrate genetic interactions between *ret* and the

syndromic-HSCR associated genes *bbs4/bbs5* using morpholino injections (16) and a bowel colonization assay similar to the one used in our screen. This assay could be scaled-up using fluorescent reporter strains (17) and a prioritized list of candidate genes culled from the regions linked to HSCR. Such a screen could also be adapted to probe gain-of-function mutations since overexpression within the developing zebrafish ENS can be achieved through mRNA injection into the early embryo (18). Exome and genome sequencing of patient samples will likely allow finer mapping intervals to be obtained and may even identify specific candidate genetic lesions that can then be tested in animal models.

In closing, these studies demonstrate that maternal medications can, in principle, induce HSCR-like defects in isolation and in cooperation with permissive genetics. Mycophenolic acid serves as a proof-of-concept environmental factor that modifies birth defect penetrance and expressivity in susceptible genetic backgrounds by reducing ENS precursor proliferation. Both pharmacologic inhibition of IMPDH and its genetic disruption through the tissue-specific ablation of *Impdh2* can impair ENS precursor colonization of the bowel, implicating a requirement for de novo guanine nucleotide synthesis in the developing ENS. However, *IMPDH2* mutations probably do not contribute to HSCR.

6.4 References

1. Fu M et al. Vitamin A facilitates enteric nervous system precursor migration by reducing Pten accumulation. *Development*. 2010;137(4):631–640.
2. Anderka MT, Lin AE, Abuelo DN, Mitchell AA, Rasmussen SA. Reviewing the evidence for mycophenolate mofetil as a new teratogen: Case report and review of the literature. *Am J Med Genet A*. 2009;149A(6):1241–1248.
3. Genentech Inc., South San Francisco, CA. CellCept [package insert] [Internet] 2012; http://www.gene.com/download/pdf/cellcept_prescribing.pdf. Accessed March 7, 2013
4. Nosten F, White NJ. Artemisinin-Based Combination Treatment of Falciparum Malaria. *Am J Trop Med Hyg*. 2007;77(6 Suppl):181–192.
5. Li Q, Weina PJ. Severe Embryotoxicity of Artemisinin Derivatives in Experimental Animals, but Possibly Safe in Pregnant Women. *Molecules*. 2009;15(1):40–57.
6. Emison ES et al. A common sex-dependent mutation in a RET enhancer underlies Hirschsprung disease risk. *Nature*. 2005;434(7035):857–863.
7. Merck & Co., Inc., Whitehouse Station, NJ. Mevacor [package insert] [Internet] 2012; http://www.merck.com/product/usa/pi_circulars/m/mevacor/mevacor_pi.pdf. Accessed September 10, 2013
8. Spagnuolo PA et al. The antihelmintic flubendazole inhibits microtubule function through a mechanism distinct from Vinca alkaloids and displays preclinical activity in leukemia and myeloma. *Blood*. 2010;115(23):4824–4833.
9. Chong CR, Chen X, Shi L, Liu JO, Sullivan DJ. A clinical drug library screen identifies astemizole as an antimalarial agent. *Nat Chem Biol*. 2006;2(8):415–416.
10. U.S. Food and Drug Administration. *Approved Drug Products with Therapeutic Equivalence Evaluations 33rd Edition*. 2013:
11. Danielian PS, Muccino D, Rowitch DH, Michael SK, McMahon AP. Modification of gene activity in mouse embryos in utero by a tamoxifen-inducible form of Cre recombinase. *Curr Biol*. 1998;8(24):1323–1326.
12. Echelard Y, Vassileva G, McMahon AP. Cis-acting regulatory sequences governing Wnt-1 expression in the developing mouse CNS. *Dev Camb Engl*. 1994;120(8):2213–2224.
13. Uesaka T, Enomoto H. Neural precursor death is central to the pathogenesis of intestinal aganglionosis in ret hypomorphic mice. *J Neurosci*. 2010;30(15):5211–5218.

14. Luo W, Enomoto H, Rice FL, Milbrandt J, Ginty DD. Molecular Identification of Rapidly Adapting Mechanoreceptors and Their Developmental Dependence on Ret Signaling. *Neuron*. 2009;64(6):841–856.
15. Laranjeira C et al. Glial cells in the mouse enteric nervous system can undergo neurogenesis in response to injury. *J Clin Invest*. 2011;121(9):3412–3424.
16. De Pontual L et al. Epistasis between RET and BBS mutations modulates enteric innervation and causes syndromic Hirschsprung disease. *Proc Natl Acad Sci*. 2009;106(33):13921.
17. Park HC et al. Analysis of upstream elements in the HuC promoter leads to the establishment of transgenic zebrafish with fluorescent neurons. *Dev Biol*. 2000;227(2):279–293.
18. Shepherd IT, Pietsch J, Elworthy S, Kelsh RN, Raible DW. Roles for GFR α 1 receptors in zebrafish enteric nervous system development. *Development*. 2004;131(1):241–249.

JONATHAN IAN LAKE

EDUCATION

2006-present Washington University School of Medicine St. Louis, Missouri
M.D./Ph.D Medical Scientist Training Program

2002-2005 Cornell University Ithaca, New York
B.Sc. *magna cum laude*. College of Agriculture and Life Sciences

RESEARCH

2008-2013 Washington University School of Medicine St. Louis, Missouri
Ph.D candidate Department of Pediatrics
Robert O. Heuckeroth
Project: Gene-environment interactions in development and disease: a model interaction producing Hirschsprung disease-like pathology in mice.

2005 National Institutes of Health Bethesda, Maryland
Post-baccalaureate fellow
Allen M. Spiegel
Project: Structural investigation of the seven-transmembrane domain of the human calcium sensing receptor (CaSR).

2003-2005 Cornell University Ithaca, New York
Undergraduate researcher Department of Developmental Biology
Kenneth J. Kemphues
Project: Intronic elements responsible for the resistance to germline silencing of npp-1 transgenes in *C. elegans*.

PRESENTATIONS

July Invited Lecture
2013 *Gene-environment interactions in Hirschsprung disease: studies in model systems.*
Slone Epidemiology Center, Boston.

March Conference Presentation
2012 *The de novo guanine nucleotide synthesis inhibitor mycophenolic acid impairs enteric nervous system development in vivo and in vitro.* 3rd International Symposium on Development of the Enteric Nervous System, Hong Kong.

PUBLICATIONS

Research Article

Lake JI, Tusheva OA, Graham BL, Heuckeroth RO. *Hirschsprung-like disease is exacerbated by reduced de novo GMP synthesis*. J Clin Invest 2013;123(11):4875–4887

Review Article

Lake JI, Heuckeroth RO. *Enteric nervous system development: migration, differentiation, and disease*. Am J Physiol Gastrointest Liver Physiol. 2013;305(1):G1–G24.

TEACHING

2008-2009 Teaching Assistant

Cell & Organ Systems Biology: Physiology

HONORS AND AWARDS

- Young Investigator Travel Award, 3rd International Symposium on Development of the Enteric Nervous System
- Medical Center Alumni Scholarship Fund Prize
- Cornell University: Ho Nun De Kah Honors Society
- Cornell Presidential Research Scholar
- Novartis Corporate Merit Scholarship